IFPRI Research Project Brief

Wetting and Dispersion of Organic and Biologically-Derived Powders

The International Fine Particle Research Institute (IFPRI) wishes to fund a project in the broad area of dispersion and dissolution of organic particles. The overall objective of the project is to develop systematic understanding of wetting, imbibition, dispersion, and dissolution to facilitate proactive design of powder formulations for optimal dispersibility.

The project should explore and demonstrate approaches to control, design, and engineer nano to meso scale particle surface topology and surface chemistry of organic and biologically-derived materials to promote wetting and dissolution, in concert with addition of surface modifiers (surfactants, ions, polymers, etc.). Dispersion by liquid incorporation into powders and powder addition to liquids should *both* be investigated. A mechanistic model for dispersion and dissolution should be developed and validated. This model should describe both modes of dispersion.

IFPRI's interest is in dispersion of powders common in food and pharmaceutical applications, with an emphasis on water dispersible, bio-derived materials of which, fully soluble particles and mixed soluble/insoluble particles are explored. A phenomenological mechanistic model of the particle/powder wetting, dissolution and dispersion kinetics should be developed and validated as a predictive tool for assessing wetting/dissolution issues of powders/powder beds in both confined and unconfined vessels. The model should address powder to liquid ratios that are representative of localized conditions in transforming a wetted bed of powder having capillary or even funicular wetting at liquid-particle interfaces to a fully dispersed suspension of particles in excess liquid. An understanding of the development of films, gelatinous layers, and fish eyes should be considered, as these are some of the most common issues encountered with reconstitution of powders. Systems where little to no agitation is available to promote wetting and dispersion, such as gravimetric liquid incorporation are of particular interest.

Wetting and Dispersion of Organic and Biologically-Derived Powders

Executive Summary

- Investigate the effect of dry-mixing, wet-mixing and addition of surfactants to modify the rehydration behaviour of a representative biological powder;
- Use high resolution imaging to capture *bulk* rehydration dynamics with *high spatial and fine time resolution* and use microscopy to understand *individual* particle rehydration;
- Design *novel and bespoke image processing* to extract rehydration rate information that can be used to build a rehydration model;
- Build a rehydration model which incorporates into it the *stochastic* nature of powders, as our experience has shown that powder *heterogeneities* are critical in describing powder rehydration.

1.0 Background

Food products are often dehydrated into powder form for more economical transport and an extended shelf life so consequently require rehydration before consumption. The rehydration therefore is a critical key attribute for the performance of food powders such as milk, protein, instant coffee, cocoa, instant soups and beverages, and gives rise to the term “instant”.

Organic and biologically-derived powders often have a complex composition, which results in similarly complex rehydration characteristics. Therefore chemical composition is key for governing the rehydration of powders. However, the bulk composition is not necessarily reflective of the surface composition, and it is the surface that governs not only the interaction between the fluid and particles, but also the particle to particle interactions (Burgain *et al.*, 2017) and hence the all-important dissolution characteristics. Controlling composition, especially at the surface, through formulation and manufacturing can result in profound changes in the rehydration abilities of powders, such as through the addition of surfactants, such as lecithin. Other modifications include dry-mixing in a more soluble compound, such as lactose (Richard *et al.*, 2013); or combining wet ingredients before drying, so that one compound can interfere with the structural formation of another during dehydration (Gaiani *et al.*, 2007).

However, the surface or bulk chemistry is not the only modifiable factor affecting powder rehydration. Powder structure also plays an important role. For example, our work in particle size and morphology characterisation (Boiarkina *et al.*, 2016; Boiarkina *et al.*, 2017; Li, 2017; Cen, 2018; Zhang, 2015) have shown the important role of these characteristics during industrial scale production. It is possible for individual particles to rehydrate well, but the bulk powder to rehydrate poorly due to strong inter-particle interactions preventing water penetration.

One way to understand *a priori* which formulation process is the best method for modifying the rehydration characteristics is to understand the underlying mechanistic kinetics of rehydration. However, most industrial rehydration tests are not designed for monitoring kinetics, but rather take a pragmatic approach by taking a single ‘snapshot’ of the rehydration process at a particular time, such as the ISO method for wettability (ISO/TS 17758:2014) or the IDF method for dispersibility (IDF Standard 129A:1988).

While alternative methods have been proposed for measuring rehydration, such as measuring the change in turbidity (Gaiani *et al.*, 2009); monitoring the change in particle size using laser diffraction (Mimouni *et al.*, 2009; Syll *et al.*, 2012); and focused beam reflectance measurement (Fang *et al.*, 2011), these techniques work either only at concentrations that are significantly lower than that used in industry, or are bulk characterisation techniques and cannot effectively pick up the local development and presence of lumps and gelatinous layers which are key for industrial powder rehydration. They can also be limited in not being able to gather the initial, but crucial, first few seconds of rehydration.

Therefore the overall aim of this work is to develop a mechanistic kinetic model to predict the rehydration behaviour of different powders. We will do this through the investigation of the effect of three different formulation techniques of dry-mixing, surface modification/addition of surface modifiers, and wet incorporation prior to dehydration via spray drying. In a novel approach, we propose

to program *bespoke algorithms for image processing* to extract kinetic rates of the rehydration process. Image processing for bulk rehydration monitoring is seen as a novel way to observe the dynamics of rehydration with both *high spatial and fine time resolution, at high solids concentrations*. The high spatial resolution is seen as a novel way to observe the *stochastic* nature of the process. The project aims are presented graphically in Figure 1.

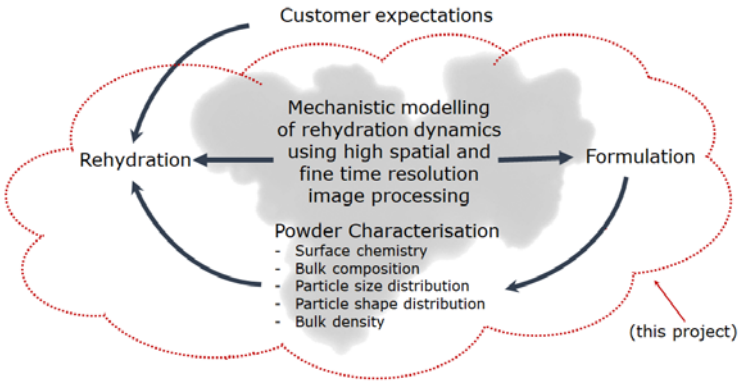

Figure 1: Diagrammatic representation of project.

2.0 Three Year Project Outline

In order to do develop a mechanistic model, a representative powder will be initially used and modified using surface modification, dry-mixing and mixing pre-manufacture. The powders will be manufactured using a spray dryer at the University of Auckland, New Zealand. The representative powder selected will have a wide range of macro constituents (e.g. fat, protein, fibre, sugars, minerals), that can be used to represent different biological systems, such as a protein powder formulation or a cocoa or instant coffee beverage. If time permits, multiple different types of powders will be studied. The powders will be characterised using a range of techniques, including particle size and shape, scanning electron microscopy and bulk density, and surface composition using x-ray photoelectron spectroscopy (XPS) and confocal laser microscopy.

A design of experiments approach will be used in order to understand the effect of formulation on rehydration. This will draw on experience of our team looking into the particle size, shape and surface fat coverage on the rehydration of dairy powders (Boiarkina *et al.*, 2016; Boiarkina *et al.*, 2016a; Boiarkina *et al.*, 2017; Zhang, 2015; Munir *et al.*, 2017) and the interaction of wettability, dispersibility and inadequate lecithination (Khor, 2018; Li, 2017). The rehydration kinetics of the individual powder constituents and the reformulated powders will then be measured, using both novel image processing to build a mechanistic model, and standard industrial rehydration tests for validation of the results.

A mechanistic kinetic model is best developed through *monitoring and measurement* of rehydration at the *appropriate scale*. Kinetic models of the rehydration of dairy powders were explored in the past by our research team in the thesis of Zhang (2015), where the team used laser diffraction to fit the Noyes-Whitney model (Fang *et al.*, 2011) and extract kinetic rehydration parameters. However, our experience has shown that these techniques, as discussed in section 1, cannot resolve rehydration at the appropriate powder solids loadings, at low stirring speeds, or in the first 10 to 20 s which are critical for determining the dispersibility of the powder. It is for this reason that the team has proposed the use of image processing for monitoring the rehydration of powders.

Image processing for understanding the mechanisms behind powder rehydration will be done at two different scales: the *individual particle scale, and the bulk powder scale*. Our team has found that some powder characteristics (e.g. morphology) are important when particles are monitored individually (or at low concentrations), but that other characteristics dominate (e.g. particle size distribution) when particles agglomerate, due to inter-particle interactions (Boiarkina *et al.*, 2016a). Understanding the difference between these mechanisms is important, because this governs what formulation mechanism should be focused on for improving rehydration.

Monitoring of individual particle rehydration will be done using microscopy to determine how much individual particle solubility contributes to total powder rehydration. Image processing with microscopy enables us to follow a specific particle through its changes during rehydration. This microscopy work will build on our past experience of our image processing work on the quantitative analysis of the morphology of instant whole milk powder (Boiarkina *et al.*, 2017; Boiarkina *et al.*, 2018).

Monitoring of bulk rehydration will be done using a high resolution digital camera with a high magnification lens using a set up custom built for this purpose (including lighting), as shown in Figure 2. The *high spatial* resolution of this technique is important for resolving the *stochastic nature of rehydration*, as a portion of the powder may rehydrate effectively, and at the same time another portion form lumps or gelatinous layers. This will leverage our previous experience with this camera set up using imaging for powder characterisation (confidential work with Fonterra, co-funded by the NZ government). Transparent vessels will be constructed to work with higher concentrations of solids (e.g. 12 – 25 %). Image processing through water penetration front tracking using dyes will be used for extracting the following mechanistic information for modelling:

1. Velocities of powder particles sinking without agitation, the rate of breakdown of powders into smaller particles, and size distribution change of lumps remaining/appearing during wetting under the powder's own weight.
2. Rate of liquid penetration into the powder under gravimetric liquid incorporation. This will be used for understanding wetting and the rehydration state transitions from pendula to funicular to capillary and to the final state.
3. Dynamic wettability changes using image processing to monitor how the wetting angle changes as the water is absorbed into the powder. This will also be used to track powder swelling upon imbibition.

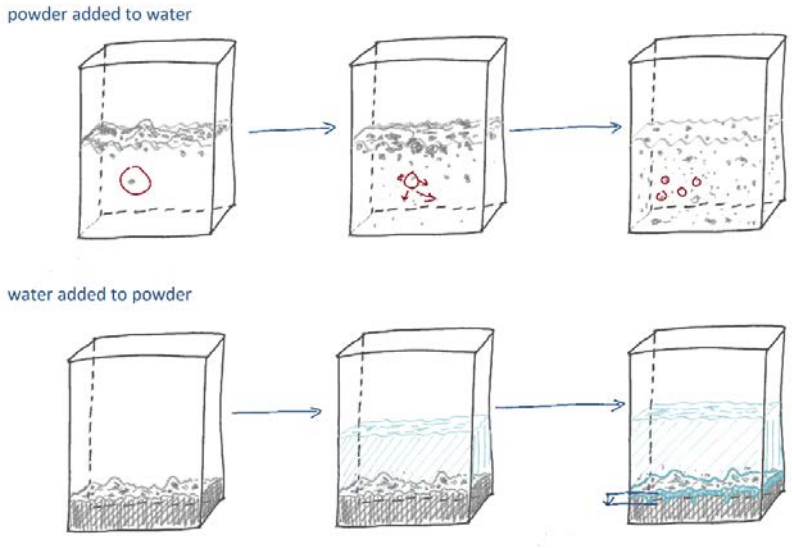

Figure 2: Schematic of set up to be used for examining rehydration.

This study is unique in that we can study *dynamic processes* over comparatively *short time scales* by analysing many particles to build up a statistically valid ensemble average given that this is a stochastic process. During past rehydration characterisation work we have found that rehydration is a highly *stochastic process*, especially when powder exhibits poor rehydration performance (Li, 2017; Zhang, 2015), and current mechanistic models, such as the Noyes-Whitney, tend to use average, or representative size, quantities for modelling rehydration. The average approach does not capture events of interest, the heterogeneity of powder rehydration.

2.1 Yearly Breakdown

Much of the work will be carried out in parallel, however key objectives for each year are listed below.

Year	Achievements for the Year
1	Formulation, manufacture and characterisation of powders with different rehydration properties. The characterisation will be done using standard industry tests for validation, particle sizing, morphology measurement, XPS and confocal laser for surface composition analysis, moisture content and particle and bulk density measurement.
2	Measurement of powder rehydration dynamics using image processing, with custom code developed in MATLAB
3	Mechanistic model development and validation using MATLAB

2.2 IFPRI Member Support

We have in-depth experience with rehydration issues in the dairy industry, however it would significantly enhance our project to understand the specific customer rehydration problems and requirements of IFPRI members. Additionally, IFPRI member support in terms of provision of testing material for validation of the model built would be invaluable. Working together and exchanging knowledge would make our project more effective.

2.3 Project Unknowns and Risks

Risk/Unknown	Mitigation
Finding the right PhD student in a timely fashion with the appropriate skill set.	Starting the project with a research assistant (RA)/research project student, to start the immediate building of the equipment and training. This RA/student could be a good doctoral candidate.
Current camera lens not having enough magnification for process.	Consideration of buying an additional lens or equipment to observe phenomena at a higher magnification.
Regular camera being too slow to capture dynamic rehydration events.	The department has a high speed camera, with appropriate lighting that can be used instead. Dr Boiarkina has experience in using a high speed camera with dye tracing for imaging from her PhD thesis work.
Importing food powder samples from overseas encounters road blocks due to customs approval - validation powders from IFPRI members not available quickly enough for testing.	Starting the approval process and discussions early. Powders will be bought off-the-shelf. Powders for initial model development will be manufactured at the University of Auckland.

3.0 Leverage of Existing Programme and Expertise

Dr Irina Boiarkina has been working with Fonterra, the world's leading dairy exporter[1], on milk powder processing for the last five years, and has experience in the characterisation of powders and understanding the role of processing in powder rehydration. This project would leverage this experience and her current focus on particle technology and process data analytics. She received a Faculty Research Development Fund grant from the University of Auckland in 2016 into understanding the role particle size and morphology on the packing of powders, and funding from the Department of Chemical and Materials Engineering into the determination of surface lecithin coverage of milk powder using XPS in 2018. Her interest in kinetics and dynamic processes extends into teaching, and she has recently received a Mathworks grant to develop Matlab learning resources for students into reaction kinetics. Understanding powder rehydration using image processing combines her interests in particle technology, image characterisation, kinetics and modelling, and is already an area she is working in.

Dr Boiarkina works closely with Dr Nick Depree[2], Dr Wei Yu[2], Ass Prof David Wilson[3] and Prof Brent Young[2] on statistical modelling and large scale regression for the application of real time quality in the dairy industry (Depree *et al.*, 2018; Boiarkina *et al.*, 2017; Boiarkina *et al.*, 2017a). This work was

[1] https://www.fonterra.com/nz/en/about-us.html

[2] University of Auckland

[3] Auckland University of Technology

originally funded as part of NZ's Ministry of Primary Industries' Primary Growth Partnership Programme. We have expertise in process simulation, image analysis, modelling, experimental design and control.

4.0 Budget

This is a fundamental study, with significant scope for further expansion into a wide variety of powders and further in-depth understanding, potentially using different characterisation methods. Current support is available from the University of Auckland from the Principal Investigator's Department and her new faculty start up grant. A Discovery grant from the NZ Government's Marsden Fund will also be sought[4] in 2018. The Marsden Fund is a prestigious "blue sky" research fund from the New Zealand Government, similar to a US National Science Foundation Grant.

Yr.	Cost Description	IFPRI	University of Auckland		Justification
1	Research assistant	$4,000			Three months for initiating research while suitable PhD student is found.
	PhD Stipend + Fees	$24,200			PhD for carrying out the work.
	Annual AGM Reporting	$3,500			Travel and Accommodation to the USA to report findings to IFPRI
	Post-doc 0.1 FTE	$6,300			Development of complex aspects of experimental rig design and image processing
	Consumables		$2,000	PReSS Account[1]	Manufacturing of imaging set up, project materials for powder formulation, powders and associated characterisation costs.
	Macro lens		$1,400	Department	Higher magnification lens for capturing the dynamic behaviour at sufficiently high resolution.
3	PhD Stipend + Fees	$24,200			PhD for carrying out the work.
	Annual AGM Reporting	$3,500			Travel and Accommodation to the USA to report findings to IFPRI
	Post-doc 0.2 FTE	$10,300			Image processing development.
	Consumables		$1,500	PReSS Account	Project materials for powder formulation, powders and associated characterisation costs.
3	PhD Stipend + Fees	$24,200			PhD for carrying out the work.
	Annual AGM Reporting	$3,500			Travel and Accommodation to the USA to report findings to IFPRI
	Post-doc 0.2 FTE	$10,300			Mechanistic model development.
	PhD Student International Conference		$2,500	PReSS Account	Travel for PhD student to present at an international conference
	Total	**$114,000**		**$7,400**	

Assuming an exchange rate of 1NZ$ = 0.69 US$

[1] Research account associated with PhD allocated by the University of Auckland

[4] https://www.royalsociety.org.nz/what-we-do/funds-and-opportunities/marsden

5.0 References

Boiarkina, I., Depree, N., Yu, W., Wilson, D. & Young, B. (2017) Rapid particle size measurements used as a proxy to control instant whole milk powder dispersibility. *Dairy Sci Technol* **96(6)**, 777-786

Boiarkina, I., Depree, N., Yu, W., Wilson, D. & Young, B. (2017a) Fault diagnosis of an industrial plant using a Monte Carlo analysis coupled with systematic troubleshooting. *Food Control* **78**, 247-255.

Boiarkina, I., Sang, C., Depree, N., Prince-Pike, A., Yu, W., Wilson, D. & Young, B. (2016) The significance of powder breakdown during conveying within industrial milk powder plants. *Adv Powder Technol* **27(6)**, 2363-2369.

Boiarkina, I., Ye, J., Prince-Pike, A., Yu, W., Wilson, D. & Young, B. (2016a) The morphology of instant whole milk powder from different industrial plants, in `Chemeca 2016, 25-28th September', Adelaide, Australia.

Boiarkina, I., Yu, W., Prince-Pike, A., Depree, N., Wilson, D. & Young, B. (2018) Classification and regression modelling for investigating the effect of particle size and morphology on the functionality of industrial spray dried milk powder, in 'AIChE Particle Technology Congress, 2018, 22-26th April', Orlando, USA.

Burgain, J., Petit, J., Scher, J., Rasch, R., Bhandari, B. & Gaiani, C. (2017) Surface chemistry and microscopy of food powders. *Prog Surf Sci* **92(4)**, 409-429.

Depree, N., Young, B., Wilson, D., Boiarkina I., Prince-Pike, A. & Croy, R. (2017) Challenges and benefits of aligning and reconciling process data for seasonal process industries, in 'AIChE Spring Meeting, 2017, 26-30th March', San Antonio, USA.

Fang, Y., Selomulya, C., Ainsworth, S., Palmer, M. & Chen, X. (2011) On quantifying the dissolution behaviour of milk protein concentrate. *Food Hydrocolloids* **25(3)**, 503-510.

Gaiani, C., Scher, J., Schuck, P., Desobry, S. & Banon, S. (2009) Use of a turbidity sensor to determine dairy powder rehydration properties. *Powder Technol* **190(1-2)**, 2-5.

Gaiani, C., Schuck, P., Scher, J., Desobry, S. & Banon, S. (2007) Dairy powder rehydration: influence of protein state, incorporation mode, and agglomeration. *J Dairy Sci* **90(2)**, 570-581.

Khor, S. (2018) Investigation of the interaction between the dispersibility and wettability of whole milk powder. Master of Engineering Studies, University of Auckland. *To be completed in June*

Li, B. (2017) Investigation of industrial dispersibility testing of instant whole milk powder and causes of poor quality results. Master of Engineering Studies, University of Auckland.

Mimouni, A., Deeth, H., Whittaker, A. Gidley, M. J. & Bhandari, B. (2009) Rehydration process of milk protein concentrate powder monitored by static light scattering. *Food Hydrocolloids* **23(7)**, 1958-1965.

Munir, M., Wilson, D., Depree, N., Boiarkina, I., Prince-Pike, A. & Young, B. (2017) Real-time product release and process control challenges in the dairy milk powder industry. *Curr Opin Food Sci* **17**, 25-29.

Richard, B., Le Page, J., Schuck, P., Andre, C., Jeantet, R. & Delaplace, G. (2013) Towards a better control of dairy powder rehydration processes. *Int Dairy J* **31(1)**, 18-28.

Syll, O., Richard, B., Willart, J., Descamps, M., Schuck, P., Delaplace, G. & Jeantet, R. (2012) Rehydration behaviour and ageing of dairy powders assessed by calorimetric measurements. *Innov Food Sci Emerg* **14**, 139-145.

Zhang, K. (2015) Investigation in Variation of Dispersibility of Instant Whole Milk Powder. Master of Engineering, Chemical and Materials Engineering, University of Auckland.

IFPRI Research project

A multi-scale study of powders reconstitution phenomena

LIBio – Laboratoire d'Ingenierie des Biomolecules (University of Lorraine, France)

I - State of the art on powder reconstitution

Organic and biologically-derived materials under a powder form are involved in the manufacturing of many products available in the food industry (cosmetics, food, pharmaceutics…). In the food field (but not only), powders are ranging from raw materials and ingredients, such as flours and spices, to processed products like instant coffee or powdered milk. They originate either from liquid conversion into powder by various techniques such as spray-drying, freeze-drying, drum-drying, belt-drying or crystallization, or from size reduction of solid materials induced by grinding, crushing, milling, attrition, or pulverization (**Karam et al., 2016**). It should be noted that particle surfaces, in that case, are essentially constituted by broken structures (**Bhandari, 2013**). Because of these various origins, their particle size and shape distributions, chemical composition, surface composition, and physical properties are highly variable. Therefore, more than one analytical technique is often required to obtain a full set of information about a given scientific question (**Burgain et al., 2017**).

Among these questions, the reconstitution of powders is of upmost importance for the industry considering that most powdered ingredients are dissolved or infused before use. In order to improve understanding, the reconstitution process is often divided into four separated but often overlapping steps. First, the wetting step can be described as the displacement of the solid/air interface by the solid/liquid interface as the powder enters into contact with the liquid. Then, the capillary step (leading to swelling) occurred thanks to the presence of intra- and inter-particle voids in which the liquid penetrates due to the action of capillary forces. The disaggregation step appears when the powder disperse into smaller units. Finally, during the final dissolution step, the particles dissolve into individual molecules and/or ions only if the particles are soluble (**Marabi, 2008**). The entire reconstitution mechanism was investigated by **Forny et al., (2011)** or **Gaiani et al., (2006)** but also focus on some individual steps was done (**Mitchell et al., 2015**).

Many techniques were used to describe and characterize these successive steps and interesting advancements have been made. Nevertheless, deeper mechanistic understanding and systemic research is still needed regarding the great variety of powders industrially available. Also, fundamental understanding enabling improvement of the reconstitution of these powders is still lacking. Moreover, elements are still missing in the understanding of reconstitution in complex industrial environment (e.g. heterogeneous surface composition created upon spray-drying or dispersion in complex liquid flow).

This project aims at:

(1) Bringing new knowledge in the reconstituability of industrial powders with a focus on the particle surface. Even if the powder surface is one of the main players during the reconstitution (from particle/air to particle/water), it has been poorly studied in the literature.

(2) A reconstituability index will then be defined to draw a predictive criterion for the classification of unknown industrial powders according to their reconstitution behavior from the knowledge of their physical and chemical characteristics.

II – Limitation in current understanding of powders reconstitution

Limitation 1. A number of analytical methods have already been developed to measure the reconstitution performance of powders (**Felix da Silva et al., 2018**). Many of them are routinely used at the LIBio (turbidimetry, conductimetry, light scattering and rheology…). Powder reconstitution kinetics must be monitored simultaneously *in situ* and for a huge variety of industrial powders to develop predictive models. Also, powders screening and classification as a function of their reconstitution performance are not available for a large variety of materials.

Answer: Part 1 of the PhD work will deal with this issue through the systemic analysis of hundreds of powders and their classification in terms of reconstituability. Kinetic data of powder reconstitution steps will be necessary to develop models.

Limitation 2. It is well known that some reconstitution steps depend strongly on particle surface (chemical composition, structure…). For instance, studies demonstrated that surface chemical composition of food particles could differ significantly

from their bulk composition (**Fäldt et al. 1993**). Correlations between hydrophobicity/hydrophilicity and/or hardness of powder surface with their reconstitution behavior are needed.

Answer: Part 2 of the PhD work will deal with this issue through surface characterization of particles (from representative powders studied in part 1) at different scales (from micro, nano- to atomic scale). Our team is a leading group on that topic.

Limitation 3. The influence of the addition of surface modifiers in relation with their nature, amount and location in powder structure was also poorly studied. Location of these modifiers within the particle and links with the powder reconstitution are not available.

Answer: This issue will be studied in part 2 of the PhD work to establish relationships between structure, function and processes for powders containing surface modifiers.

Limitation 4. The huge number of parameters influencing powder reconstitution kinetics is a critical limitation for the development of predictive mechanistic models able to deduce reconstitution times from the knowledge of powder characteristics. Moreover, the complexity of the different steps occurring in particle reconstitution precludes from establishing a single analytical model taking into account the multiple influences of powder physical and chemical characteristics.

Answer: To overcome these limitations, the PhD work in part 3 will first be focused on correlation between powders properties to select the most significant parameters and model powder reconstituability from its physicochemical characteristics.

III – Our proposal: an engineering approach of the reconstitution phenomena based on multi-scale study

This proposal is divided into three phases (**Figure 1**).

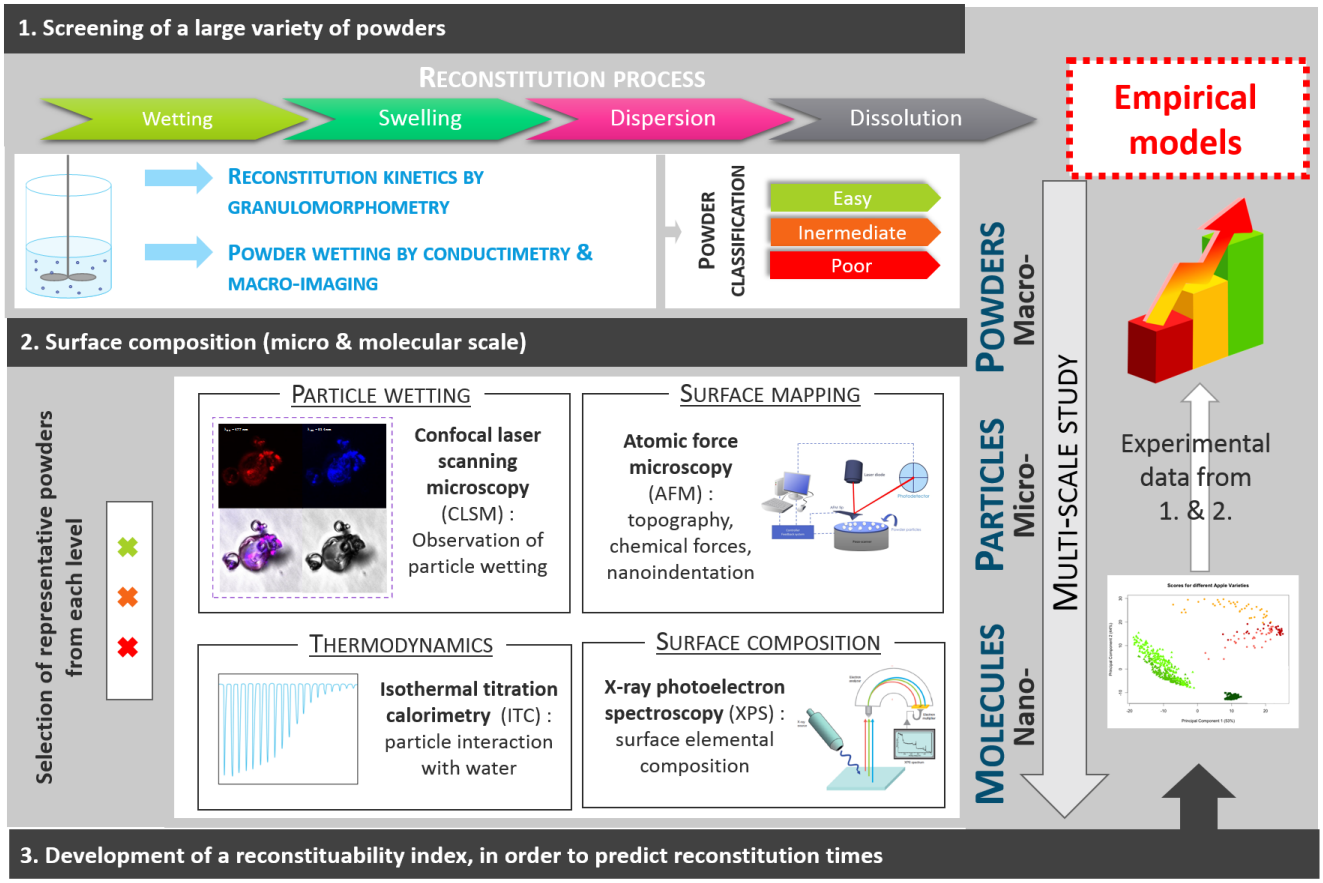

Figure 1: General organization of the PhD project.

First, the reconstitution performance of a large variety of powders will be assessed in order to create three groups: i.e., easy, intermediate and poor reconstitution performance. For this purpose, hundreds of powders will be selected in agreement with the IFPRI consortium. During reconstitution, powder reactivity is directly linked to the surface composition and structure. Therefore, powder surface is a locker to really master the reconstitution. This is why the second part of the thesis will focus on the characterization of particle surface heterogeneity, structure and composition with new and promising techniques already mastered at the LIBio. In a last phase, the surface and bulk characteristics of powder, as well as thermodynamic parameters describing the kinetics of powder reconstitution steps will be integrated into empirical models in order to calculate a reconstituability index, able to reflect differences in reconstitution times of the various investigated powders.

1 - Screening of a large variety of powders (macroscale)

A maximum of materials (around a hundred of industrial food powders) will be screened to be able to classify the powders into three reconstituability levels: easy, intermediate and poor. Tested powders should present variable proximate compositions (water, fat, protein, carbohydrate and mineral contents), structural properties (size, shape, porosity and density), physical properties (amorphicity/crystallinity…) and process origins (spray-drying, drum-drying, freeze-drying) to obtain a wide range of reconstitution profiles.

Two techniques will be concurrently used to screen both the wetting (1) and the swelling, dispersion, and dissolution steps (2).

(1) The **wetting step** will be studied similarly to **Mitchell et al. (2015)**, with the construction of rate-limiting regime maps (**Table 1**).

Table 1. Example of powder wetting classification used by **Fitzpatrick et al., (2016)**

Speed (rpm)	salt	sugar	Skim milk	flour	chocolate	NaCas	MPI
100	Sedimentation	Sedimentation	Sedimentation	Floating + sedimentation	Floating	Floating and big clumps in dispersion	Floating
200							
300	Dispersed		Clumps in dispersion	Clumping + sedimentation			
400		Dispersed					
500			Dispersed				
600							
700				Dispersed	Dispersed		Dispersed
classification	Easy	Easy	Intermediate	Poor	Poor	Poor	Poor

(2) The **swelling, dispersion and dissolution steps** will be investigated by dynamic image analysis. The equipment uses a high-speed mega-pixel camera to simultaneously characterize the particle size and shape at an unrivaled particle numbers (Yu and Hancock, 2008). In the present study, powders will be fed into a reactor with a controlled temperature and stirring speed, connected to the equipment. The advantage of this apparatus is its flexibility: large temperature scales, different solvents, various stirring speeds, possibility to visualize particles in opaque media (like in milk for example)… Particle size and shape evolution during the reconstitution process, but also other parameters (numbers of particles and fibers, final number of insoluble particles…) will be collected to construct reconstitution kinetics.

Deliverables:

(1) Powder classification according to their reconstituability behavior.

(2) Reconstitution kinetics in different conditions of temperature, stirring, and solvent nature.

(3) Statistical correlation between the various powder characteristics and reconstitution ranking (to be in depth investigated in part 3 of the thesis).

Duration: year 1

2 - Surface composition (micro & molecular scale)

Only representative powders classified into poor, intermediate and easy reconstitution behaviors will be in depth investigated in the second part of the PhD work. The selection of powders will be based on the statistical approach mentionned above, and the support/validation of IFPRI members that will "mentor" this project. Here, we will focus on single particle behavior

(and not the whole powder bulk contrary to part 1 of the PhD work) and more particularly the particle surface. Two important limitations to a good reconstitution are directly linked to the particle surface. First, the surface composition of the powder will influence the wetting behavior (**Burgain et al., 2016b**). Also, the surface hardness/softness was found to be responsible for a poor dispersion behavior for some powders (**Burgain et al., 2016a**) as well as the structure (roughness, porosity).

- Particle wetting/swelling

The wetting step of single particles will be investigated at micro-scale by CLSM. Particle size increase, fish eyes, and chemical composition of the external layer can be determined. CLSM is regularly used to visualize structures based on autofluorescence of particle compounds or, more commonly, by using fluorescent labels. However, labelling can affect particle structure and/or their wetting behavior. To avoid these problems, we will use a label-free imaging method such as Coherent anti-Stokes Raman scattering (CARS) microscopy that is based on molecular vibrations in the sample. CARS microscopy is a dye-free method and the prominent advantage of this method is that the sample remains almost unaffected. The technique is also suitable for 3D imaging since the method is confocal and the signal is generated from a small focal spot that can be scanned in all spatial directions. By a judicious selection of wavelengths, it will be possible to observe location of molecules in the particle and the evolution during particle wetting.

- Powder surface mapping

After being initially used as a high resolution imaging technique, AFM is currently often used for measuring interaction forces in a mode called force spectroscopy (**Butt et al., 2005**). Force–distance curves are a very sensitive and quantifiable way to determine probe–sample interactions, used both in force spectroscopy and nanoindentation. Force curves can be recorded either at a well-defined location or at multiple locations leading to a so-called "force–volume image". In the latter case, spatially-resolved maps of sample properties and molecular interactions forces are produced. With AFM, surface structure and chemical properties can be correlated thanks to the combination of surface topography analysis and force measurements. To this end, the AFM probe should be carefully grafted with functional groups presenting well-known properties.

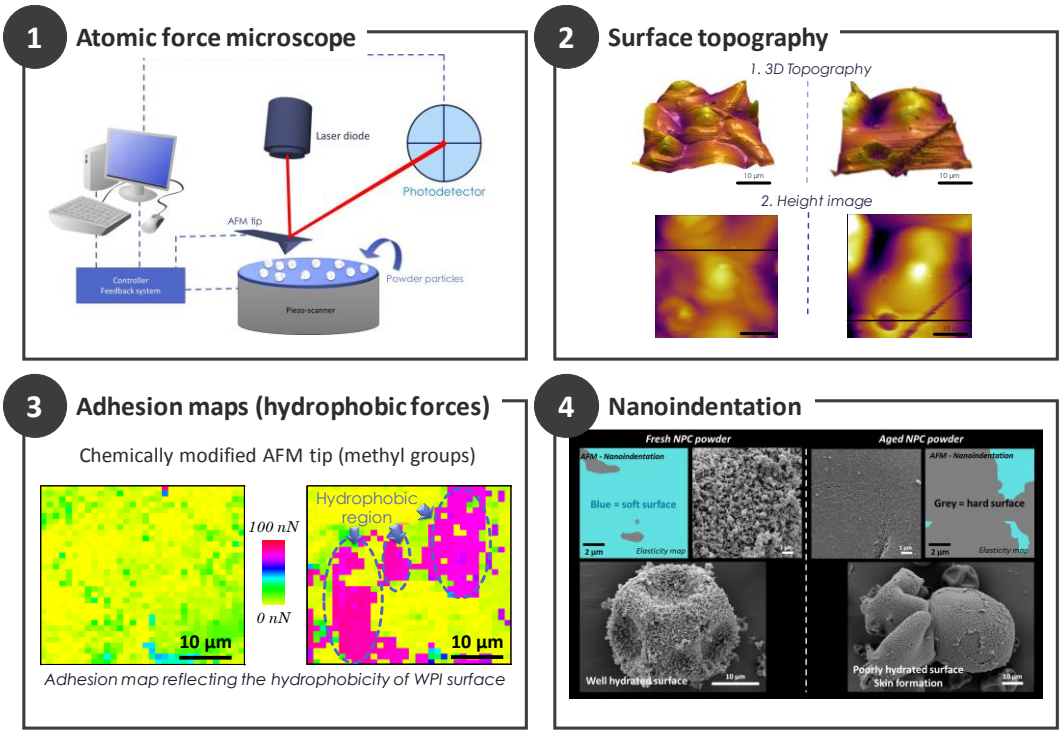

Figure 2: AFM as a tool to analyze particle surface: 1- Experimental set up; 2- Particle surface topography; 3- Examples of adhesion maps recorded on a whey particle submitted to storage; 4- Surface hardening of casein powders associated with reconstituability after storage.

We will use the two modes (chemical force microscopy and nanoindentation) on selected powders as they showed interest in some of our previous works in understanding two important limitations to a quick powder reconstitution: presence of components making the surface hydrophobic (*i.e*. whey powders – **Burgain et al., 2016b**) and/or powder surface hardening during storage (*i.e.* casein powders– **Burgain et al, 2016a**). In the first case, the presence of Maillard reaction end-products was found to impair the reconstitution, the surface being more and more covered by hydrophobic patches during its storage. In the second case, no evolution of surface hydrophobicity was noticed but the surface became harder during storage with the formation of a crust at the particle surface making a barrier to water penetration. Complementary techniques to screen the particle surface such as X-ray Photoelectron spectroscopy (XPS) will be also used to qualify and quantify the surface chemical composition. XPS was first developed by **Fäldt et al, (1996a, 1996b)** but is now routinely used for this purpose.

- Powder surface mapping after surface modifier addition

The same powders containing variable quantities and nature of surface modifiers (furnished by industrial partners) will be investigated. Surface characteristics will be correlated with the powder behavior during reconstitution (macroscale). It should be possible to determine the preferential location of the modifier (at the surface, in the bulk, in the porosities) and its distribution at the particle surface (patches or homogeneously distribution), and to correlate with the powder classification established in part one.

Deliverables:
(1) Surface chemical mapping and nanoindentation to establish correlations with powder reconstituability
(2) Determine the effect of surface modifiers (quantities to cover the surface, surface distribution, minimal quantity necessary to improve wetting. etc.).
Duration: year 2

- Development of a new technique for the determination of thermodynamic parameters of the water/particle interaction

Isothermal titration calorimetry (ITC) is used to study binding interactions. It consist in injecting successive amounts of titrant (water) into the sample solution (powder in ethanol) present in a cell. The heat exchanged during the water/particle interaction is measured. The strength of this technique lies in its unique ability to provide not only the binding affinity, but also the thermodynamical characteristics of the binding.
As injection of titrant can be done through very small volume, it is expected to allow deciphering all the reconstitution steps whereas techniques described in the first part of the project (and in the literature) are either able to follow the reconstitution globally (*i.e.* depending on the powder, some reconstitution steps may be impossible to check owing to their quickness) or to analysis some steps. Here, powder wetting which describes the affinity between the material constituting the powder and the liquid as well as the capillary/swelling which describes the process of water penetration inside the particle may be more easily followed. Also thermodynamic parameters can be obtained and then injected into the models. This part is challenging but can bring very accurate data on powder reconstituability.

Deliverables: Thermodynamic parameters identification at the molecular level: the binding affinity (K_a), enthalpy changes (ΔH), and binding stoichiometry (n) of the interaction between two or more molecules in solution. From these initial measurements, Gibbs energy changes (ΔG) and entropy changes (ΔS) can be determined using the relationship: $\Delta G = -RT.\ln K_a = \Delta H - T\Delta S$
Duration: end of year 2 and year 3

<u>3 - Development of a reconstituability index, in order to predict reconstitution times in given process conditions</u>

The aim of this last part is to predict reconstitution times in given conditions from the numerous powder characteristics that are susceptible to affect the powder behavior. Indeed, reconstitution times are known to be affected by various properties of powder bulk and surface, such as proximate composition (water, fat, protein, carbohydrate, and mineral contents), physical properties (size, shape, porosity, and density), chemical properties (amorphicity/crystallinity…) and manufacturing process (spray-drying, drum-drying, freeze-drying) that may impact powder structure and interactions with water.
The first task will be to identify the main powder characteristics influencing the reconstitution behavior. Two approaches will be employed. On one hand, statistical analysis methods (ANOVA, Pearson correlation coefficients, principal component

analysis, etc.) will be applied to determine what powder characteristics mainly influence reconstitution times measured in given conditions (obtained in part 1 of PhD work). This will allow to obtain a relevant set of parameters related to powder characteristics only that control powder reconstitution times. On the other hand, it will be tried to link thermodynamical parameters describing the kinetics of each reconstitution step (determined in part 2 of the PhD work) to powder characteristics. In this purpose, statistical analysis methods will also be employed to identify the main powder characteristics affecting thermodynamical parameters of reconstitution kinetics.

The second task will intend to model the influence of the main powder characteristics on reconstitution times. Empirical models for the prediction of reconstitution times will be built with thermodynamical parameters of reconstitution kinetics only as input parameters. After that, empirical models will be established to convert the significant powder characteristics (deduced from task 1 of part 3 of the PhD work) into thermodynamical parameters describing the reconstitution process kinetics. Finally, a unique empirical model taking into account the great variability of investigated powders in matter of physical, chemical, structural characteristics will be built by using the main influencing parameters (deduced from task 1 of part 3 of the PhD work) as input parameters to predict reconstitution times. This will be achieved by combining the two kinds of models previously obtained (the first one linking powder characteristics to thermodynamical parameters, the second one calculating reconstitution times from thermodynamical parameters), but also by performing direct modelling without recourse to thermodynamical parameters of reconstitution kinetics.

The last task of part 3 of the PhD work will be intended to go one step further by defining a reconstituability index that is independent from the process conditions used to determine reconstitution times. Indeed, models developed in task 2 of part 3 of the PhD work may successfully predict reconstitution times in given (lab-scale) conditions, but will not be applicable to other reconstitution conditions. Dimensional analysis approaches will be employed to translate the reconstitution time obtained in given conditions into a dimensionless reconstituability index, similarly to **Jeantet et al. (2010)** who showed that powder reconstitution in agitated vessels is mainly controlled by Reynolds number (representative for flow conditions, *i.e.* powder-water mixing intensity) and solid content (*i.e.* weight ratio between powder and water). Finally, values of reconstituability indices calculated for all investigated powders will be used to draw a criterion for the classification of powders according to their reconstitution behavior into easily, moderately, and hardly reconstitutable powders (determined in part 1 of the PhD work).

Deliverables: (1) empirical models able to predict reconstitution times;
(2) definition of a reconstituability index reflecting powder reconstitution behavior independently from reconstitution conditions in agitated vessels
Duration: year 3

IV - Leveraging into LIBio existing programs

The workpackages outlined above will be carried out by a dedicated full time PhD student 100 % funded by the IFPRI Consortium. Materials and consumables will be covered by the LIBio. This project can be leveraged to obtain local funds from the Grand Est region and the University of Lorraine Impact “Biomolecules” program leaded by a LIBio professor. These organizations provide 2-to-1 support for industrial cash grant.

The PhD student will be embedded in the LIBio laboratory under the direct supervision of Prof. Claire GAIANI. Since her recruitment in 2007, she has received more than of 2 000 k€ funding for projects on which she was the principal investigator. Among other important activities, she successfully managed **fundamental competitive programs** including the French ANR and European projects. She also participated in **international collaborations**. Finally, she managed many **industrial partnerships** with leading international food companies (including Nestlé, Lactalis, Bel, Bongrain, and Senoble).

V - Indications where IFPRI members could support the program through provision e.g. of model test materials, test methods, industrial experience

This project will be in close collaboration with the IFPRI members with regular meetings and reports. We will test powders of interest for the industry and if possible directly from the industrial partners.

VI – References

Bhandari, B., 1 - Introduction to food powders, in: Handb. *Food Powders*, Woodhead Publishing, (**2013**) 1–25.

Burgain, J., Petit, J., Scher, J., Rasch, R., Bhandari, B., & Gaiani, C. Surface chemistry and microscopy of food powders: A review, *Prog. Surf. Sci.* 92 (**2017**) 409-429.

Burgain, J., Scher, J., Petit, J., Francius, G., & Gaiani, C. Links between particle surface hardening and rehydration impairment during micellar casein powder storage, *Food Hydrocol.* 61 (**2016a**) 277-285.

Burgain, J., El Zein, R., Scher, J., Petit, J., Norwood, E.A., Francius, G., & Gaiani, C. Local modifications of whey protein isolate powder surface during high temperature storage, *J. Food Eng.*, 178 (**2016b**) 39-46.

Butt, H.J., Cappella, B., & Kappl, M. Force measurements with the atomic force microscope: Technique, interpretation and applications, *Surf. Sci. Reports* 59 (**2005**) 1–152.

Fäldt, P., Bergenståhl, B., & Carlsson, C. The surface coverage of fat on food powders analyzed by ESCA, *Food Structure*, 12 (**1993**) 225-234.

Fäldt, P., & Bergenståhl, B. Spray-dried whey protein/lactose/soybean oil emulsions. 1. Surface composition and particle structure, *Food Hydrocol.*, 10 (**1996a**) 421-429.

Fäldt, P., Bergenståhl, B. Spray-dried whey protein/lactose/soybean oil emulsions. 2. Redispersibility, wettability and particle structure, *Food Hydrocol.*, 10 (**1996b**) 431-439.

Felix da Silva, D., Ahrné, L., Ipsen, R., & Hougaard, A.B. Casein-based powders: characteristics and rehydration properties, Comp. Rev. *Food Sci. Food Saf.* 17 (**2018**) 240-253.

Fitzpatrick, J.J., van Lauwe, A., Coursol, M., O'Brien, A., Fitzpatrick, K.L., Ji, J., & Miao, S. Investigation of the rehydration behavior of food powders by comparing the behavior of twelve powders with different properties, *Powder Tech.* 297 (**2016**) 340-348.

Gaiani, C., Étude des mécanismes de réhydratation des poudres laitières : influence de la structure et de la composition des poudres, *Institut National Polytechnique de Lorraine* (**2006**) 228 pp.

Jeantet, R., Schuck, P., Six, T., Andre, C., & Delaplace, G. The influence of stirring speed, temperature and solid concentration on the rehydration time of micellar casein powder, *Dairy Sci. Technol.* (**2010**) 225-236.

Karam, M.C., Petit, J., Zimmer, D., Baudelaire Djantou, E., & Scher, J. Effects of drying and grinding in production of fruit and vegetable powders: A review, *J. Food Eng.* 188 (**2016**) 32–49.

Marabi, A., Mayor, G., Burbidge, A., Wallach, R., & Saguy, I. Assessing dissolution kinetics of powders by a single particle approach, *Chem. Eng. J.* 1 (**2008**) 118-127.

Mitchell, W.R., Forny, L., Althaus, T.O., Niederreiter, G., Palzer, S., Hounslow, M.J. & Salman, A.D. Mapping the rate-limiting regimes of food powder reconstitution in a standard mixing vessel, *Powder Technology* 270 (**2015**) 520-527.

Forny, L., Marabi, A., & Palzer, S. Wetting, disintegration and dissolution of agglomerated water soluble powders, *Powder Tech.* 206 (**2011**) 72-78.

IFPRI Research Project Brief

Atomization Under Industrially-Relevant Conditions

The International Fine Particle Research Institute (IFPRI) wishes to fund a project to investigate the atomization of fluids and slurries under conditions relevant to spray drying. The approach to spray drying varies broadly by industrial application, using several different spray nozzle types and a wide range of operating parameters (mass flow, velocity and pressure), spraying fluids with myriad rheological properties in different chamber conditions (temperature and pressure). Although, there is a large body of literature on spray characteristics, little is focused on comparing sprays at conditions relevant to spray drying industry. The purpose of this research is to map the breadth of spray characteristics for a broad range of industrially relevant fluid systems and operating conditions to enable the selection of a set of nozzles and conditions for a given application. The best choice of nozzle for an application depends in most cases strongly on specifics of the application. For example, it may be critical to limit oversize particles in some application or undersize particles in other. Just focusing on an average particle size, as most of the current correlations do, is rarely sufficient.

More specifically, the project should focus on the spatial variation of droplet size distribution for a variety of nozzle types under a range of operating parameters and fluid rheology. Results should be used to develop a "comparison map" of the different nozzles, identifying their operating range and limitations in terms of quality of atomization, i.e. droplet size distribution, spray pattern, and spray stability.

While the scope of the project should be defined by the PI, IFPRI members come from many industry sectors and therefore utilize a broad range of atomizers and fluids. For this reason, at least two nozzle types and 2-3 different scales should be investigated. Fluids should be selected to span the range fluid rheologies used in spray drying, including Newtonian and non-Newtonian solutions and suspensions over a range of solid fractions.

Characterization of Spray Drying Nozzles at Industrially Relevant Conditions

Nasser Ashgriz
Department of Mechanical and Industrial Engineering
University of Toronto, ON, Canada M5S-3G8
ashgriz@mie.utoronto.ca

Proposal to
IFPRI

Summary

This proposal is aimed at developing a set of benchmark experimental data and better models for the droplet size distributions of sprays formed by nozzles relevant to spray drying technology. Despite decades of research on the atomization process, the current models still fail to properly predict droplet sizes at industrially relevant conditions. Almost all correlations are based on droplet size measurement far downstream of the nozzle, when the spray is fully established. However, changes in the fluid properties, in particular changes in the rheological properties, as well as changes in the ambient conditions can significantly alter the spray droplet size distribution. For this purpose, we propose to characterize near-nozzle atomization process. Fluids with different rheological properties will be tested to determine ligament sizes and shapes close to the nozzle and also further downstream of the nozzle. Droplet size distributions as well as correlations for the mean droplet sizes will be developed for industrially relevant fluids. In addition, effect of chamber temperature on the ligament formation and final droplet sizes will be considered.

1 Introduction

In the spray drying process, active ingredients are dissolved in solvents and the solution is atomized into small droplets, which are dried in a heated gas stream to form particles [1]. The morphology of the particles is intimately related to the droplet size distribution of the spray. The droplet size distribution, in turn, depends on the choice of the nozzle, fluid properties, the operating conditions, such as liquid and gas mass flow rates, velocities, pressures and temperatures, as well as the ambient conditions.

In order to determine the proper operating conditions, the desired fluid is tested at a pilot scale system, the results of which are then extrapolated to the production scale. Because of the lack of having proper scaling parameters, such extrapolations require several trials before satisfactory conditions are determined. This is a time consuming and costly process. A better understanding of the atomization process for industry relevant fluids would allow development of better scaling models, which can significantly reduce time and cost from pilot to production scale sprays.

There are numerous spray nozzles, the choice of which depend on the liquid properties and the application area. The more commonly used nozzles for spray drying have been pressure swirl nozzles for the production scale and twin-fluid nozzles for the pilot scale tests. And the most important property that influences the atomization process is the rheological properties of the fluid. Generally, it is more difficult to atomize viscoelastic liquids than viscoinelastic liquids [2]. The breakup pattern of viscoinelastic liquids are similar to those of low viscosity fluids, like water. However, viscoelastic liquids generate ligaments that undergo large stretching motion before they

breakup into droplets. It is shown [2] that the extensional viscosity is the most significant rheological property that inhibits breakup. For shear thinning fluids the quality of atomization closely relates to the apparent viscosity of the fluid in the limit of infinite shear rate. The Sauter Mean Diameter (SMD) is found to increase with this viscosity (μ_∞) according to [2]:

$$SMD \propto \mu_\infty^{0.42} \quad (1)$$

However, such relations for pharmaceutically relevant fluids are lacking.

There are several correlations for the average droplet sizes generated by complex fluids. We have selected two of them, which have used complex fluids as provided in Table 1, for comparison in this study. One is by Mansour and Chigier for power law liquids [2]:

$$SMD = d_o\left(1+\frac{\dot{m}_g}{\dot{m}_l}\right)\{0.0707We_g^{-0.39}+0.275Oh_l^{0.78}\} \quad (2)$$

and the other is by Aliseda et al. [3] for complex liquids, including polymers:

$$SMD = d_o C_1\left(1+\frac{\dot{m}_g}{\dot{m}_l}\right)\left(\frac{b_g}{d_o}\right)^{1/2}\left(\frac{\rho_l}{\rho_g Re_g}\right)^{1/4}\frac{1}{\sqrt{We_g}}\left\{1+C_2\left(\frac{b_g}{d_o}\right)^{-1/6}\left(\frac{\rho_l}{\rho_g Re_g}\right)^{-1/12}We_g^{1/6}Oh_l^{2/3}\right\} \quad (3)$$

where, d_o is the nozzle diameter, $\dot{m}_g$ and $\dot{m}_l$ are the gas and liquid mass flow rates, respectively, and Weber, Ohnesorge, and Reynolds numbers are defined as: $We_g = \rho_g(u_g-u_l)^2 d_o/\sigma$, $Oh_l = \mu_l/\sqrt{\rho_l\sigma d_o}$, and $Re_g = b_g\rho_g u_g/\mu_g$, where $b_g$is the thickness of the gas layer that impinges on the liquid. These correlations are selected since they have some theoretical base. In particular, equation (3) uses jet instability models to come up with the form given. The correlation constants are then determined based on a set of experimental results.

None of the spray nozzles can provide satisfactory atomization outcome for the full range of desired viscosities and operating conditions [4]. Therefore, it is important to determine the operating range of each nozzle that results in the desired atomization. For instance, an internally mixed nozzle may result in more ligaments than externally mixed nozzles. This may not be good for drying conditions, since long ligaments may dry quickly before they breakup into droplets.

Many high viscosity liquids also have solid suspensions. Solid particles not only change the effective viscosity of the liquid, but also have added atomization complexity [5]. For instance, larger solid particles may separate from the liquid after atomization resulting in a bimodal droplet size distribution. A correlation for fluids with suspension is given by Mulhem et al. [6] (an IFPRI supported project):

$$SMD = 0.21 d_o Oh_l^{0.0622}\left(\frac{\dot{m}_g}{\dot{m}_l}We_g\right)^{-0.4} \quad (4)$$

And another by Dooher [7]:

$$SMD = \frac{10^4 d_o\sqrt{Oh_g}We_g^{-1.09}}{\sqrt{A_s}} \quad (5)$$

where A_s is the cross sectional area of the spray at the measurement distance from the nozzle.

Inspection of correlations given in equations (2-5) shows a large variation in the exponents of the scaling parameters, We_g, Re_g, and Oh_l. For instance, the coefficients of the We_g are 0.39, 0.4, 0.5, and 1.09, and those of Oh_l are 0.06, 0.5, 0.6, 0.78. This limits each correlation only to the conditions and the fluids that it is developed for.

There are many more studies and correlations for high viscosity liquids using twin fluid nozzles [8-15]. They all indicate that high viscosity liquids generate ligaments that take longer times to breakup or even do not breakup. No study has yet fully characterized the ligaments formed

by polymeric fluids. This is one of the main objectives of the present research. We intend to map different sprays based on ligament sizes (length and diameter), and determined a non-dimensional time and length that it takes for the ligaments to breakup into droplets.

Table 1-Fluid properties tested

Fluid	Viscosity (mPa.s)	Viscosity at the upper shear rate (mPa.s)	Ref.
Xanthan gum + water	30-14,761	1.58-2.82	[2]
Polyacrilamide E10 Polymer +water	2.1-9342	1.2-12.1	[2]
Glycerol+water	1-78	62	[3]
CA-PEG	146	152	[3]
Opadry-HPMC 15% solids	192	133	[3]
Opadry-PVA 20% solid	235	66	[3]
Maltodextrin + water	60-308		[4]

2 Issues and Objectives

Issue I: Currently there are no quantitative spray characteristics on the ligaments and fibers generated close to the nozzle. The literature provides correlations for the average droplet diameter (e.g., SMD) at relatively long distances from the nozzle. The distance has to be long enough that all ligaments and fibers are broken into relatively spherical droplets, so that they can be measured. The literature also shows that high viscosity fluids do not turn into droplets immediately after breakup. The higher the fluid viscosity, the longer it takes for ligaments to breakup, if they breakup at all. This becomes an important issue in spray drying, when the ligaments are exposed to high gas temperature and dried. In such conditions, the ligament and fibers may not have enough time to breakup and the atomization is not completed.

Issue II: The information on the droplet size distribution for the atomization of high viscosity and polymeric liquids is very limited. Although the prior studies measure the droplet size distributions, they mainly report the average size and not the distribution itself. Although, correlations for the average droplet size are useful for design and scaling, they do not provide any information on the size distribution. For instance, a size distribution with a long tail can result in the formation of very large particles, significantly reducing the particle quality.

Issue III: Correlations that provide droplet size information for a large range of nozzle scales are needed. The available correlations are mainly obtained by using a narrow range of nozzles sizes but a wide range of operating conditions. Therefore, they cannot reliably be used for large scale production nozzles and conditions.

Issue IV: Effect of high ambient temperatures, as in the spray dryers, on the evolutionary process of primary and secondary atomization is not available. This information is needed since ligaments may quickly dry before secondary atomization, completely changing the final spray size distribution. The currently available literature on the droplet size distributions are obtained at normal ambient conditions.

Objectives:

I. **Develop a benchmark data set for the near nozzle spray characteristics for high viscosity and polymeric fluids.** Sprays will be characterized based on the size and shape of the ligaments at different distances from the nozzle. Such data would provide information on the evolution of the droplet size distribution and the influence of the secondary atomization on the final droplet sizes. We will
   - develop a comparison map for different nozzles identifying their operating range and limitations in terms of the quality of the atomization, including, near-field droplet and ligament shape and length distributions, and far field droplet size distribution, and
   - determine the characteristic times and distances that takes for ligaments with certain initial characteristics (length, thickness, and fluid properties) to breakup into droplets.
   - A wide range of fluids including some organic solvent systems in conjunction with common spray drying polymers such as HPMC, HPMCAS hypromellose acetate succinate), and PVP-VA (N-vinylpyrrolidone and polyvinylpyrrolidone-co-vinyl acetate), and concentrated aqueous suspensions of Titanium dioxide with varying amounts of a water soluble high molecular weight polymer (such as PVA) will be considered. PVP's have been used as carriers for amorphous solid dispersion formulation of poorly soluble drugs prepared by different methods.

II. **Determine correlations for the nozzle scaling.** We will perform spray characterization at several different scales to identify the governing parameters for proper scaling of the nozzles. We will determine how the nozzle and flow parameters need to be changed for a production scale nozzle to generate the desired droplet size distribution as obtained from the pilot scale nozzle.

III. **Develop correlations for the effect of ambient temperature,** on the droplet size distribution.

3 Proposed Research

3.1 Near Nozzle Spray Characterization

The atomization process of high viscosity fluids is different than those of low viscosity liquids mainly because of two important factors. One, it takes more energy to atomize a high viscosity fluid and the other, it takes a much longer time for the atomized ligaments to become somewhat spherical droplets. These effects are loosely referred to as the primary atomization (for the initial atomization process) and the secondary atomization (for the later breakup of ligaments). For low viscosity liquids, there is basically no secondary atomization, and the ligaments formed are small enough that they quickly become spherical. However, for high viscosity liquids, the ligaments can be very long, and they may stretch to become even longer once they are separated from the core flow, as depicted in Fig. 1. This effect is exasperated for fluids containing polymers.

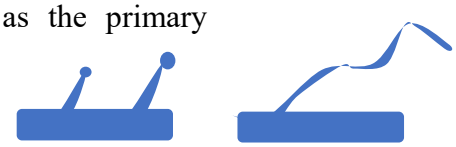

Figure 1- Ligament breakup

Figure 2 [4] shows images of a spray close to two different types of twin-fluid nozzles, and for inlet air pressures of 0.14 and 0.28MPa and gas to liquid ratios of 10% and 20%. The solution is water-maltodextrin-50% at room temperature, resulting in a 308mPa.s. It is observed that the

atomization process generates long filaments close to the nozzle. Such filaments were observed for solutions as low as 40% maltodextrin with viscosity of 60 mPa.s, however, the filaments were thinner [4]. Another observation is that the atomization behavior of the ligaments depends on the nozzle type.

Although, spray images, such as those in Fig. 2 [4] are sporadically available in the literature, none have been quantitatively characterized. One of the objectives of the present research, which distinguishes it from other studies, is that we intend to characterize the primary atomization, i.e., the spray close to the nozzle. Filament sizes (e.g., length, diameter, and shape) will be characterized for different nozzles and operating conditions, and for changes in the elongational and shear viscosities.

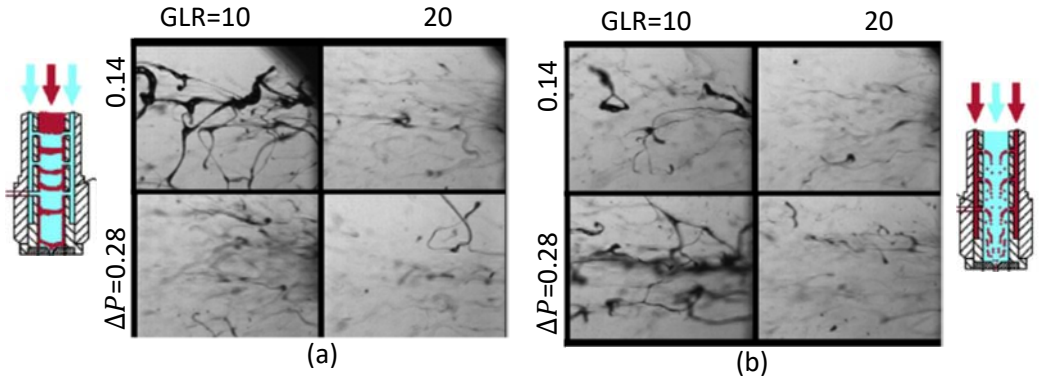

Figure 1- Near-nozzle spray pattern for two different nozzles and for $\mu_l = 308\ mPa.s$ and for different injection pressures (ΔP) and gas to liquid ratios (GLR) [4].

3.2 Droplet Size Distribution

Although most studies that measure and provide correlations for the average droplet size in the spray actual have data for the droplet size distribution, they do not report them. For low viscosity fluids the droplet size distributions curves are mainly similar and authors do not report them to limit redundancy. However, for high viscosity fluids, the size distribution can significantly change from one condition to another.

Figure 3 shows the droplet size distributions for three different water/glycerin mixtures (120, 30, 1.3mPa.s) and at three different distances from the nozzle ($x^* = x/d_o$) [16]. An internal mix twin-fluid nozzle was used in this study. The figure shows bimodal distributions for high viscosity cases. The results also show that close to the nozzle, x^*=17, the large droplet volume fraction is large for the high viscosity solution. This difference shows that the primary atomization for the high viscosity solution is worse than low viscosity solution. As atomization proceeds, fragments break up further and small drops begin to merge. The distribution changes to unimodal when x^*= 50 for two lower viscosities. With a further

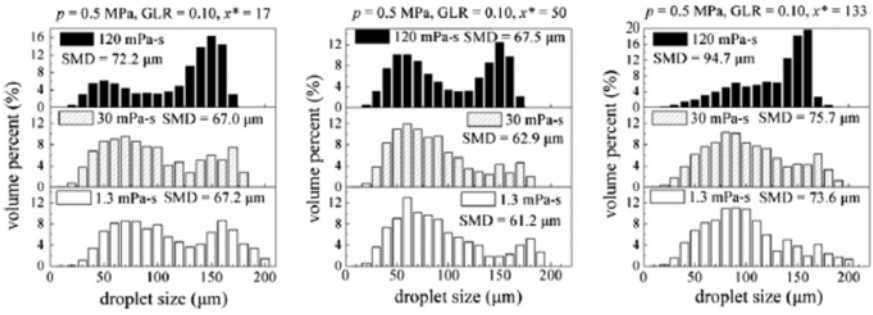

Figure 3- Droplet size distribution for different liquid viscosities and different distances form the nozzle [16].

increase in distance, x^*= 133, right shifts of the peaks are observed, probably due to droplet coalescence. At this distance, the distributions for the two lower viscosities becomes almost unimodal.

Clearly, reporting only the SMD does not provide any of the significant changes that is observed in the spray. Therefore, we intend to measure and report all droplet size distributions across the spray and at different distances from the nozzle. Such data would allow the user to determine whether there are size segregations and significant secondary atomization along the spray axes or if there are many large droplet sizes.

3.3 Droplet Size Correlations

Correlations for droplet sizes for pharmaceutically relevant fluids are very limited. Currently, correlations similar to those given in equations (2-5) are used to scale different nozzles. We intend to develop similar correlations for pharmaceutically relevant fluids. Our correlations will most likely be in the following form:

$$SMD = d_o\left(1+\frac{\dot{m}_g}{\dot{m}_l}\right)\{C_1 We_g^{-a} + C_2 Oh_l^b\} \quad (6)$$

which is shown to include all relevant scaling parameters. Except that we need to provide Oh in terms of relevant viscosity of the solutions. This requires a knowledge of the shear rate at the nozzle so that the fluid viscosity can be estimated. The liquid viscosity (shear and elongational viscosities) will be fully characterized in this study and will be incorporated in the correlations to determined the relationship between the size and viscosity: $SMD \propto \mu_l^n$.

By exploring a broad selection of fluids and operating conditions, we can determine the effects of key non-dimensional parameters (We, Oh, and Re numbers) on the atomization phenomena. In addition, studies with two-fluid nozzles have shown that the spray characteristics depend on the atomization gas to liquid flow rate. This study would help us elucidate the atomization mechanism with changes in the gas to liquid ratios.

3.4 Scaling of a Nozzle

Studies on the utilization of spray drop size correlations in the production scale [e.g., 17] have shown that the correlations do not work for high viscosity fluids, even though they were developed for such fluids at the pilot scale. One explanation for this is that the correlations have not used a wide enough nozzle scales to extrapolate the results to the production scale.

One of the important variables involved in the control of droplet size for a two-fluid nozzle is the mass ratio of atomization gas flow rate to liquid flow rate (GLR). An increase in this ratio should cause a decrease in droplet size. At a critical GLR value the atomization gas reaches its maximum velocity, which is the speed of sound for a convergent nozzle, and subsequent increases in the atomization gas flow rate only increases the atomization gas pressure (density). This will have a much smaller effect on atomization than the atomization gas velocity (i.e., the SMD is constant).

At the lower atomization gas flow rates, the SMD is found to increase with faster liquid flow. At the higher operating gas flows, no difference in SMD is found among the investigated liquid flows. The degree of atomization is determined by the velocity difference between the atomization gas and the liquid. Therefore, the liquid flow rate has lower importance when operating at higher atomization gas flow rates.

The above information is currently used to scale up a nozzle. However, scaling studies [17] have shown that GLR leading to the same droplet size distribution is substantially lower for the production scale nozzle than the pilot scale nozzle. This is attributed to higher atomization gas

velocities for the production scale nozzles when compared to the pilot scale nozzles resulting in smaller droplets for identical atomization gas to liquid flow ratio. Therefore, scaling up just using the GLR is not correct.

We intend to increase the nozzle size until the changes in the GLR can be properly quantified, before reaching the critical conditions for the pilot scale. Then, the knowledge of the droplet size distribution for the pilot scale nozzle in combination with a model can be used to predict nozzle operation conditions resulting in same droplet sizes for a larger nozzle of similar design.

3.5 Effect of Ambient Conditions

If long ligaments and filaments are introduced inside a hot gaseous environment, they may dry before they breakup, resulting in long dried filaments. Therefore, the secondary atomization is needed to breakup these ligaments into small droplets, otherwise, they will remain as such in the flow. One of the main issues with scaling pilot scale tests to production scale is the time requirement for the secondary atomization of the filaments, which may be incorrectly scaled.

We will test different sprays inside a temperature controlled chamber to determine the effect of ambient temperature on the droplet and ligament size distribution. An environmentally controlled chamber, as shown in Fig. 4, already exists in our labs, which can be used for this study.

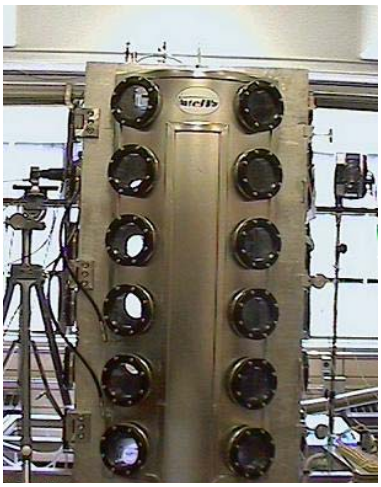

Figure 4- Environmental Chamber

3.6 Measurement Technique

The prior studies have mainly used light scattering techniques to measure the droplet sizes. The commonly used instruments are the Spraytec system by Malvern and PDPA systems by TSI, Dantec, and Artium. These systems cannot properly work if the liquid is the form of long ligaments. An imaging system is a better choice for characterizing such sprays.

We will use an imaging instrument as shown in Fig. 5. This system can generate high intensity flashes at as low as 15 nanoseconds, and can resolve sizes down to 5 microns. An image processing software analyzes the images at a fast rate to determine the particle size and morphology. Particle shapes can be characterized based on their length and thickness which can be used to map different types of sprays.

Figure 5- The spray sizer based on imaging.

4 A detailed outline of the proposed program

1) Testing of twin fluid and swirl nozzles to identify and map the dominant atomization mechanisms for high viscosity and polymeric solutions, and fluid having inorganic

particles. Develop correlations for the characteristic times and distances for which the ligaments formed in the primary atomization form droplets through the secondary atomization (Year One).

2) Development of droplet size distribution and mean droplet size correlations for high viscosity and polymeric solutions, and fluid having inorganic particles (Year Two).
3) Measurement of the variation of the sizes of droplets and ligaments along the axis of the sprays at elevated ambient temperatures to develop models for the secondary atomization of relevant fluids (Year Three).

5 Critical unknowns that may influence the direction/outcome of the project.

Determining a correlation for drop size distribution in terms of rheological properties of the fluid requires a detailed understanding of atomization process that occur near the nozzle. For low viscosity liquids droplets are instantly separated from the liquid core, however, for high viscosity and non-Newtonian liquids fibers and ligaments are formed that later will break into droplets. Therefore, a unified correlation that defines all fluids may not be possible. It may be necessary to identify, categorize and map the spray based on atomization mode and rheological properties.

In addition, the filaments may be too convoluted to be able to measure their lengths. It may be necessary to only categorize the filaments, as long, medium or short, in order to map different types of sprays.

Many spray size distributions follow log-normal distribution pattern. In such cases, it is possible to identify the distribution based on two parameters, mainly mean and standard distribution. However, based on the type of atomization there might be flow conditions that do not necessarily follow a log-normal behavior, namely, multi-mode atomization, where different sizes are produced due to different type of atomization.

6 What will be accomplished: Accomplishments Tasks and goals.

- Selection of the nozzles and identification of the operating conditions.
- Capturing near-field and far-field images of the spray for a range of fluids.
- Identify the atomization regimes for various mixtures and nozzles.
- Obtaining characteristic times and distances for the completion of the secondary atomization.
- Provide droplet size distributions for all operating conditions.
- Compare size distribution of fluids with varying rheological properties.
- Obtain SMD correlations for all the tested conditions with emphasis on the fluid properties and nozzle scaling.

7 How this project could leverage into existing programs in which your research team is engaged

This project can be leveraged to obtain government funds from Canadian research organizations, including NSERC, MITACS, and OCE. These organizations provide 2 to 1 support for any industrial cash grant. In many cases, if the scope of the project is expanded, it is possible to receive funds from two of the above three organizations, making the leverage 4 to 1. Therefore, $38,000 USD annual grant from IFPRI, which is equivalent to $48,640 Canadian dollars, can be increased to $145,920 or possibly to $243,200.

The spray labs at the university of Toronto is equipped with Spraytec instrument by Malvern, PDPA system by TSI, and IPI (interferometric particle imaging) by Dantec, as well as a particle imaging system. Therefore, all spray characterization system are already available and there in no requirement to acquire new systems.

Out lab is also equipped with an environmental chamber to control the ambient temperature and pressure. The chamber is equipped with a set of windows for using instruments from the outside of the chamber, and it is large enough to put instruments inside the chamber for closeup imaging.

8 Indications where IFPRI members could support the program through provision e.g. of model test materials, test methods, industrial experience.

This project will be in close collaboration with the IFPRI members with regular conference calls. We will test fluids of interest to the industry and the operating conditions for their pilot scale and if possible the production scale.

9 References

[1] Masters, K., "Part V. Applications of spray drying in industry", in Spray Drying Handbook, 5th Ed.; Longman Scientific & Technical U.K.: Harlow Essex, England, 1991; 491–680.

[2] Mansour, A. and Chigier, N., "Air blast atomization of non-Newtonian liquids," *Journal of non-Newtonian Fluid Mechanics,* 58, 1995, pp:161-194.

[3] Aliseda, A., E.J. Hopfinger, J.C. Lasheras, D.M. Kremer, A. Berchielli, E.K. Connolly, "Atomization of viscous and non-Newtonian liquids by a coaxial, high-speed gas jet. Experiments and droplet size modeling", International Journal of Multiphase Flow, Volume 34, Issue 2, February 2008, Pages 161-175.

[4] Mlkvik, M., Stähle, P., Schuchmann, H.P., Gaukel, V., Jedelsky, J., Jicha, M., "Twin-fluid atomization of viscous liquids: The effect of atomizer construction on breakup process, spray stability and droplet size," International Journal of Multiphase Flow Volume 77, December 2015, Pages 19-31.

[5] S.Y. Son, K. K. (1998). Effect of coal particle size on coal water slurry atomization. *Atomization and Sprays*, 503-519.

[6] Mulhem, B., Gunther Schulte, Udo Fritsching, "Solid-liquid separation in suspension atomization", Chemical Engineering Science, Volume 61, Issue 8, April 2006, Pages 2582-2589

[7] Dooher, J. P. (2005). Fundamental Considerations for coal slurry atomization . *Atomization and sprays*, 585-602.

[8] U. Fritsching, B. M. (2009). Influence os suspended solid particles on suspension atomization process.

[9] Semiao, V., Pedro Andrade, Maria da Graca Carvalho, Spray characterization: Numerical prediction of Sauter mean diameter and droplet size distribution, Fuel, Volume 75, Issue 15, November 1996, Pages 1707-1714

[10] M. Sacchetti, and M. M. Van Oort. Spray-drying and supercritical fluid particle generation techniques. In A. J. Hickey (ed.), Inhalation Aerosols, Physical and Biological Basis for Therapy, Vol. 94, Lung Biology in Health and Disease, Marcel Dekker, New York, 1996, pp. 337–384.

[11] Bittner, and T. Kissel. Ultrasonic atomization for spray drying a versatile technique for the preparation of protein loaded biodegradable microspheres. J. Microencapsul. 16:325–341 (1999).
[12] B. S. Freitas, H. P. Merkle, and B. Gander. Ultrasonic atomisation into reduced pressure atmosphere—envisaging aseptic spray-drying for microencapsulation. J. Control. Release 95:185–195 (2004).
[13] S.C. Tsai, B. Viers, Airblast atomization of viscous liquids, Fuel 69 (1990) 1412–1419.
[14] S.C. Tsai, K. G. (1991). Air blast atomization of micronized coal slurries using a twin fluid jet atomizer . *Fuel*, 483-490.
[15] L. Zhouhang, W. Yuxin, Y. Hairui, C. Chunrong, Z. Hai, H. Kazuaki, T. Keiji, L. Junfu, Effect of liquid viscosity on atomization in an internal-mixing twin atomizer, Fuel 103 (2013) 486–494.
[16] Li, Z., Wua, Y., Yang, H., Cai, C., Zhang, H., Hashiguchi, K., Takeno, K., Lu, J., "Effect of liquid viscosity on atomization in an internal-mixing twin-fluid atomizer," Fuel 103 (2013) 486–494.
[17] Thybo, P., Hovgaard, L., Anderson, S.K., and Lindelov, J.S., "Droplet size measurement for spray dryer scale-up," Pharmaceutical Development and Technology, 13, 2008, pp: 93-104.

Research Proposal for IFPRI Project 2018-2020

Mapping the spray characteristic within atomization of non-Newtonian liquids and suspensions for spray drying applications

Dr.-Ing. Lydia Achelis and Prof. Dr.-Ing. habil. Udo Fritsching
Particles and Process Engineering, University of Bremen, Bremen, Germany
Leibniz-Institute of Materials Engineering IWT, Bremen

Introduction

The most suitable or ideal spray for spray drying operation contains monodispersed (equally sized) droplets homogeneously spreading at constant concentration (resp. mass flux distribution), a condition that can practically not be achieved. The atomization process of the liquid feed in spray drying delivers a spray of liquid droplets that is characterized by its **spray quality** in terms of drop size distribution (DSD, typically given in terms of some overall mean or characteristic drop size of the distribution) and the **spray homogeneity** (spray shape and / or morphology, spray angle, or more precisely the spatial mass flux distribution). Practical spray drying operations and spray dried products need to address problems of oversized particles (e.g. causing process problems due to sticking within the dryer, or afterwards in the product e.g. the need to be comminuted / milled or grinded in post processing) or undersized particles (dust removal from product or agglomeration necessity for instance by fines return into the dryer atomization zone). Therefore, in order to characterize the atomizer characteristics and process performance in spray drying correctly it is necessary to describe the **shape and the width of the specific drop size distribution** (in terms of distribution moments or characteristic span values) and its spatial variation together with the spray homogeneity.

Spray drying atomization fundamentals regarding nozzle design and operations with respect to the specific fluids to be atomized are important for proper layout of the drying process for specific feed streams [Maj14, Mas02]. The liquid feed in spray drying is to be characterized in terms of its specific **rheological behavior**. Typical fluids to be operated in spray drying are **melts or solutions** (typically at higher viscosities) with Newtonian or non-Newtonian viscosity behavior and **suspensions / slurries or emulsions** with non-Newtonian behavior [Mew12, Wil13]. The rheological liquid behavior directly impacts the disintegration behavior of the feed and thus the spray quality.

Atomizer or nozzle types in spray drying applications are utilizing either potential (pressure), kinetic or centrifugal energy (in rotary atomizers, twin-fluid nozzles, or pressure swirl atomization devices). Thus either jet or sheet fragmentation is found. Choosing the most appropriate nozzle for a specific spray drying task is always challenging. However, typical operation conditions and relations of spray quality and homogeneity can be found in literature and from manufacturers.

Though myriads of investigations can be found in literature that are known to describe the spray quality of specific atomizer configurations (see summaries in: [Lef17, Wal05] a **lag of**

knowledge and data needs to be postulated especially when it comes to scale –up of nozzle systems with respect to:

- industrial scale atomizers (at relevant throughputs)
- spatial (or temporal) variations in the spray characteristics
- inhomogeneous liquids (suspensions, emulsions, ...) and non-Newtonian liquids.

Challenges in experimental spray characterization and spray analysis at these industrially-relevant conditions arise especially from the highly dynamic processes (impeding the identification of disintegration mechanisms) and the high spatial drop densities (dense sprays) that may lead to measurement problems and inaccuracies.

Aims

This proposal and investigation of spray drying atomizers operating with non-Newtonian liquids aims the **derivation of scaling maps and correlations for the basic spray parameters spray quality (DSD) and spray homogeneity (flux)** for the

- Droplet-size-distribution DSD (not just mean size, but also distribution width - in terms of e.g. characteristic deviation, span value, or RRSB parameter)
- local (or spatial) variations in the DSD,
- local spray homogeneity (spray angle and mass flux distribution).

All **relevant types of nozzles systems** and atomizers found in spray drying operations will be addressed throughout the course of the project: **pressure / rotary / twin-fluid**.

The **parameters to be investigated** are reflecting typical conditions in spray drying operations in terms of:

- atomizer or nozzle type (jet or sheet, centrifugal, ...)
- process parameters (throughput, ...)
- liquid parameters (rheology, ...)

The project aims at derivation of scaling and / or comparison maps describing the spray quality and spray homogeneity for typical spray drying nozzle types and operation conditions especially for non-Newtonian liquid feed rheology. The correlations should enable **scaling possibilities for different operational conditions** and principles of atomizer devices.

Critical unknowns / State of the art in atomizer design for spray drying

Characteristics of industrial scale atomizer systems within spray drying applications principally are based on:

- correlations on basic atomizer setups from scientific or technical application literature, typically derived at **labscale devices**
- operational charts and diagrams from atomizer device manufacturers, typically derived for **water as operating liquid**.

The most appropriate nozzle for a specific spray drying task and operation is not easily found. Scaling typically is not possible as mechanism limits are not indicated. Typical operation conditions and spray information can be found in literature and from manufacturers for "simple" fluids only.

Atomization of a liquid stream depends on inherent liquid instabilities and the interaction of the fluid stream with the surrounding gas (at the interface). As a result, liquid fragmentation occurs in different modes depending on liquid and process parameters. Engineering derivations typically summarize these specific modes in mode charts and correlations depending on dimensionless influencing numbers (as Reynolds, Weber, Ohnesorge, Bond, Froude, ...). It is important that specific correlations are only valid within the device and process window and atomization mode where these have been derived for (or the experiments have been done).

Such **mode charts and correlations development for nozzle scale-up** in spray drying are in the core focus of the investigation.

Research program for initial three years

Characterization of non-Newtonian liquid atomization behavior for spray drying applications needs a fundamental approach. Thus the initial phase of the project is devoted to **generic atomization experiments**. In the first instance, the disintegration of (laminar) liquid jets and sheets (from rotary as well as pressure nozzles) is analyzed. Here, individual threads and planar sheets will be investigated and analyzed in basic studies. It is postulated in this context that conventional disintegration charts, scaling laws and drop size correlations need to be extended by one (at minimum) additional parameter (repectively dimensionless number) characterizing the **non-Newtonian behavior of complex liquids resp. suspensions**. Starting from a description of the rhelogical behaviour in a pseudoplastic approach with shear thinning behavior based on the Ostwald/deWaele equation (power law), the exponential factor of shear thinning will be taken as base of the correlation. However, further approaches need to be taken into account. The models to be derived will be transferred to **spray dryer scaled atomization systems** that will be specified and investigated in the course of the project.

Schedule and Milestones

The tentative working program and the intended milestones/deliveries within **the first period (years 1 - 3)** are as follows:

<u>Year 1</u>

Subject: Setup of experimental facility (spray rig) for pressure and centrifugal atomization in lab and industrial scale
Installation of measurement devices for **local** measurements: laser diffraction, light sheet, patternator, high-speed video, ...
Spray and breakup characterization for water based (water/glycerol) liquids

Milestones: Proof of principle for the experimental and measurement systems
Setting up of an evaluation procedure for description of:
- local DSD (mean and width)
- spray homogeneity (mass flux)
- breakup mode

Year 2

Subject: Generic studies of laminar Newtonian and non-Newtonian jets and sheets
Installation and testing large scale atomization systems

Milestones: Disintegration chart for non-Newtonian jets and sheets (pressure and rotary),
Initial formulation of local DSD correlations
Identification of relevant dimensionless parameters for non-Newtonian fragmentation behavior
Creation of break-up mode charts for non-Newtonian liquids and suspensions

Year 3

Subject: Investigating the role of turbulence on jet and sheet breakup in non-Newtonian liquids
Analyzing (some) commercial or equivalent based atomization nozzle systems (at least in 2 different scales)

Milestones: correlations and scaling laws for pressure and centrifugal atomization of non-Newtonian liquid jets and sheets in commercial spray drying application nozzle systems

Outlook onto second period (years 4 to 6):

Topics to be addressed in the second period of the project are mainly on **extension of the program to a broader scope and other nozzle systems** (e.g. twin-fluid) and other rheological feed parameters. The close-up of the investigation to commercial nozzle systems is to be checked. The exact definition of the research program and its parameter to be evaluated is to be defined (in cooperation with IFPRI industrial members) after the first period. Some possible topics for the second period are:

- Other atomization principle: Atomization of non-Newtonian liquids in twin-fluid (gas assisted) nozzle configurations.
- Other feed systems: Evaluating relevant suspension liquids in terms of: particle concentration (Bachelor) and particle shape (thus including Krieger/Doherty and shear hardening behavior)
- Other nozzle system: The relation and relevance of commercial nozzles in spray drying (e.g. GEA/Niro, Spraying Systems, Delavan, BETE, ...) will be screened.
- Other nozzle systems: Evaluating the potential of hybrid atomization systems (e.g. gas assisted pressure swirl) in spray drying applications [Fri12]

Fitting into the PI research portfolio / Preliminary investigations

The research group at the University Bremen investigates multiphase flows and atomization processes of complex liquids with demanding rheological properties within the past 30 years. Here e.g. metal melts (high surface tension) [Fri06, Ach08, Hen17], high-viscosity liquids and melts [Loh02, Czi08], suspensions [Lix11, Mul03, Mul06] and emulsions [San17] among others have been studied. In this context the development of tailored atomization systems has been performed that are described in [Czi08, Fri12]. The atomization process in spray drying and its impact on spray quality and agglomeration processes has been studied [Lit12, Ver04].

Several general overview articles and handbook contributions on atomization and spray systems have been published [Fri06, Fri16, Hen17, Lix17].

The Particles and Process Engineering group at the University Bremen is one of the promoting and inventing institutions for laser diagnostics in sprays and multiphase processes, namely for Phase-Doppler-Anemometry (PDA) [Men03], and in-process spectroscopy [Gil01, Gla15].

Intended IFPRI support within project

This research proposal intends cooperation and proper support of IFPRI member institutions and industrial partners, especially by:

- identification of relevant operational conditions in spray drying
- identification and delivery of typical feed materials for spray drying purposes: suspension particles, commercial and technical liquids, ….
- identification and characterization/description of rheological properties of spray drying relevant liquids
- identification of commercial relevant atomization systems and suppliers

References

General

[Maj14] Majumdar, A.S.: Handbook of Industrial Drying, CRC Press 4th Edition 2014

[Mas02] Masters, K.: Spray Drying in Practice, SprayDryConsult Int. ApS Denmark 2002

[Mew12] Mewis, J.; Wagner, N.: Colloidal Suspension Rheology, Cambridge Univ. Press 2012

[Lef17] Lefebvre, A.; McDonnel, V.: Atomization and Sprays, CRC Press, 2nd Edition 2017

[Wal05] Walzel, P.: Spraying and Atomizing of Liquids, Ullmann´s Encyclopedia of Industrial Chemistry, 2005

[Wil13] Willenbacher, N.; Georgieva, K.: Rheology of Disperse Systems, in: Bröckel, U.; Meier, W.; Wagner, G. (Eds): Product Design and Engineering, Wiley-VCH Verlag GmbH, Weinheim, pp. 7-49 (2013)

Bremen contributions

[Ach08] Achelis, L., Uhlenwinkel, V. "Characterisation of metal powders generated by a pressure-gas-atomizer.", MSE A 477, Volume 477 (Issues 1-2) 15-20 (2008)

[Czi08] Czisch, C; Fritsching, U.: Atomizer design for viscous-melt atomization; Mat. Sci. Engng. A 477 (2008) 1-2, 21-25

[Fri06] Fritsching, U.; Bauckhage, K.: Sprayforming of Metals in: Ullmann´s Encyclopedia of Industrial Chemistry, 7th Edition, 2006 Electronic Release, Wiley VCH, Weinheim 2006

[Fri12] Fritsching, U.; Uhlenwinkel, V.: Hybrid Gas Atomization for Powder Production; In: Kondoh, K. (Ed.): Powder Metallurgy, InTech Publ., March 2012, pp. 99-124

[Fri16] Fritsching, U. (Ed.): Process-Spray: Functional Particles Produced in Spray Processes; Springer Int. Publ. Switzerland (2016)

[Gil01] Gillandt, I.; Fritsching, U.; Bauckhage, K.: Measurement of Phase Interaction in Dispersed Gas / Particle Two Phase Flow; Int. J. Multiphase Flow 27 (2001), 1313 – 1332

[Gla15] Glasse, B.; Riefler, N.; Fritsching, U.: Intercomparison of Numerical Inversion Algorithms for Particle Size Determination of Polystyrene Suspensions Using Spectral Turbidimetry; Journal of Spectroscopy Volume 2015, Article ID 645879

[Hen17] Henein, H.; Uhlenwinkel, V.; Fritsching. U. (Eds.): Metal Spray and Spray Deposition; Springer International Publishing, Switzerland (2017)

[Lit12] Littringer, E.M., Mescher, A., Schroettner, H., Achelis, L., Walzel, P., Urbanetz, N.A. "Spray dried mannitol carrier particles with tailored surface properties - The influence of carrier surface roughness and shape", European Journal of Pharmaceutics and Biopharmaceutics, 82 (1) 194-204 (2012).

[Lix11] Li, X.G.; Heisterüber, L.; Achelis, L.; Uhlenwinkel, V.; Fritsching, U.: Spray Process Modelling in Metal Matrix Composites Powder Production; Atomization and Sprays 21 (2011) 11, 933–948

[Lix17] Li, X.; Fritsching, U.: Spray Systems, In: Multiphase Flow Handbook Second Edition (Eds: Michaelides, E.E.; Crowe, C.T.; Schwarzkopf J.D.); CRC Press - Taylor & Francis Boca Raton 2017, pp. 1091-1250

[Loh02] Lohner, H.; Fritsching, U.; Bauckhage, K.: Melt Atomization by Heated Gases; ILASS-Europe 2002, Zaragoza, Spanien, 9-11 September 2002, Proceedings

[Men03] Menn, P.; Schulte, G.; Fritsching, U.: Phasen-Doppler-Anemometrie bei Zerstäubung von Prozessfluiden in der Sprühtrocknung, GALA Laser Anemometry 2003

[Mul03] Mulhem, B.; Fritsching, U.; Schulte, G.; Bauckhage, K.: Effect of Solid Particle Characteristics on Suspension Atomization; Atomization and Sprays 13 (2003) 2&3, pp. 321-343

[Mul 06] Mulhem, B.; Schulte, G.; Fritsching, U.: Solid-liquid separation in suspension atomization, Chem. Eng. Sci. 61 (2006) 8, 2582-2589

[San17] Sander, S.; Tischler, C.; Achelis, L.; Henein, H.; Fritsching, U.: Production of Polymer Microparticles by Electrospray Atomization; Atomization and Sprays, 27(5): 457–464 (2017)

[Ver04] Verdurmen, R.E.M.; Menn, P.; Ritzert, J.; Blei, S.; Nhumaio, G.C.S.; Sonne Sørensen, T.; Gunsing, M.; Straatsma, J.; Verschueren, M.; Sibeijn, M.; Schulte, G.; Fritsching, U.; Bauckhage, K.; Tropea, C.; Sommerfeld, M.; Watkins, A.P.; Yule, A.J.; Schønfeldt, H.: Simulation of Agglomeration in Spray Drying Installations: The EDECAD Project; Drying Technology 22 (2004) 6, S. 1403-1461

UFri / LA 24.04.18

IFPRI Atomization Proposal

Udo Fritsching to me, achelis Apr 24

Dear Jim,

please find attached the more specified and revised research proposal from Bremen.

Some remarks to your requests:

- Suspensions are in the very focus of the project. This has been done before by including suspensions in the term "complex liquids with non-Newtonian" behaviour. However, as this term seems the cause of some misunderstanding we now explicitely included the target of the project as "compex liquids and suspensions".

- Same holds for nozzle scale-up. The point has been more explicitely addressed in the revised proposal.

- The project is outlined for analysis of spray drying operations with all relevant nozzle types, namely: pressure, rotary and twin-fluid. However, in our opinion, the project clearly would be overloaded when such a broad scope of nozzles will be handled in parallel. Thus the outline of the project intends two different nozzle systems in the first period (year 1 - 3) of the project and extending the scope in years 4 - 6 to a greater number of nozzle systems. We feel that otherwise the project would explode. Details of nozzle specifications and ranks of nozzle systems may be done during the start of the project in discussion with the IFPRI members.

Best regards from Bremen
We hope to cooperate with IFPRI in future on this project.
Udo

PS: Unfortunately I cannot attand the WCPT 2018 in Florida. I wish you a nice meeting and excellent discussions.

…

--

Prof. Dr.-Ing. habil. Udo Fritsching

Leibniz-Institut für Werkstofforientierte Technolgien - IWT
Hauptabteilung Verfahrenstechnik

Fachgebiet Mechanische Verfahrenstechnik / Fachbereich Produktionstechnik
Universität Bremen

Badgasteiner Str. 3
28359 Bremen

phone: +49 - 421 - 218 - 51230
fax: +49 - 421 - 218 - 9851230

ufri@iwt.uni-bremen.de
www.iwt-bremen.de\vt\mps

IFPRI Research Project Brief

Adhesion of Powders to Metal Surfaces During Compaction

The International Fine Particle Research Institute (IFPRI) wishes to fund a research project to develop fundamental understanding and predictive relationships between a powder's physical and chemical properties and its propensity to adhere to metal surfaces of compaction tooling. The project should include the following elements:

- Identification of appropriate test powders and characterization of their relevant physical and chemical properties. Note that IFPRI is comprised of member companies from many industry sectors, so the choice of powder should not be constrained to those of pharmaceutical interest. Powders of interest range in mean particle size from 5 to 500 microns.

- Establishment of a test method to quantify material adhesion on compaction tooling over an industrially relevant range of process and environmental conditions

- Identification of key factors affecting the amount and/or rate of powder adhesion on compaction tooling such as:
    - molecular, crystal, surface, and mechanical properties of the powder
    - surface finish and chemistry (including coated surfaces)
    - process conditions (e.g. pressure/stress)
    - environmental conditions (temperature, relative humidity)

- Establish predictive criteria for the propensity of adhesion given a set of molecular/crystal properties and process/environmental conditions

Adhesion of powders to metal surfaces during compaction

IFPRI Research Project Proposal (revised)

Dr. Csaba Sinka

Department of Engineering, University of Leicester, UK

ics4@le.ac.uk

30 April 2018

Adhesion of powders to metal surfaces during compaction (referred to as "sticking") is a significant problem in powder pressing sectors including pharmaceuticals, food, detergents, batteries etc. Sticking is difficult to predict in early stage of product formulation and process development and usually manifests during full production scale where high productivity machines such as rotary tablet presses are used. The remedy consists of stopping production, remove, clean, reassemble tooling and continue processing until the material builds up on the tooling surfaces again. In pharmaceuticals it is believed that 25% of solid dosage forms are affected by sticking.

Review of state of the art research on sticking

Empirical research on sticking reported in the literature include observations and mitigating procedures based mostly on lubrication of the powder and/or change of surface finish of the tooling. Toyoshima et al. (1988) correlated sticking tendency with the surface roughness of the tablets and alleviated sticking by lubrication. Bakar et al. (2007) characterised sticking by measuring the damaged area on the surface of the tablet and used granulation to mitigate the problem. Reed et al. (2015) used different tools on a rotary press at the same time and evaluated the sticking tendency visually. Mullarney et al. (2012) assessed tablet-sticking propensity by weighing the powder accumulated on a removable punch tip. They observed that increasing internal lubrication increased sticking for ibuprofen but decreased sticking for mannitol. Roberts et al. (2014) confirmed that increasing lubrication increased sticking of ibuprofen but noted stearic acid didn't. McDermott et al. (2011) examined sticking using electron microscopy and X-ray diffraction mapping and observed that increased solid fraction and increased lubricant concentration led to decreased sticking tendency. Waimer et al. (1999) developed an instrumented upper punch to measure the adhesion force to the top of the tablet. Hamid and Betz (2012) associated sticking with high radial stress transmitted to the die wall. Simmons and Gierer (2012) reported empirical observations using a number of punches, Wang et al. (2015) related sticking to surface roughness while Uchimoto et al. (2013) related sticking to punch surface roughness.

Research on sticking, however, is not limited to empirical observations. Wang et al. (2003) used molecular simulations and atomic force microscopy to determine the work of adhesion and linked this information with bulk scale compaction experiments (Wang et al. 2004). A project 'Tabletting Science Anti-stick Research' project (TSAR) involving a UK pharmaceutical punch manufacturer and academic partners used punch profilometry, contact angle, atomic force microscopy (to determine surface energy and adhesion force), scanning electron microscopy and spectrospy to develop a model to help choose punch material and coating for a given formulation. Markarian (2013) describes an adhesion map which included input from discrete element modelling. In summary, the research above identified the following potential factors affecting sticking: Van der Waals forces, capillary action, morphology

(surface roughness), deformation mechanics of the granule, environment (humidity), chemistry. Sticking is related to competing mechanisms between interparticle bonding and particle-wall adhesion.

Research on sticking published in 2017 continues along the same lines, and some basic ideas linked to mechanistic models emerge, which are consistent with our hypotheses developed independently (described later). Paul et al. (2017) measured the mass of powder adhering to a punch during successive compaction events and fitted the data with a classic chemical reaction rate equation leading to a conceptual model for sticking while still requires linking parameters to underlying sticking mechanism. Tsosie et al. (2017) used electron microscopy observations and identified that material not only sticks to tool surfaces but can also be removed during compaction. They proposed a mechanism for sticking which includes fragmentation at the interface of the tooling. Jasevičius and Kruggel-Emden (2017) applied discrete element modelling and an adhesive contact law to analyse the sticking of bacteria to glass; this framework is also relevant to this proposal. Samiei et al. (2017) links sticking to electrostatic properties of the powders, which can be considered as a special case of contact law. Empirically, Al-Karawi et al. (2017) looked at powder lubrication and tool coating while Swaminathan et al. (2017) reported on the use of an instrumented punch to evaluate sticking.

An engineering analysis relevant to sticking

Before a suitable research methodology for sticking could be constructed it is instructive to reduce the problem to its essential features and consider a mechanical engineering analysis to identify potential sticking mechanisms.

At 10 mm (tablet) scale: the contact between two bodies is generally described by normal and tangential interactions. Normal interaction involves contact pressure and adhesion forces. These are influenced by the constitutive behaviour of the bulk powder (including elasticity, plasticity and densification), while adhesion can be considered using classical cohesive zone models. Tangential interaction (e.g. friction) can be described by the coefficient of friction (which may depend on contact pressure, sliding velocity and surface properties such as roughness, contamination treatment etc.). The build-up of material on the tool faces during successive compaction events will result in an evolution of the interface properties (friction and adhesion).

At 1 mm (embossing) scale: sticking can be triggered in regions where features (grooves for letters and symbols) are present on the punch faces. Mechanisms of adhesion and friction aided interlocking are present at this scale also but the geometric details became important for the compaction stage as well as unloading. A model at this scale should include the mechanical deformation of the steel punch. This mechanical interlocking can be present at tablet scale too (e.g. deep punch curvatures).

At 0.1 mm (granule) scale: contact laws developed in the field of contact mechanics provide a detailed description of the complex mechanical pressure distributions and adhesive forces acting between two particles in contact or a particle and a metal surface (adhesive models such as JKR, DMT etc. are extensively used). This is further complicated by the breakage of granules during compaction; important for sticking are the processes at granule - tool interface. Lubricants affect local friction and adhesion. The granule breakage results in new surfaces which behave according to the lubricant admixing method (intra-granular or during granulation vs. extra-granular, where a thin coating is thought to be forming on the outer surface of the granule during lubrication just before compression).

At angstrom (10^{-10} m), or atomic scale: The interaction between atoms is governed by force fields (e.g. Lennard-Jones type potentials). This is complicated by the anisotropy of the crystal and presence of functional groups attached to the surface.

A preliminary thermo-mechanical analysis of the powder-tool interface was carried out in order to provide insight into sticking mechanisms and help identifying the material characterisation requirements and experimental device development. Sticking is a problem inherent to compaction,

thus detailed knowledge of stress and deformation is necessary between tooling and particles as well as bulk level.

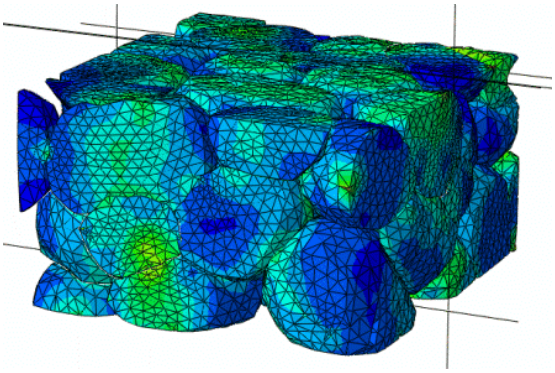

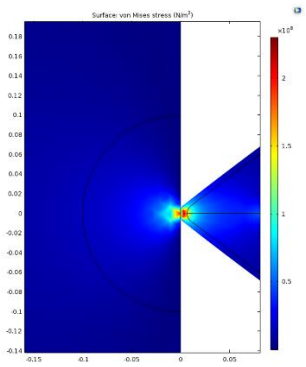

Heat is generated by 1) densification work and 2) friction between powder and tooling during compaction. Heat is transferred between the tooling and powder and influences adhesion, friction and the mechanical properties of the particles. The multi-particle finite element method (see figure on the left) was used to resolve the rearrangement of particles (leading to changing contact areas and contact stress between particles and tooling), and the deformation of the particles (flattening of features of irregular particles subject to high contact stresses), exposing of fresh, high energy surfaces by fracture. This analysis also provided realistic stress states in a particle next to the tooling to enable detailed analysis of an interaction of a single asperity with the tooling wall (see figure on the right). This analysis provides input into formulating hypotheses for sticking and developing material characterisation requirements detailed below.

Sticking hypotheses and critical unknowns

1. Sticking can be understood as a coupled thermo-mechanical problem which involves mechanisms such as particle rearrangement, elastic deformation, plastic deformation and/or breakage, which in turn lead to further rearrangement. Relevant to sticking are the detailed processes occurring at the interface between particles and tooling, usually made of stainless steel. The interaction between particles and tooling requires consideration of friction and adhesion. Powder compaction involves dissipative processes that generate heat. At the tool interface heat is also generated due to friction. As sticking (gradual deposition of the material to surfaces) progresses the properties of the materials and surfaces evolve:
    a. Stress, strain rates, and temperature causes phase transformations, particularly in materials with low melting points.
    b. Contact areas of deforming particles increase, exposing new pristine surfaces
    c. Particle breakage exposes new pristine surfaces with high surface energy

Unknowns: what are these properties and how do they evolve?

2. Sticking can be understood as a balance between material deposition on the surface and material removal (similar to wear as the powder itself continues to slide along the surface during compaction). The formulation can include abrasive components.

Unknowns: what are the rates and how are the parameters are related to mechanisms?

3. Sticking often initiates at small geometric features (embossing) of the tooling, which requires consideration of the elastic deformation of the punch subject to pressure from powder during compaction.

Unknowns: geometric effects of embossing on compaction

4. There may exist high energy hot-spots on the surface of the metal tooling and on the surface of particles. Unknowns: origin and activation of these sites.

5. Sticking is linked to segregation during die fill, resulting in a non-homogeneous powder blend before compaction. Unknowns: segregation patterns during die fill.

Project planning

WP1: Identification of test materials and characterisation procedures following consultation with IFPRI members covering the industries of interest. These measurements will provide input into testing of the hypothesis above. The testing methods will be standard and available at Leicester and industrial partners, leveraging existing programmes and capabilities (months 1-6).

WP2: Characterisation of single component materials and surfaces. The following material methods are proposed to characterise single particle properties: a) mechanical properties using nano-indentation (Young's modulus, Poisson's ratio, yield stress and strain hardening), b) thermal properties (heat capacity, thermal conductivity and heat transfer coefficients across the powder-tooling interface) and c) surface energy. Some of these data are already available from previous work or from the industrial partners. This work package will standardise the characterisation methodology and characterise the materials of interest from WP1 for which there is no data available. Metal surfaces will be characterised in terms of a) surface roughness (using a profilometer), b) chemical composition (using XRD) and c) surface energy (using AFM), (months 3-12 and 24-30).

WP3: Development of an apparatus to characterise sticking at particle scale: a micromanipulator will be designed to work in an environmental SEM to study the interaction between a single particle and a range of target metal surfaces. The system will include a resistive element to control the temperature of the metal substrate up to 100 °C. The facility will provide direct observation of and control over the conditions where sticking will take place, including contact pressure, sliding velocity, and temperature of substrate (months 6-18).

WP4: Development of apparatus to characterise sticking of multi-component mixtures at bulk scale:

1) heated die and punch system: expertise with designing dies instrumented with radial stress sensors for pharmaceutical powder compaction research will be used to develop a heated die system to study the sticking behaviour of formulations to dies and punches. The heated die will be integrated into a general purpose mechanical testing machine and used to study temperature dependent sticking at compaction rates up to 50 mm/min. A series of punches with different geometric features will be made to study the effect of embossing geometry. The tips will be integrated in a purpose built punch with a local resistive element to control the temperature at the tip (months 6-18)

2) rotary friction system to study the sticking behaviour over time: a load adjustable anvil will be used to press a powder compact of a given composition against a rotary base with adjustable speed. Tool materials will be used similar to the other proposed systems. The heat produced as the tablet slides against the plate will be monitored using thermocouples and the sticking behaviour will be observed over time (months 6-18).

Note: In the second stage of the project (years 3-6) the heated die and punch design will be implemented on a rotary tablet press to characterise sticking at production rates and over time.

WP5: Establish predictive criteria for sticking propensity. The three experimental rigs develop in WP3-4 will be used to identify sticking mechanisms and verify the hypotheses. The facilities developed will discern effects from: molecular, crystal, surface, and mechanical properties of the powder; surface finish and chemistry (including coated surfaces); and will apply representative stress at the interface between powder and tooling at macroscopic (compact) and microscopic (particle) level. A range of powders, surfaces and formulations will be characterised and functional relationships will be developed to predict sticking propensity for a new powder or formulation against tooling made from materials and finishes used in tabletting operations. During the compaction process the material properties, friction and adhesion change with temperature, which are Characterised in WP2. The combinations favourable

for material sticking will be identified in terms of 1) material properties (elastic, plastic, fracture), 2) particle-surface interactions laws (adhesion in normal direction and friction in tangential direction) and 3) processing conditions (stress, strain rate) prevailing at the interface between powder bed and surface. The functional relationships for sticking will be incorporated into a software tool with a hierarchical input structure to predict sticking using 1) particle characteristics and 2) formulation composition. **Deliverable**: predictive software tool for practical use (months 12-36).

Leveraging into existing programmes

A dedicated PhD student will carry out the work packages and will lead the investigations in all areas. The PhD student will be embedded in my group of 5 PhD students who working on the following topics:

- Understanding densification and crack propagation in pharmaceutical tablet manufacturing (provides support to verifying hypothesis 3).
- Influence of contact strength between particles on the constitutive law for powder compaction (provides support to verifying hypothesis 4)
- Modelling of solid-solid and air-solid interactions for particulate handling and processing (provides support to verifying hypothesis 5)
- Swelling and disintegration of multi-component polymeric structures
- Single particle drying mechanisms

The group owns bespoke facilities to characterise compaction, powder flow, and mechanical behaviour in general at all length scales described above. The PhD student will also benefit from the outputs from final year undergraduate and Masters level projects on sticking which produced feasibility work leading to some of the hypotheses proposed above.

The experiments will be performed in the Mechanics of Materials Laboratory (Department of Engineering) and the Advanced Electron Microscopy Centre (College of Science and Engineering), both free at point of use (excluding consumables). We anticipate that IFPRI partners will contribute their publically available data and share their industrial experience to guide the programme. We have strong collaboration with other institutions to cover characterisation needs.

The project will be leveraged with the EPSRC (UK research council) project EP/N025261/1 “Virtual Formulation Laboratory (VFL) for prediction and optimisation of manufacturability of advanced solids based formulations”. The project runs until 2020 and involves 2 post-doctoral research associates (PDRAs) at Leicester and 3 PDRAs based in Chemical Engineering Departments at Leeds, Imperial and Greenwich. VFL is low TRL project addressing flow, segregation, compaction and caking. The VFL philosophy for addressing these 4 manufacturing problems was considered in developing this proposal to address the problem of sticking.

References

Abdel-Hamid S. and Betz G. 2012. A novel tool for the prediction of tablet sticking during high speed compaction. *Pharmaceutical Development and Technology*, 17 (6), 747–754.

Abu Bakar N.F., Mujumdar A., Urabe S., Takano K., Nishii K., Horio M. 2007. Improvement of sticking tendency of granules during tabletting process by pressure swing granulation. *Powder Technology*, 176, 137-147.

Al-Karawi C., Lukášová I., Sakmann A., Leopold C.S. 2017. Novel aspects on the direct compaction of ibuprofen with special focus on sticking. *Powder Technology*, 317, 370-380.

Bunker M., Zhang J., Blanchard R., and Roberts C.J. 2011. Characterising the surface adhesive behavior of tablet tooling components by atomic force microscopy. *Drug Development and Industrial Pharmacy*, 1–11.

I Holland Limited. 2014. Solving Tablet-Sticking Problems with I Holland's Predictive Model. P*harmatech*.

Jasevičius R., Kruggel-Emden H. 2017. Numerical modelling of the sticking process of a S. aureus bacterium. *International Journal of Adhesion and Adhesives*, 77, 15-28.

Markarian J. 2013. Tablet-Sticking Solutions. Screening methods and predictive models address tenacious tablet-sticking problems. *Pharmaceutical Technology,* 37 (10).

McDermott T.S., Farrenkopf J., Hlinak A., Neilly J.P., Sauer D. 2011. A material sparing method for quantitatively measuring tablet sticking. *Powder Technology*, 212 (1), 240-252.

Mullarney M.P., MacDonald B.C., Hutchins A. 2012. Assessing tablet-sticking propensity, by weighing accumulated powder on a removable punch tip. *Pharmaceutical Technology*. 36 (1), 57-62.

Paul S., Taylor L.J., Murphy B., Krzyzaniak J.F., Dawson N., Mullarney M.P., Meenan P., C.C. Sun C.C. 2017. Powder properties and compaction parameters that influence punch sticking propensity of pharmaceuticals, *International Journal of Pharmaceutics*, 521 (1–2), 374-383.

Reed K., Davies C., Kelly K. 2015. Tablet sticking: Using a 'compression toolbox' to assess multiple tooling coatings options. *Powder Technology*, 285, 103-109.

Roberts M., Ford J.L., MacLeod G.S., Fell J.T., Smith G.W., Rowe P.H., Days A.M. 2004. Effect of lubricant type and concentration on the punch tip adherence of model ibuprofen formulations. *Journal of Pharmacy and Pharmacology*, 56 (3), 299-305.

Samiei L., Kelly K., Taylor L., Forbes B., Collins E., Rowland M. 2017. The influence of electrostatic properties on the punch sticking propensity of pharmaceutical blends. *Powder Technology*, 305, 509-517.

Simmons D.M. and Gierer D.S. 2012. A material sparing test to predict punch sticking during formulation development. *Drug Development and Industrial Pharmacy*, 38 (9), 1054–1060.

Swaminathan S., Ramey B., Hilden J., Wassgren C., 2017 Characterizing the powder punch-face adhesive interaction during the unloading phase of powder compaction. *Powder Technology*, 315, 410-421.

Toyoshima K., Yasumura M., Ohnishi N. and Ueda Y. 1988. Quantitative evaluation of tablet sticking by surface roughness. *International Journal of Pharmaceutics*, 46, 211-215.

Tsosie H., Thomas J., Strong J. et al. 2017. Scanning Electron Microscope Observations of Powder Sticking on Punches during a Limited Number (N < 5) of Compactions of Acetylsalicylic Acid. *Pharm Res* 34, 2012.

Uchimoto T., Iwao Y., Yamamoto T., Sawaguchi K., Moriuchic T., Noguchi S., Itai S. 2013. Newly developed surface modification punches treated with alloying techniques reduce sticking during the manufacture of ibuprofen tablets. *International Journal of Pharmaceutics,* 441, 128– 134.

Waimer F., Krumme M., Danz P., Tenter U., Schmidt P.C. 1999. A novel method for the detection of sticking of tablets. *Pharmaceutical Development and Technology*, 4 (3), 359-367.

Wang J.J., Guillot M.A. T, Bateman S.D., Morris K.R. 2004. Modeling of Adhesion in Tablet Compression. II. Compaction Studies Using a Compaction Simulator and an Instrumented Tablet Press. *Journal of Pharmaceutical Sciences*, 93, 407–417.

Wang J.J., Li T., Bateman S.D., Erck R., Morris K.R. 2003. Modeling of Adhesion in Tablet Compression—I. Atomic Force Microscopy and Molecular Simulation. *Journal of Pharmaceutical Sciences*, 92, 798–814.

Wang Z., Shah U.V., Olusanmi D., Narang A.S., Hussain M.A., Gamble J.F., Tobyn M.J., Heng J.Y.Y. 2015. Measuring the sticking of mefenamic acid powders on stainless steel surface. *International Journal of Pharmaceutics*, 496, 407–413.

Adhesion of Powders to Metal Surfaces During Compaction

Changquan Calvin Sun, Ph.D.

Pharmaceutical Materials Science and Engineering Laboratory

Department of Pharmaceutics, University of Minnesota

Original submission: October 30, 2017

Second submission: April 30, 2018

308 Harvard Street S.E., 9-127B WDH, Minneapolis, MN 55455, USA

Email: sunx0053@umn.edu; Tel: 612-624-3722; Fax: 612-626-2125

Introduction and Background

Powder adhesion onto tooling, known as punch sticking, is a common problem in cold welding processes to manufacture compacts from powders of pharmaceutical, metallurgy, and energy materials. Without being properly addressed, it can result in significant problems in manufacturing. Punch sticking requires intermittent stoppage of the tableting process to clean the punch sets, which grossly reduces production efficiency. In addition to poor aesthetic quality, inconsistent weight will lead to rejection of an entire batch of compacts in severe cases. Tooling can also be damaged leading to costly down time. The punch sticking phenomenon is a complex problem, known to be affected by process conditions (compaction pressure, dwell time)[1-3], particle properties (size, shape, surface roughness, surface energy, deformability) [4-8], environmental factors (humidity, temperature) [9, 10], formulation composition [11], and punch tip properties (coating, surface asperity and roughness) [12, 13]. Punch sticking has been investigated using several techniques, including atomic force microscopy to quantify adhesion [14, 15], measuring tablet detachment force [7], scanning electron microscopy [16], HPLC analysis of quantitatively extracted adhering mass [11, 17, 18], and monitoring weight of sticking mass using a punch with a removable punch tip [19].

The removable punch tip method is a material-sparing method capable of generating data for quantitatively assessing punch sticking kinetics. In this experimental approach, the material of interest is blended with a non-sticking matrix material, e.g., microcrystalline cellulose. The mixture is then compressed under a controlled pressure and speed. The amount of material adhering to the punch tip is measured periodically to obtain the adhering mass – number of compression data, which quantifies punch sticking kinetics. It is suitable for rank ordering sticking propensity of compounds as well as different batches of the same compound. For example, the generated data can be used to characterize different batches of a drug, which helps flag potential sticking problems during manufacturing due to batch-to-batch variations.

Using the removable punch tip technique, we have quantified the punch sticking propensity of a large number of pharmaceutical materials by tracking the kinetics of mass accumulation during compression [20]. The role of various factors on punch sticking, such as compaction force, drug surface area, drug mechanical properties have also been investigated [4, 6, 21]. Our studies led to a punch sticking model (Figure 1) [20].

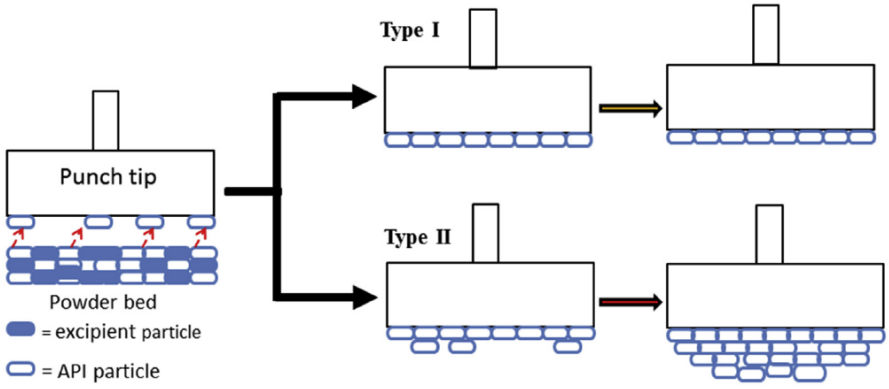

Figure 1. Schematic representation of the punch sticking kinetics based on interactive forces.

To apply this model, the formulated powder is considered to be a mixture between a main component (such as a drug or fine iron ore), **A**, and a matrix. This model predicts punch sticking outcome based on the interplay among three competing forces, i.e., F1 (**A**-punch adhesion), F2 (**A**-**A** cohesion), and F3 (**A**-matrix adhesion). Punch sticking is avoided if F1 is lower than F2 and F3, but sticking occurs when F1 is greater than F2 and F3. When a monolayer of sticking mass is present on punch surface, F1 has no further role in controlling the sticking kinetics. Instead, the relative magnitude of F2 and F3 determines the kinetics of subsequent mass build-up. Only a monolayer of sticking mass (or filming) is expected when F2 < F3, but continued build-up of material is expected when F2 ≥ F3.

This model is consistent with several known features of punch sticking, including a) APIs are enriched in the punch adhered mass [20]; b) mechanical properties and particle size impact sticking propensity [6]; and c) tooling construction materials can influence punch sticking by the same powder [8]. This model suggests the possibility of modulating sticking propensity by controlling the magnitude of F2 and F3. While F2 is constant for a given batch of **A**, punch sticking propensity can be minimized by elevating F3 through appropriate selection of excipients in a formulation. For example, simply choosing a binder that exhibits higher F3 should reduce sticking severity. The model was supported by our recent work where two model drugs, Celecoxib and ibuprofen, were studied in four excipient matrices (Microcrystalline cellulose Avicel PH102 and Avicel PH105, hypromellose, and starch). Punch sticking indeed decreased with increasing F3 for both drugs and at both compaction pressures investigated (Figure 2).[22]

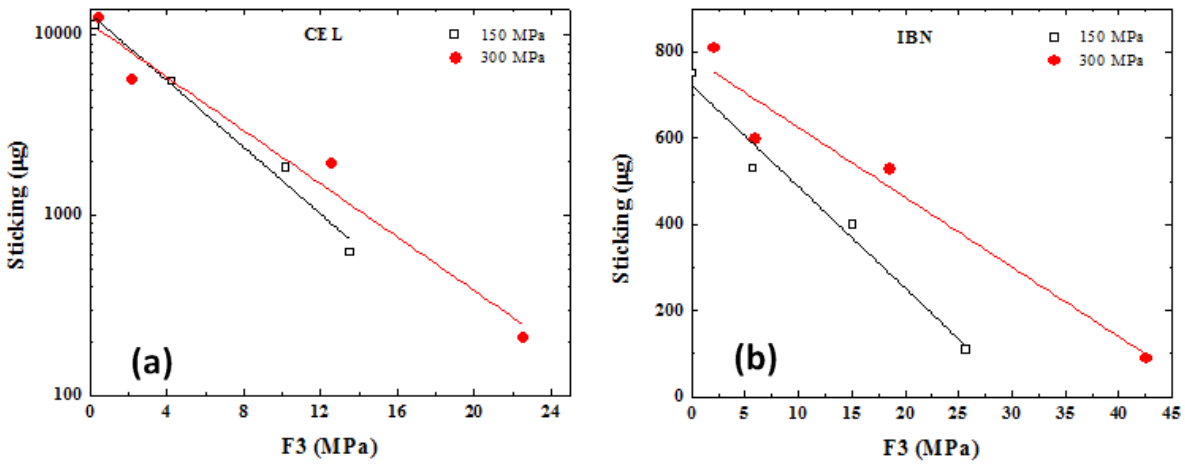

Figure 2. Dependence of sticking on F3 for (a) celecoxib and (b) ibuprofen. Tableting was performed at two pressures, 150 MPa and 300 MPa.

Despite the extensive earlier efforts, a mechanistic understanding of punch sticking phenomenon remains elusive. Systematic further investigation of this phenomenon is required to elucidate the punch sticking mechanism, which is critical for effective formulation design or process engineering. The goal of following research is to ultimately eliminate punch sticking problems during manufacturing.

Research Plan

Although useful in rank ordering sticking propensity among different powders, the removable punch tip method faces two problems for broad adoption for reliably predicting sticking behavior during manufacturing: 1) only flat punch surface has been used, which is different from real punch tips having curvature and embossed letters and numbers. 2) an absence of correlation between data from the removable punch tip study and sticking propensity during actual manufacturing. Therefore, the first stage of this research is to develop an improved removal tip method for reliable prediction of punch sticking that can be applied over any desired compaction pressure and environment conditions using a compaction simulator. In the following experiments, a total of 100 tablets will be compressed and the weight of adhered mass will be measured every 20 compression. During the entire project, environmental conditions will be monitored and controlled, if needed, by humidifying or de-humidifying an isolated space that houses the instruments. All samples will be equilibrated under controlled relative humidity (RH) in suitable RH chambers. For a selected model compound, effects of RH on punch sticking will be assessed. Compaction pressure has been shown to influence punch sticking in the published work, including those by us. As a standard practice in our work, punch sticking propensity experiments for each formulation will be performed at two pressures, 150 MPa and 300 MPa, which cover the typical range of pressure during commercial tablet manufacturing. For different drugs in the same matrix, tablet solid fraction (or porosity) may slightly differ. The use of two pressures also allows interpolation of sticking data to a common solid fraction for different drugs.

Goal #1. Optimize the design of removable punch tip for conducting laboratory punch sticking assessment. In this part of the research, punch tips with different curvatures and embossed with selected letters and numbers will be compared. The hypothesis is that such tips are more sensitive in detecting punch sticking. Using such tips, future punch sticking assessments can be performed more quickly and reliably using less material. Punch tips will be prepared using standard tool steel, with and without embossed letters and numbers (O, A, R, 0, 6, 8, 9). Along with monitoring the amount of adhering mass, the locations of punch sticking will be documented by microscopic images. Three powders (exhibiting low, medium, and severe punch sticking propensity) will be used. Based on the results, tips with different curvatures will be made and evaluated to identify the most sensitive tip design for use in subsequent studies.

Goal #2. Establish a calibrated scale that allows reliable predictions of punch sticking during manufacturing from the laboratory assessments using the optimized tip. Meeting this goal requires the use of 6 - 10 powders with known punch sticking propensity during manufacturing. The comparison of laboratory punch sticking data to the known sticking propensity will lead to a calibrated scale, which can be used to reliably predict sticking propensity during commercial manufacturing based on laboratory assessment using the removable punch tip method. A critical unknown is the availability of sufficient quantity of powders (estimated 500 g) with well documented punch sticking propensity during commercial manufacturing and details on punch design and construction material. If such desired powders or information are not available from the

IFPRI members, we will prepare different model formulations in sufficient quantity and assess their punch sticking propensity using a standard concave tooling on a laboratory rotary press (Piccola). We will assess their punch sticking propensity in parallel using the optimized tooling identified in Goal #1.

Goal #3. Examine effects of tooling material and coating on punch sticking propensity. When punch sticking problems are discovered in a late stage of development, modifying formulation is rarely an option due to the high costs. In those cases, a common solution is to reduce punch adhesion using different tooling steels or coating. Here, we will compare sticking propensity of three model formulations (low, intermediate, and high sticking propensity) on three types of steel and three coatings as summarized in the table below.

Variable	**Options**		
Steel type	S7	D2	M340
Coating	Hard chrome	chromium nitride (CrN)	titanium nitride (TiN)

The PI has secured full commitment from Natoli Engineering to support this project by providing all needed tooling (punch and tips) manufactured with different materials and coating types. An engineer from Natoli will also be dedicated as a consultant on all tooling related issues or problems. There are no foreseeable critical unknowns that may influence the outcome of the project.

Goal #4. Determine effects of particle size on punch sticking. API particle size may change during the course of drug development or commercial manufacturing, for example, due to optimization of crystallization process for higher yield and purity or due to milling to enhance dissolution rate. This factor is known to have an impact on punch sticking propensity but further mechanistic understanding is needed. The conventional wisdom suggests that smaller particles always correspond to more severe sticking because of larger surface area that can be in contact with punch face. However, our preliminary work suggested this notion is not always correct. We hypothesize that very fine API particles can form large agglomerates, which actually lower its area of contact with punch face. Here, we will study the effect of size using four model drugs, exhibiting a range of mechanical properties (brittle to ductile) and sticking propensity (medium to high). Each model drug will be obtained in four different size fractions through recrystallization, milling, and sieving. Different sizes of hematite (0.005 – 1 mm), obtained commercially, will also be evaluated. Punch sticking propensity will be assessed for each of the sizes and correlated to particle size to develop a general rule. If needed, more model compounds will be investigated to ensure robustness of the proposed rule.

Goal #5. Constructing a statistic model for predicting punch sticking from surface energy and mechanical properties of actives. So far, work described in Goals 1-4 is aimed at yielding practical insight into the problem, which is valuable to the industry. However, it may not yield

mechanistic understanding, which is essential for guiding effective formulation design and process control to eliminate punch sticking problems for a wide range of active molecules. Ideally, such a model enables reliable predictions of sticking for compounds with diverse chemical structures and for crystals of the same compounds that differ in morphology. To achieve this goal, contributions of surface chemistry and crystal structure to punch sticking need to be understood first. This requires careful study of a large number of actives. In the context of punch sticking, the most relevant surface property that reflects surface chemistry of actives is surface energy. Therefore, another goal of this project is to elucidate the role of surface energy and mechanical properties of actives on punch sticking. According to the punch sticking model in Figure 1, punch sticking propensity can be predicted from properties that can affect F1, F2, and F3, regardless of the chemical composition of the active. Surface (or interfacial) energy affects strength of bonding, while mechanical properties (hardness and elastic modulus) affect area of bonding, both influence the magnitudes of these forces. Successful construction of a meaningful model likely requires the study of a large number of chemically different actives, which may require more time than available in this project. Therefore, our approach to achieving this long term goal is to, whenever possible, collect surface energy, mechanical properties, and particle size of actives, surface energy of punches in the foregoing studies (Goals 1 – 4) to gradually build a sizeable database for constructing a statistical model. Surface energy will be measured by either contact angle technique or inverse gas chromatography (IGC). Mechanical properties will be measured by nanoindentation or analysis of powder compression data. Such a successful statistical model can be used to guide effective formulation development to proactively address potential punch sticking problems both in the laboratory experiments and commercial manufacturing. However, it should be stressed that the model cannot be applied to predict sticking of a given formulation based on properties of the active. This is because punch sticking is also affected by many other factors in addition to surface energy and mechanical properties, such as lubrication, drug loading, tableting speed, and punch design.

Research beyond year 3. The long term goal of this research is to develop a classification scheme of powders punch sticking propensity based on easily accessed information, such as particle size, surface energy, and mechanical properties. For each class of materials, sticking-free formulation space will be identified and appropriate strategies for avoiding punch sticking by each class of material will be recommended. Strategies for developing sticking-free formulations will involve crystal engineering (e.g., spherical crystallization, alternate solid form), particle engineering (e.g., granulation, particle coating, and use of appropriate excipients), and process optimization (e.g., speed, pressure, tooling material and design). Effects of tooling design on punch sticking will also be elucidated.

Model compounds

1) Organic powders: Several active pharmaceutical ingredients exhibiting widely different physicochemical properties and sticking propensity will be selected based on our previous work on 24 compounds [20]. Two compounds will be obtained with different sizes by recrystallization and milling (e.g., jet milling and cryo-milling). This allows the study of effects of particle size or

impact of processing on punch sticking. **2) Inorganic powders:** Alpha alumina, Gamma alumina, and Hematite (0.005-1 mm).

Other model compounds may be included in accordance to suggestions by IFPRI members.

Summary of the key objectives and expected outcomes from the proposed research

	Key objectives	**Expected outcomes**
Year 1	Design and evaluate punch tip design on sticking assessment	1) Identify an optimal tip design 2) Annual report to IFPRI
Year 2	Establish a calibrated scale for predicting punch sticking during manufacturing based on laboratory assessment	1) Development of a calibrated scale capable of predicting sticking during manufacturing 2) Journal publication 3) Annual report to IFPRI
Year 3	1) Effects of tooling material and coating on sticking 2) Effects of particle size, shape, and mechanical properties on sticking 3) Constructing a statistical model for predicting punch sticking.	1) Clear understanding of effects of tooling material and coating on punch sticking 2) Development of a rule for predicting particle size effect on sticking 3) Journal publication 4) Annual report to IFPRI

Leverage into existing programs

The Minnesota lab is dedicated to solving problems related to solids formulation and powder processing. My research emphasizes on fundamental understanding of problems, from which solutions are identified through appropriate crystal and particle engineering. The same approach will be applied in this research. This lab has worked on the problem of punch sticking since 2014. We have accumulated a wealth of knowledge on the problem and expertise in conducting punch sticking experiments using the removable punch tip method. The punch sticking model developed by us (Figure 1) will be a foundation for investigating the role of punch material, coating, and design on sticking. We have ready access to many state-of-the-art powder and particle characterization instruments that are required to fully characterize model materials in this research. The proposed work can be efficiently conducted because the fully instrumented compaction simulator (Presster), a central piece of instrument to this research, resides in my lab. In summary, this proposed research is an important extension of ongoing work in my lab, for which we are well equipped to carry out. Also importantly, Natoli Engineering, a leading tablet tooling manufacturer, is fully committed to design and provide all required tooling as well as expert consultancy throughout this project.

IFPRI member support

IFPRI members' supports are sought in four ways: 1) Suggest suitable model compounds for this research. The current list of model compound is based on advice from one of the IFPRI members (William Ketterhagen). 2) Provide model formulations with known sticking propensity during tablet manufacturing for testing in our lab using the removable punch technique. Such results are essential for developing a calibrated scale for predicting sticking propensity during industrial manufacturing based on laboratory assessment. 3) Support on characterizing samples using instruments not available through existing resources. 4) Perform periodic review of our research and provide constructive comments to assure the success of this project.

Risks and contingency plan

1. The proposed research heavily relies on the compaction simulator. There is the chance that the simulator has mechanical or electrical parts failure due to aging or misuse. The problem of misuses can be minimized through rigorous user training and frequent refreshers. The simulator (Presster) is now marketed and served by our collaborator, Natoli Engineering. In the case of problems occurring with the compaction simulator, there will be down time but we expect speedy repair by Natoli Engineering. In the worst case scenario, we can arrange having work done at Natoli Engineering's facility if repair of our simulator will take an unexpectedly long time. We are also in the process of acquiring a Style'One Evolution. This provides double safety to ensure non-disrupted investigation of the research because software with the Style'One is capable of simulating any press, including the Presster.
2. There is also a slight risk that some of the materials characterization cannot be done at University of Minnesota due to a lack of instrument, e.g., inverse gas chromatography. In that case, help from IFPRI members will be sought first. If no IFPRI members could provide timely assistance needed for this project, we will seek help from other academic laboratories. In the worst case scenario, we will use commercial service companies for samples characterization. In all these cases, careful planning and close communication will ensure the quality of data.

References

1. Abdel-Hamid, S. and G. Betz, *A novel tool for the prediction of tablet sticking during high speed compaction.* Pharm Dev Technol, 2012. **17**(6): p. 747-54.
2. Otsuka, A., *Adhesive properties and related phenomena for powdered pharmaceuticals. .* Yakugaku Zasshi, 1998. **118**(4): p. 127-42.
3. Kakimi, K., T. Niwa, and K. Danjo, *Influence of Compression Pressure and Velocity on Tablet Sticking.* Chemical and Pharmaceutical Bulletin, 2010. **58**(12): p. 1565-1568.
4. Paul, S., et al., *Powder properties and compaction parameters that influence punch sticking propensity of pharmaceuticals.* International Journal of Pharmaceutics, 2017. **521**(1–2): p. 374-383.
5. Waknis, V., et al., *Molecular Basis of Crystal Morphology-Dependent Adhesion Behavior of Mefenamic Acid During Tableting.* Pharmaceutical Research, 2014. **31**(1): p. 160-172.
6. Paul, S., et al., *Dependence of punch sticking on compaction pressure – roles of particle deformability and tablet tensile strength.* J. Pharm. Sci., 2017. **521**: p. 374-383.
7. Hooper, D., et al., *Effects of crystal habit on the sticking propensity of ibuprofen—A case study.* International Journal of Pharmaceutics, 2017. **531**(1): p. 266-275.

8. Al-Karawi, C. and C.S. Leopold, *A comparative study on the sticking tendency of ibuprofen and ibuprofen sodium dihydrate to differently coated tablet punches.* European Journal of Pharmaceutics and Biopharmaceutics, 2018. **128**: p. 107-118.
9. Corn, M., *The adhesion of solid particles to solid surfaces. II.* Journal of the Air Pollution Control Association, 1961. **11**(12): p. 566-84.
10. Corn, M., *The Adhesion of Solid Particles to Solid Surfaces, I. a Review.* Journal of the Air Pollution Control Association, 1961. **11**(11): p. 523-28.
11. Roberts, M., et al., *Effect of lubricant type and concentration on the punch tip adherence of model ibuprofen formulations.* Journal of Pharmacy and Pharmacology, 2004. **56**(3): p. 299-305.
12. Roberts, M., et al., *Effects of surface roughness and chrome plating of punch tips on the sticking tendencies of model ibuprofen formulations.* J. Pharm. Pharmacol., 2003. **55**(9): p. 1223-8.
13. Roberts, M., et al., *Effect of punch tip geometry and embossment on the punch tip adherence of a model ibuprofen formulation.* J. Pharm. Pharmacol., 2004. **56**(7): p. 947-50.
14. Bunker, M., et al., *Characterising the surface adhesive behavior of tablet tooling components by atomic force microscopy.* Drug Development and Industrial Pharmacy, 2011. **37**(8): p. 875-885.
15. Wang, J.J., et al., *Modeling of adhesion in tablet compression—I. atomic force microscopy and molecular simulation.* Journal of Pharmaceutical Sciences, 2003. **92**(4): p. 798-814.
16. Tsosie, H., et al., *Scanning Electron Microscope Observations of Powder Sticking on Punches during a Limited Number (N < 5) of Compactions of Acetylsalicylic Acid.* Pharmaceutical Research, 2017. **34**(10): p. 2012-2024.
17. Al-Karawi, C., et al., *Novel aspects on the direct compaction of ibuprofen with special focus on sticking.* Powder Technology, 2017. **317**(Supplement C): p. 370-380.
18. McDermott, T.S., et al., *A material sparing method for quantitatively measuring tablet sticking.* Powder Technology, 2011. **212**(1): p. 240-252.
19. Hutchins, A., B.C. MacDonald, and M.P. Mullarney, *Assessing tablet-sticking propensity.* Pharm. Technol. , 2012. **36**: p. 57–62.
20. Paul, S., et al., *Mechanism and Kinetics of Punch Sticking of Pharmaceuticals.* J Pharm Sci, 2017. **106**(1): p. 151-158.
21. Paul, S., et al., *Mechanism and Kinetics of Punch Sticking of Pharmaceuticals.* Journal of Pharmaceutical Sciences, 2017. **106**(1): p. 151-158.
22. Paul, S. and C.C. Sun, *Modulating Sticking Propensity of Pharmaceuticals Through Excipient Selection in a Direct Compression Tablet Formulation.* Pharmaceutical Research, 2018. **35**(6): p. 113.

Adhesion of Powders to Metal Surfaces During Compaction

Changquan Calvin Sun, Ph.D.

Pharmaceutical Materials Science and Engineering Laboratory

Department of Pharmaceutics, University of Minnesota

Original submission: October 30, 2017

Second submission: April 30, 2018

308 Harvard Street S.E., 9-127B WDH, Minneapolis, MN 55455, USA

Email: sunx0053@umn.edu; Tel: 612-624-3722; Fax: 612-626-2125

Introduction and Background

Powder adhesion onto tooling, known as punch sticking, is a common problem in cold welding processes to manufacture compacts from powders of pharmaceutical, metallurgy, and energy materials. Without being properly addressed, it can result in significant problems in manufacturing. Punch sticking requires intermittent stoppage of the tableting process to clean the punch sets, which grossly reduces production efficiency. In addition to poor aesthetic quality, inconsistent weight will lead to rejection of an entire batch of compacts in severe cases. Tooling can also be damaged leading to costly down time. The punch sticking phenomenon is a complex problem, known to be affected by process conditions (compaction pressure, dwell time)[1-3], particle properties (size, shape, surface roughness, surface energy, deformability) [4-8], environmental factors (humidity, temperature) [9, 10], formulation composition [11], and punch tip properties (coating, surface asperity and roughness) [12, 13]. Punch sticking has been investigated using several techniques, including atomic force microscopy to quantify adhesion [14, 15], measuring tablet detachment force [7], scanning electron microscopy [16], HPLC analysis of quantitatively extracted adhering mass [11, 17, 18], and monitoring weight of sticking mass using a punch with a removable punch tip [19].

The removable punch tip method is a material-sparing method capable of generating data for quantitatively assessing punch sticking kinetics. In this experimental approach, the material of interest is blended with a non-sticking matrix material, e.g., microcrystalline cellulose. The mixture is then compressed under a controlled pressure and speed. The amount of material adhering to the punch tip is measured periodically to obtain the adhering mass – number of compression data, which quantifies punch sticking kinetics. It is suitable for rank ordering sticking propensity of compounds as well as different batches of the same compound. For example, the generated data can be used to characterize different batches of a drug, which helps flag potential sticking problems during manufacturing due to batch-to-batch variations.

Using the removable punch tip technique, we have quantified the punch sticking propensity of a large number of pharmaceutical materials by tracking the kinetics of mass accumulation during compression [20]. The role of various factors on punch sticking, such as compaction force, drug surface area, drug mechanical properties have also been investigated [4, 6, 21]. Our studies led to a punch sticking model (Figure 1) [20].

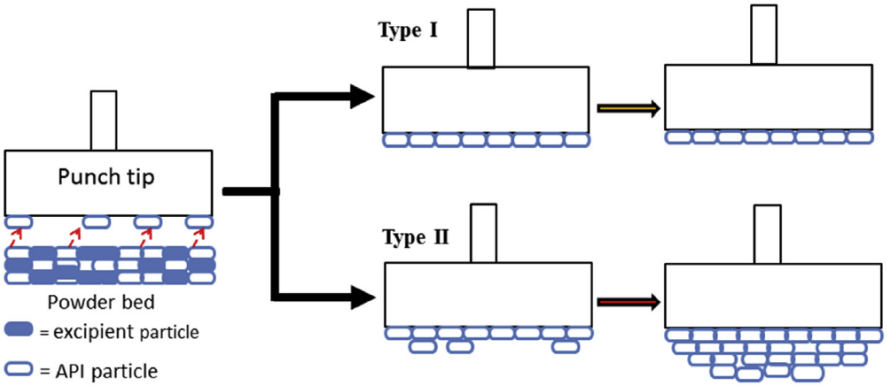

Figure 1. Schematic representation of the punch sticking kinetics based on interactive forces.

To apply this model, the formulated powder is considered to be a mixture between a main component (such as a drug or fine iron ore), **A**, and a matrix. This model predicts punch sticking outcome based on the interplay among three competing forces, i.e., F1 (**A**-punch adhesion), F2 (**A**-**A** cohesion), and F3 (**A**-matrix adhesion). Punch sticking is avoided if F1 is lower than F2 and F3, but sticking occurs when F1 is greater than F2 and F3. When a monolayer of sticking mass is present on punch surface, F1 has no further role in controlling the sticking kinetics. Instead, the relative magnitude of F2 and F3 determines the kinetics of subsequent mass build-up. Only a monolayer of sticking mass (or filming) is expected when F2 < F3, but continued build-up of material is expected when F2 ≥ F3.

This model is consistent with several known features of punch sticking, including a) APIs are enriched in the punch adhered mass [20]; b) mechanical properties and particle size impact sticking propensity [6]; and c) tooling construction materials can influence punch sticking by the same powder [8]. This model suggests the possibility of modulating sticking propensity by controlling the magnitude of F2 and F3. While F2 is constant for a given batch of **A**, punch sticking propensity can be minimized by elevating F3 through appropriate selection of excipients in a formulation. For example, simply choosing a binder that exhibits higher F3 should reduce sticking severity. The model was supported by our recent work where two model drugs, Celecoxib and ibuprofen, were studied in four excipient matrices (Microcrystalline cellulose Avicel PH102 and Avicel PH105, hypromellose, and starch). Punch sticking indeed decreased with increasing F3 for both drugs and at both compaction pressures investigated (Figure 2).[22]

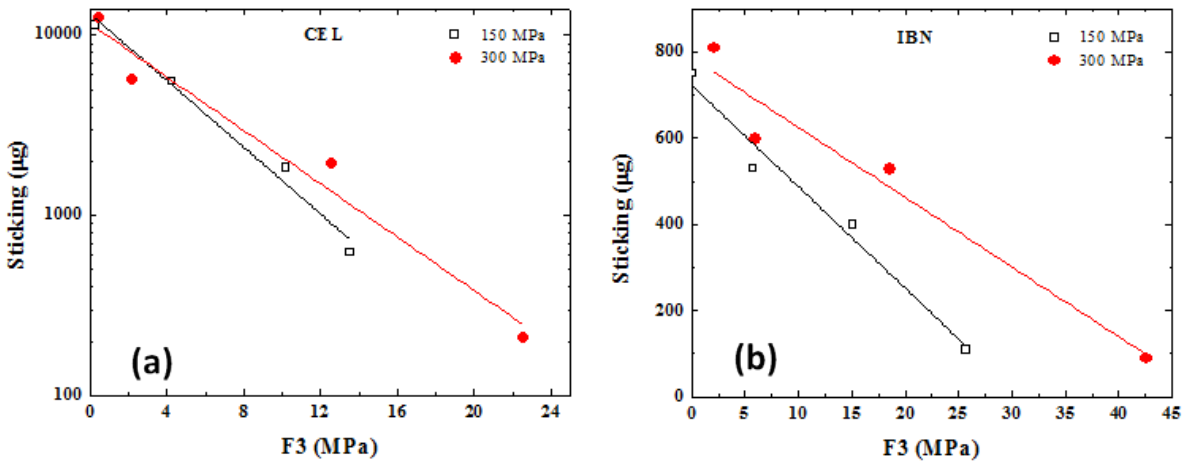

Figure 2. Dependence of sticking on F3 for (a) celecoxib and (b) ibuprofen. Tableting was performed at two pressures, 150 MPa and 300 MPa.

Despite the extensive earlier efforts, a mechanistic understanding of punch sticking phenomenon remains elusive. Systematic further investigation of this phenomenon is required to elucidate the punch sticking mechanism, which is critical for effective formulation design or process engineering. The goal of following research is to ultimately eliminate punch sticking problems during manufacturing.

Research Plan

Although useful in rank ordering sticking propensity among different powders, the removable punch tip method faces two problems for broad adoption for reliably predicting sticking behavior during manufacturing: 1) only flat punch surface has been used, which is different from real punch tips having curvature and embossed letters and numbers. 2) an absence of correlation between data from the removable punch tip study and sticking propensity during actual manufacturing. Therefore, the first stage of this research is to develop an improved removal tip method for reliable prediction of punch sticking that can be applied over any desired compaction pressure and environment conditions using a compaction simulator. In the following experiments, a total of 100 tablets will be compressed and the weight of adhered mass will be measured every 20 compression. During the entire project, environmental conditions will be monitored and controlled, if needed, by humidifying or de-humidifying an isolated space that houses the instruments. All samples will be equilibrated under controlled relative humidity (RH) in suitable RH chambers. For a selected model compound, effects of RH on punch sticking will be assessed. Compaction pressure has been shown to influence punch sticking in the published work, including those by us. As a standard practice in our work, punch sticking propensity experiments for each formulation will be performed at two pressures, 150 MPa and 300 MPa, which cover the typical range of pressure during commercial tablet manufacturing. For different drugs in the same matrix, tablet solid fraction (or porosity) may slightly differ. The use of two pressures also allows interpolation of sticking data to a common solid fraction for different drugs.

Goal #1. Optimize the design of removable punch tip for conducting laboratory punch sticking assessment. In this part of the research, punch tips with different curvatures and embossed with selected letters and numbers will be compared. The hypothesis is that such tips are more sensitive in detecting punch sticking. Using such tips, future punch sticking assessments can be performed more quickly and reliably using less material. Punch tips will be prepared using standard tool steel, with and without embossed letters and numbers (O, A, R, 0, 6, 8, 9). Along with monitoring the amount of adhering mass, the locations of punch sticking will be documented by microscopic images. Three powders (exhibiting low, medium, and severe punch sticking propensity) will be used. Based on the results, tips with different curvatures will be made and evaluated to identify the most sensitive tip design for use in subsequent studies.

Goal #2. Establish a calibrated scale that allows reliable predictions of punch sticking during manufacturing from the laboratory assessments using the optimized tip. Meeting this goal requires the use of 6 - 10 powders with known punch sticking propensity during manufacturing. The comparison of laboratory punch sticking data to the known sticking propensity will lead to a calibrated scale, which can be used to reliably predict sticking propensity during commercial manufacturing based on laboratory assessment using the removable punch tip method. A critical unknown is the availability of sufficient quantity of powders (estimated 500 g) with well documented punch sticking propensity during commercial manufacturing and details on punch design and construction material. If such desired powders or information are not available from the

IFPRI members, we will prepare different model formulations in sufficient quantity and assess their punch sticking propensity using a standard concave tooling on a laboratory rotary press (Piccola). We will assess their punch sticking propensity in parallel using the optimized tooling identified in Goal #1.

Goal #3. Examine effects of tooling material and coating on punch sticking propensity. When punch sticking problems are discovered in a late stage of development, modifying formulation is rarely an option due to the high costs. In those cases, a common solution is to reduce punch adhesion using different tooling steels or coating. Here, we will compare sticking propensity of three model formulations (low, intermediate, and high sticking propensity) on three types of steel and three coatings as summarized in the table below.

Variable	**Options**		
Steel type	S7	D2	M340
Coating	Hard chrome	chromium nitride (CrN)	titanium nitride (TiN)

The PI has secured full commitment from Natoli Engineering to support this project by providing all needed tooling (punch and tips) manufactured with different materials and coating types. An engineer from Natoli will also be dedicated as a consultant on all tooling related issues or problems. There are no foreseeable critical unknowns that may influence the outcome of the project.

Goal #4. Determine effects of particle size on punch sticking. API particle size may change during the course of drug development or commercial manufacturing, for example, due to optimization of crystallization process for higher yield and purity or due to milling to enhance dissolution rate. This factor is known to have an impact on punch sticking propensity but further mechanistic understanding is needed. The conventional wisdom suggests that smaller particles always correspond to more severe sticking because of larger surface area that can be in contact with punch face. However, our preliminary work suggested this notion is not always correct. We hypothesize that very fine API particles can form large agglomerates, which actually lower its area of contact with punch face. Here, we will study the effect of size using four model drugs, exhibiting a range of mechanical properties (brittle to ductile) and sticking propensity (medium to high). Each model drug will be obtained in four different size fractions through recrystallization, milling, and sieving. Different sizes of hematite (0.005 – 1 mm), obtained commercially, will also be evaluated. Punch sticking propensity will be assessed for each of the sizes and correlated to particle size to develop a general rule. If needed, more model compounds will be investigated to ensure robustness of the proposed rule.

Goal #5. Constructing a statistic model for predicting punch sticking from surface energy and mechanical properties of actives. So far, work described in Goals 1-4 is aimed at yielding practical insight into the problem, which is valuable to the industry. However, it may not yield

mechanistic understanding, which is essential for guiding effective formulation design and process control to eliminate punch sticking problems for a wide range of active molecules. Ideally, such a model enables reliable predictions of sticking for compounds with diverse chemical structures and for crystals of the same compounds that differ in morphology. To achieve this goal, contributions of surface chemistry and crystal structure to punch sticking need to be understood first. This requires careful study of a large number of actives. In the context of punch sticking, the most relevant surface property that reflects surface chemistry of actives is surface energy. Therefore, another goal of this project is to elucidate the role of surface energy and mechanical properties of actives on punch sticking. According to the punch sticking model in Figure 1, punch sticking propensity can be predicted from properties that can affect F1, F2, and F3, regardless of the chemical composition of the active. Surface (or interfacial) energy affects strength of bonding, while mechanical properties (hardness and elastic modulus) affect area of bonding, both influence the magnitudes of these forces. Successful construction of a meaningful model likely requires the study of a large number of chemically different actives, which may require more time than available in this project. Therefore, our approach to achieving this long term goal is to, whenever possible, collect surface energy, mechanical properties, and particle size of actives, surface energy of punches in the foregoing studies (Goals 1 – 4) to gradually build a sizeable database for constructing a statistical model. Surface energy will be measured by either contact angle technique or inverse gas chromatography (IGC). Mechanical properties will be measured by nanoindentation or analysis of powder compression data. Such a successful statistical model can be used to guide effective formulation development to proactively address potential punch sticking problems both in the laboratory experiments and commercial manufacturing. However, it should be stressed that the model cannot be applied to predict sticking of a given formulation based on properties of the active. This is because punch sticking is also affected by many other factors in addition to surface energy and mechanical properties, such as lubrication, drug loading, tableting speed, and punch design.

Research beyond year 3. The long term goal of this research is to develop a classification scheme of powders punch sticking propensity based on easily accessed information, such as particle size, surface energy, and mechanical properties. For each class of materials, sticking-free formulation space will be identified and appropriate strategies for avoiding punch sticking by each class of material will be recommended. Strategies for developing sticking-free formulations will involve crystal engineering (e.g., spherical crystallization, alternate solid form), particle engineering (e.g., granulation, particle coating, and use of appropriate excipients), and process optimization (e.g., speed, pressure, tooling material and design). Effects of tooling design on punch sticking will also be elucidated.

Model compounds

1) Organic powders: Several active pharmaceutical ingredients exhibiting widely different physicochemical properties and sticking propensity will be selected based on our previous work on 24 compounds [20]. Two compounds will be obtained with different sizes by recrystallization and milling (e.g., jet milling and cryo-milling). This allows the study of effects of particle size or

impact of processing on punch sticking. **2) Inorganic powders:** Alpha alumina, Gamma alumina, and Hematite (0.005-1 mm).

Other model compounds may be included in accordance to suggestions by IFPRI members.

Summary of the key objectives and expected outcomes from the proposed research

	Key objectives	**Expected outcomes**
Year 1	Design and evaluate punch tip design on sticking assessment	1) Identify an optimal tip design 2) Annual report to IFPRI
Year 2	Establish a calibrated scale for predicting punch sticking during manufacturing based on laboratory assessment	1) Development of a calibrated scale capable of predicting sticking during manufacturing 2) Journal publication 3) Annual report to IFPRI
Year 3	1) Effects of tooling material and coating on sticking 2) Effects of particle size, shape, and mechanical properties on sticking 3) Constructing a statistical model for predicting punch sticking.	1) Clear understanding of effects of tooling material and coating on punch sticking 2) Development of a rule for predicting particle size effect on sticking 3) Journal publication 4) Annual report to IFPRI

Leverage into existing programs

The Minnesota lab is dedicated to solving problems related to solids formulation and powder processing. My research emphasizes on fundamental understanding of problems, from which solutions are identified through appropriate crystal and particle engineering. The same approach will be applied in this research. This lab has worked on the problem of punch sticking since 2014. We have accumulated a wealth of knowledge on the problem and expertise in conducting punch sticking experiments using the removable punch tip method. The punch sticking model developed by us (Figure 1) will be a foundation for investigating the role of punch material, coating, and design on sticking. We have ready access to many state-of-the-art powder and particle characterization instruments that are required to fully characterize model materials in this research. The proposed work can be efficiently conducted because the fully instrumented compaction simulator (Presster), a central piece of instrument to this research, resides in my lab. In summary, this proposed research is an important extension of ongoing work in my lab, for which we are well equipped to carry out. Also importantly, Natoli Engineering, a leading tablet tooling manufacturer, is fully committed to design and provide all required tooling as well as expert consultancy throughout this project.

IFPRI member support

IFPRI members' supports are sought in four ways: 1) Suggest suitable model compounds for this research. The current list of model compound is based on advice from one of the IFPRI members (William Ketterhagen). 2) Provide model formulations with known sticking propensity during tablet manufacturing for testing in our lab using the removable punch technique. Such results are essential for developing a calibrated scale for predicting sticking propensity during industrial manufacturing based on laboratory assessment. 3) Support on characterizing samples using instruments not available through existing resources. 4) Perform periodic review of our research and provide constructive comments to assure the success of this project.

Risks and contingency plan

1. The proposed research heavily relies on the compaction simulator. There is the chance that the simulator has mechanical or electrical parts failure due to aging or misuse. The problem of misuses can be minimized through rigorous user training and frequent refreshers. The simulator (Presster) is now marketed and served by our collaborator, Natoli Engineering. In the case of problems occurring with the compaction simulator, there will be down time but we expect speedy repair by Natoli Engineering. In the worst case scenario, we can arrange having work done at Natoli Engineering's facility if repair of our simulator will take an unexpectedly long time. We are also in the process of acquiring a Style'One Evolution. This provides double safety to ensure non-disrupted investigation of the research because software with the Style'One is capable of simulating any press, including the Presster.
2. There is also a slight risk that some of the materials characterization cannot be done at University of Minnesota due to a lack of instrument, e.g., inverse gas chromatography. In that case, help from IFPRI members will be sought first. If no IFPRI members could provide timely assistance needed for this project, we will seek help from other academic laboratories. In the worst case scenario, we will use commercial service companies for samples characterization. In all these cases, careful planning and close communication will ensure the quality of data.

References

1. Abdel-Hamid, S. and G. Betz, *A novel tool for the prediction of tablet sticking during high speed compaction.* Pharm Dev Technol, 2012. **17**(6): p. 747-54.
2. Otsuka, A., *Adhesive properties and related phenomena for powdered pharmaceuticals. .* Yakugaku Zasshi, 1998. **118**(4): p. 127-42.
3. Kakimi, K., T. Niwa, and K. Danjo, *Influence of Compression Pressure and Velocity on Tablet Sticking.* Chemical and Pharmaceutical Bulletin, 2010. **58**(12): p. 1565-1568.
4. Paul, S., et al., *Powder properties and compaction parameters that influence punch sticking propensity of pharmaceuticals.* International Journal of Pharmaceutics, 2017. **521**(1–2): p. 374-383.
5. Waknis, V., et al., *Molecular Basis of Crystal Morphology-Dependent Adhesion Behavior of Mefenamic Acid During Tableting.* Pharmaceutical Research, 2014. **31**(1): p. 160-172.
6. Paul, S., et al., *Dependence of punch sticking on compaction pressure – roles of particle deformability and tablet tensile strength.* J. Pharm. Sci., 2017. **521**: p. 374-383.
7. Hooper, D., et al., *Effects of crystal habit on the sticking propensity of ibuprofen—A case study.* International Journal of Pharmaceutics, 2017. **531**(1): p. 266-275.

8. Al-Karawi, C. and C.S. Leopold, *A comparative study on the sticking tendency of ibuprofen and ibuprofen sodium dihydrate to differently coated tablet punches.* European Journal of Pharmaceutics and Biopharmaceutics, 2018. **128**: p. 107-118.
9. Corn, M., *The adhesion of solid particles to solid surfaces. II.* Journal of the Air Pollution Control Association, 1961. **11**(12): p. 566-84.
10. Corn, M., *The Adhesion of Solid Particles to Solid Surfaces, I. a Review.* Journal of the Air Pollution Control Association, 1961. **11**(11): p. 523-28.
11. Roberts, M., et al., *Effect of lubricant type and concentration on the punch tip adherence of model ibuprofen formulations.* Journal of Pharmacy and Pharmacology, 2004. **56**(3): p. 299-305.
12. Roberts, M., et al., *Effects of surface roughness and chrome plating of punch tips on the sticking tendencies of model ibuprofen formulations.* J. Pharm. Pharmacol., 2003. **55**(9): p. 1223-8.
13. Roberts, M., et al., *Effect of punch tip geometry and embossment on the punch tip adherence of a model ibuprofen formulation.* J. Pharm. Pharmacol., 2004. **56**(7): p. 947-50.
14. Bunker, M., et al., *Characterising the surface adhesive behavior of tablet tooling components by atomic force microscopy.* Drug Development and Industrial Pharmacy, 2011. **37**(8): p. 875-885.
15. Wang, J.J., et al., *Modeling of adhesion in tablet compression—I. atomic force microscopy and molecular simulation.* Journal of Pharmaceutical Sciences, 2003. **92**(4): p. 798-814.
16. Tsosie, H., et al., *Scanning Electron Microscope Observations of Powder Sticking on Punches during a Limited Number (N < 5) of Compactions of Acetylsalicylic Acid.* Pharmaceutical Research, 2017. **34**(10): p. 2012-2024.
17. Al-Karawi, C., et al., *Novel aspects on the direct compaction of ibuprofen with special focus on sticking.* Powder Technology, 2017. **317**(Supplement C): p. 370-380.
18. McDermott, T.S., et al., *A material sparing method for quantitatively measuring tablet sticking.* Powder Technology, 2011. **212**(1): p. 240-252.
19. Hutchins, A., B.C. MacDonald, and M.P. Mullarney, *Assessing tablet-sticking propensity.* Pharm. Technol. , 2012. **36**: p. 57–62.
20. Paul, S., et al., *Mechanism and Kinetics of Punch Sticking of Pharmaceuticals.* J Pharm Sci, 2017. **106**(1): p. 151-158.
21. Paul, S., et al., *Mechanism and Kinetics of Punch Sticking of Pharmaceuticals.* Journal of Pharmaceutical Sciences, 2017. **106**(1): p. 151-158.
22. Paul, S. and C.C. Sun, *Modulating Sticking Propensity of Pharmaceuticals Through Excipient Selection in a Direct Compression Tablet Formulation.* Pharmaceutical Research, 2018. **35**(6): p. 113.

IFPRI Research Project Brief

Powder Flow Near Boundaries

The International Fine Particle Research Institute (IFPRI) wishes to fund a project to develop extensions for dry-flowing powder rheology that describes flow, stress, and packing densities at boundaries including a free surface. Given IFPRI's industrial focus, the project should include industrially-relevant powder flow characterization techniques that are appropriate for studying flows at boundaries.

The flow of powders under low consolidation stress and with a free surface is relevant to a range of industrial processes and emerging technologies. Conditions of low consolidation stress are encountered in many applications: fluidized bed, small silos, capsule filling, additive manufacturing, etc. In these applications, cohesion may induce flow intermittences, waves and complex density fluctuations [1]. These phenomena are relevant in processing, for example in powder-bed-based additive manufacturing where the creation of successive thin and homogenous powder layer is needed [2]. To select the best powder properties and to optimize the process, we need modeling and characterization methods relevant to flows that are dominated by boundary-layer physics. Ideally, measurement methods should reflect the flow, stress and packing fields of powders in thin-layer flows.

Validation should include a practical range of boundary conditions on the thin-layer substrate (e.g., previous free surface, belt, etc.) and underflow boundary (e.g., weir or roller) used to control layer thickness. Experimental and computational techniques should be able to capture a range of particle size, shape and density distribution, as well as variations in bulk cohesion and particle mechanical properties (e.g. modulus, roughness).

More specifically, we are interested in flows relevant to thin layers of particles, where layer thickness (H) is no more than 10X the median particle size (D), spread over a width (W) that is relatively large: $H/D < 10$; $W/H > 100$. The flow regime should include quasi-static and intermediate flows, where the regime is defined at the point of metering the powder into the layer.

References:

[1] M. Wojtkowski, O. I. Imole, M. Ramaioli, E. Chávez Montes and S. Luding, Behavior of cohesive powder in rotating drums, AIP Conference Proceedings 1542 (2013)

[2] G. Yablokova, M. Speirs, J. Van Humbeeck, J.-P. Kruth, J. Schrooten, R. Cloots, F. Boschini, G. Lumay, J. Luyten, Rheological behavior of β-Ti and NiTi powders produced by atomization for SLM production of open porous orthopedic implants, Powder Technology 283, 199–209 (2015)

Dear Dr. Louge and Dr. Michaels:

Thank you for the review of our proposal entitled "A Validated Rheometry-aware, Tribology-aware approach to elucidating powder flow behavior near boundaries". Your comments were very helpful and most of them have been addressed or added to the proposal as needed. Below are my point-by-point responses to your questions and comments (shown in italics).

(1) *Members suggested that you reinforce your analysis of flow fundamentals and place less emphasis on result interpretation based on machine learning. Specifically, please consider fundamental flow regimes spanning relevant particle packing and shear rate conditions, including quasi-static, intermediate and collision-dominated regimes*

The machine learning aspects of the original proposal have been removed and replaced an analysis based on fundamental mechanics. The flow regimes ranging from quasi-static to collision-dominated will be probed by varying the nominal shear rate (please see Table 2).

(2) *If you intend to show Fig. 6, could you justify its form based on physical principles?*

This figure has now been replaced by a figure showing the validation of spreading model against experimental single layer spreading.

(3) *Members suggested that you clarify your statement of work and deliverables.*

Industrial funding that bears no overhead cannot have deliverables or statements of work. However, a new section has been added on "Research Output". It involved voluntary sharing of key items expected from this work.

(4) *Could you indicate which range of particle size and shape distributions you intend to deploy in experiments?*

An exhaustive table on model and experimental test matrix has been added. Please see Table 2. Powders to be characterized in this proposal will have spherical, angular and blocky shapes.

(5) *Members suggested that you consider broader characterization of particle properties than what the FT4 alone will provide. In particular, it is unclear how you intend to derive K, mu and beta from the FT4 data (Literature references would be useful). It would be especially worthwhile to indicate how control of boundary conditions in characterization equipment (e.g. controlled stress vs controlled volume) can be related to flows in processing equipment, -- such as variable underflow weir or roller conditions in your AM example*

Thanks for the comment. We will answer these concerns in three parts.
1] The FT4 is one of the many characterization tools used to ascertain particle properties. Table 1 has been added to show all the instruments which will be used in this work and the properties these instruments will measure.
2] The properties K, β and μ are derived when calibrating and obtaining a virtual avatar of a powder. The section (see Task 2.1) has been revised to explain how these parameters can be

determined. This method has also been introduced by the author (see Ref. Desai 2017, PhD thesis and Desai et al. 2018 pending journal paper) and others (see. Ref. Bharadwaj et al. 2010).
3] A new section explaining the fundamental knowledge gained from this work, such as how the boundary conditions on an AM spreader (e.g., layer thickness or layer volume) affect the spreading throughput (i.e., the flowrate per unit width), has been added to the revised RFP.

References:

R. Bharadwaj, W. R. Ketterhagen, B. C. Hancock, Discrete element simulation study of a Freeman powder rheometer, Chemical Engineering Science 65 (2010)
P. Desai, Tribosurface Interactions involving Particulate Media with DEM-calibrated Properties: Experiments and Modeling. Ph.D. thesis, Carnegie Mellon University, (2017).
P. Desai, A. Mehta, P. Dougherty, C. F. Higgs, A rheometry based calibration of a first-order DEM model to generate virtual avatars of metal additive manufacturing (AM) powders, Peer reviewed journal

Cheers,

C. Fred Higgs III
John & Ann Doerr Professor of Mechanical Engineering (MECH)
Faculty Director, Rice Center for Engineering Leadership (RCEL)
Director, Particle Flow and Tribology Laboratory (PFTL)
RICE University (Houston, TX)

A Validated Rheometry-aware, Tribology-aware approach to elucidating powder flow behavior near boundaries

PI: C. Fred Higgs III
Affiliation: Mechanical Engineering Department, Bioengineering Department
Place: Rice University, 6100 Main St., 101 Mech. Engineering Building, Houston, TX 77005
Lab: Particle Flow & Tribology Lab (PFTL)
Contact: 713-348-5923 (ph); higgs@rice.edu (email); https://higgslab.org/ (web)

1. Introduction

Granular and powder flows are the core components of many industries, including additive manufacturing, pharmaceuticals, solids and food processing, biotechnology, and energy technology. The International Fine Particle Research Institute (IFPRI) recently supported a collaborative study in dense granular flows [1]. It did not address the more complex tribological-rheological particle-surface interactions at the boundaries and so the planned effort seeks to do this. The three-year overall objective of the planned work involves researching, developing, and experimentally validating fundamental powder dynamics model so that it can form the nucleus of a predictive framework that intelligently guides and improves performance in various applications, such as additive manufacturing (i.e., powder bed 3D printing/spreading, powder-weir/blade flow interactions, silo/hopper flows-wall interact spreading processes. A couple of these relevant applications are expanded upon below.

Additive Manufacturing. Powder bed 3D printing involves numerous modes of powder dynamics that are of concern to powder companies. For example, there is unconfined gravity-driven powder flow out of a hopper to dispense the powder on to the build plate. Next, there is a thin film spread (by a recoater) or rolled during the powder spreading process just prior to the printing step. During spreading, there are interactions of the powder with the interfacial surfaces, which in the field tribology are known as the 'tribosurfaces'. In a system involving powder media in relative motion between surfaces, the topography and micro-scale surface features in concert with the powder rheology dictate the performance of the powder. However, the powder spreading step is far from ideal [2,3] and a lack of fundamental understanding of the powder rheology and particle-boundary surface effects is often the central cause to two powder layer defects: varying heights (or high roughness) and high porosity.

Hopper/Silo Powder Flows. Some of the most common shear flow geometries seen in industrial applications are hoppers and silos, which are containers of varying shapes used in the aforementioned solid processing industries. The geometry of hopper and silo designs is dependent on the materials being used and particle-surface interaction parameters, namely the coefficients of friction (COF) and restitution (COR), surface roughness, size of the materials, and other parameters [5]. Understanding particle-boundary surface interactions can result in high mass flow (discharge) rates without jamming [7]. Another design issue is "inadequate emptying" that occurs in silos when the container cone or exit angles are too low, resulting in an undesirable remnant of un-discharged bulk material [4].

Free surface mixer/blender flows. Powder flows over weirs (or single blades) must be understood to ensure predictable performance in applications such as mixers and blenders [6].These granular material devices abound in pharmaceutical and solid processing industries. However, the mixing of granular material are not well understood because of the lack of constitutive relation descriptions, but also because of the lack of understanding of the particle-boundary interactions especially when the particles are on the order of the dimensions of the surface asperities. This is often the case when using fine powders. Similar to mixers or weirs where powder moves over single blades, the Freeman FT4 rheometer has a rotating blade, which descends into a powder-filled cylinder.

Summary of overall strategy. In this work, *Rice University* (Rice) will pursue research to elucidate the behavior of powder near boundaries. The strategy is that by introducing rheometry measurables plus tribology-level fidelity (which involves intensive mechanical and surface characterization of the particle media and the surfaces

involved), the most sensitive parameters in the 'near boundary' region can be identified. Methods for measuring and mathematically representing these parameters (e.g., surface roughness, friction coefficient, cohesion/adhesion) in DEM models will be established. Beyond the current effort, the outcomes of this work can be used to inform continuum model boundary conditions [7, 8].

Preview of 3-year research plan. Figure 1 shows how the PI's lab plans to achieve the aforementioned strategy. They will be pursuing a 3-year research plan that consists of three independent yet overlapping phases. **Phase 1** will focus on full characterization of the powders' rheological and tribological properties using a powder rheometer (measures the energy and resistance required to spread powders under different states), powder tribometer (measures the friction between thin powder films and prescribed surfaces). **Phase 2** focuses on the research and development of a computational modeling framework for elucidating the rheology of powder in the rheometer and then extended to various applications such as additive manufacturing. Once the powder rheology is obtained from an experimentally-validated model of the powder rheometer, the accurate rheology can then be combined with the advanced surface parameter descriptions to form the basis for predicting the behavior of the powder in industrial applications. For example the spreading process variables (e.g., spreading speed, spreading flowrate, and layer thickness) can be related to the spreading process output variables (e.g., powder layer roughness and porosity). The **Phase 3** work will be comprised of model validation, where experiments with a powder rheometer and a 3D printer's spreader package are conducted.

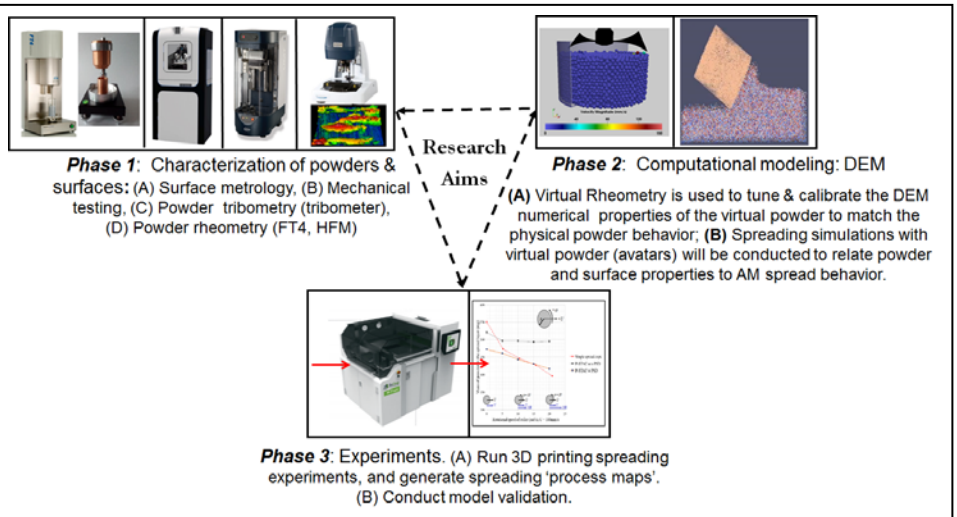

Fig. 1: Overall Three Phase Research Plan:
(1) Characterization of the powder behavior. Powder is analyzed with rheometry (FT4, Hall flow), nanoindenter/material testers. Tribometer used to obtain inter-particle and wall friction. Surface profilonmetrs used to measure roughness.
(2) Computational modeling is employed. (2A) First the virtual rheometer helps compute the numerical values to represent the physical powder with the virtual powder ('avatar). (2B) Powder spreading DEM simulations are run to determine the optimal spreading speed V, layer thickness H to obtain virtual layer. Spreading process curves relating the process variables (velocity U, layer thickness) to the process outputs (layer roughness, porosity) are generated.
(3) Experiments will be conducted to: validate the model in Phase 2, run parametric tests (e.g., varying powder size distributions, sizes, materials, etc.); experimental validation of spreading process curves from Phase 2 model will be conducted.

IFPRI collaboration. Beyond unrestricted financial support, IFPRI members can support this work with in-kind contributions of powder materials, free surface experimental rigs (e.g., chutes, small silos), and feedback on results. The PI also plans to write NSF GOALI proposals on this work in collaboration with the appropriate IFPRI members to support the PI's students/postdocs. Internships for the PI's students are also welcomed.

How this planned research will impact PI's existing program. The PI wants to affect two key sectors: solid processing and additive manufacturing. He is developing a suite of experimentally-validated models, experimental tests methods, and data libraries. This work will help make strides towards these goals.

Historical Review

History of AM powder spreading modeling.
The history of AM powder spreading modeling is brief. Only a handful of studies [9-12] have attempted to answer the influence of spreading step in the entire 3D printing process. None of them works in real size simulation domains with massive particle numbers, as the proposed work will.

A major goal for powder-bed AM end-user companies, such as P&G, is to spread any powder anytime, or less ambitiously, to spread more than a few powder systems. In other words, 3D printing companies and researchers would be greatly aided if a model or perhaps a 'spreading process map' (derived from the model) existed, where such as model or map could link the main spreader inputs, layer height H and spreader velocity V to the spread process outputs of layer roughness and porosity. The planned research will contribute to the R&D of an experimental and modeling platform to study the mechanics of powders in the powder-bed AM spreading process. A key scientific deliverable is to uncover the relationship between the spreading process inputs and the spread powder layer quality and defects.

2.2 Spreadability of powder films in AM processes.
Most powder industries are transporting powders through aeration process or through hopper and silo discharge nozzles, which means that 'powder flowability' is of the appropriate governing parameter to evaluate various powders [13]. A hall flow meter, which is a gravity driven device where the time it takes to discharge different powders are record, is the common instrument. A powder's flowability, which is intrinsic to the powder, is assumed to directly correlate with its 'spreadability' in the context of direct metal AM processes and it does not. Spreadability relates to the ability of a powder candidate to spread a powder layer with uniform thickness, density, and coverage for a prescribed AM process environment.

Relation of powder properties to spreadability in AM
'Spreadability' refers to the ease with which a powder will **spread** under a specified set of conditions. Normally, powders are 'spread' within a sliding contact (i.e., relatively moving surfaces). In order to quantify the spreadability of a powder film, one must measure the properties of the discrete and bulk properties of the powder. The properties help describe the potential of a spread powder film to be uniform.

The cohesion or friction between the particles (i.e., the internal friction), would greatly affect the final configuration of the particles; the surface roughness on the particles would likely have a similar effect. Smaller particles might not have enough weight to overcome the short-range cohesive (e.g., Van der Waals, capillary) or repulsive (e.g., electrostatic, tribo-electrification) surface forces. These surface forces would affect the particle packing and the energy required to spread the powder film. As opposed to cohesion, which occurs between particles, adhesion involves the interaction between the powder media and the boundaries; tools such as powder rheometry and tribometry can provide quantitative insight here. The interplay of the large number of variables that effects powder flowability is severe.

2. Preliminary work conducted by the PI
The preliminary work is broken into two segments: (1) Powder tribology (friction in the interface, including the interfacial media and surface features) work conducted by the PI's group and (2) Powder rheology conducted by his group. Figure 2 shows an image from the PI's white light interferometer (optical profilometer) which captures powder coverage on a surface

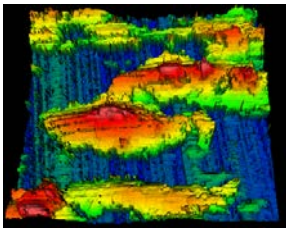
Fig. 2: Spread powder layer is fractionally covering a substrate (blue)

3.1 Preliminary work by the PI: Measuring the tribology when spreading powder layers
Higgs and Wornyoh [14-17] conducted powder film experiments on a pellet-on disk with slider pad tribometer (instrument for measuring friction, wear, and interfacial conditions).

3.2 Preliminary work by PI: Analyzing AM Materials through Powder Rheometry

The PI has also conducted investigations into the spreadability of candidate AM materials using powder rheometry. In utilizing one of the state-of-the-art powder FT4 rheometers, this technique focuses on the elucidation of key parameters involved in a powders ability to flow. Sample measurables include the Bulk Flow Energy (BFE), is a measurement for the energy to spread over confined powder such as the powder in the binded powder sub-layer (BSL); it represents the average energy during this downward motion. The Specific Energy (SE) represents the energy to spread over loose unbinded powder. The *bulk density* is also captured which represents the packing state of the loose powder. ***One key outcome of this work will be a detailed use and elucidation of the FT4 powder rheometer for broad applicability to any industry that needs a tool to predict the behavior of powder media in their applications.***

3.3. Preliminary work in DEM simulations of powder flows

A discrete element method (DEM) solver was developed in PI Higgs's research group to study complex granular flows. The solver possesses capabilities to model the physics, which dominate granular flows such as particle-particle heat transfer and particle-fluid coupling [18-22]. Material properties become important for quantitative comparison to experiments conducted in the PI's laboratory [23]. The work culminated in our in-house multi-physics code called as the **Particle-Surface Tribology Analysis Code (P-STAC)**. The code has computational modules for modeling the fluid dynamics; particle mechanics, solid/contact mechanics, thermal physics, and material wear [*26*]. Cohesion and adhesion modules have also been incorporated.

3.4 Preliminary work obtaining virtual 'powder avatars'

DEM simulations of real powders can only be done after the Preliminary modeling work for the RAPID 2015 conference [*28*] was carried out to study rheometry of a benchmark granular media- 2mm glass beads. A DEM solver is faced with two competing effects: accurate modeling of the bulk behavior of the discrete medium and computational efficiency. The choice of the interaction model, from now on referred to as the contact model, is a difficult one considering the absence of a constitutive law for DEM solvers. There is no single holistic contact model capable of replicating the bulk behavior of the medium without applying some sort of calibration procedure. Therefore, a simple, first-order contact model is chosen for this study.

A calibration process has been employed wherein the parameters of the contact model are iteratively changed until the bulk behavior of virtual glass beads matches that of the real glass beads seen in the published experimental results. Sample P-STAC simulation snapshot is shown in Fig. 3 (a) with a tuning of micro-parameters or contact model parameters to obtain a good match with the published experimental and numerical results is shown in Fig. 3 (b) for the force experienced by the rheometer blade as it penetrates through the glass beads.

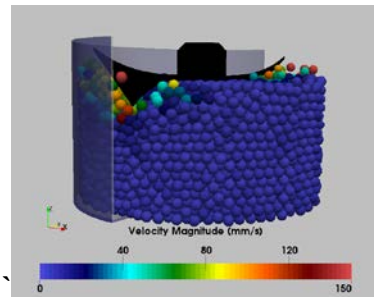

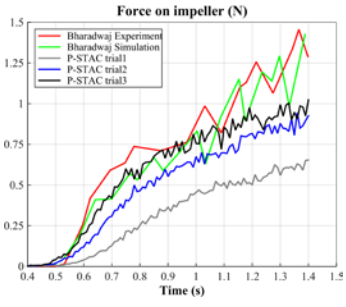

(a) (b)

Fig. 3: (a**)** Simulation snapshot for confined-compressive loading inside 48mm virtual rheometer w 2mm glass beads. The particles are colored by the magnitude of their velocity. (b) P-STAC tuning t micro-parameters to match the experimental results.

3. The planned technical approach:

The planned research consists of three independent yet overlapping phases aimed at elucidating powder mechanics, with a focus on characterizing the particle-boundary surface interactions in order to understand industrial processes, namely powder spreading (in additive manufacturing) and powders in a FT4 rheometer which is a mixing type of device albeit primarily used for characterization of homogenous powders. **Phase 1 (characterization)** will involve characterization of the powder rheological, mechanical, and tribological properties and the boundary surface properties as well. **Phase 2 (modeling)** consists of computational modeling DEM framework which will be developed as an *in silico (virtual)* tool for relating the FT4 powder rheometry variables to the AM powder spreading variables. **Phase 3 (experiments)** will focus on running FT4 experiments to characterize the behavior of powder samples in the FT4 rheometer; 3D printing (i.e., layer spreading) experiments of varying parameters will also be conducted.

Phase 1: Characterization of the powder's rheology and spreading behavior

Task 1.1 Mechanical, materials, and surface characterization

As shown in characterization instruments and measured parameter Table 1, single particle nanoindentation is difficult but if successful elastic modulus (similar to stiffness K) and hardness H can be measured. Scanning electronic microscopy can be used to measure particle shape, roughness, and size-based parameters. Profilometer and interferometers can get roughness information of surfaces and thin powder layers. In concert with high-speed camera imaging, an in-house designed coefficient of restitution (COR) tester has been made to measure the COR of impacting particles.

	K	R_q	β	COR	AIF	σ_{pp}	$\sigma_{rolling}$	σ_{wall}	E	H	ϕ	cohesion	Flowability*
Nanoindenter	■								■	■			
Tribometer				■	■	■	■	■					
FT4 powder rheometer					■	■		■				■	■
Hall flow meter					■	■							
SEM		■									■		
Laser profilometer (wide area)		■											
White light interferometer											■		
COR rig	■		■										
High speed camera													

* = FT4 assesses flowability using parameter SE (i.e., specific energy) and the Hall flow meter assesses it from the Δt_{Flow}

Task 1.1 characterizing the powder flow behavior via powder **rheometry**

The powders being tested for spread and/or flow behavior using rheometry tools. *First*, experiments will be conducted with the Freeman FT4 powder rheometer. Second, a Hall flow meter will be used to analyze the flowability of the powder candidate materials. This type of flow has a free surface, and cane be qualitatively compared (for powder to powder) to the specific energy measurement in the FT4, which is for unconfined flows as found in free surface conditions. For AM, powders exhibit many properties, but the key is to determine which variable are most sensitive to good 'spreadability', namely for powders that are moving under low consolidation stress (e.g., in AM spreading).

Task 1.2 In situ characterizing the powder spreading behavior of powder materials via powder **tribometry**

The powders from the rheometer will be tested in a pin (i.e., roller, sphere, flat slider, etc.) on disk tribometer experiments (see diagram in Fig. 4). The slider can be fabricated to resemble a smaller version of the spreader in the 3D printer. The friction when spreading the slider over the powder of various states can be measured. The pin/slider can also be made with the same materials of a small silo to directly measure the friction at the powder media-to-boundary interfaces. The tribometer allows the layer height H and sliding speed V, which will be linear and reciprocating to be varied. The slider on the tribometer will be run over the different substrates, which match those of interest in the targeted industrial applications.

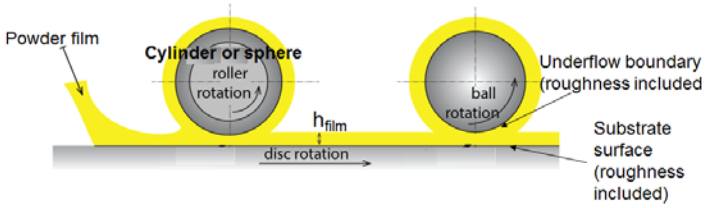

Fig 4: Pin-on-disk powder tribometery. Thin powder film on disk moves under a 'pin' (i.e., a fixed or rotational roller, sphere, or slider flat (not shown) which can be used interchangeably). A load can be applied to, or disengaged from, the pin. The coefficient of friction (COF) between the powder and relevant surfaces can be measured as a function of the surface topographies. The tribological behavior during spreading can also be obtained. This will yield detailed transient tribological (friction and wear/attrition) data for powder samples.

Task 1.3 characterizing the powder spreading behavior of powder materials via 3D printer spreading

The powders will be put in the 3D printer and spreading tests will be conducted. Spread powder layers and the underlying substrate will be characterized to examine the spread layer quality and to measure for powder layer roughness (layer height varying with position) and powder layer holes (porosity).

Phase 2: Computational Modeling of Powder Spreading

In Phase 2 of the planned research, the discrete element method (DEM) will be used to construct a computational modeling framework capable of accurately simulating the behavior of the different powder media during spreading and the resulting frictional response.

Task 2.1: Obtain 'virtual avatar' of powder media for DEM simulations

The preliminary work explained in section 3.4 will be extended to generate virtual bulks for real AM powders like Ti-64 and stainless steel. The particle sizes of such micro-powders vary from 10's to a few 100's of microns. This will result in drastic increase in the number of particles and thereby computations to be performed. These computations though large in numbers will still be simple enough to be carried out speedily on a slower processor. This type of computational burden can be economically tackled by parallelizing P-STAC to work on GPU (Graphics Processing Unit) comprising of thousands of less powerful processors instead of CPU with few highly powerful processors. So P-STAC will be upgraded to work on a GPU.

The contact model to study rheometry of real AM powders will be built on the one discussed in section 3.4 with the addition of cohesive forces and particle size effects. For a powder in a DEM framework to match a physical powder, the appropriate DEM micro-parameters—stiffness **K**, damping **β** and sliding friction coefficient **μ**—must be tuned as shown in the flowchart diagram Fig. 5. This process will involve a two-step validation where the qualitative behavior of the virtual powder is validated by performing angle of repose tests (Virtual Experiments 1 and 2) and the quantitative behavior of the virtual powder is validated by performing a confined compressive test in a virtual rheometer. Here ρ stands for density, e for coefficient of restitution, p for particle, v for vessel, i for impeller and the three possible interactions are particle-particle (p,p), particle-vessel (p,v), and particle-impeller (p,i).

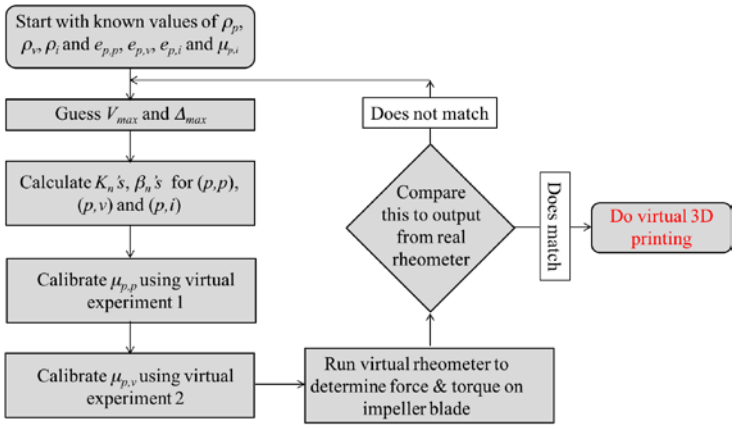

Fig. 5: DEM calibration process: Bulk behavior of virtual powders is matched to real powders by tuning the DEM stiffness and damping micro-parameters.

For particle-particle properties, the FT4 powder rheometer will be used for each candidate powder to find the internal friction angle (AIF), which can be correlated to the normal (n) and tangential (t) DEM powder stiffness **K**, sliding friction coefficient **μ**, and damping **β**; damping is determined from the coefficient of restitution (COR). COR values for micro-powders must be extrapolated from COR curves generated from FEM simulations (see PI's prior work [24]). Information on the PI's DEM approach can be found, here [25-27]. The virtual powder bulk thus obtained can be extended to in simulations of other industrial applications, such as powder spreading or small silo flow.

Task 2.2: Develop DEM simulation of spreading. This task will try to address the issue of spreadability by performing virtual spreading experiments. An outcome for this task will be to relate powder and roller/substrate surface properties to the layer properties. These relations can be obtained as a function of spreading input parameters such as layer thickness h, nominal shear rate (ratio of spread velocity U to h), etc. Figure 6 shows a DEM spreading simulation where a heap of powder is spread at different lateral speeds V_x (or U) and roller spin rates ω.

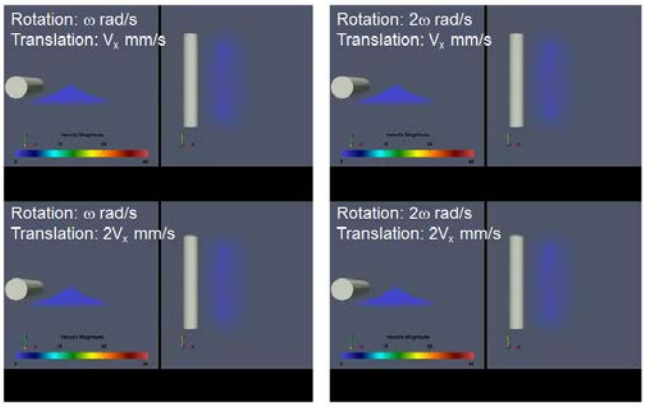

Fig. 6: DEM spreading simulations. The virtual powders can be spread in simulation to determine their layer roughness, segregation effects, layer porosity, and the effects of particle and surface properties on the thin powder layer for different shear rates (and thus regimes, e.g., quasi-static, intermediate).

Future extension of this work. This also has implications for the pharmaceutical industry as well. For example, with the correct powder rheology known from this framework, a simulation can be developed to optimize *capsule filling* or small *silo flow*.

Phase 3: Experiments: spreading thin layer powders

The goal here in Phase 3 is to validate the Phase 2 model with experiments. Spreading experiments will be conducted with the PI's 3D printer. Spreading experiments for varying parameters as shown in Table 2, where the parameters to be varied are in the left column and the values or parameter levels are in the right column.

Task 3.1: For the instances where the model and the experiments are run for the same cases, the parameter or particular numerical value is marked by an asterisk (*). Parameters such as the particle and substrate roughness (see Fig. 7) are difficult to prescribe or controllably vary so the values will be measured and used as-is as input. The spread powder layer roughness and porosity will be evaluated.

Parameters	Values
Powder materials#	Ti-6Al-4V, Stainless steel, TiO_2
Particle size* ϕ (μm)	10-250
Particle shape	Spherical*, angular, blocky
Particle size distribution (PSD)	Normal, Uniform (DEM only)
Particle roughness	As measured using SEM, AFM
Roller roughness	Low*, medium, high, textured*
Substrate roughness*	As measured by profiler
Layer height ratio*, h/ϕ_{avg}	1-10
Spread length (W)	$(50\text{-}200)\phi_{avg}$
Spreader translation speed (U)	40-100 mm/s
Nominal shear rate (U/h)	$133s^{-1}$ to $2000s^{-1}$
Roller rotation speed (ω)	-20 to 20
Model predictions	Layer roughness, packing fraction, layer porosity, segregation, spread throughput rate

* = Parameter will be modeled

= Elastic modulus, E and hardness, H vary with materials

Table 2: Experimental and modeling parametric test matrix

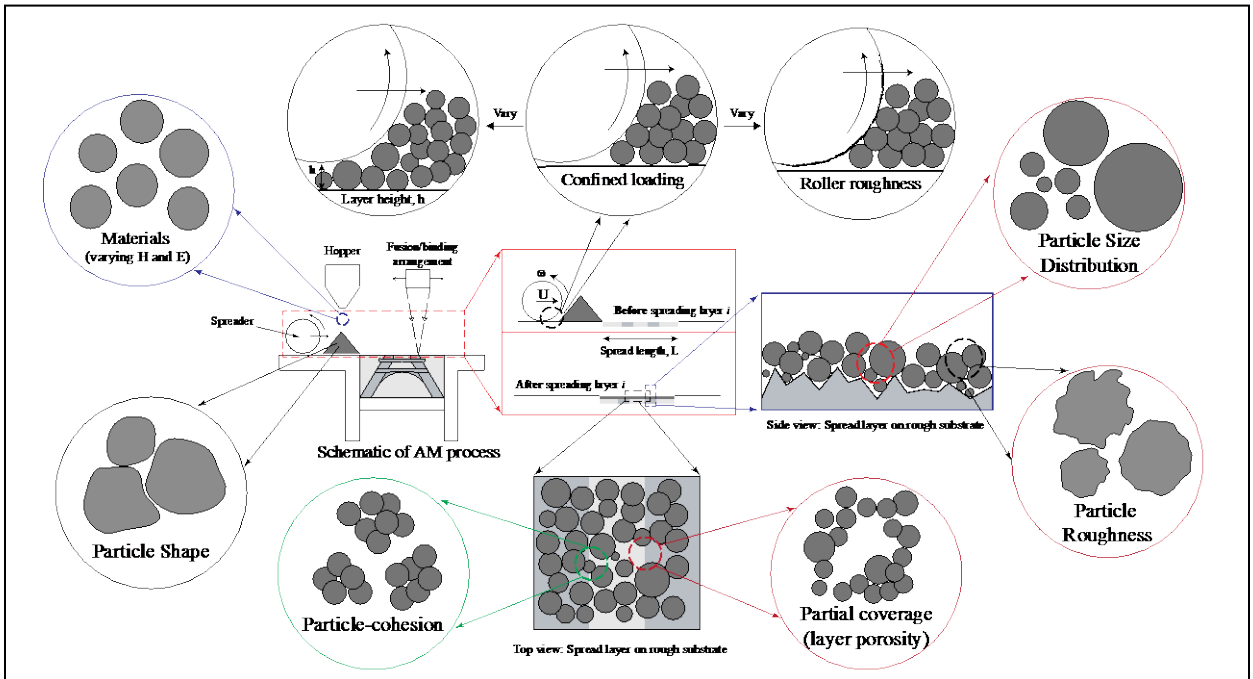

Fig. 7: Overview diagram of key parameters to be measured or modeled for powder spreading.

Task 3.2: Experimental validation of DEM spreading model

Of the various spread layer properties discussed, the only spread layer property which can be easily measured after performing spreading experiments is the mass of the powder left on the spreading coupon, M_s. Figure 8 shows an expected remaining mass M_s for the experimental spreading along with anticipated simulation results for a translation speed of 100mm/s and varying rotational speeds. As the rotational speed (in the direction of translation) increases, the interaction of the roller surface with the powder increases and thereby more energy is imparted to the powder and a decline in M_s Expected model predictions with and without probability size distributions (PSD) are also displayed, as PSD can be varied in P-STAC as well.

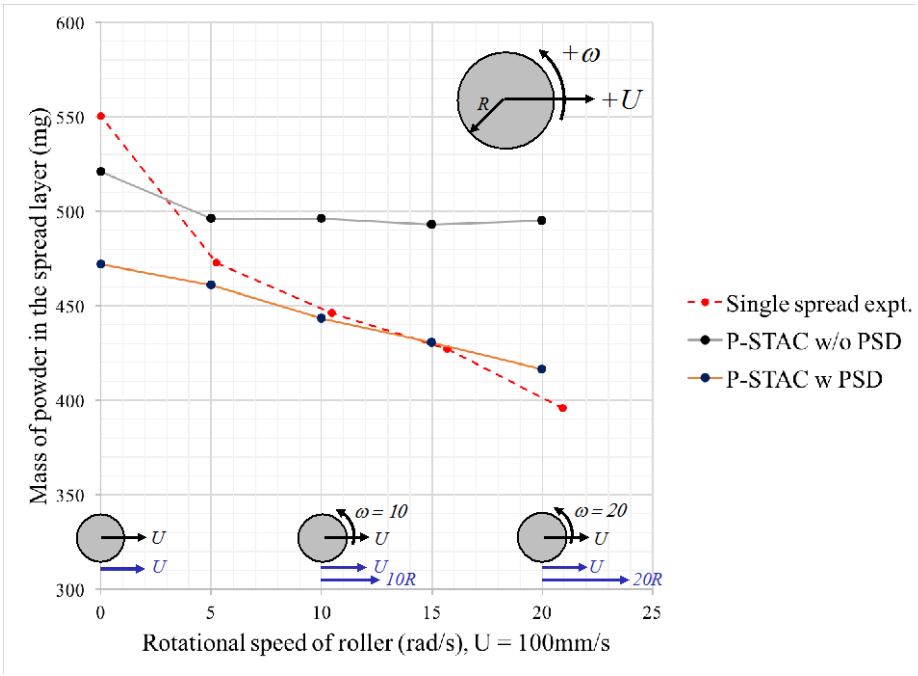

Fig. 8 Variation of spread layer property Ms with changing spreader rotational speeds: Experiments and Modeling

4. Fundamental knowledge gained from analysis of results.

This work proposes an intense experimental-modeling companion study with direct experimental validation of models to gain fundamental insights into real thin layer powder problems. This work will help describe powder flow, stress, and packing densities near boundaries. Flowability tests of powders using Hall flow meter and an FT4 powder rheometer will give some insight on powder flows with free surfaces. The project will also involve real additive manufacturing (AM) spreading experiments using a commercial 3D printer. Further, industrially-relevant powder flow characterization techniques such as powder rheometry and tribometry (measuring friction behavior of powders sliding against each other and against substrate surfaces) will be employed for studying flows at boundaries.

In AM spreading, there is exist spreading powders, which are effectively powders under low consolidation stress. Powder of different cohesivity will be sought from IFPRI member companies to assess their effect on spreading, as cohesion causes flow intermittences and possible segregation. The problem of powder spreading (via the 3D printer) and mixing (via the FT4) is governed by boundary-layer physics. The metrology tools the PI proposes to use (see APPENDIX for equipment available at Rice University for this work) appropriate for this work with powders in thin-layer flows. Experimental validation in this work will primarily relate to controlled layer thickness, which is a variable parameter in the 3D printer for use in this study. As shown in Table 2, the modeling and experiments proposed in this work will be able capture a range of particle size, shape and materials (and thus varying densities) and mechanical (e.g., hardness, elastic modulus) and surface properties (roughness). This work specifically

addresses flows involving thin layers of particles, where the ratio of layer thickness to particle diameter (h/f) is 1 -10, and the powder layer is spread over a length of 50 – 200 particle diameters. The nominal shear rates (U/h) are expected to create varying flow regimes from quasi-static to intermediate flows.

Management and Timeline

The PI will advise research assistants to conduct the proposed research. Additionally, they will continue to work with undergraduate researchers, who will assist with lab experiments, and parametric studies. Each four-month period is shown as "*Tri*" in **Table 3** below. The black bars indicate the proposed work period.

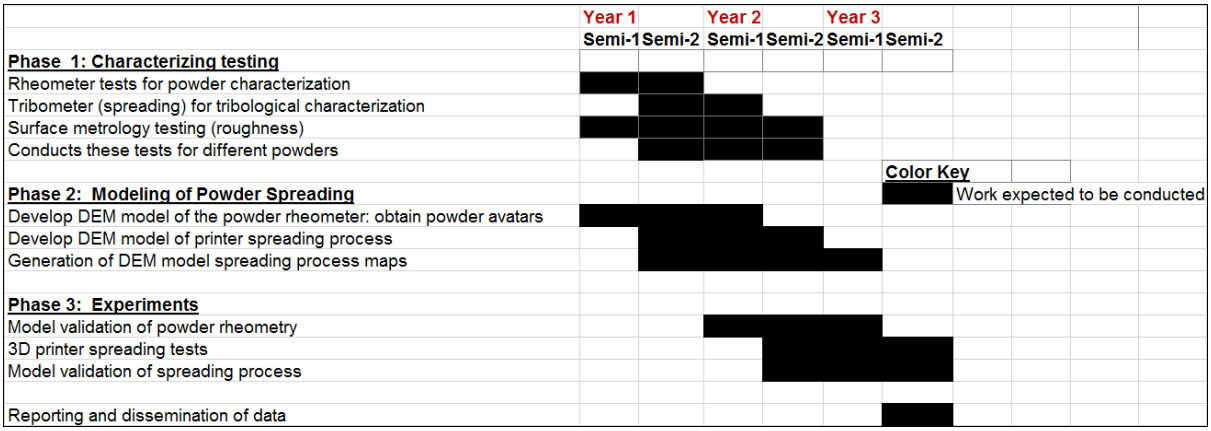

Table 3: Gantt chart with the milestone and objectives for the three research phases.

Research Output

Research goals include voluntarily sharing with the IFPRI and AM/granular community: (i) particle, substrate surface, and spreading experimental data, (ii) model validation approaches and data, (iii) and our summary report. This research is expected to lead to follow-on research through the NSF GOALI (university-industry) program.

References

1. Mort, P., Michaels, J. N., Behringer, R. P., Campbell, C. S., Kondic, L., Langroudi, M. K., ... & Wassgren, C. (2015). Dense granular flow—A collaborative study. Powder Technology, 284, 571-584.
2. Bertrand, P.H., F. Bayle, C. Combe, P. Goeuriot, and I. Smurov, Ceramic Components Manufacturing by Selective Laser Sintering. Applied Surface Science, 2007.
3. Gu, D.D., W. Meiners, K. Wissenbach, and R. Proprawe, Laser Additive Manufacturing of Metallic Components: Materials, Processes, and Mechanisms. International Materials Reviews, 2012. 57(3): p. 133-164.
4. Pereira, M. and U. Thombansen. Contributions for the next generation of 3D metal printing machines. in SPIE LASE. 2015. International Society for Optics and Photonics.
5. Frazier, W.E., Metal additive manufacturing: a review. Journal of Materials Engineering and Performance, 2014. 23(6): p. 1917-1928.
6. Radl, S., Brandl, D., Heimburg, H., Glasser, B. J., & Khinast, J. G. (2012). Flow and mixing of granular material over a single blade. Powder technology, 226, 199-212.
7. Higgs, C. F., & Tichy, J. (2008). Effect of particle and surface properties on granular lubrication flow. Proceedings of the Institution of Mechanical Engineers, Part J: Journal of Engineering Tribology, 222(6), 703-713.
8. Higgs, C. F., & Tichy, J. (2004). Granular flow lubrication: continuum modeling of shear behavior. TRANSACTIONS-AMERICAN SOCIETY OF MECHANICAL ENGINEERS JOURNAL OF TRIBOLOGY, 126(3), 499-510.
9. Haeri, S., Wang, Y., Ghita, O. and Sun, J., 2017. Discrete element simulation and experimental study of powder spreading process in additive manufacturing. Powder Technology, 306, pp.45-54.
10. Herbold, E.B., Walton, O. and Homel, M.A., 2015. Simulation of Powder Layer Deposition in Additive Manufacturing Processes Using the Discrete Element Method (No. LLNL--TR-678550). Lawrence Livermore National Lab.(LLNL), Livermore, CA (United States).
11. Mindt, H.W., Megahed, M., Lavery, N.P., Holmes, M.A. and Brown, S.G.R., 2016. Powder bed layer characteristics: the overseen first-order process input. Metallurgical and Materials Transactions A, 47(8), pp.3811-3822.
12. Parteli, E.J. and Pöschel, T., 2016. Particle-based simulation of powder application in additive manufacturing. Powder Technology, 288, pp.96-102.
13. Sun, C.C., Setting the bar for powder flow properties in successful high speed tableting. Powder technology, 2010. 201(1): p. 106-108.
14. Higgs III, C.F. and E. Wornyoh, An In Situ Mechanism for Self-replenishing Powder Transfer Films: Experiments and Modeling. Wear, 2008. 264(1-2): p. 131.
15. Wornyoh, E.Y.A. and C.F. Higgs III, An asperity-based fractional coverage model for transfer films on a tribological surface. Wear, 2011. 270(3-4): p. 127-139.
16. Higgs, C.F. and E.Y.A. Wornyoh, An in situ mechanism for self-replenishing powder transfer films: Experiments and modeling. Wear, 2008. 264(1-2): p. 131-138.
17. Wornyoh, E.Y.A. and C.F. Higgs III. Self-replenishing, self-repairing solid lubrication: Modeling and experimentation. 2005. Washington, D.C., United States: American Society of Mechanical Engineers, New York, NY 10016-5990, United States.
18. Terrell, E.J. and C.F. Higgs, A particle-augmented mixed lubrication modeling approach to predicting chemical mechanical polishing. Journal of Tribology, 2009. 131(1): p. 012201.
19. Mpagazehe, J.N., G.A. Thukalil, and C.F.H. III. A Study to Estimate the Number of Active Particles in CMP. in Materials Research Society Spring Meeting. 2009. San Francisco, CA.
20. Mpagazehe, J.N., G.A. Thukalil, and C.F.H. III. A Multi-Physics Computational Framework to Predict Dishing and Erosion in Patterned Wafers. in ASME/STLE 2009 International Joint Tribology Conference (IJTC2009) 2009. Memphis, Tennessee, USA

21. Mpagazehe, J.N., A.F. Queiruga, and C.F.H. III, Towards an Understanding of the Drilling Process for Fossil Fuel Energy: A Continuum-Discrete Approach. Tribology International, 2012, submitted.
22. Marinack Jr., M.C., J.N. Mpagazehe, and C.F. Higgs III, An Eulerian, Lattice-based Cellular Automata Approach for Modeling Multiphase Flows. Powder Technology, 2012. 221: p. 47-56.
23. McCarthy, J.J., V. Jasti, M. Marinack, and C.F. Higgs, Quantitative validation of the discrete element method using an annular shear cell. Powder Technology, 2010. 203(1): p. 70-77.
24. Marinack Jr, M.C., B.G. Gaudio, R.E. Musgrave, C.E. Rizzo, M. Lovell, and C.F. Higgs Iii. Coefficient of restitution testing: Explicit finite element modeling and experiments. in STLE/ASME 2010 International Joint Tribology Conference, IJTC2010, October 17, 2010 - October 20, 2010. 2010. San Francisco, CA, United states: American Society of Mechanical Engineers.
25. Marinack, M.C., J.N. Mpagazehe, and C.F. Higgs, An Eulerian, lattice-based cellular automata approach for modeling multiphase flows. Powder Technology, 2011.
26. Mpagazehe, J.N., A Physics-Based, Eulerian-Lagrangian Computational Modeling Framework to Predict Particle Flow and Tribological Phenomena, in Mechanical Engineering2013, Carnegie Mellon University.
27. Mpagazehe, J.N., A.F. Queiruga, and C.F. Higgs Iii, Towards an understanding of the drilling process for fossil fuel energy: A continuum-discrete approach. Tribology International, 2013. 59: p. 273-283.
28. Desai P., Dougherty P. and Higgs III C. F., Towards an understanding of the spreadability of metal additive manufacturing (AM) powders, RAPID Conference, 2016.
29. Zhang, W., Mehta, A., Desai, P., Higgs, C. F., “Machine Learning-enabled Powder Spreading Process Maps for Metal Additive Manufacturing (AM)”, 2017 Solid Freeform Fabrication Symposium Proceedings, 2017.

Fascilities and Equipment

(Below is the equipment for coPI Higgs' Particle Flow & Tribology Lab at Rice University)

Nvidia GPU cluster for modeling

Multiphysics modeling simulations with the coPI's in-house modeling software, the Particle-Surface Tribology Analysis Code (P-STAC), are carried out using GPU-based nVIDIA GeForce GTX 970 graphics card on a multicore computer platform.

Granular shear cell (GSC)

This granular shear cell helps to study the flowing and shearing behavior of grains between relatively moving surfaces. This cell allows one to study the grain flow velocity, solid fraction, granular temperature (i.e., velocity fluctuation), energy dissipation during flow, and slip velocities.

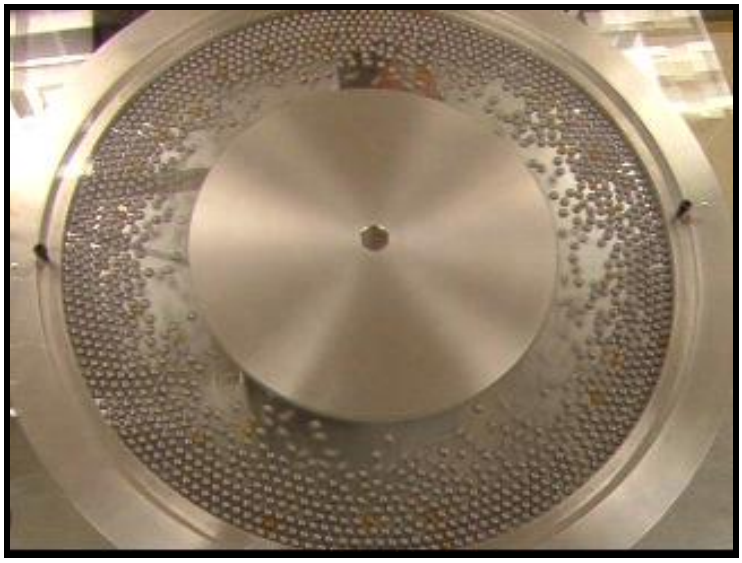

Granular shear cell (gravity acts into page)

To impose shear on test grains within the GSC, the inner rotating wheel has can be given a prescribed roughness. The GSC has an aluminum frame with a transparent body so that the dynamic behavior of the grain flow can be observed using high-speed photography where the particle position and velocimetry data are known as a function of time. The moving wheel is attached to a 1/16 HP motor capable of achieving rotational speeds of 53–280 rpm, which corresponds to a linear velocity of 0.55–2.89 m/ s.

Vision Research's Phantom VEO® 710S (High-speed camera)

Vision Research's Phantom VEO® 710S high-speed camera is compact, rugged and fully equipped for research, namely traditional and advanced imaging applications.

The VEO 710 is the fastest VEO model and features a one megapixel sensor with over 7 Gigapixels/second (Gpx/s) throughput. This translates to the ability to record up to 7,400 frames-per-second (fps) at its full 1280 x 800 resolution, or over 8,200 fps at 720p HD. The top speed at reduced resolution is 680,000 fps standard or 1,000,000 fps via the FAST option, which also provides exposure times as low as 300 nanoseconds. With the RAM configuration of 72 GB, at 7,400 fps the VEO 710 provides over six seconds of record time.

All Phantom VEOS 710S camera model includes everything needed for traditional software-based capture and motion analysis. It also includes additional signal availability, on-camera controls, ruggedized connectors and compatibility with removable CFast 2.0 storage media. Lastly, it includes HD-SDI and HDMI outputs and a versatile Programmable I/O infrastructure.

Phantom VEO 710S

- Small, rugged, powerful high-speed camera
- 7Gpx/second throughput, 1 Megapixel resolution
- 7400 frames per second (fps) at 1280 x 800
- 72GB RAM
- Exposure Index range: Mono- Color
- FAST option (1M frames/sec)

.

Applications include slurry (multiphase) flows, tribology debris generation, fluid dynamics, biomechanics, material test, airbag development and test, microscopy and granular flow. The high-speed CCD camera is used to capture images of granular media data such as solid fraction, particle velocity, and slip.

Particle attrition tester (PAT)

A particle attrition tester (PAT) allows test particles to be sheared in sliding contacts under load and high-shear to induce attrition or particle wear for the test materials. The PAT works similar to a journal bearing in that the center shearing wheel imposes a load on to the grain materials as they are sheared. The varying eccentricity between the inner rotating wheel and the outer stationary ring depends on the dynamic state of the granular materials in the interface. Thus, grains are entrained into a high-load, high-shear zone which causes high contact stresses within the grain flow, which leads to particle fracture and attrition. The PAT allows different loads and shear rates to be applied to the granular material. Following the PAT tests, particles are characterized for surface and bulk damage, and attrition levels are measured.

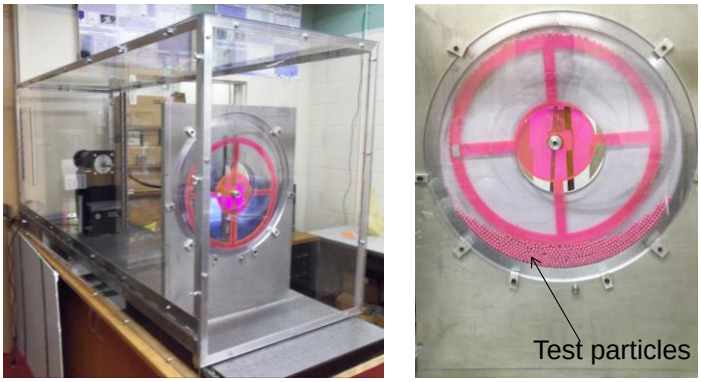

Particle Attrition Tester (PAT)

Impact and Coefficient of restitution (COR) tester

Single granular particles can be dropped from various heights and COR based on height or velocity is computed. The apparatus is used to measure the coefficient of restitution (COR) between colliding materials. The figure shows a photograph (a) and an annotated diagram (b) of the experimental apparatus. In the right figure b, the labeled components (A – G) are defined as a Plexiglas casing (G), air hose/pump (E/F), base plate and plate holder (A and B), sphere being tested (D), and device for holding the sphere being dropped (C). The casing (G) provides holes which fix the

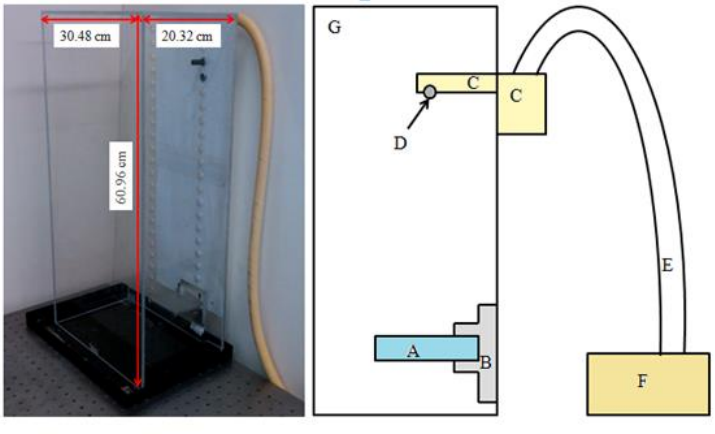

Coefficient of Restitution (COR) Tester

holding device (C) in place at different heights. The air hose/pump (E/F) provides a suction force to the holding apparatus (C), which is turned on to hold a sphere (D) in place, and then switched off to allow the sphere to drop from rest. This type of setup minimizes spin during the drop. The base plate (A) is secured in place at the bottom of the apparatus by a holder (B). This plate is what the test particle or sphere collides with during each trial. Consequently, the COR can be obtained between the sphere and plate materials.

Advanced multi-scale load & speed tribometer

The RTEC Multi-functional Tribometer is specifically designed for multiple modes of tribometery across multiple scales of force and speed. It performs complex, automated synchronized control of several specimen motions. It can switch from linear to rotational.

Multi-functional tribometer from RTEC

- Load: mN to 8000N
- •In-line optical profilometers and imaging
- •Reciprocating frequency: 0 to 300 Hz
- •Rotational speed: 0 to 10000 RPM
- •Temp: -60 to 1000C
- •Environment: 5 to 95% RH, Inert gas
- •Multiple ASTM/ DIN/ ISO standards
- •Rotary, reciprocating
- Measurements:
  - Wear, Friction, Hardness, Fatigue, Wear life, Surface roughness, Adhesion, Cracks, Chemistry

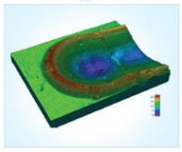

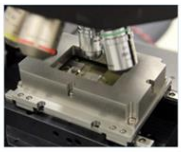

Bruker UMT-3 Multi-Scale Tribometer

Conidered by some to be the state of art tribometer, the MFT is used for measuring the friction, lubrication, and wear behavior in sliding contact.

A Hysitron "TriboIndenter" 980 Nanoindenter

The Hysitron "Triboindenter" (TI) 980 is a nanoindenter that performs mechanical nano-characterization and measurements of 3D surface topography of particles and surfaces using scanning probe measurement (SPM) capabilities. TI 980 TriboIndenter®

The World's Most Powerful Nanomechanical & Nanotribological Test System for All Your Material Analysis Needs

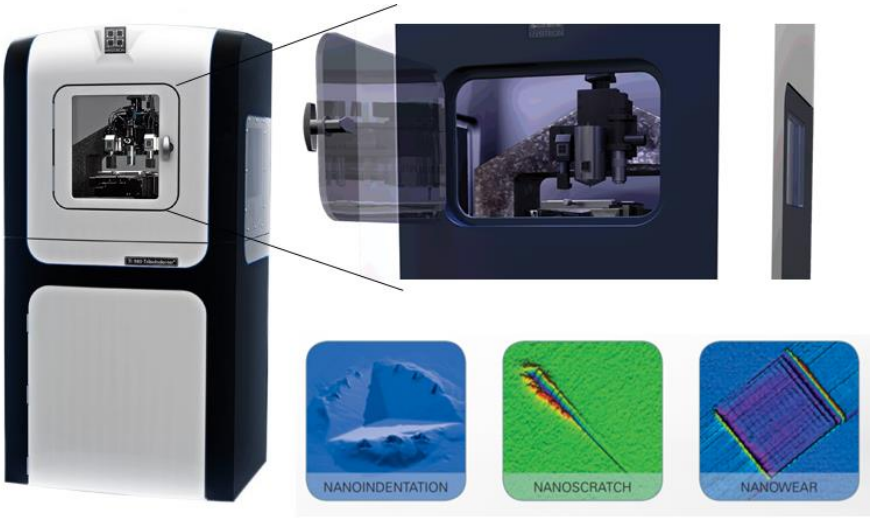

A Hysitron "TriboIndenter" 980 Nanoindenter

The TI 980 TriboIndenter is Hysitron's latest, most advanced nanomechanical test instrument that lies at the intersection of maximum performance, flexibility, reliability, usability, and speed. The TI 980 Nanoindenter is the next-generation of Hysitron's renowned TriboIndenter product family, building upon decades of technological innovation to deliver a new level of extraordinary performance, enhanced capabilities, and ultimate versatility in nanomechanical and nanotribological characterization.

Features include:

- Force and displacement noise floors that enable nanomechanical and nanotribological characterization to the low end of the nanoscale
  - Capacitive Transducer Noise Floors: 20nN force, 0.1nm Displacement
  - Hysitron's xProbe™ Transducer Noise Floors: 1nN Force, 0.01nm Displacement
- Powerful base configuration includes quantitative nanoscale-to-microscale indentation, nanoscratch, nanowear, high resolution in-situ Scanning Probe Microscopy imaging, dynamic nanoindentation, and high speed mechanical property mapping
- Accelerated Property Mapping for fast nanoindentation for rapid, high-resolution property mapping and statistically significant data sets
- SPM^{+} high resolution *in-situ* Scanning Probe Microscopy imaging enables nanometer precision test placement accuracy and characterization of post-test deformation behavior
- Tribo iQ™ software enables adaptable data analysis and reporting, with user-writable analysis modules that are shareable amongst the Hysitron community

Bruker Optical Profilometer

The Countour GT-K1 white light interferometer is for characterizing and quantifying surface roughness, step heights, critical dimensions, and other topographical features with excellent precision and accuracy. All measurements are nondestructive, fast, and require no sample preparation. Profile heights ranging **down to sub-1nm** at high speeds, independent of surface texture, magnification, or feature height.

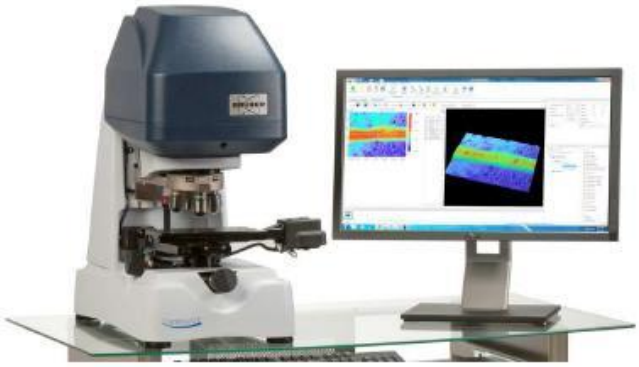

Countour GT-K1

Bruker Atomic Force Microscope

MultiMode8 with SPM with Application Module-ready Optical Head performs major SPM imaging techniques including PeakForce Tapping, ScanAsyst contact and non-contact atomic force, lateral force, and TappingMode (air) without additional hardware. On axis tip view head,2mm x 2mm range sample stage accepts samples up to 15mm diameter and 6mm thick. The AFM can be operated in an environmental chamber with:

Standard Imaging

- Basic Contact AFM and DFM
- Lateral Force Microscopy (LFM)
- True Non-Contact AFM

Chemical Properties

- Chemical Force Microscopy with Tip
- Electrochemical Microscopy

Dielectric/Piezoelectric Properties

- Electric Force Microscopy (EFM)
- Dynamic Contact EFM (DC-EFM)

Electrical Properties

- Conductive AFM (Ultra-Low & Variable Current)
- Scanning Capacitance Microscopy (SCM)

In-liquid Imaging

- Ion Conductance Microscopy (ICM)

Magnetic Properties

Bruker Multimode 8
Atomic Force Microscope
(AFM)

Chemical mechanical polishing (CMP) R&D test machine *(G&P POLI-300)—Coming Soon*

Chemical mechanical polishing (CMP) is a complex process in which a wafer surface is planarized by mounting it on a rotating chuck and pressing it against a rotating pad that is flooded with slurry consisting of a fluid and abrasive nanoparticles.

CMP R&D machine (*G&P POLI-300)*

The GNP POLI-300 is designed for R&D CMP process development applications such as integrated circuits, MEMS, as well as CMP parametric study.

Specifications:

- Head, Table: 30~200 rpm, Rotational Motion, Head Oscillation (±12mm)
- Size: 960W * 1000D * 1950H mm
- Table Size: Φ 406 mm (16 inch)
- Pressing Method: Variable Air Pressure Electronic Controller
- Carrier Type: 70~700 g/cm2 (1 psi ~ 10 psi) for 4" Wafer
- Membrane Type: 50~500 g/cm2 (0.7psi ~ 7 psi)

Options:

- Conditioning: Oscillating Head Type or Swing Arm Type
- Double Head System
- Friction Force & Temperature Monitoring System

Applications:

- Workpiece: Max 6 inch wafer, MEMS Structure, Coupon Wafer
- CMP Process: Si CMP, Oxide CMP (BPSG, TEOS, SC), Metal CMP (W, Cu), STI.

Particle rheometer

The FT4 Powder Rheometer® was designed to characterise the rheology, or flow properties, of powders. This remains a primary function today, but the instrument, accessories and methodologies have been continuously developed to the point where the FT4 is now considered a universal tester.

Freeman Particle rheometer

In addition to the dynamic methodology, where a powder's resistance to flow is measured whilst the powder is in motion, the FT4 also includes a shear cell for measuring the powder's shear strength, a wall friction kit to quantify how a powder shears with respect

to the surfaces of process equipment (in accordance with ASTM Standard D7891), as well as accessories for measuring bulk properties, such as density, compressibility and permeability. This range of measurement capabilities makes the FT4 a truly universal powder tester and the world's most versatile instrument for measuring and understanding powder behavior.

Fluid Erosion Jet tester

Erosive wear is caused by the impact of particle-laden fluid jets impinging on a solid surface. Erosion leads to loss of material, bio-films, or coatings.

The Ducom Fluid Jet Erosion Tester facilitates determination of wear rates under wide range of conditions. Wear rate can be used to identify the best material under given operating conditions. It can also be used to predict service life and life cycle costs.

Ducom Fluid Jet Erosion Tester

Erosive wear is caused by the impact of particles air jet impinging on a solid surface. Erosion leads to loss of life of components in aerospace, gas turbines, boilers and power plants. In order to maximize life, proper selection of materials used in such applications is required.

The Fluid Jet Erosion Tester facilitates determination of wear rate under wide range of conditions. Wear rate can be used to identify the best material under given operating conditions. It can also be used to predict service life and life cycle costs.

Powder-bed 3D printer and supplement AM equipment

Additive Manufacturing Equipment

3D Printer

- Ink jet binder printer
- Powder bed based
- Metal and Non-Metal part

Metals

- Stainless Steel
- IN Alloy
- Iron/Bronze
- Cobalt-Chrome
- Tungsten carbide, Tungsten

Non-Metals

- Ceramic beads
- Sand
- Zircon
- Soda lime glass

ExOne Powder-bed 3D printer

Powder rheometer

Light-gas gun

A light-gas gun is used to accelerate small projectiles to hypervelocity. The gun consists of two stages: 1) a chamber in which helium or hydrogen is compressed to high pressure, and 2) a long barrel with very low, near vacuum pressure.

A rupture disk separating the two stages eventually fails at sufficiently high pressure in the first stage. The pressured light-gas rapidly expands into the vacuum barrel, which propels a projectile down the barrel towards a target. The projectile can be accelerated to a velocity as fast as 8 km/s.

The light-gas gun can be used to study micrometeriod and space debris impact on orbiting and reentry spacecraft.

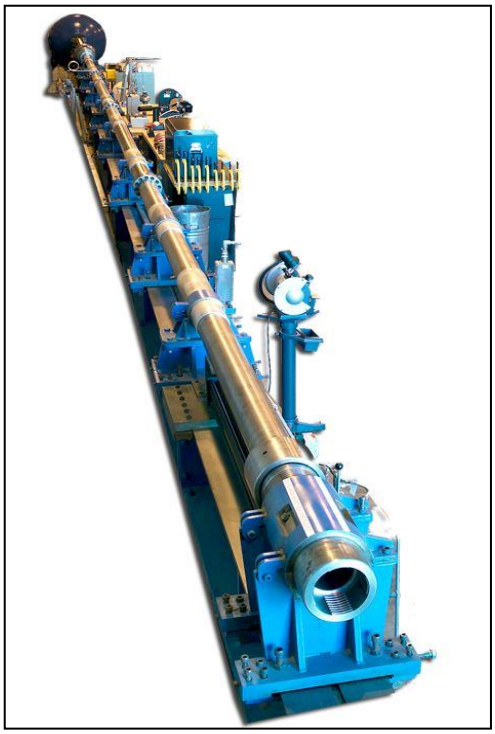

GPU Workstation

A GPU optimized workstation was constructed to perform computations using the PFTL's parallelized, in-house Multiphysics framework, P-STAC (particle-surface tribology analysis code). GPU parallelization uses thousands of cores within a graphical processing unit to carry out parallel workloads. The specifications for the GPU workstation constructed for use in the PFTL are:

- 2 x nVIDIA GTX 1070 GPU
- Intel i7 processor (6 cores @ 3.4 GHz)
- 2 x 16 GB RAM
- 512 GB SSD
- 2 x 3 TB HDD

PFTL Microfabrication Station

PI Higgs has a hood-based microfabrication station, which is a fully autonomous soft-lithography laboratory, which allows for the fabrication of complex microfluidic channels. Completely bypassing expensive cleanroom environments, microfluidic channels containing features down to ~6 um may be fabricated with this setup. The station features the primary components that are typically found in most soft-lithography stations; however, they are all contained within a single fume-hood rather than a cleanroom. A spin coater is used for dispersing SU-8 onto a silicon wafer at extremely precise thicknesses. The digital hotplate is used for the many baking steps required, and a user-friendly UV light system exposes the SU-8 that is revealed from under a custom-designed photomask. A PDMS mixture is poured over the SU-8 mold and is allowed to cure in a special oven. Finally, to close the flow network, the PDMS chip is bonded to a glass slide via an advanced plasma treatment system.

BlackHole Lab Full Soft-Lithography Fabrication Station

SEA Co-op: KSV CAM 200 Optical Tensiometer

(Surface tension, surface energy, contact angle measurement and droplet formation analysis)

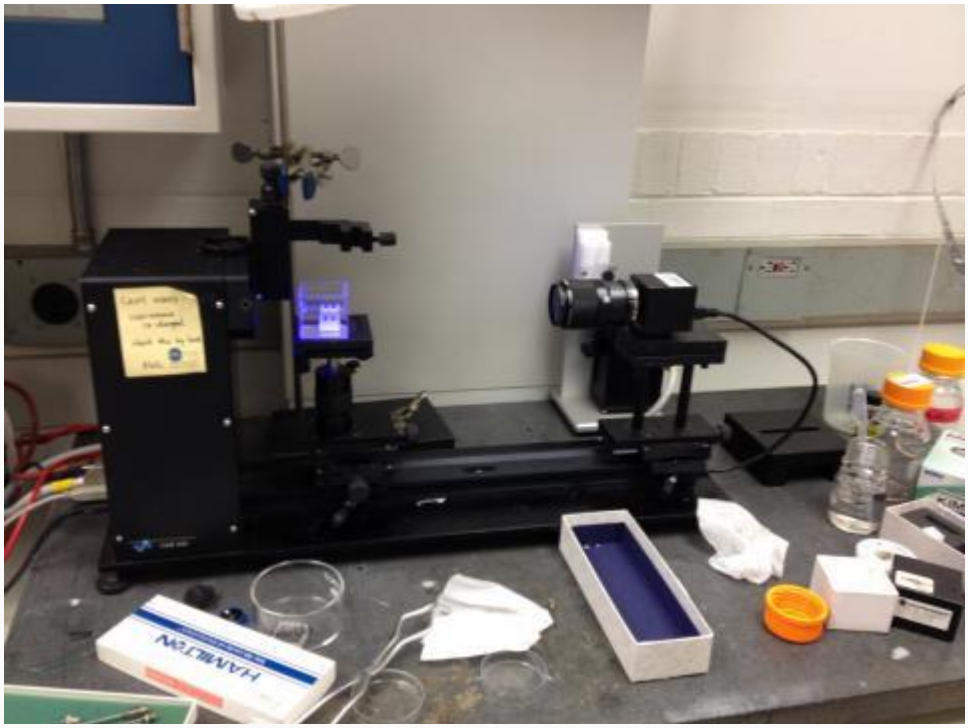

The KSV CAM 200 Optical Tensiometer is a fully computer controlled instrument based on video capture of images and automatic image analysis for measuring static or dynamic contact angles, **surface or interfacial tensions of liquids**, surface free energies (γ), and absorption of liquids into porous materials. This instrument is a part of the Rice University BRC Instrument Cooperative.

Rice Shared Equipment Authority (SEA)

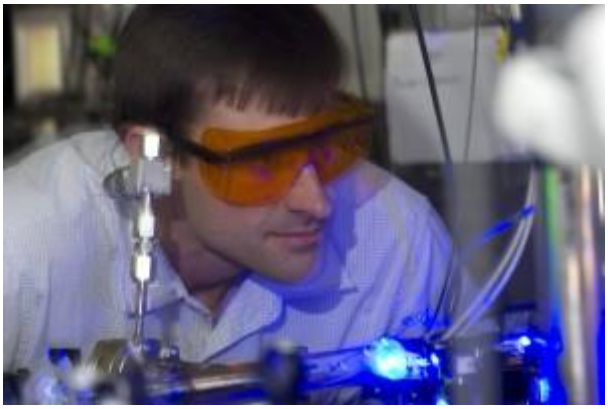

Tom Killian

As today's researchers in science, engineering, and medicine seek to address ever more complex problems, they require access to an increasingly robust research infrastructure. Recognizing this critical need, Rice University established the Shared Equipment Authority (SEA) in 2001 as a way to provide its faculty superb experimental facilities, research equipment, and support services at an affordable cost.

The SEA's management structure is an innovative one. The Authority is governed by an active group of faculty who are committed to the principles of shared infrastructure and fiscal responsibility. These faculty oversee and manage more than 85 pieces of highly sophisticated research equipment, develop administrative policies governing the operation of this equipment, and set schedules and fees for use of it.

Rice's research infrastructure includes the following categories of shared equipment:

- X-ray diffraction
- Optical microscopy
- Electron microscopy
- Scanning probe microscopy
- Optical spectroscopy
- Nuclear magnetic resonance
- Mass spectrometry
- Thermal analysis
- Clean room class 100/1000
- Micro/nano fabrication

The SEA has been awarded state, federal, and industry funds totaling more than $18 million, and continually strives to raise additional funds to expand the categories – and quality – of shared equipment available for faculty.

Complementing the SEA's work in managing shared equipment is a team of 10 full-time professional Research Scientists who run and maintain the equipment, set and enforce safety procedures, educate and train users, and provide research assistance. In short, these research scientists, whose positions are supported by the University, provide users with outstanding service for shared equipment.

To ensure maximum and fair use of the shared equipment, the SEA created a flexible framework so that both Rice researchers and their many colleagues in the Texas Medical Center and in Houston's larger academic and commercial research and development community may easily access and use this equipment. A welcome result has been the development of new and productive collaborations among researchers across multiple disciplines and institutions.

The SEA's effectiveness and efficiency in managing Rice's shared equipment has been nationally recognized. The National Research Council has pointed to Rice's SEA as a model for midsize research universities seeking to maintain and grow their shared instrumentation (NRC, Midsize Facilities: The Infrastructure for Materials Research, National Academies Press, 2006, pp 53-56). Today, the SEA continues to maintain the high standards and exemplary service that led to this recognition.

INSTABILITIES OF FLOWING COHESIVE GRAINS AND POWDERS

Pr. Nicolas Taberlet
University of Lyon, France
Physics Laboratory ENSL

In this project, I propose to study the instabilities of powders and grains flowing on an inclined plane. Namely, I propose to study the roll waves and traffic waves instabilities in thin flowing layers of powders and granular material, through laboratory-scale experiments as well as DEM simulations. Such instabilities are of great fundamental interest but can also be the cause of malfunctioning in industrial processes such as additive manufacturing.

IFPRI Call for Proposals

I. State of the art and Scientific goals

At the frontier between physics and mechanics, the flow of powders and granular materials has become a very active research domain [1-4]. The behavior of assemblies of particles can be very complex. Indeed, even in the simple case of dry cohesionless particles, where the mechanical properties of the material are only controlled by the momentum transfer during collision or frictional contacts between grains, a universal constitutive law is still lacking. Moreover, capillary forces, van der Waals forces or viscous interactions render the mechanical behavior of cohesive powders even more complex and difficult to model [5-7].

The project I would like to develop consists in studying the instabilities that exist in shallow granular flows. Flow instabilities are of fundamental interest but are also of great importance for industrial processes as they create large fluctuations in the flow rate (or discharge rate) and may cause clogging and jamming.

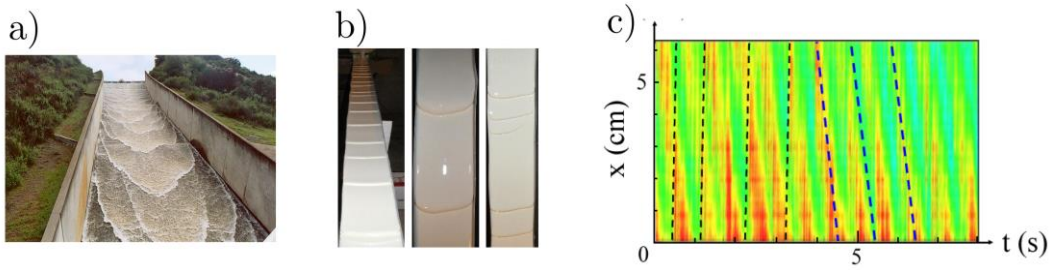

Figure 1. a: Roll waves in a shallow flow of water [10]. b: Roll waves in flow of cornstarch mixtures [11]. c: Traffic waves in granular flows (N. Taberlet).

Roll waves are a classical instability of shallow liquid flows. When a thin layer of water flows down an inclined plane, the surface may become unstable and surge waves, which travel faster than the average speed of the flow can develop (see Figure 1a). This phenomenon is known to exist in viscous and complex fluid (Fig. 1b shows roll waves in flowing mixtures of cornstarch) as well as in dry granular material (see references [8,9]). I propose to bridge the gap between the complex fluids and the dry cohesionless granular material by studying the conditions under which roll waves appear in thin flowing layers of cohesive powders and grains. The phenomenon will be investigated through numerical simulations as well a laboratory experiments.

A second type of instability can occur in shallow granular flows. Recently, I observed waves at the surface of an inclined plane flow traveling against the direct of the flow (see Fig. 1c). In this figure, *x* is the position along the direction of the flow and the colors encode the thickness of the flowing layer. Periodic oscillations of the thickness are clearly visible but the most striking feature is that these waves travel upstream (the oblique lines indeed indicate that the propagation is against the direction of the flow). Such upstream waves are reminiscent of traffic waves which occurs on congested roads [12]. Again, I will investigate, both experimentally and numerically, the conditions under which such granular traffic flow appear and fully characterize their physical properties (amplitude, velocity, dispersion…).

II. Experimental and numerical tools

a. Experimental techniques

I will study the instabilities of cohesive powders and grains flowing over an inclined flat surface (smooth and/or rough) between confining walls. This configuration has proven to be a reliable tool for probing the rheological properties of flowing granular matter [6]. It allows one to easily vary quantities such as the flow rate, the thickness and density of the flowing layer of material. Figure 2 shows a variety of experimental setups I have built and used in the laboratory in recent years.

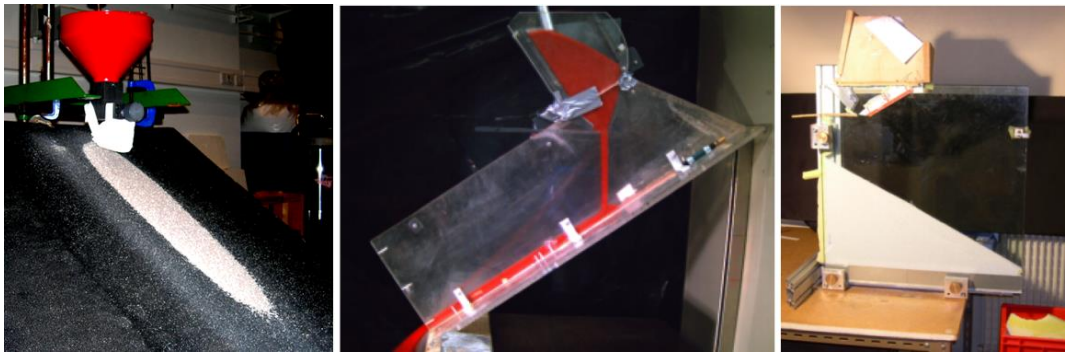

Figure 2. Variety of experimental setups developed by the author of this proposal for the study of granular and powder flows. From left to right: unconfined flows over a rough surface, shallow flow over an incline, flow over an erodible sand-bed.

The velocity profiles will be obtained through Particle Imaging Velocimetry (PIV) using a fast camera (such as the Phantom VEO4K 590L), monitoring the flow both directly from above and from the side through transparent side-walls. Measurements of the thickness of the flow (which is expected to fluctuate quickly when roll waves have developed) will be achieved using a laser scanner such as the Micro-Epsilon scanCONTROL 2900-100, which allows one to measure the profile at a rate of 300 Hz and with an accuracy of 12 µm. The boundary bottom plane will be equipped with force sensors (Honeywell FSG15N1A and Omega LCMKD-2KN) which can simultaneously measure the normal and tangential stress applied by the flowing material onto the base.

The cohesion of the material at rest can be determined through classical bi-axial or tri-axial compression but my research group is equipped with two rheometers (Anton Paar MCR 102 and TA Instruments AR 2000) which can also be used to measure the internal cohesive stress of material under an applied shear stress. Recently, while studying the Washboard Road instability [13], I have used a simpler method for measuring the cohesive stress of a powder. A variable normal stress is applied onto a plane resting on the material and the tangential force required to create a slippage is measured. The results are in excellent agreement with more complex experimental methods.

b. Discrete Element Method for numerical simulations

In this project, I will use the soft-sphere molecular dynamics method, one of the Discrete Elements Methods (DEM). This method deals with deformable frictional grains colliding with one another. Although not flawless, it has been widely used in the past two decades and has proven to be very reliable [14-15].

The DEM method aims at simulating granular assemblies using physical laws, rather than ad hoc rules (as opposed to cellular automata for instance). When two grains collide, they experience a repulsive elastic normal force, given by Hertz' law, and a dissipative term is added in order to model the inelasticity of the collisions. Grains also experience a tangential force (based on the Cundall and Strack model [16]) which models a history-dependent solid friction and which allows residual stress to be maintained within the simulated material. The method is time-driven and the position, velocity and rotation speed of all grains are simultaneously (unlike in Monte-Carlo simulations) calculated using Newton's law of mechanics at the next time step using the forces and torques acting on each individual grain.

I have been using this method actively in the past decade and the numerical results I have obtained are essential elements to 25 of my 50 publications in peer-reviewed journals. Figure shows a few examples of physical phenomena that I have simulated using the DEM method (gravity driven flows, flow in a rotating tumbler, fluidized beds).

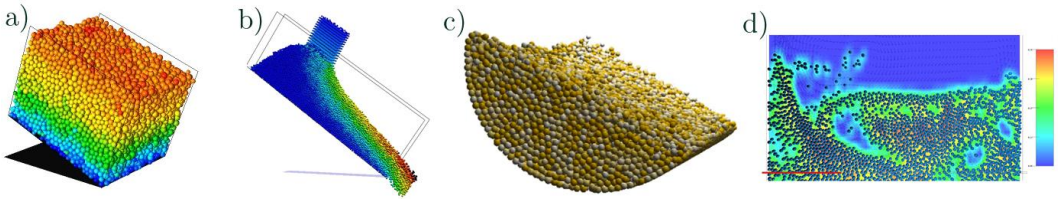

Figure 3: Examples of DEM simulations by the author of this proposal. a) and b): gravity-driven flows, c): flow in a rotating tumbler and d): fluidized bed (granular suspension)

One of the great advantages of DEM simulations is that all parameters can be varied easily. One can choose the size distribution over a wide range, a variety of shapes can be simulated by "gluing" particles together and the mechanical properties of the material (friction, elastic modulus, inelasticity, cohesion…) can be chosen independently. Most importantly, since all the positions, velocities and forces are known at all time, one can easily compute (or measure) any relevant quantity. More particularly, the stress tensor can be defined from individual particle-particle interactions, f, and the distance between two grains in contact, r, and averaged over a control volume V [17]:

$$\sigma_{ij} = \frac{1}{V} \sum_{contacts} r_j \, . \, f_i$$

DEM simulations have been widely used to simulate dry grains but cohesive forces can be easily implemented in order to simulate powders and attractive suspensions (due to capillary forces for instance). Recently, in another project, I have simulated cohesive powders by adding an attractive force between two contacting grains. Figure 4 shows the result of preliminary tests, showing the angle of repose of simulated powders with increasing internal cohesive stress. I will apply this method to simulations of flowing powders and study the effect of cohesion on the characteristics of the flow (thickness, basal stress, flow rate, instabilities…).

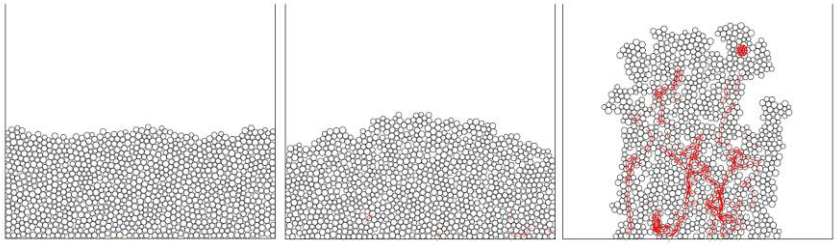

Figure 4: Simulated powder at rest (released from a hopper) with increasing internal cohesive stress (from left to right). The red lines indicate the intensity of inter-particle attractive forces.

III. Interaction with the industrial partners

I am hoping to develop strong interactions with the industrial partners within the IPRI. I see this funding opportunity as a chance to learn what challenges the industrial world is facing in powder technology, and to offer my expertise in the physics of granular material.

a. Additive Manufacturing

It is my understanding that Powder-based Additive Manufacturing (AM) and Laser-Metal Deposition (LMD) or Laser Sintering are becoming increasingly important for industrial applications. However, these techniques have to face a number of technical challenges, some of which caused by irregularities in the deposited layer.
I believe that my research proposal could shed some light on these issues. Indeed, as seen in Fig 1, a simple thin flow of grains or powder, bounded between confining walls, can already develop two types of instabilities: roll waves ad traffic waves. A better understanding of these phenomenon could lead to an improved control of the layer deposition in AM.

Moreover, in some manufacturing processes, a layer of powder is sometimes compacted using a roller. Under conditions which remain to fully be identified, this compaction process can be the cause of irregularities in the powder surface, which evidently deteriorates the manufacturing.
I have been studying a similar phenomenon, known as washboard road or corrugated road, for over a decade [18-21]. When vehicles repeatedly roll onto a granular surface, a rippled pattern gradually appears over time. I have investigated this instability through laboratory-scale experiments as well as DEM numerical simulations, using either dry sand or cohesive powders. We have identified the conditions under which a layer of sand or powder is unstable (i.e. develops ripples or bumps) or instead remains flat, regardless of any initial perturbations. I believe that our conclusions could help understand why imperfections appear when a layer of cohesive powder is submitted to the passage of a roller.

b. Test materials and flow characterization

As a physicist I have been using model materials such as spherical glass or steel beads, as well as sand-blasting grains (which have been washed and sieved). I understand that such materials can be far from those handled in civil engineering, in food processing or in the pharmaceutical industry. Instead of purchasing a given powder, I believe that members of the IFPRI could provide me with test samples of the powders and grains

that are relevant to their industrial applications. Namely, I am hoping that large companies such as Chemours, DuPont or Corning might share some of the material used in their industrial processes.

Moreover, again, I am hoping that interactions within the IFPRI could be very fruitful and I would be happy to characterize the chosen materials using tools manufacture by GranuTools or by FreemanTechnology. The GranuFlow, GranuHeap and GranuDrum are very efficient tools in characterizing the mechanical properties of powders and grains, and the FT4 Powder Rheometer allows one to fully characterize the flow of powders in a shear cell. Maybe I could rent some of these equipment. If these manufacturers are interested, maybe a partnership where all sides learn from each other could be established.

IV. Project timeline and deliverables

a. Timeline

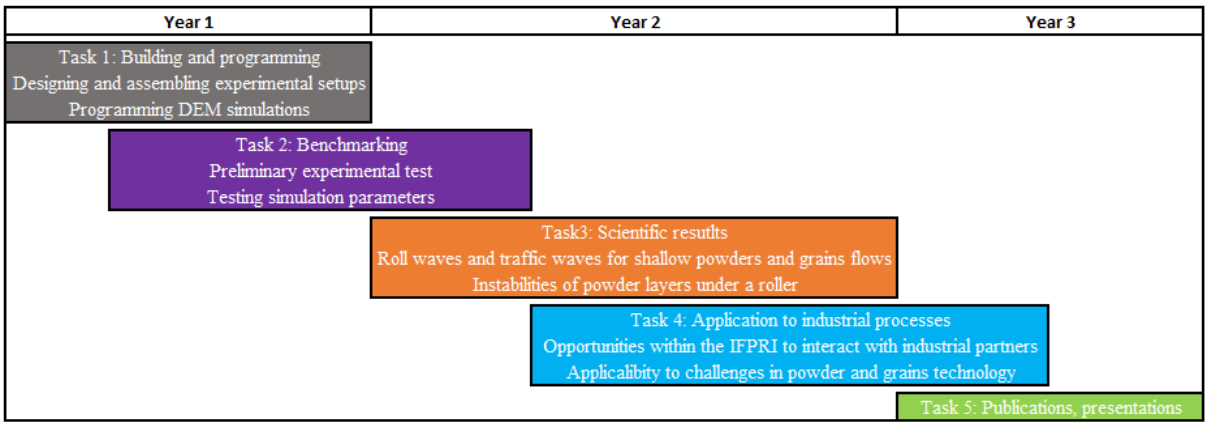

b. Deliverables

I propose to send an annual report on the scientific and technical achievements, explaining the progress made, the difficulties encountered, and the goals and the direction of research for the future year.
I will also send an annual summary of the use of the budget.

V. Budget

Equipement			USD
Linear aluminium rail	Bosch		4000
Fast Camera	Phantom VEO4K 590L		20000
Laser Scanner	Micro-Epsilon scanCONTROL		6000
Force sensors (10 units)	Omega LCMKD-2KN		7000
Data aquisition card	National Instruments DAQ USB		3000
Computer			1500
Other costs			
Travel expenses	annually	3000	9000
Publication Costs	annually	2000	6000
Partial PhD student wage	annually	18000	54000
Total			**110500**

References

[1]. R. L. Brown and J. C. Richards, Principles of Powder Mechanics,
Pergamon, New York, 1970.

[2]. J. Duran. Sand, Powders and Grains,
Springer-Verlag, New-York, 1999.

[3]. H. J. Herrmann, J.-P. Hovi, and S. Luding, editors, Physics of Dry Granular Media.
Kluwer Academic Publishers, Dordrecht, 1998.

[4]. P.G. De Gennes, Reflections on the mechanics of granular matter
Physica A, 261:267–293, 1998.

[5]. M. Wojtkowski, O. I. Imole, M. Ramaioli, E. Chávez Montes and S. Luding, Behavior of cohesive powder in rotating drums
AIP Conference Proceedings 1542, 2013.

[6]. G.D.R Midi, On dense granular flows
Eur. Phys. J. E 14: 341, 2004.

[7]. Pierre Jop, Yoël Forterre and Olivier Pouliquen, A constitutive law for dense granular flows
Nature 441, 727-730, 2006.

[8].Cristiana Di Cristo, Michele Iervolino, Andrea Vacca, Barbara Zanuttigh
Journal of Hydrology, Volume 377 (1) 50-58, 2009.

[9]. Andrew Neal Edwards, Roll waves and erosion-deposition waves in granular flows
PhD Thesis, University of Manchester, 2004.

[10]. San Diego State University, College of Engineering
http://eh.sdsu.edu/chow_froude_and_vedernikov_presentacion.html

[11]. Neil Balmforth, University of British Columbia
https://www.math.ubc.ca/~njb/Research/rollo.htm

[12]. Hayakawa, H., & Nakanishi, K. Universal behavior in granular flows and traffic flows. Progress of Theoretical Physics Supplement, 130, 57-75, 1998.

[13]. B. Percier, Washboard Road Instability
PhD Thesis, University of Lyon, 2013.

[14]. Radjai et al. Journal de Physique I 7(9), 1053-1070, 1997.

[15]. Schafer et al. J. Phys. I France 6, 5 1996.

[16]. Cundall, P. A., & Strack, O. D. A discrete numerical model for granular assemblies.
Geotechnique, 29(1), 47-65., 1979.

[17]. Andreotti, Bruno, Yoël Forterre, and Olivier Pouliquen. *Granular media: between fluid and solid*.
Cambridge University Press, 2013.

[18]. B. Percier, S. Manneville, N. Taberlet, Modeling a washboard road: From experimental measurements to linear stability, , Phys. Rev. E 87, 012203 (2013)

[19]. B. Percier, S. Manneville, J.N. McElwaine, S.W. Morris, N. Taberlet, Lift and drag forces on an inclined plow moving over a granular surface, Phys. Rev. E 84, 051302 (2011)

[20]. A.F. Bitbol, N. Taberlet, S.W. Morris, J.N. McElwaine, Scaling and dynamics of washboard roads, Phys. Rev. E 79, 061308 (2009)

[21]. N. Taberlet, S. Morris, J. McElwaine, Washboard road: the dynamics of granular ripples formed by rolling wheels, Physical Review Letters 99, 068003 (2007).

Curriculum

Dr. Nicolas Taberlet
UCBL - ENS-Lyon, Laboratoire de Physique, 46, Allée d'Italie F-69007 Lyon, France
Born March 12, 1978, Countries of citizenship: France and Switzerland

Experience

Since 2006	**Professor** at University of Lyon **Université Claude Bernard, École Normale Supérieure de Lyon, France** Research topics: granular flows, granular compaction, complex fluids in complex flows, ultrasound velocimetry, soft glassy materials.
Since 2015	**Elected Vice-chair** of the Physics Department, ENSL
Oct 2005- Sept 2006	**Postdoc at DAMTP, University of Cambridge, UK** **Department of Applied Mathematics and Theoretical Physics**, "Laterally unconfined flows of complex fluids", under the supervision of Prof. E.J. Hinch
2002-2005	**Ph.D. at Université de Rennes 1, France** & **University of Maryland, USA** "Gravity-driven Granular Flows": channelised flows, confined flows, segregation and diffusion in a rotating drum, long runout avalanches.

Funding & Contrats

Research projects
Projet Emergent PALSE, 2013-2015, 300 k€, Principal Investigator
ERC USoft, 2010-2015, 1.3 k€, Associate Investigator
National Swiss Fund, 2005-2007, 50 k€, Principal Investigator

International collaborations
CECAM fund (France), with Pr. Sobral, U. Brasilia, 6k€
CAPES fund (Brazil), with Pr. Sobral, U. Brasilia, 20k€
Laboratoire international associé (LIA) – France – Argentine
ECOS program (Chile), 20k€
MIT (USA), 20k€

Miscellaneous

50 peer-reviewed publication & 2 patents

5 graduated PhD students under my supervision

h-index: 20 (Google scholar), 18 (Research Gate), 15 (Isi Web of Science)

Reviewer for scientific journals: ~25 papers / year

Reviewer for research projects
FNS, Fond National Suisse
EPSRC (Engineering and Physical Sciences Research Council), UK
CONICYT (Comisión Nacional de Investigación Científica y Tecnológica), Chile

List of selected publications – on granular flows

1. Grains unchained: local fluidization of a granular packing by focused ultrasound
   P. Lidon, N. Taberlet, S. Manneville
   Soft Matter, Volume: 12, Issue: 8, Pages: 2315-2324 (2016)

2. Insights on the local dynamics induced by thermal cycling in granular matter
   B. Percier, T. Divoux, N. Taberlet
   Euro. Physics Letters 104, 24001(2013)

3. Lift and drag forces on an inclined plow moving over a granular surface
   B. Percier, S. Manneville, J.N. McElwaine, S.W. Morris, N. Taberlet
   Phys. Rev. E 84, 051302 (2011)

4. The effect of side-wall friction on dense granular flows
   N. Taberlet, P. Richard, R. Delannay,
   Computers and Mathematics with Applications 55, 230 (2008).

5. Density inversion in rapid granular flows: the supported regime
   N. Taberlet, P. Richard, E. Henry, R. Delannay,
   European Physical Journal E. 22, 17 (2007).

6. Towards a theoretical picture of dense granular flows down inclines
   R. Delannay, J. T. Jenkins, M. Louge, P. Richard, N. Taberlet, A. Valance,
   Nature Materials 6, 99 (2007).

7. Rock avalanche dynamics: Insights from the granular physics experiments
   J. Friedmann, N. Taberlet, W. Losert,
   International Journal of Earth Sciences 95, 911 (2006).

8. 2D and 3D Confined Granular Flows: Experimental and Numerical Results
   W. Bi, R. Delannay, P. Richard, N. Taberlet, A. Valance,
   Journal of Physics: Condensed Matter 17, S2457 (2005).

9. Super Stable Granular Heap in a Channel
   N. Taberlet, P. Richard, A. Valance, W. Losert, JM. Pasini, J.T. Jenkins, R. Delannay,
   Physical Review Letters 91, 264301 (2003).

10. Two-dimensional inclined chute flows: transverse motion and segregation
    G. Berton, R. Delannay, P. Richard, N. Taberlet, A. Valance,
    Physical Review E 68, 051303 (2003).

11. Leidenfrost granular flows
    N. Taberlet, P. Richard, R. Delannay
    Proceedings of Traffic and Granular Flows 07, Pages: 565-576, Springer (2009).

12. How sidewalls influence granular flows
    N. Taberlet, P. Richard, R. Delannay, M. Louge,
    in Powders & Grains 2005, Balkema, Rotterdam, 873 (2005).

13. Volume fraction profile in channelled granular flows down an erodible incline
    M. Louge, A. Valance, N. Taberlet, P. Richard, R. Delannay,
    in Powders & Grains 2005, Balkema, Rotterdam, 885 (2005).

feedback on your proposal to IFPRI

Nicolas Taberlet to Michel, me, Willie, Filip, mort.pr@pg.com 9:51 AM

Dear all,

please find attached the revised version of my research proposal.
I have reworked it along the lines suggested in your previous e-mail. Please find below answers to your comments.

(1) The brief emphasized the need for 'modeling and characterization methods relevant to flows that are dominated by boundary-layer physics, (...) It would be especially worthwhile to indicate how control of boundary conditions in characterization equipment (e.g. controlled stress vs controlled volume) can be related to flows in processing equipment, -- such as variable underflow weir or roller conditions in AM.
I have removed the first part of my proposal which in retrospect seem to be further from industrial applications. I have tried to explain how the proposed work could be useful of industrial processes such as additive manufacturing.

(2) Members suggest that you specify a list of deliverables to that end.

I've added a paragraph in the revised version of the proposal.

(3) Members wondered what powder material and particle-size-distribution you intend to deploy in experiments and characterize in your rheometer. The PSD's role is illustrated, for example, in references of the recent article https://doi.org/10.1016/j.powtec.2017.11.042 . How will you consider particle shape and shape distributions, as mentioned in the brief?

In my opinion, the best solution would be for some of the (numerous) industrial partners within the IFPRI to provide me with test samples of powders that are relevant to their industrial applications.

(4) Questions arose on the budget, particularly with respect to your purchase of a high-speed camera. If such camera is needed in the first year, how do you intend to support a student and retain adequate funds for travel?

I can also rely on other sources of funding, especially regarding support for students. Moreover, PhD students usually join a PhD program in fall, and therefore the funding required during the first year is very limited.

Looking forward to hearing from you,
Nicolas

IFPRI Research Project Brief

Predicting and Characterizing Crystal Surface Modification in Milling

The International Fine Particle Research Institute (IFPRI) wishes to fund a project in the broad area of crystalline structure modification during milling. Milling (size reduction) is often the final step in production of crystalline powders, used to control the particle size distribution of the product. It is not unusual that milling also causes undesirable structural changes, in the bulk and on the surface of crystals. The mechanism of these transformations is not understood, and it is not possible to predict whether a given crystalline phase will be sensitive to milling or not. This project aims to build a mechanistic understanding of mechanically-induced *surface* transformations, with the expectation that this will provide the basis for prediction of, aiding characterization of, and potentially avoiding surface damage in milling.

More specifically, the objective of the project is computational prediction of transformation (energy absorption and potentially fracture, disorder and/or phase change) in a brittle or semi-brittle crystalline structure caused by a mechanical shock at a surface due to a collisional impact that applies stress at rate and extent relevant to impact milling. There is no restriction on the modelling approach used in the project. The project should likely focus on physical phase modification; chemical (damage /reactivity) prediction is presumed to be too challenging to be within initial scope. Both organic and inorganic crystals are in scope; semi-crystalline thermoplastics are out of scope.

Reply to IFPRI members' feedback on the research proposal

"*Molecular Dynamics simulations of Aspirin and Sodium Chloride Impact Loading*"

by D.N. Theodorou and C. Tzoumanekas

We thank the members of the IFPRI committee for their constructive criticism and their comments.

- The proposal objectives, computational approach and materials (1 inorganic and 1 organic) address the IFPRI intent quite well. There is very good literature coverage – including awareness that mechanical properties are strain rate sensitive. Overall, great job!

Thank you very much.

- Some revision should made after consideration of this abridged comment:

- The argument on brittle-ductile transition with reference to milling is misleading.
- Single nanocrystals do not typically undergo fracture.
- The strain energy causes plastic deformation only for both NaCl and aspirin.
- Particles smaller than this transition size undergo size reduction by ductile tearing
- The brittle-ductile transition refers to the state in which the strain energy is inadequate to supply the energy required for crack propagation [according to]… K Puttick, K Kendall, and Hagan. For NaCl, particles smaller than micron size undergo plastic deformation without cracks."

We agree with the comments. We refer to the brittle-ductile transition in the sense discussed by Puttick, Kendall, and Hagan, as mentioned. These studies are based on single compression experiments which do not take into account temperature and stress rate effects, or fatigue fracture. For small crystals they predict a limiting size (of the order of 1 μm) below which only plastic deformation can take place. In general, they predict that yielding occurs prior to fracture due to the absence of preexisting cracks, and/or insufficient elastic energy to promote either crack nucleation, or crack propagation in case of existing, necessarily small cracks that require high stresses for particle breakage.

Therefore, we have asked ourselves if simulated atomistic nanocrystals of size approximately 50 nm would break after impact, as mentioned in the comments. Recent work [1] has shown that, by stabilizing the particles (elimination of agglomeration), monocrystal sizes of the order of 10 nm can be obtained, for example for a ceramic material such as SnO_2. It was also shown that, at the very late stages, size reduction proceeds by the fracture of single crystallites (monocrystals). Note that the feed material was already in the nm range (200 nm). However, the breakage mechanisms of nanoparticles are still poorly understood. In ref [1] the general mechanism was characterized as fatigue fracture promoted by cyclic loading, for example by some kind of ductile fracture, as mentioned in the comments. Plastic deformation leads, somehow, to the generation of some kind of defect which grows as a subcritical crack under the

action of repeated stress events. Since a monocrystal of size 10 nm must have been created after the fracture of another larger monocrystal, it may be possible that monocrystals of size 50 nm, as in our atomistic simulations, would break down to form smaller ones, especially after repeated impact events. The situation is certainly not clear. If, for the selected materials, a breakage mechanism at the nanometer scale is present, in the atomistic simulations it will appear naturally and we will be able to track it. We note that in ref [1] a gross trend for smaller limiting particle sizes for materials with higher melting points was observed. Thus, fracture is much less likely for Aspirin nanocrystals (melting temperature 135^o C) than for NaCl nanocrystals (melting temperature 801^o C).

[1] Knieke, C., "Fracture at the nanoscale and the limit of grinding" (2012), PhD Thesis, Cuvillier Verlag Göttingen.
[2] Armstrong, P., Knieke, C., Mackovic, M., Frank, G., Hartmaier, A., Göcken, M., Peukert, W. "Microstructural evolution during deformation of tin dioxide nanoparticles in a comminution process" (2009) *Acta Materialia*, 57, pp. 3060-3071.

- It would be helpful to have more details on the multiscale model.

We have clarified the description of the model in the proposal with intuitive figures and comments. The MD/FE interface has been simplified by 'dressing' the continuum model with a thick atomistic surface.

- For example, is it intended to allow simulation of an impacting particle with size of at least 0.1 – 1 um, the approximate minimum size range of typical relevance to industrial milling?

Certainly, this is the target length scale of the model.

- Will establishing, through MD, a constitutive equation for stress-deformation in the FEM domain be more challenging than the thermal balance?

The constitutive equations for heat transfer and stress-deformation, and the corresponding thermal conductivity and elastic stiffness tensor in the FEM domain, are input to the model. Information from the atomistic MD surface layer is passed to the continuum domain, during impact, through coupled MD/FE boundary conditions, in a self-consistent manner. The outer, interfacial FEM nodes are immersed in MD subdomains. By statistical averaging of the velocities and displacements of MD subdomain atoms, the local temperature and displacement of interfacial MD subdomains are given as boundary conditions to the interfacial FEM nodes. Then, the generated reaction forces and heat flux from the FEM domain update the local forces and velocities of interfacial MD subdomain atoms, and so on.

- The full atomistic MD is expected to be practical up to approximately what size scale for each material (presuming perhaps that you are focused on prediction of crystalline damage/transformation rather than a parametric milling study that requires a very large number of impact simulations)?

Approximately up to 50-100 nm particle size, for both materials (see refs [20,48] in the proposal).

- NaCl seems like a fine choice for an inorganic material based on substantial literature, physical behavior, etc. It would be helpful to mention, very briefly, why NaCl is a superior choice, for this research, relative to some common milled industrial inorganic powders with reportedly "interesting phase behavior" [specifically TiO_2, Al_2O_3, PbO were mentioned by IFPRI members], based on need to avoid systems where chemical bond cleavage is critical for milling-induced surface transformation or other factors.

We did consider the TiO_2 system (melting temperature 1843^o C, 3 major polymorphs) for which nanocrystals of size 20 nm have been produced with ball milling. The discussed materials would constitute excellent choices. NaCl was selected in order to avoid the classical modeling of chemical bond cleavage, as mentioned in the comment, with the molecular mechanics force field employed for atomistic modeling. Also, in order to focus on physical change modification and avoid chemical damage, which is presumed to be too challenging (and we think it is) to be within the initial scope of the research project, as discussed in the IFPRI project call.

Molecular Dynamics simulations of Aspirin and Sodium Chloride Impact Loading

A Research proposal
submitted to the
International Fine Particles Research Institute

by

Prof. Doros N. Theodorou

and Dr. Christos Tzoumanekas

Department of Materials Science and Engineering
School of Chemical Engineering
National Technical University of Athens
9 Heroon Polytechniou Street, Zografou Campus
Tel. +30 210-772-3157, Fax +30 210-772-3112
e-mail doros@central.ntua.gr

website http://comse.chemeng.ntua.gr

April 2018

Introduction and Background

The outcome of a milling process depends upon a complex interaction between material properties, mill type, and operational conditions (number of stress events, type of stresses, their intensity, etc.) [1]. Understanding and quantifying this interaction is essential for predictive modeling of the size-reduction process [2]. It has been shown that the primary material properties responsible for the breakage of solid particles are Young's modulus (E), hardness (H), and critical stress intensity factor (K_c), representing the resistance of the material to elastic deformation, plastic deformation and crack propagation, respectively [3-6]. Microscopic processes related to particle breakage, such as cleavage along slip planes, generation of surface steps, point defects and dislocations, and crack nucleation, are manifested in these properties. In parallel, it is widely accepted that changes in surface/bulk structure, particle shape, and surface energetics are equally important [7,8]. Milling increases the total surface area but also changes the relative exposure of different crystal faces in the powder and therefore the surface chemistry [9,10]. Moreover, the strong heat generation of most dry milling processes can lead to surface melting of small particles. These changes can lead to enhanced agglomeration and affect milling sensitivity and powder processing (e.g., flowability, compactibility, mixing) [1]. In addition, critical product properties can be altered [11]. A prominent example is the modification of the dissolution behavior of active pharmaceutical ingredients (APIs) whose size reduction by milling increases their surface area, hence their dissolution rate (the majority of screened drug candidates have low solubilities). Changes in crystal habit, surface melting, recrystallization, amorphization, and stress-induced transformation to a different crystal polymorph (stable/unstable), can affect wetting, aerosolization, mixing, compaction, thermodynamic stability, and dissolution behavior of the API [11]. Understanding fundamentally the effects of milling on particle surface properties has become even more important with the advent of nanomilling [11-13]. Among other applications, the dispersion of nanocrystalline particles in a host material, leading to reinforcement and tailored mechanical/electrical properties [14], as well as the stabilization of API nanocrystals by polymers or surfactants [15], are of utmost technological importance.

Overview. The mechanical properties of a material measured at low strain rates may be inadequate for describing its breakage and deformation behavior at high strain rates. During milling the particles are subjected to different kinds of loads. Impact testing can conform to strain rates operating in various milling machines and is more relevant than nano-indentation for strain-rate hardening materials. Single particle impact studies have been employed to develop an understanding of failure processes and mechanisms under different loading conditions, as well as to provide useful data that can be used for predictive analysis of milling [3,16-18]. In the proposed work we will undertake molecular dynamics (MD) simulations of acetylsalicylic acid (aspirin) and sodium chloride (NaCl) nanoparticles hitting an impact surface, analyze the resulting changes in the size/shape, crystallinity, defect generation, stress distribution, surface free energy, and surface charge of the particles, and perform an energy balance on the process. Furthermore, we will design a multiscale MD/continuum thermomechanical approach for conducting analogous studies on μm sized particles.

Proposed Work. The particle will approach an immovable wall (impact surface) with prescribed impact angle (orientation) and initial translational and angular velocities. The plan is to simulate the entire collision process and record all changes (energetic, thermal, structural, local stress) taking place in the particle during/after impact, including 'crunching' and possible particle breakage into fragments. (Distributions of) initial particle velocities and angular velocities should be chosen so as to be representative of the actual milling process (in the range 10-300 m/s, or much larger to simulate jet mill processes). The roughness of the impact surface (height and wavelength of asperities) should also be

representative of the process; varying it systematically would give us the opportunity to conduct an interesting parametric study.

To probe surface and bulk crystal structure modifications, the particle and the impact surface (IS) *should be described with atomistic resolution*. If the duration of impact is of the order of one μs, atomistic impact simulations of nanoparticles using MD with molecular mechanics-type force fields, by exploiting parallel computing, are possible. However, milling is an intrinsically multiscale process, and in industrial practice the target size distribution can be centered in the mm, μm, or nm length scale. Therefore, starting from atomistic simulations, our intention is to formulate a multiscale modeling approach that would smoothly interface with continuum approaches to large length and time scale phenomena.

Fully Atomistic Simulations. *Particle*. Two compounds whose equilibrium structure are known from X-rays will be studied. Aspirin, an organic molecular crystal, and NaCl, a prototype ionic crystal. The shot particles will be single nanocrystals without defects, as shown in Figure 1. Their habitus will be representative of the compound with typical linear size between 50 and 150 nm. The selected crystals have been simulated with MD in the past [20,24] and used in milling and single particle impact studies [3,6,18,33].

Figure 1: (a) crystal habit of Aspirin, form I [19], (b) Aspirin nanocrystal [19,20], (c) NaCl nanocrystals [21]

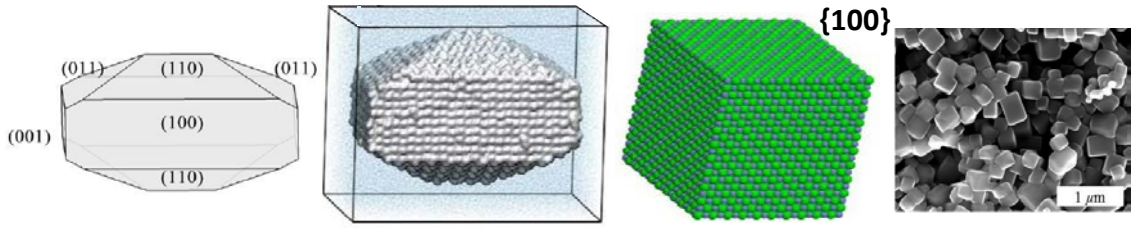

Aspirin has two ambient mechanically stable polymorphs, forms I and II [22], distinguished by a small lateral shift of layers and very small energy differences, 2.56 kJ/mol (298K) [23]. Sodium chloride exhibits a high pressure transition from the low pressure B1 phase (rocksalt structure) at ambient conditions to the B2 phase (CsCl structure) at 30GPa [24].

Force field. Given the significant computational effort required and our focus mainly on physical and not chemical phenomena, the use of a simple force field is appropriate. Minimum requirements of the force field are that it have a minimum near the correct (X-ray) crystal structure of the particle, that it yield a good estimate of the cohesive energy density (lattice energy), and that the matrix of isothermal elastic coefficients extracted from it be reasonable. It would be nice if, in addition, it can reproduce the equilibrium melting point and heat of fusion, and give a good estimate of the thermal conductivity and of the attachment energies of primary slip planes.

Impact Surface (IS). It will be represented as a semi-infinite medium (Fe atomistic lattice) with lateral dimensions much larger than the particle. No periodic boundary conditions will be applied. Atoms on the impact surface are expected to mainly execute vibrations around their average positions. No significant plastic deformation of the impact surface is expected; most of the damage due to the collision will be experienced by the particle. Asperities can easily be introduced on the IS with

prescribed height and wavelength. Rough surfaces have been simulated in the past [25]. Since the particle is much less massive than the impact surface, three to five atomic layers and asperity atoms near the approaching particle will be allowed to move in the MD in order to allow for heat dissipation through the IS, while the rest will be treated as a medium consisting of stationary atoms. A molecular mechanics-type potential corresponding to Fe will be used to describe interactions within the IS and interactions between the IS and particle atoms. The potential due to the stationary atomic layers of the semi-infinite part of the IS can be precomputed and pretabulated in three dimensions [26]. The moving atoms of the IS will be thermostated with Brownian dynamics. Sophisticated thermostating schemes exist which can reproduce the thermal conductivity of Fe [27]. It will probably be satisfactory to assume that the IS has infinite thermal conductivity in relation to the particle. Whatever scheme is adopted, we will be able to calculate the energy that is conducted away as heat through the IS during the collision.

Notes on the selected materials. ▪ Fragmentation occurs through cleavage along preferential slip planes or crack propagation. The primary slip planes of both crystals are well known and characterized [18,32]. Additionally, there is wealth of published data on the thermophysical and mechanical properties of the materials. ▪ A relative measure of the resistance to fracture and grinding is the brittleness index, BI=H/K_C, where H is the hardness and K_C is the fracture toughness. K_C and BI of aspirin and NaCl crystals are very different: between 0.02 and 0.034 MPa $m^{1/2}$, and $2.9 \times 10^3 – 10.5 \times 10^3$ $m^{1/2}$, respectively, for aspirin (due to fracture anisotropy [6,18]); 0.5 MPa $m^{1/2}$ and 0.4×10^3 $m^{1/2}$ for NaCl [28]. It would be interesting to see how this one order of magnitude difference in BI alters impact behavior. ▪ Single crystals of both aspirin polymorphs have been grown from solution, while it has been shown that the two phases are frequently intergrown [29]. Form I was found to undergo a reversible phase transition to a new polymorph (form III) at 2 GPa (hydrostatic pressure) [30]. Form II did not undergo any phase transition for pressures up to 10 GPa, but exhibited a disordered structure above 7 GPa [30]. It has been reported that it transforms to form I slowly (over several months) at ambient conditions but the transformation is accelerated by shear stress upon mechanical grinding [31]. Shear slip along {100}<001> provides a mechanistic rationale for the observed solid-state II/I transformation [30,31]. ▪ The thermal expansion of aspirin is larger by a factor of two perpendicular to the direction [010]. The anisotropy of the longitudinal elastic stiffness is less pronounced; the difference between the minimum and maximum values is approximately 30% [32].

Multiscale simulations. The μm size grinding limit, imposed by theoretical studies of the brittle to ductile transition, driven by a decreasing particle size [34], has been superseded by current milling technology (wet milling in stirred media mills, jet mills, etc.) [11-13]. The true grinding limit [35] lies in the nm range, which falls within strain rates and length scales treated with MD. In industrial practice, however, the need for controlled and energetically efficient milling, with target particle size distribution in the μm or mm size, will always exist. Such length scales are many orders of magnitude larger than the systems we can simulate atomistically with MD.

In order to scale up the system, only the domains of the particle and the impact surface which come into close contact during the collision will be represented *with atoms* and simulated with full MD (MD domains). The remaining (largest) domains of the particle and IS will be represented with Finite Element (FE) meshes (i.e., with *mesh nodes*, see Fig. 2). As far as their motion is concerned, *they will be treated as rigid bodies*. As far as heat transfer and stress distribution is concerned *they will be treated as continua* with given constitutive law and boundary conditions (temperature and loading), and known elastic stiffness and thermal conductivity tensor. The thermomechanical problem within the continua will be solved with the Finite Element Method (FEM). No periodic boundary conditions will

be applied. An outline of how multiscale simulations can be conducted is given below. The discussion will be restricted to the particle. The extension to the impact surface is fairly obvious. A sketch of the model system, as envisioned before the collision, is given in Figure 2. Note that the inner continuum part of the particle is 'dressed' with an atomistic, fully enclosing, thick surface layer. The contact between particle and IS will be treated atomistically, even if the particle would roll on the IS during impact.

The multiscale scheme is based on the Embedded Statistical Coupling Method (ESCM) for coupling MD with FE [36,37]. The method uses statistical averaging over both time and volume of atomistic subdomains at the MD/FE interface to provide nodal displacement boundary conditions to the continuum FE domain. In response to the atomic displacements, the FEM generates interface reaction forces that are uniformly distributed over the interface atoms in the form of constant traction boundary conditions to the MD domain [36].

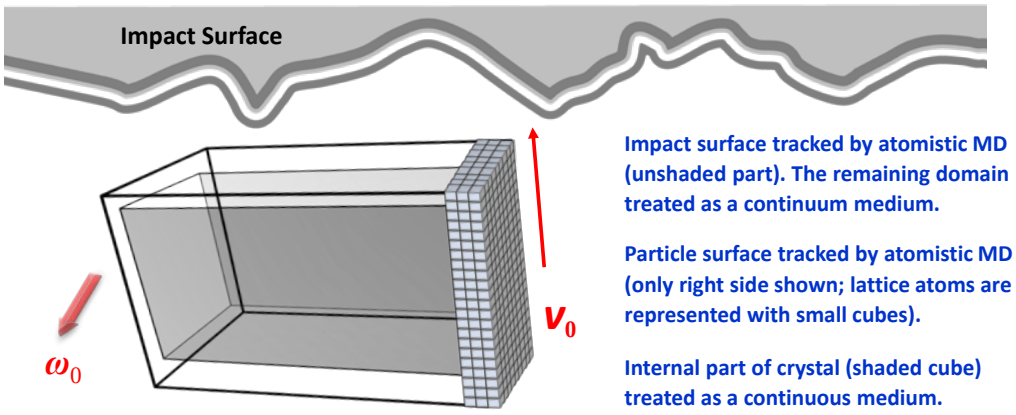

Figure 2: Schematic representation of the multiscale model. $\mathbf{V_0}$, $\boldsymbol{\omega_0}$, linear and angular velocity of particle.

The FE and MD computational systems (describing the particle) communicate only through an iterative update of the boundary conditions at the MD/FE interface (coupled boundary value problem, see Fig. 3). The continuity of material properties at the interface, and of the interface itself, is achieved by the immersion of interfacial FE nodes within the MD region. Each one of these nodes is surrounded by certain atoms (specified by geometric criteria) of the local MD region. Thus, the interface becomes a set of interfacial FE nodes surrounded by corresponding MD subdomains. MD subdomains are defined only at the MD/FE interface. The MD simulation proceeds in time steps of Δt 1 ps or less. During this time the interfacial nodes are kept still and apply constant forces (tractions) to the atoms of MD subdomains, transferring the static FE domain stress field to the MD domain. Because of the collision each atom at the MD/FEM interface will experience an average net displacement (with reference to the average atom positions in the previous Δt step). These displacements are much smaller for atoms in MD subdomains than for particle atoms in contact with and near the interface. By averaging the displacements within MD subdomains a displacement for each interfacial node is calculated. This way an iterative update of the coupled boundary conditions at the MD/FEM interface is achieved. The nodal displacements will generate new reaction forces from FEM that will be then applied to MD subdomains. The latter, after time Δt, will generate new FEM nodal displacements, and so on.

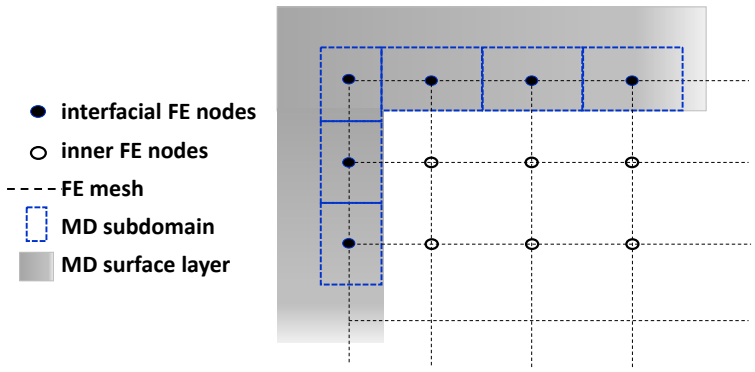

Figure 3: Schematic representation of the MD/FE interface structure in the multiscale model.

Any conventional FEM code, including commercial packages, can be used to solve the continuum mechanical problem. The FEM and MD computational systems are effectively independent, making the multiscale model convenient and extendable to different chemistries. Additionally, the continuum thermal problem, which plays a crucial role in the energy balance of the collision, can be solved with FEM in parallel with the mechanical problem and on the same continuum FE mesh. The mechanical/thermal analogy is the following: displacement becomes temperature, stress becomes heat flux, load (force) becomes heat, and the elastic stiffness matrix becomes the thermal conductivity matrix. From the short-time averaged kinetic energy of molecules in MD subdomains the temperature distribution at all FE nodal points of the interface will be known, and the continuum heat transfer problem will be solved with FE. The heat flux at the MD/FE interface will be fed back to the atomistic MD and used to rescale atomic velocities of MD subdomains. In this way, a seamless representation of heat transfer within the particle will be accomplished. The heat generated from the collision will be transferred from the MD to the FE domain. The thermal problem can be coupled with the mechanical one to take into account the temperature dependence of elastic constants and thermal expansion coefficients of the crystal [32,38].

Technically, the multiscale model poses many challenges, and it needs to be developed at increasing levels of sophistication. The surfaces changes due to the collision can be investigated with an elastic or elasto-plastic constitutive model employed in the FE domain. However, one can also envision solving the continuum equations of elasticity within the continuum with surface tractions derived from the atomistic part and thereby tracking cleavage along primary slip planes, or crack propagation [39], in the FE domain. This would require a more complex constitutive model and FE treatment.

Observables to be tracked

- Movies of the entire collision process with defect accumulation and/or stress scale coloring; Duration of the collision.
- Detection of face, edge or vertex impact, and insight on outcome differences.
- Energetic analysis of the collision: Energy balance. Fraction of the initial kinetic energy that goes to increase the internal energy of the particle. Increase in potential energy and its components (inter- vs intra-molecular, stretching, bending, torsional etc.). Increase in kinetic energy of molecules after subtracting overall translational and rotational motion. Spatial distribution of the increase in internal energy. Fraction of the initial kinetic energy that is dissipated as heat through the impact surface. Overall particle momenta and angular momenta before and after collision. Overall kinetic energies before and after collision. Coefficient of restitution of the collision.

- Structural and specific surface energy changes brought about by the collision and their time evolution. Local density $\rho(\mathbf{r},t)$ as a function of position and time. Crystalline defects (point, dislocations [40], grain boundaries, surface steps), with respect to the initial crystalline structure, their spatial distribution and their evolution with time. Presence of plastic deformation. Cleavage plane analysis based on attachment energy of nanocrystal slip planes. Development of voids by analysis of clusters of accessible volume: void shape, orientation, spatial distribution and evolution. Onset and propagation of surface/internal cracks. Detection of surface melting, amorphization, recrystallization. Transition into different polymorphs in the surface/bulk region. Particle structure factor and interpretation of its features based on observed structural changes. Profiling of the damage region and its time evolution based on the above structural measures. Overall charge developing in NaCl as a result of the collision and distribution of surface charges.
- Stress distribution as a function of time, $\boldsymbol{\sigma}(\mathbf{r},t)$. Both atomic-level stresses and locally averaged stresses will be computed through the virial theorem. Analysis of local stress in the light of continuum criteria for fracture.
- Temperature distribution throughout the particle as a function of time, $T(\mathbf{r},t)$, from short-time averaging of atomic kinetic energies after subtraction of overall particle motion. Detection of surface melting or phase transitions based on the temperature-time history at specific points.

System parameters whose effect will be studied

- Particle size, habit or shape.
- Initial velocity and angular velocity of particle with respect to the impact surface. A distribution of those should be studied. At a later stage, this distribution could be connected to a macroscopic simulation of the actual milling process.
- Frequency and height of asperities on the impact surface.
- Effect of repeated collisions of the same particle. At a later stage, subsequent collision simulations could be conducted on the fragments obtained from an initial particle.
- Effect of temperature [41] (e.g., cryogenic vs ambient milling conditions).
- Initial particle orientation with respect to the impact surface and asperities (for example, the two following cases). Several interesting variations can be envisaged.
- Shear vs compressive stress effects, by comparing impact with zero angular velocity and particle face oriented parallel to a flat impact surface for near-0° and 90° impact angle (promoting development of shear vs compressive stresses on the particle/impact-surface interface, respectively).
- Single (one loading 'point') vs double (two loading 'points') impact. On double impact the orientation of the particle will be adjusted to hit the surface on two points simultaneously: a point on the flat part of the surface and a point located on a protruding asperity near the flat part.

Future extensions could include the simulation of particles of various chemical constitutions, the simulation of multicrystalline or defective particles, an analysis of particle-particle collision along the same lines (jet mills), simulation in the presence of moisture in the mill, etc.

Critical unknowns, and limitations. ▪ Setup and validation simulations will be performed on the 128 core cluster of our group. To analyze the scaling of required computational resources vs. system size we will exploit the use of preparatory access projects (for setting large-scale simulations) granted (after application) by High Performance Computing (HPC) centers. This is the first stage for getting access to

powerful large-scale computational platforms to perform production simulations (proof of scaling is a must when applying). Post-processing can be performed in our lab. We will apply for access to at least two HPC centers, PRACE (European) and ARIS (Greek) [42,43], where we have carried out recent projects. ▪ By searching the literature we found out that there is limited work (if any) concerning impact (breakage) simulations of solid particles with real chemistry, though impact problems have been studied with large-scale MD simulations [44,45]. Considering this gap, atomistic impact simulations are considered absolutely necessary before embarking on a multiscale approach ▪ If a breakage mechanism is present for Aspirin or NaCl atomistic nanocrystals of size apprx. 50-100 nm that will be studied, it will appear naturally in the simulations. ▪ We note that in ref [61] a gross trend for smaller limiting particle sizes for materials with higher melting points was observed. Thus, fracture is much less likely for Aspirin nanocrystals (melting temperature 135^o C) than for NaCl nanocrystals (melting temperature 801^o C). ▪ Another issue is whether or not continuum mechanics can be used to describe a particle at the nanometer scale [14]. Recent simulations have shown that Hertzian theory of the deformation, due to an external load, of two elastic NaCl nanocrystals in contact can be applied down to sizes of 5 nm [48]. ▪ The simulated wavelength of asperities will be limited by the spatial extent of the impact surface. A plane IS will be simulated first. ▪ A compromise between the size of the system and the total number of simulated impact events is necessary. A cubic NaCl nanocrystal with edge length 170 Å contains approximately 216000 atoms (226 Å, 512000 atoms).

Targets and accomplishments in each of the three years

First year. Setup of the single particle impact simulation engine for given impact angle, velocity and angular velocity of aspirin particles. We will use the freely available Large-scale Atomic/Molecular Massively Parallel Simulator (LAMMPS) MD software [49,50]. Selection of suitable force field for aspirin and IS (Fe). Computational generation of the particle/IS system. Automatic scheme for generating atomistic nanoparticles of given linear dimensions and habit. Application for preparatory access project (code scaling & optimization) to HPC centers [42,43]. Surface/bulk characterization of structure/energetics of the known aspirin and NaCl polymorphs. Mechanical characterization of aspirin for the selected force field (material model). Estimation of the elastic stiffness matrix and yield strength of the particle bulk phase and comparison with previous simulation/experimental work. Impact simulations of small/moderate size Aspirin systems and validation of setup. Development of software for post processing analysis of the observables to be tracked.

Second year. Effect of system parameters. Preparatory large-scale simulations of aspirin, estimation of computing and storage needs according to system size. Application for computationally intensive project to HPC centers. Optimization and selection of system parameters (especially size) for large-scale impact simulations of Aspirin. Visualization of impact trajectories with color filters for detecting generated surface/bulk defects and regions of high local stress in particle and its fragments. Large scale Aspirin simulations. Analysis of observables. Setup and deployment of large scale NaCl impact simulations.

Third year. Continuation of large scale Aspirin, NaCl impact simulations. Variation of initial conditions; initial particle orientation, etc. Analysis and collection of data/results for as many possible impact events. Setup of the multiscale simulation scheme. Integration of MD with FEM for the thermomechanical problem for one of the systems.

How this project could leverage into existing programs in which your research team is engaged. The Computational Materials Science and Engineering (CoMSE) group at NTUA is engaged in several

research programs aiming at the design, development, and implementation of powerful, yet tractable multiscale modeling and simulation strategies for the prediction of properties of materials from chemical constitution and processing conditions. Ongoing programs relevant to the proposed project focus on dispersing nanoparticles in polymer matrices by tuning interactions or use of surface-grafted chains, as well as on the thermal and mechanical properties of the resulting nanocomposites [51-55]; on predicting surface tension, work of adhesion, and dynamics at interfaces from atomic-level interactions [59,60]; on cavitation of soft materials under imposition of external stress [56]; on polymer crystallization [57]; and on nonlinear rheology under high deformation rates [58]. The knowhow, methodology, software, and collaborative ties with Industry developed in the context of these research programs will be highly useful in the proposed project.

Indications where IFPRI members could support the program through provision e.g. of model test materials, test methods, industrial experience. Consultation on particle characteristics and impact conditions relevant to real milling processes; prioritization of system parameters for study according to their relevance for industry; validation of predicted material properties and impact simulation outcomes based on experimental findings and accumulated industrial knowhow; guidance in planning next steps.

References

1. Roberts, R.J. "Particulate Analysis - Mechanical Properties" (2011) in '*Solid State Characterization of Pharmaceuticals*', pp. 357-386, John Wiley and Sons

2. Vogel, L., Peukert, W. "Breakage behaviour of different materials - Construction of a mastercurve for the breakage probability" (2003) *Powder Technology*, 129 (1-3), pp. 101-110.

3. Ghadiri, M., Zhang, Z. "Impact attrition of particulate solids. Part 1: A theoretical model of chipping" (2002) *Chemical Engineering Science*, 57 (17), pp. 3659-3669.

4. Kwan, C.C., Chen, Y.Q., Ding, Y.L., Papadopoulos, D.G., Bentham, A.C., Ghadiri, M. "Development of a novel approach towards predicting the milling behaviour of pharmaceutical powders" (2004) *European Journal of Pharmaceutical Sciences*, 23 (4-5), pp. 327-336.

5. Vogel, L., Peukert, W. 'From single particle impact behaviour to modeling of impact mills' (2005) *Chemical Engineering Science*, 60 (18), pp. 5164-5176.

6. Meier, M., John, E., Wieckhusen, D., Wirth, W., Peukert, W. "Influence of mechanical properties on impact fracture: Prediction of the milling behaviour of pharmaceutical powders by nanoindentation" (2009) *Powder Technology*, 188 (3), pp. 301-313.

7. Williams, D.R. "Particle engineering in pharmaceutical solids processing: Surface energy considerations" (2015) *Current Pharmaceutical Design*, 21 (19), pp. 2677-2694.

8. Luner, P.E., Zhang, Y., Abramov, Y.A., Carvajal, M.T. "Evaluation of milling method on the surface energetics of molecular crystals using inverse gas chromatography" (2012) *Crystal Growth and Design*, 12 (11), pp. 5271-5282.

9. Heng, J.Y.Y., Bismarck, A., Williams, D.R. "Anisotropic surface chemistry of crystalline pharmaceutical solids (2006) AAPS *PharmSciTech*, 7 (4), art. no. 84, .

10. Heng, J.Y.Y., Thielmann, F., Williams, D.R. 'The effects of milling on the surface properties of form I paracetamol crystals' (2006) *Pharmaceutical Research*, 23 (8), pp. 1918-1927.

11. Scheler, S. "Micro- and Nanosizing of Poorly Soluble Drugs by Grinding Techniques" (2013) in *Drug Delivery Strategies for Poorly Water-Soluble Drugs*, pp. 509-550, John Wiley and Sons

12. Mende, S. "Industrial Production of Nanomaterials with Grinding Technologies" (2015) in '*The Nano-Micro Interface: Bridging the Micro and Nano Worlds*', Second Edition, 2-2, pp. 629-646, Wiley Blackwell

13. Knieke, C., Steinborn, C., Romeis, S., Peukert, W., Breitung-Faes, S., Kwade, A. "Nanoparticle production with stirred-media mills: Opportunities and limits" (2010) *Chemical Engineering and Technology*, 33 (9), pp. 1401-1411.

14. Guo, D., Xie, G., Luo, J. "Mechanical properties of nanoparticles: Basics and applications" (2014) *Journal of Physics D: Applied Physics*, 47 (1), art. no. 013001, .

15. Peltonen, L., Hirvonen, J. "Pharmaceutical nanocrystals by nanomilling: Critical process parameters, particle fracturing and stabilization methods" (2010) *Journal of Pharmacy and Pharmacology*, 62 (11), pp. 1569-1579.

16 Tavares, L.M., Austin, L.G., King, R.P. "Breakage and damage of particles by impact" (2006) in '*SME Annual Conference - Advances in Comminution*', pp. 205-223.

17. Meier, M., John, E., Wieckhusen, D., Wirth, W., Peukert, W. "Characterization of the grinding behaviour in a single particle impact device: Studies on pharmaceutical powders" (2008) *European Journal of Pharmaceutical Sciences*, 34 (1), pp. 45-55.

18. Olusanmi, D., Roberts, K.J., Ghadiri, M., Ding, Y. "The breakage behaviour of Aspirin under quasi-static indentation and single particle impact loading: Effect of crystallographic anisotropy" (2011) *International Journal of Pharmaceutics*, 411 (1-2), pp. 49-63.

19 Hammond, R.B., Pencheva, K., Ramachandran, V., Roberts, K.J. "Application of grid-based molecular methods for modeling solvent-dependent crystal growth morphology: Aspirin crystallized from aqueous ethanolic solution" (2007) *Crystal Growth and Design*, 7 (9), pp. 1571-1574.

20. Greiner, M., Elts, E., Briesen, H. "Insights into pharmaceutical nanocrystal dissolution: A molecular dynamics simulation study on aspirin" (2014) Molecular Pharmaceutics, 11 (9), pp. 3009-3016.

21. Range, S., Bernardes, C.E.S., Simões, R.G., Epple, M., Da Piedade, M.E.M. "Size matters: An experimental and computational study of the influence of particle size on the lattice energy of NaCl" (2015) *Journal of Physical Chemistry C*, 119 (8), pp. 4387-4396.

22. Bond, A.D., Solanko, K.A., Parsons, S., Redder, S., Boese, R. "Single crystals of aspirin form II: Crystallisation and stability" (2011) *CrystEngComm*, 13 (2), pp. 399-401.

23. Reilly, A.M., Tkatchenko, A. "Role of dispersion interactions in the polymorphism and entropic stabilization of the aspirin crystal" (2014) *Physical Review Letters*, 113 (5), art. no. 055701.

24. Zhang, S., Chen, N.-X. "Molecular dynamics simulations for high-pressure induced B1-B2 transition in NaCl by Möbius pair potentials" (2003) *Modeling and Simulation in Materials Science and Engineering*, 11 (3), pp. 331-338.

25. Li, J., Fang, Q., Zhang, L., Liu, Y. "The effect of rough surface on nanoscale high speed grinding by a molecular dynamics simulation" (2015) *Computational Materials Science*, 98, pp. 252-262.

26. June, R.L., Bell, A.T., Theodorou, D.N. "Molecular Dynamics Study of Methane and Xenon in Silicalite" (1990) *J. Phys. Chem.*, 94, 8232-8240; erratum (1991) *J. Phys. Chem.*, 95, 1014.

27. Berro, H., Fillot, N., Vergne, P., Tokumasu, T., Ohara, T., Kikugawa, G. "Energy dissipation in non-isothermal molecular dynamics simulations of confined liquids under shear" (2011) *Journal of Chemical Physics*, 135 (13), art. no. 134708.

28. Duncan-Hewitt, W.C., Weatherly, G.C. "Evaluating the hardness, Young's modulus and fracture toughness of some pharmaceutical crystals using microindentation techniques" (1989) *Journal of Materials Science Letters*, 8 (11), pp. 1350-1352.

29. Boese, R., Desiraju, G.R. "On the polymorphism of aspirin: Crystalline aspirin as intergrowths of two "polymorphic" domains" (2007) *Angewandte Chemie - International Edition*, 46 (4), pp. 618-622.

30. Crowell, E.L., Dreger, Z.A., Gupta, Y.M. "High-pressure polymorphism of acetylsalicylic acid (aspirin): Raman spectroscopy" (2014) *Journal of Molecular Structure*, 1082, pp. 29-37.

31. Varughese, S., Kiran, M.S.R.N., Solanko, K.A., Bond, A.D., Ramamurty, U., Desiraju, G.R. "Interaction anisotropy and shear instability of aspirin polymorphs established by nanoindentation" (2011) *Chemical Science*, 2 (11), pp. 2236-2242.

32. Bauer, J.D., Haussühl, E., Winkler, B., Arbeck, D., Milman, V., Robertson, S. "Elastic properties, thermal expansion, and polymorphism of acetylsalicylic acid" (2010) Crystal Growth and Design, 10 (7), pp. 3132-3140.

33. Zhang, Z., Ghadiri, M. "Impact attrition of particulate solids. Part 2: Experimental work" (2002) *Chemical Engineering Science*, 57 (17), pp. 3671-3686.

34. Hagan, J.T. "Impossibility of fragmenting small particles: brittle-ductile transition" (1981) *Journal of Materials Science*, 16 (10), pp. 2909-2911.

35. Knieke, C., Sommer, M., Peukert, W. "Identifying the apparent and true grinding limit" (2009) *Powder Technology*, 195 (1), pp. 25-30.

36. Saether, E., Yamakov, V., Glaessgen, E.H. "An embedded statistical method for coupling molecular dynamics and finite element analyses" (2009) *International Journal for Numerical Methods in Engineering*, 78 (11), pp. 1292-1319.

37. Saether, E., Yamakov, V., Glaessgen, E. "New developments in the embedded statistical coupling method: Atomistic/continuum crack propagation" (2008) *Collection of Technical Papers - AIAA/ASME/ASCE/AHS/ASC Structures, Structural Dynamics and Materials Conference*

38. Thomas, L.M., Shanker, J. "Temperature dependence of elastic constants and thermal expansion coefficient for NaCl crystals" (1996) *Physica Status Solidi (B) Basic Research*, 195 (2), pp. 361-366.

39. Yamakov, V.I., Warner, D.H., Zamora, R.J., Saether, E., Curtin, W.A., Glaessgen, E.H. "Investigation of crack tip dislocation emission in aluminum using multiscale molecular dynamics simulation and continuum modeling" (2014) *Journal of the Mechanics and Physics of Solids*, 65 (1), pp. 35-53.

40. Kelchner, C.L., Plimpton, S.J., Hamilton, J.C. "Dislocation nucleation and defect structure during surface indentation (1998) *Physical Review B*, 58 (17), pp. 11085-11088.

41. Olusanmi, D., Wang, C., Ghadiri, M., Ding, Y., Roberts, K.J. 'Effect of temperature and humidity on the breakage behaviour of Aspirin and sucrose particles' (2010) *Powder Technology*, 201 (3), pp. 248-252.

42. Partnership for Advanced Computing in Europe (PRACE), http://www.prace-ri.eu

43. Greek research and technology network; Advanced Research Information System (ARIS) https://grnet.gr/en/

44. Germann, T.C. " Large-scale molecular dynamics simulations of hyperthermal cluster impact' (2006) *International Journal of Impact Engineering*, 33 (1-12), pp. 285-293.

45. Yamaguchi, Y., Gspann, J. "Large-scale molecular dynamics simulations of cluster impact and erosion processes on a diamond-surface" (2002) *Physical Review B*, 66 (15), art. no. 155408, pp. 1554081-15540810.

46. Doye, J.P.K., Wales, D.J. "Structural transitions and global minima of sodium chloride clusters" (1999) *Physical Review B*, 59 (3), pp. 2292-2300.

47. Kendall, K., Yong, C.W., Smith, W. "Deformation of NaCl particle in contact at the nano-scale" (2007) Powder Technology, 174 (1-2), pp. 2-5.

48. Miesbauer, O., Götzinger, M., Peukert, W. "Molecular dynamics simulations of the contact between two NaCl nano-crystals: Adhesion, jump to contact and indentation" (2003) *Nanotechnology*, 14 (3), pp. 371-376.

49. Pavia, F., Curtin, W.A. "Parallel algorithm for multiscale atomistic/continuum simulations using LAMMPS" (2015) *Modeling and Simulation in Materials Science and Engineering*, 23 (5), art. no. 055002.

50. Silani, M., Talebi, H., Arnold, D., Ziaei-Rad, S., Rabczuk, T. "On the coupling of a commercial finite element package with LAMMPS for multiscale modeling of materials" (2012) *Steel Research International*, SPL. ISSUE, pp. 1371-1374.

51. Vogiatzis, G.G., Voyiatzis, E., Theodorou, D.N. "Monte Carlo simulations of a coarse-grained model for an athermal all-polystyrene nanocomposite system" (2011) *Eur. Polym. J.*, 47, 699-712.

52. Ndoro, T.M., Voyiatzis, E., Ghanbari, A., Theodorou, D.N., Böhm, M., Müller-Plathe, F. "Interface of grafted and ungrafted silica nanoparticles with a polystyrene matrix: Atomistic Molecular Dynamics simulations" (2011) *Macromolecules*, 44, 2316-2327.

53. Vogiatzis, G.G., Theodorou, D.N. "Structure of polymer layers grafted to nanoparticles in silica-polystyrene nanocomposites" (2013) *Macromolecules*, 46, 4670-4683.

54. Skountzos, E. N., Anastasiou, A., Mavrantzas, V.G., Theodorou, D.N. "Determination of the mechanical properties of a poly(methyl methacrylate) nanocomposite with functionalized graphene sheets through atomistic simulations" (2014) *Macromolecules*, 47, 8072-8088.

55. Mathioudakis, I.G., Vogiatzis, G.G., Tzoumanekas, C., Theodorou, D.N. "Multiscale simulations of PS-SiO_2 nanocomposites: from melt to glassy state" (2016) *Soft Matter*, 12, 7585-7605.

56. Morozinis, A.K., Tzoumanekas, C., Anogiannakis, S.D., Theodorou, D.N. "Atomistic simulations of cavitation in a model polyethylene network" (2013) *Polym. Sci. – Ser. C*, 55, 212-218.

57. Romanos, N.A., Theodorou, D.N. "Melting point and solid-liquid coexistence properties of α_1 isotactic polypropylene as functions of its molar mass: A molecular dynamics study" (2016) *Macromolecules*, 49, 4663-4673.

58. Vogiatzis, G.G., Megariotis, G., Theodorou, D.N. "Equation of state based slip spring model for entangled polymer dynamics" (2017) *Macromolecules*, 50, 3004-3029.

59. Theodorou, D.N., Vogiatzis, G.G., Kritikos, G. "Self-consistent field study of adsorption and desorption kinetics of polyethylene melts on graphite and comparison with atomistic simulations" (2014) *Macromolecules*, 47, 6964-6981.

60. Sgouros, A.P., Vogiatzis, G.G., Kritikos, G., Boziki, A., Nikolakopoulou, A., Liveris, D., Theodorou, D.N. "Molecular simulations of free and graphite capped polyethylene films: Estimation of the interfacial free energies" (2017) *Macromolecules*, 50, DOI: 10.1021/acs.macromol.7b01808

61. Knieke, C., "Fracture at the nanoscale and the limit of grinding" (2012), PhD Thesis, Cuvillier Verlag Göttingen

IFPRI Research Project Brief

Rheology of Suspensions at High Solids Content: Bridging the Gap from Colloids to Grains

Pumping, flow, conveyance, and the long-term flow stability of highly concentrated particle systems remain and industrial challenge. Advancements in understanding surface turnover and chemistry-mediated particle interactions have improved our understanding of highly concentrated colloidal systems. Improvements in understanding of jamming phenomena, particle shape and inertial streams have similarly improved understanding of granular systems. A recent revolution has taken place in understanding the rheology of high-solid-content dispersions (HSCDs), viz., that at sufficiently high stress, particles are pressed into contact, so that many ideas from granular flow may become transferable to suspension flow in this regime. This project aims to explore how this new paradigm can be applied to optimize the processing of HSCDs by understanding how their rheology is controlled by many of the classic variables (e.g. morphology and size distribution) viewed under the new paradigm, and by some of the variables made relevant by these recent advances themselves (e.g. roughness, friction).

A key idea from recent advances is that HSCDs jam at a packing fraction ϕ_m substantially below random close packing, so increasing solid content involves increasing ϕ_m. *The overall objective is therefore to understand what controls* φ_m. Research themes under this heading may include:

- The friction coefficient matters, but how this can be systematically modified on the micro to nano scales is not yet mastered.
- Roughness almost certainly matters on some scale, but again, no systematic study yet exists.
- Badly packed aggregates lower ϕ_m, so that it may be fruitful to study wet milling in this context. In particular, wet milling applies stress to an HSCD at $\phi > \phi_m$ to break up aggregates, thereby lowering ϕ_m in the process; the new paradigm should give insight into how best to do this.
- Polydispersity is known to affect random close packing; how it affects ϕ_m is largely unknown.
- Identify key/dominant particle characteristics (e.g., morphology, surface friction, modulus, size distribution) that impact particle assembly, jamming and overall rheological behavior across the transition zone between low and high particle Peclet number concentrated (>40% vol) slurry systems for predictive modeling applications.
- Explore the link between system level and particle level characteristics on the packing/jamming transitions and corresponding rheology of concentrated suspensions across the transition regime between surface dominated interactions and inertially dominated particle systems.

To make progress, the contractor should be able to perform studies in well characterized systems using one or more of the following methodologies: monitor structure and dynamics under flow using a mixture of real-space and scattering methods; develop framework linking measured structure and dynamics to constitutive properties of suspension; develop toolkit for systematic variation of relevant parameters (friction, roughness, etc.).

Bridging the Rheological Gap:
Exploring Shear Thickening in non-Ideal Dispersions

Daniel L. Blair, Dept. of Physics and I(SM)^2, Georgetown University, USA

The response of concentrated collections of solid particles subjected to external shear stresses exhibits a rich variety of nonlinear flow behavior [1, 2]. In particular, colloidal dispersions and granular slurries can undergo dramatic increases in viscosity as the shear rate (stress) is increased above a critical value. For low to moderate concentrations, the increase in viscosity as a function of shear stress (or strain rate) will remain smooth resulting in continuous shear thickening. However, above a critical, and in many cases suspension specific concentration, the viscosity increase can become divergent, leading to a dramatic solidification of the suspension at a finite applied stress, known as discontinuous shear thickening. This illustrative example indicates that very small changes in processing conditions can have extreme outcomes that may result in the loss of time, energy and equipment. Understanding the role of structural heterogeneities and the spatial distribution of flow instabilities in concentrated suspensions is of ever increasing importance when considering the correct processing conditions of these value added materials.

The goal of this proposal is to outline a set of IFPRI relevant projects designed to quantify the impact that particle structure, collective flow dynamics, surface interactions, and particle stiffness have on the rheology of dense suspensions. To achieve this, we will perform innovative fundamental measurements on the flowing state of colloidal to granular scale suspensions by developing a new set of experiments that simultaneously describe the *bulk* and *local* rheology with real-space quantification of structural properties by utilizing our opto-rheological platform. We will work closely with all interested partners within IFPRI to identify ways that we can extend the applicability of our methods to existing systems to provide the best possible synergy between our work and broader needs.

To this end, we will directly address specific aspects of the *Project Brief* that align most effectively with our current experimental capabilities while providing a collaborative position for IFPRI partners to utilize our experimental resources. By investigating a broad range of systems, we will provide insights into the connections between single the attributes of single particles to the collective behavior of suspensions as they approach jamming at the packing fraction ϕ_m. Our proposed experiments provide a new way to link the structural evolution of sheared HSCDs in three dimensions, to the bulk and local rheology. We will explore what controls ϕ_m at the particulate level by using the experimental method we have developed, known as confocal-rheology, which provides both rheology and imaging over a broad range of length and time scales. Moreover, we will work to identify the impact that key microscopic physico-chemical parameters (*e.g.* polydispersity, friction, anisotropy) have on the flow and structure of HSCDs. These important experimental challenges are far from understood for these important materials.

Leveraging current work:
My group has focused on the development of experimental techniques that extend our ability to quantify the mechanical aspects of soft materials subjected to shear deformations. We have developed tools for the quantitative integration of high speed three dimensional confocal microscopy data with simultaneous rheology to provide real space analysis of the structure and dynamics of HSCDs at shear rates that span six orders of magnitude ($10^{-4} - 10^{2}\,\mathrm{s}^{-1}$) [3, 4]. Using these capabilities, we have investigated the microscopic origins of single particle rearrangements in polydisperse emulsions above ϕ_m and discovered that the observed Hershel Bulkley steady shear rheology can be explained through a microscopic description of the single particle rearrangement events[4].

Many of our experiments will utilize a new experimental method for quantifying the spatially and temporally resolved rheological response of suspensions. Our approach, known as *Boundary Stress Microscopy* (BSM) is a generalization of the traction force microscopy (TFM) method developed by biological physicists, applied to rheological measurements. TFM has also been used in non-rheological soft matter experiments to study fracture of slurries, dewetting of films and adhesion [6]. Briefly, BSM utilizes thin ($\sim 30\mu$m) transparent elastomeric substrates with controllable stiffness, that are spin coated onto glass slides. In our confocal rheology experiments, the elastomer coated glass slides replace the bottom plate of the stress controlled rheometer providing direct optical access to the suspension. The shear stress at the bottom boundary is measured using colloidal particles that are covalently linked to the elastomer (see Figure 1a). As the suspension is sheared by the upper plate of the rheometer tool, the stress in the fluid displaces the elastomer resulting in a displacement of the attached particles. These displacements are recorded with a high speed confocal microscope and then analyzed with particle tracking or velocimetry methods. Particle displacements are then converted into spatially resolved stresses using mathematical inversion methods. What results is a spatially and temporally resolved visual "read out" of the magnitude of the shear stress that is applied by the suspension to the bottom boundary. These local shear stress are resolvable over a broad range of length scales ranging from the single particle (the smallest area we can resolve a single stress value is $\sim 2\mu\mathrm{m}^2$) to as large as the entire rheometer tool (possible for small cones and plate geometries). Moreover, the technique is insensitive to particle size, shape and stiffness, making it an ideal methodology for investigating the local rheological properties of sheared HSCDs.

To provide context and to motivate the importance and applicability of BSM to our IFPRI projects, I will provide a brief overview of an example BSM from our recent publication of its application to HSCDs [7]. As is well known, bulk rheology provides spatially, and to varying degree, temporally averaged information about how fluids respond to an external imposed stress that originate and are subsequently measured through interactions

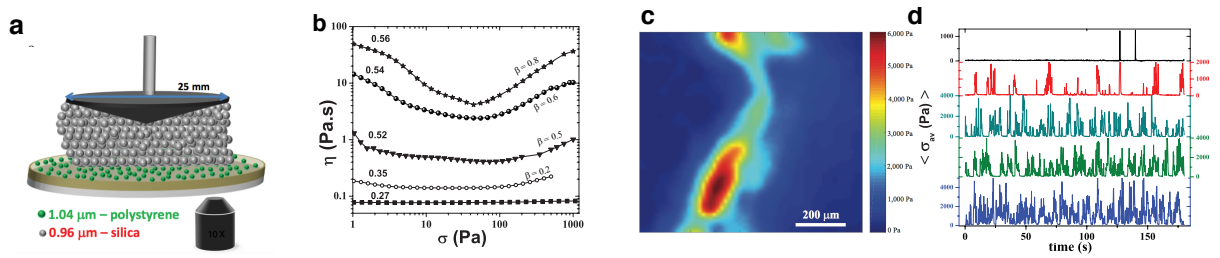

Figure 1: (a) Schematic of Boundary Stress Microscopy setup. The bottom cover slide is shown in silver and the thin elastic PDMS layer in light green. Fluorescent microspheres attached to the PDMS are shown in green and the silica colloids in silver. The rheometer cone defines the top surface of the suspension and is attached to a stress controlled rheometer. (b) Viscosity vs. applied stress flow curves for suspensions of different concentrations ϕ with the approximate shear-thickening exponent β. (c) Representative calculated stress field (component of the stress in the flow direction) showing heterogeneous boundary stress for a concentration $\phi = 0.56$ in the CST regime. The field of view, slightly less than 1x1 mm, is large compared to the particle size (1 μm) and small compared to the radius of the rheometer tool (25 mm), but the extent of the high stress region in the velocity (flow) direction is of the order of the space between the rheometer plates (200 μm). (d) Time series of average stress per frame from BSM in the CST regime ($\phi = 0.56$). From top to bottom, applied stress of σ = 100, 200,500,750, 1000 Pa (From [7]).

between the fluid and the boundaries of the rheometer tools. For example, in continuous shear measurements, the relationship between boundary displacement and applied torque is interpreted by the rheometer software to provide physical quantities such as viscosity, stresses, and shear rates that are constructed from constitutive models and tooling parameters. However, critical information about the existence of spatially non-uniform fluid stresses (force/stress chains), or nonlinear flow profiles (shear banding) are lost to averaging, removing any ability to link these important instabilities or heterogeneities to the bulk response. Boundary stress microscopy and real space 3-D imaging of suspensions during flow provide a route for directly quantifying these important features.

Figure 1(a-d) provides an example of how BSM is used to explore the structure and dynamics of a shear thickening suspension of hard colloidal particles. The bulk rheology of this fluid is typical for HSCDs composed of stiff and solid particles, showing a ϕ independent critical stress for the onset of thickening (Fig.1b). BSM reveals that the shear stress at the boundary is not uniform, indicating that the suspension is behaving like two fluids of highly varied local viscosities. We discern this from the strong stress fluctuations observed in Fig.1c; if the suspension had a spatially homogeneous viscosity, the stress map would have a uniform magnitude given by the stress applied to the suspension. If we spatially average the stress maps, we observe the magnitude of the total shear stress applied to that region at a given time. The time traces of the stress are shown in Fig.1d, showing that the frequency of the appearance of large local stress "events" increases, while the magnitude stays nearly

constant for a tenfold increase in the applied stress. This indicates that shear thickening is determined by the number of these localized solidification events. This is highly consistent with the models of shear thickening proposed by Wyart and Cates, where shear thickening is described as a transition between two fluid states [2]. Our results indicate that these two fluid states actually seem to coexist within the same suspension and that shear thickening is a phase separation phenomenon. Just to clarify the meaning of the stress maps relative to the bulk rheology – if we divide the temporal and spatial averages of the stress maps by the average shear rate reported by the rheometer, we simply reproduce the suspension viscosity. However, the stress maps provide a much richer picture of the suspension rheology.

Aspects of the Project Brief to be Covered:
We have identified numerous aspects of the Brief that are very closely aligned with our experimental expertise described above. In the themes identified below, we will perform complementary experiments that provide project outcomes that overlap both in technique and analysis, thus optimizing our ability to deliver results. We will address the following aspects described in the project brief.

- The role of polydisperisity and friction on the approach to ϕ_m will be explored. We will combine silica microspheres of particular size distributions with controlled number densities and final volume fractions (particles will be produced by our group using a Stöber-type synthesis). By directly controlling the polydispersity index of these suspensions, we will be able to *formulate* systems with known packing. We will use this as a model for the wet milling process and a method for understanding the role of packing efficiency on the fluidization of suspensions. We will quantify and link the microscale structure of the three dimensional packing directly to the rheology as a way to identify the onset of a yield stress and other rheological signatures that indicate an approach to ϕ_m. We will also utilize boundary stress microscopy to identify the types of flow instabilities that result in stress heterogeneities by measuring the local stress fluctuations. We hypothesize that these types of events are linked to the onset of shear thickening.

- To explore the role of friction, we will extend our synthesis capabilities to alter the surface of silica colloids by the addition of a thin polymeric coat. This soft coating will alter the contact dynamics of particle interactions. Using atomic force microscopy, we will quantify the relative frictional interactions between the coated to uncoated particle to identify the magnitude of force required to slide the particles past each other. We will then vary the relative number density of coated to uncoated particles, while keeping the overall volume fraction fixed. We will quantify the changes to the

rheological behavior, compared to unmodified suspensions, as the overall concentration is increased to ϕ_m. These experiments will provide a model system for altering the sliding friction of the system.

- We will explore how particle shape, morphology, frictional interactions, and stiffness impact the onset of jamming. We will investigate each aspect and combinations of physical attributes in model systems where each aspect can be adjusted independently and systematically. By extending our core shell approach to producing varied surface interactions we can also investigate the impact of particle stiffness on the overall rheological signatures of HSCDs. We will increase the thickness of the outer shell relative to the size of the individual particles. The relative size variation will will determine the overall stiffness of the particle resulting in suspensions of well understood surface interactions with variable stiffness. We will also utilize AFM in a tapping mode to quantify the overall change in particle stiffness with shell thickness. We will also explore the rheology of anisotropic particles using a method for synthesizing colloidal rods. We expect that the addition of anisotropy in the particle shape will become important as the isotropic-nematic transition is approached.

- We will explore rheology of suspensions and slurries as they traverse the transition from colloidal (interfacial) to granular (inertial) through the systematic increase in particle size. Using our boundary stress microscopy method, which is scalable across particle size, stiffness, shape, and surface chemistry, we will identify if the size of the particle impacts the local signatures of rheology as the system approaches jamming. In particular, we will explore how local instabilities in the flow, which is the mechanism for shear thickening, change (or not) as the Peclet number changes.

We will apply both our rheological and optical methods to each of the projects outlined below. Of course, BSM is just one type of quantitative technique that we have at our disposal. We have also developed a set of particle-scale microscopy tools for identifying the three dimensional structure and dynamics within sheared suspensions. Using these techniques we can investigate the packing geometry statistics from Voronoi-style spatial tessellation of the packing. By tracking individual particles in time, we can also determine the and displacement statistics and the velocity autocorrelation functions to determine a type of statistical mechanics for particle motion under shear.

Time-line:
We are providing a rough outline of the time-line for the work to be performed by the student that will focus on this project.

Y1. In this first year we will perfect the synthesis and AFM technique for producing suspension of variable surface interactions and stiffnesses. We will explore the proper types of polymer coats starting with polyacrylamide. In Y1, we expect to start producing rheological results and identifying structural features in the flow profiles as the interactions between particles are varied. Because the synthesis methods are linked, the results from Y1 will feed into our plan for Y2.

Y2. We will extend our formulations of suspensions by using the synthesis and characterization to produce systems with variable effective particle stiffness. I presume that within this year we will also start the process of mixing particle sizes to produce our model packings. We will also utilize time in Y2 to explore shape anisotropy through rheology and imaging.

Y3. In the final year of support we explore the colloidal to granular transition by identifying particle types and sizes that have similar surface friction and stiffness. This will be an important aspect of quantifying the impact of Peclet number on the rheological behavior of these suspensions.

References

[1] N. J. Wagner and J. F. Brady. "Shear thickening in colloidal dispersions." *Physics Today* 62, 27–32 (2009).

[2] M. Wyart and M. E. Cates. "Discontinuous shear thickening without inertia in dense non-brownian suspensions." *Phys. Rev. Lett.* 112, 098302 (2014). URL https://link.aps.org/doi/10.1103/PhysRevLett.112.098302.

[3] S. K. Dutta, A. Mbi, R. C. Arevalo, and D. L. Blair. "Development of a confocal rheometer for soft and biological materials." *Review of Scientific Instruments* 84, 063702 (2013).

[4] V. V. Vasisht, S. K. Dutta, E. Del Gado, and D. L. Blair. "Rate dependence of elementary rearrangements and spatiotemporal correlations in the 3d flow of soft solids." *Phys. Rev. Lett.* 120, 018001 (2018). URL https://link.aps.org/doi/10.1103/PhysRevLett.120.018001.

[5] E. Brown and H. M. Jaeger. "Shear thickening in concentrated suspensions: phenomenology, mechanisms and relations to jamming." *Reports on Progress in Physics* 77, 046602 (2014).

[6] R. W. Style, R. Boltyanskiy, G. K. German, C. Hyland, C. W. MacMinn, A. F. Mertz, L. A. Wilen, Y. Xu, and E. R. Dufresne. "Traction force microscopy in physics and biology." *Soft Matter* 10, 4047 (2014).

[7] V. Rathee, D. L. Blair, and J. S. Urbach. "Localized stress fluctuations drive shear thickening in dense suspensions." *Proc. Natl. Acad. Sci. U.S.A.* 114, 8740–8745 (2017).

IFPRI Project proposal: Erin Koos

1. State of the art

Suspensions can exhibit a wide range of rheological behaviors such as shear thinning, shear thickening, and normal stress differences. These behaviors are closely linked, not necessarily to the bulk particle structure, but more to the microstructure and direct particle contacts. For instance, discontinuous shear thickening (DST) is closely linked to friction, and hence on the number of number of particle contacts. In their numerical study, Mari et al. showed a link between the fraction of frictional contacts and the shear stress [1]. This fraction of frictional contacts, defined as the number of contacts where the normal force exceeds the critical load for the onset of friction in their model divided by the total number of particle contacts, was independent of volume fraction.

Confocal microscopy allows us to image model suspensions to gain information about their microstructure [2–4]. Recently, we have used this method to determine the structure of suspensions with attractive capillary interactions [5, 6]. Confocal microscopy is a powerful tool that can be used to study the link between the network microstructure and the rheological response of the material. Typically, the structure is analyzed using the local volume fraction ϕ_{local} or coordination number z [7, 8]. We propose using an additional parameter c, the clustering coefficient. The clustering coefficient is a measure, taken from graph theory, describing the clique-ishness of a network. The difference between the coordination number and the clustering coefficient is shown in Figure 1. In this figure, the center two configurations both have a coordination number of 3. In the case were the particles are distributed around the particle, the bonds are able to rotate as shown by a low clustering coefficient ($c = 0$). The case where the particles form close-packed dimers will be much more rigid and the clustering coefficient is closer to unity ($c = 2/3$).

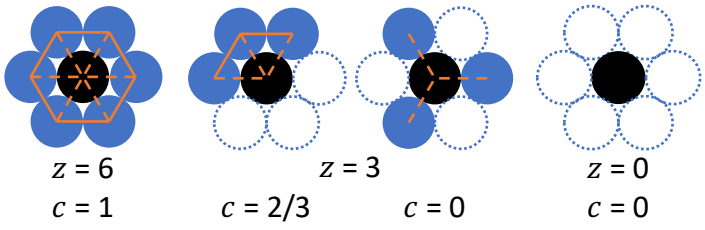

Figure 1: Difference between the coordination number z, the number of bonds per particle (dashed lines), and the clustering coefficient c. The clustering coefficient is defined as $c = \frac{2e}{z(z-1)}$, where the number of bonds between neighbors (solid lines) is e.

We have applied this concept to networks with capillary interactions (Figure 2). A slice of the confocal image is shown on the left in this figure. As the solid phase, we used monomodal silica spheres with a mean particle size of $d_{50,3} = 6.40 \pm 0.02$ µm and a polydispersity of $(d_{90,3} - d_{10,3})/d_{50,3} = 0.697 \pm 0.005$. The nanoporous particles were fluorescently dyed with rhodamine B isothyocyanate and are shown in red in this image. The secondary fluid, aqueous glycerine is dyed using PromoFluor-488 premium carboxylic acid and shown in yellow in this image. The oil, a mixture of 1,2-cyclohexane dicarboxylic acid diisononyl ester (Hexamoll DINCH) and n-dodecane, is undyed. The three components are all index matched and the silica contact angle modified (see [5] for more information). The computationally reconstructed body for this network is shown on the right where the particles are colored using their individual clustering coefficient. To determine the particle positions and sizes, the computational code of Weeks [9] (based on the method of Crocker and Grier [10]) was used

where multiple mask sizes were employed to account for the polydispersity in the particle diameters. Particle contacts were determined using a separation threshold.

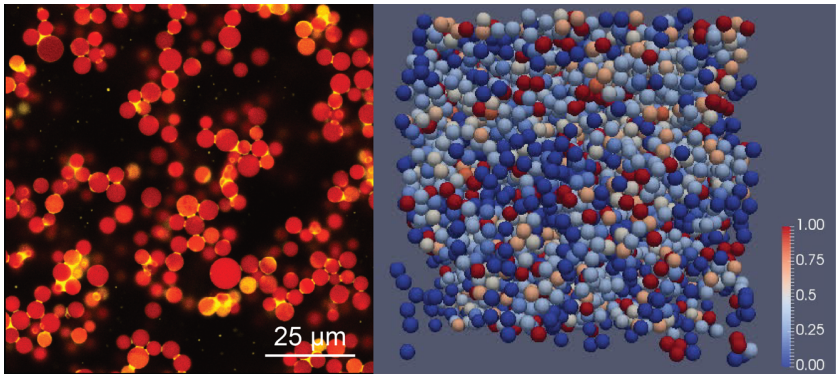

Figure 2: (left) Confocal image and (right) reconstructed body colored by the clustering coefficient for each particle. This solid-liquid-liquid system has $\phi_{\text{solid}} = 0.25$ and $\phi_{\text{sec}}/\phi_{\text{solid}} = 0.09$.

The average coordination number and clustering coefficient compare well with transitions observed in the rheology of these capillary networks as shown in Figure 3. The transition from a granular pile to a pendular network corresponds to a drop in both z and c as a loose sample-spanning network is formed. (There is no rheological data for $\phi_{\text{sec}}/\phi_{\text{solid}} = 0$ as phase separation prevented these measurements.) The transition from a pendular network, where particles are connected by binary bridges, to the funicular state, where larger clusters are formed, occurs at $\phi_{\text{sec}}/\phi_{\text{solid}} = 0.09$ (case shown in Figure 2), which corresponds to a peak in the coordination number and beginning of a plateau in clustering coefficient. While not shown here, the distribution of clustering coefficients in the system changes from a monomodal to bimodal distribution.

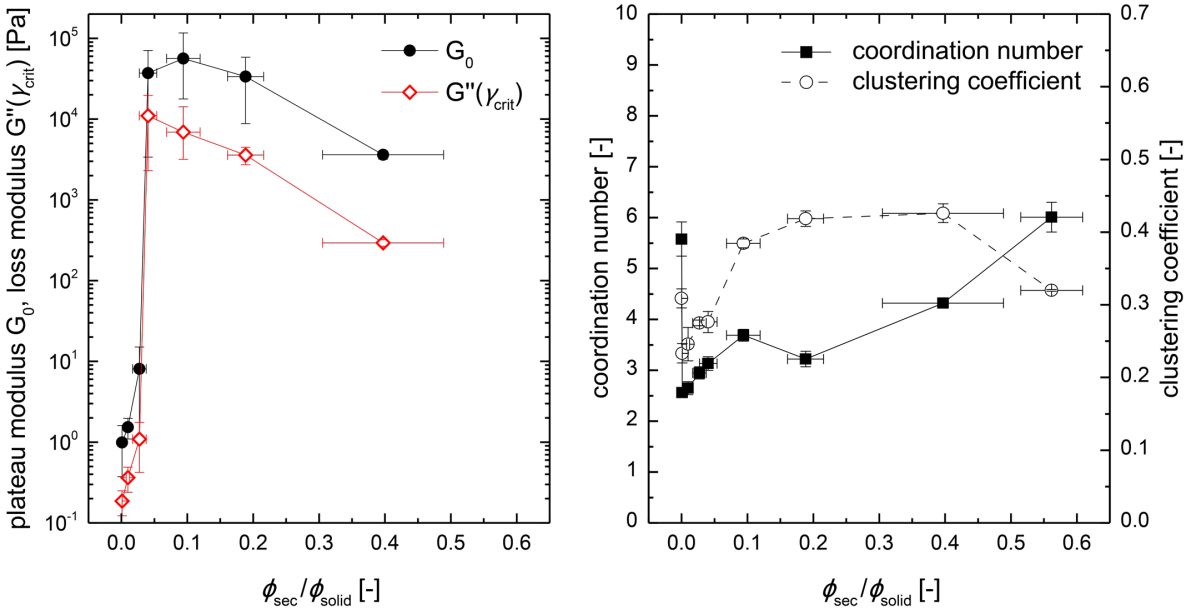

Figure 3: (left) Plateau modulus G_0 and loss modulus G'' at the critical oscillatory amplitude γ_{crit}. (right) Mean coordination number and clustering coefficient computed from confocal imaging. The rheological properties at $\phi_{\text{sec}}/\phi_{\text{solid}} = 0$ (granular bed) and $\phi_{\text{sec}}/\phi_{\text{solid}} = 0.56$ (inside a dense floc) were not measured as phase separation occurred in these systems.

This method can be used to investigate several phenomena in granular systems. One particularly promising area is in understanding yield. Yield occurs on a plane with some critical number of defects or where key rearrangements are possible. As these materials are

disordered, this is a statistical process. A better understanding of the specific microstructure around yielding plane. These particle contacts are equally important in situations where chains of particles lead to a dramatic increase in the shear stress or even the stoppage of flow.

2. Proposed work

2.1. General methodology

The general methodology can be described as follows:

1. Samples for confocal microscopy will be created using an index matched system of SiO_2 or polymeric particles in a suitable oil (Hexamoll DINCH, BASF) or aqueous glycerol. The particle surface chemistry can be controlled to create attractive or repulsive interactions. Cubic particles can be printed (IP-Dip, Nanoscribe) and raspberry particles created using a UV curing polyurethane resin (Conathane, Cytec Solvay).
2. The micro-and network structure will be imaged using confocal microscopy and analyzed using a custom-designed IDL code. This code determines the particle positions and their size (for polydisperse particles) as well as the size and location of the secondary fluid. From this information, various parameters can be calculated.
3. The particle positions and microstructure will be monitored during shear using a thermo-shear cell that fits on top of the confocal microscope. This shear cell applies a linear shear profile using the deformation of microscope slides. The structure can be either monitored continuously during shear (if the continuous shear profile is sufficiently slow) or using a step profile.
4. The bulk rheological properties of the materials will be measured under steady and oscillatory shear. In addition to the shear stress, the first normal stress differences will be measured.

2.2. Specific work packages

WP1: Particle tracking under shear

Using the custom IDL code and the thermo-shear cell, we can track the particle positions and interactions under step or oscillatory shear profiles. Of particular interest is the development of the coordination and clustering coefficient during shear. We hypothesize that particles clusters with a high clustering coefficient undergo rigid-body motion and should be associated with frictional shear thickening. By tracking the individual particle deformation and that of the neighboring particles, we can correlate this motion to the local clustering. We will begin using a very slow, step shear profile to test and optimize the particle tracking. We will then investigate profiles with a larger shear step. As the tracking of individual particles may be difficult at large steps, we may employ a small proportion of tracer particles with a fluorescein isothiocyanate (FITC) dye and track their dynamics. Using the microscope, we can look at the number and type of particle collisions and bonds at yield, during shear thickening, and also between the different layers in the shear banding system.

These shear profiles will be repeated on the rheometer so that the force measurements can be compared to the changes in microstructure. These rheometer tests can also be used to highlight interesting regions for the confocal study. The thermo-shear cell uses piezoelectric

actuators to create a smooth shear profile, which means that the force data cannot be independently measured. We might be able to use the applied voltage to monitor changes to the force, but this cannot be used to make reliable rheometric measurements. Thus, we must rely on correlations between the two devices.

WP2: Particle size distribution

The particle size distribution influences both the packing of particles and the resultant rheological properties. A microfluidic chip using UV curing polymers can be used to create particles with a uniform size. Uniform particles are particularly interesting as they are associated with a very high degree of local ordering or crystallization. Such ordering is interesting as yielding typically occurs at regions with low local order. We will then investigate a unimodal particle size distribution having wider and narrower size ranges, which change the effective packing and the effective viscosity of these systems. The particles currently used (Figure 2) already have a size distribution, so modification of the particle-tracking algorithm will not be necessary.

Systems with mixtures of large and small particles, varying the relative fractions and size ratios, will then be employed. Such mixtures are associated with a decrease in the effective viscosity at intermediate fractions of small spheres, with the degree of reduction depending on the relative size ratio of the spheres. With our method, we can investigate the local packing around both sphere sizes individually as well as the influence on the direct local deformation of the system.

Finally, by using a combination of silica and polymeric particle types or by modifying the particle hydrophobicity, we can include variations in the charge or surface chemistry. These interactions modify the effective size and softness of the particles as well as the importance of frictional collisional interactions in the shear dynamics. Such repulsive interactions have been shown to reduce or even prevent shear thickening whereas attraction between the particles acerbate this problem. We must be careful in conducting experiments with repulsive systems, however. A very thin layer of fluid, below the optical resolution of the microscope, may separate the particles. This fluid layer complicates the calculation of particle bonds. Thus, we will probably need to look at the motion of neighboring particles to determine bonds.

WP3: Raspberry-shaped particles, cubic particles, and particle mixtures

UV curing polymers allow a variety of particle shapes to be created. We can print cubic particles using a Nanoscribe, or raspberry-shaped particles using a microfluidic double emulsion templating (DETA) Pickering emulsion route. Depending on the size of the asperities, we can either treat the particles as spheres or individually detect the size and orientation of the asperities. In this latter case, the use of two different fluorescent dyes may improve the detection. The cubic particles have an orientation and the current IDL code (as well as Week's algorithm) uses a cross correlation between the particle and a mask. Therefore, the IDL code will have to be modified using a FFT to determine the particle orientation as the mask is applied. Both the raspberry particles and the cubic particles will significantly increase the effective friction during collisional interactions and cause groups of particles to undergo solid-body motion. Thus we want to closely track the relative motion (and rotation) of particles.

We can then use a combination of spherical and raspberry particles and spherical and cubic particles. (Raspberry and cubic particles will also be included if possible.) This will effectively introduce different types of interactions: smooth-smooth interactions with low friction, rough-rough interactions with high friction, and smooth-rough interactions with an intermediate friction. The aggregate behavior will be monitored as a function of the ratio of the particle types and relative particle sizes. By using two different dyes, we can easily distinguish the two particle types and hopefully track the change in particle velocity before and after collisions depending on the particle types.

2.3. Gantt chart

This research is divided into three work packages. The first three quarters will consist of improving the IDL code and tracking the particles under shear. This code will have to be improved for each subsequent work package. The other two work packages investigate particle size distribution and particle shapes.

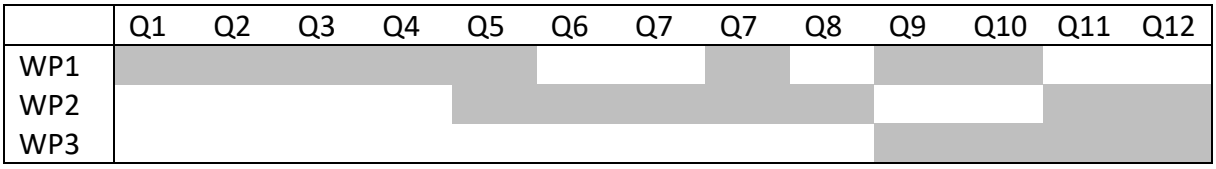

3. Leverage opportunities

3.1. Existing research programs

I have already started to investigate the structure of capillary suspensions using these confocal microscopy techniques. Thus, the developments we make within this proposal can benefit from and contribute to these efforts. Our initial study (highlighted above) shows that the microstructure can be used to predict the bulk rheological data under quiescent conditions. Naturally, we would like to adapt this method to monitor dynamic changes to the network, especially during yielding. The advanced made in this program, in combination with the work with capillary suspensions, also lends itself to a future expansion in the dynamics of wet granular media.

In addition, I have a doctoral student who recently started to model capillary suspensions using the coarse-grained MD code ESPResSo. He will determine the structure of these networks and to make pseudo-rheology experiments under various conditions. This student has experience in analyzing the particle networks once the particle positions and sizes are determined. In addition, we can use the confocal experimental results as the initial conditions for the MD model. The rheological results made in this project will improve the force-interaction curves in his model and give us more insight into the direct influence of the particle interactions on the resultant behavior, especially as such particle interactions can be selectively altered computationally.

3.2. Collaboration within IFPRI

The industrial expertise of the IFPRI members will be invaluable in identifying areas of specific interest for this project. This research should be a platform that we can use to gain a clear understand the dynamics on a limited scale. Thus, the problems and test methods should be used as a starting point in this project. We can then identify the specific microstructural changes occurring during these tests or under these specific conditions. By highlighting the microstructural changes, especially in relation to the particle interactions, we can have a positive feedback loop with industry to suggest minor changes and tackle increasingly more complex problems.

While this research project concentrates on the use of model systems due to the limitations of confocal microscopy, we should push towards making experiments on real systems. Assistance in bridging this gap using more ideal, industrial materials would be appreciated. Coating seed particles with silica can be used as one such method. This can even be used to create irregular particles that still have the necessary index of refraction for confocal microscopy. We aim to start with more well-defined particle shapes, but angular and irregular particles are the natural end goal.

4. References

1. Mari, R., Seto, R., Morris, J. F., Denn, M. M. (2014). Shear thickening, frictionless and frictional rheologies in non-Brownian suspensions. *Journal of Rheology*, *58* (6), 1693–1724.
2. Cheng, X., McCoy, J. H., Israelachvili, J. N., Cohen, I. (2011). Imaging the Microscopic Structure of Shear Thinning and Thickening Colloidal Suspensions. *Science*, *333* (6047), 1276–1279.
3. Dinsmore, a D., Weitz, D. a. (2002). Direct imaging of three-dimensional structure and topology of colloidal gels. *Journal of Physics: Condensed Matter*, *14* (33), 7581–7597.
4. Dinsmore, a. D., Prasad, V., Wong, I. Y., Weitz, D. a. (2006). Microscopic structure and elasticity of weakly aggregated colloidal gels. *Physical Review Letters*, *96* (18), 185502.
5. Bossler, F., Koos, E. (2016). Structure of Particle Networks in Capillary Suspensions with Wetting and Nonwetting Fluids. *Langmuir*, *32* (6), 1489–1501.
6. Bossler, F., Maurath, J., Dyhr, K., Willenbacher, N., Koos, E. (2018). Fractal approaches to characterize structure of capillary suspensions using rheology and confocal microscopy. *Journal of Rheology*, *62* (1), 183.
7. Aarons, L., Sundaresan, S. (2006). Shear flow of assemblies of cohesive and non-cohesive granular materials. *Powder Technology*, *169* (1), 10–21.
8. Wenzl, J. (2013). *Wet and dry model granulates under mechanical load A confocal microscopy study*. Johannes-Gutenberg-Unversität, Mainz.
9. Weeks, E. R. (2000). Three-Dimensional Direct Imaging of Structural Relaxation Near the Colloidal Glass Transition. *Science*, *287* (5453), 627–631.
10. Crocker, J. C., Grier, D. G. (1996). Methods of Digital Video Microscopy for Colloidal Studies. *Journal of Colloid and Interface Science*, *179* (179), 298–310.

IFPRI Review Brief
Milling Aids

The International Fine Particle Research Institute wishes to commission a comprehensive review of the use of grinding aids in milling of organic and inorganic materials. The review should include an overview of the types of grinding aids that are used and how they are used (i.e. in what types of mills for what materials), and what their impact is on energy consumption and milling rate. It should also include a critical discussion of the current understanding of the mechanisms by which grinding aids work. The scope of the review is limited to dry grinding of inorganic or organic materials with dry or liquid grinding aids (including steam), and it should include discussion of both positive and negative effects of the aids.

IFPRI Review Brief

Characterization of Fluid Boundary Layers in High-Shear Multiphase Flows

The International Fine Particle Research Institute wishes to commission a comprehensive critical literature review of experimental methods and modeling approaches to describe high-shear flow of suspensions and dispersions, slurries, and pastes in confined flows at wall boundaries in processes such as extrusion and injection molding. This review should identify current practices and the state of the art in both experimental methods and modeling approaches. Of particular interest is the phenomenon of wall slip, which is fundamental to the response of high-solids fraction suspensions to mechanical deformation.

CONTROLLING RHEOLOGY VIA BOUNDARY CONDITIONS IN DENSE GRANULAR FLOWS

Karen Daniels
Dept. of Physics, NC State University
kdaniel@ncsu.edu
(919) 513-7921
http://danielslab.physics.ncsu.edu

April 30, 2018

Introduction & Completed Work

In the field of granular rheology, one of the most promising advances of the past decade has been the development of various *nonlocal* rheologies [1, 3, 4, 12, 14, 19, 34]. These constitutive models hold the promise of permitting the determination of a small number of empirical parameters for a particular set of particles, which then can be used to predict flow fields and stresses over a large range of intermittent, creeping, quasi-static, and intermediate flows. In order for these models to be useful, the aim is to make a set of flow measurements for a set of particles in one geometry, and then determine the constitutive parameters for use in predicting flows in other geometries (for the same particles). Doing this requires a quantitative understanding of which properties are set by both the particle properties, and the boundary conditions at the walls.

Constitutive models can be postulated on very general empirical grounds, relating the applied stresses to the properties of flow. For granular materials, such constitutive models are a generalization of elastic theory (applied stress causes reversible elastic deformations) and viscous theory (applied stress causes flow) that allows the continuum modeling of a broad class of materials. In a dense granular flow, the starting point for describing a flow is to consider the dimensionless inertial number [12, 17, 22, 26]

$$I \equiv \frac{\dot{\gamma} d}{\sqrt{P/\rho}}.$$

This arises from the ratio between two timescales: a microscopic timescale $T = d/\sqrt{P/\rho}$ (the time for a particle of density ρ to fall into a hole of grain size d, under pressure P) and a macroscopic timescale $1/\dot{\gamma}$ (the mean deformation time due to shear rate $\dot{\gamma}$). While the modeling of rapid flows ($I \gg 1$) is in an advanced state [6, 13], intermediate flows ($I \sim 1$) must account for both shear and compression effects [7], and slow flows ($I \ll 1$) remain particularly challenging to model. It is convenient to similarly measure the applied stress (the cause of the flow) via the nondimensional stress ratio μ, the ratio between the local shear stress τ and the local pressure P:

$$\mu \equiv \frac{\tau}{P}.$$

Constitutive measurements of $\mu(I)$ were first modeled by purely local considerations: any point with $\mu \geq \mu_s$ (the yield criterion) would be flowing, and those with $\mu < \mu_s$ would be blocked. While these local rheologies have been broadly successful at describing fully-developed flows [12], they fail to quantitatively capture the transition from inertial to quasistatic ($I \ll 1$ but still creeping) flow [20], explain the dependence of shear band width on geometry and grain size [8, 22],

or describe how shear/vibration in one region of a granular material can fluidize distant regions [23, 27]. Due to these limitations of local rheology, several nonlocal rheology models have recently been developed. The nonlocal rheology model proposed by Kamrin and Koval [14, 19] extends a local Bagnold-type granular flow law to include a Laplacian term governing the diffusion of *fluidity* via cooperative effects. The nonlocal rheology model of Bouzid *et al.* [3, 4] performs a gradient expansion of a general constitutive relation. In both models, a Laplacian term models the diffusion of nonlocal effects within the granular material, but with a different physical interpretation; we will refer to these models as *cooperative* and *gradient*, respectively. The diffusive aspect of nonlocal models also introduces a characteristic mesoscopic lengthscale between the particle (micro) and bulk (macro) scales. In this renewal proposal, we will focus our efforts on the cooperative model of Kamrin et al. This is both for the more physical basis for its underlying assumptions, and because it does an equivalent job of modeling the data, but with one fewer free parameter.

Local Rheologies

the local shear rate is determined by only the local shear stress
resistance to flow is a function of only the local shear rate
constitutive parameters μ_s, b

Non-Local Rheologies (NLR)

particle rearrangements in one part of a flow trigger rearrangements elsewhere
resistance to flow is a function of both the local shear rate and these non-local events
constitutive parameters, in addition to nonlocal parameter A

Figure 1: Summary of Local vs. Non-Local Rheologies. More detailed descriptions of the models are provided in Tang et al. [30] (included as Appendix A).

These nonlocal models provide an important advance in our ability to write continuum models with quantitative predictive powers, with all parameters determined from empirical experiments. These nonlocal rheological models (NLR) complement discrete element models (DEM, [9]) in important ways:

- While DEM are currently limited to simple shapes such as circles (or a aggregates thereof), NLR permit modeling of any particle shape/size distribution, once the empirical parameters are determined.
- Because DEM requires solving the Newtonian equations of motion ($\vec{F} = m\vec{a}$) for all particles, the computational time grows significantly with the size of the system; NLR (like the Navier-Stokes equations for fluids) are scaled to the system size after the simulation is completed and therefore do not.
- DEM provide the details of every particle's dynamics and stresses, required for some applications, while NLR only give velocity, fluidity and stress fields.

(a)

(b)

	Vishay circles/ellipses	acrylic ellipses	acrylic circles	acrylic pentagons
μ_s	0.26 ± 0.02	0.24 ± 0.02	0.24 ± 0.02	0.17 ± 0.01
b	1.1 ± 0.3	1.1 ± 0.5	1.1 ± 0.6	1.1 ± 0.6
A	0.402 ± 0.003	0.231 ± 0.003	0.280 ± 0.003	0.101 ± 0.001

Figure 2: (a) Example laser-cut particles from our particle library. Opaque (acrylic) particles are laser-cut to include a central hole to aid in more accurate and precise particle-tracking. (b) Table of NLR parameters determined for each shape (**Q2**).

- Both DEM and NLR are expected to be able to capture intermittency, flow/no-flow, and large spatial gradients, but the NLR have not been well-tested in these regimes.
- For both DEM and NLR, the choice of boundary condition must be specified. For DEM, the choice of interparticle interactions directly guides this choice, while for NLR it is an open question.

This project aims to address current shortcomings in how to calibrate and apply NLR to real granular systems, beyond calibrating them against DEMs as has been the primary validation to date. During the first two (of three) years of our IFPRI funding, our team has performed quantitative tests [30] of both the cooperative [19, 34] and gradient [3, 4] nonlocal rheologies. Although only the cooperative model was mentioned in the original proposal, it later became clear that multiple, competing models were available. We therefore adjusted our aims to evaluate both of them simultaneously.

Our experiments (see Fig. A.1) have established the following successes of both these two models, addressing our original 3 questions.

- **Q1**: We have measured the flow field $v(\vec{r})$ and fluidity field $g(\vec{r})$ in 2D annular flows [30], and found that both models describe the data well, using a single set of parameters across

many different flow conditions. We observed that the diverging length scale $\xi(\mu)$ behaves as predicted from models, the first such observation in experiments. These comparisons were enabled by the development of a new type of experiment wall in which the wall itself acts as a sensor to measure $\mu(r)$ (see Tang et al. [29] for details). The key results addressing **Q1** are presented in Fig. A.5a and A.7b from [30] (attached as Appendix A).

- **Q2**: We are currently measuring the shape- and size-dependence of both the fitting parameters and the diverging length scale. Preliminary results are presented in the annual report, and further research is continuing this year, with some current results presented in Fig. 2. In all cases, the NLR model was able to successfully model the flows. We observe that μ_s differs for angular vs. rounded particles, and the nonlocal parameter A varies based on both particle material and shape.

- **Q3**: Using photoelastic particles [11], we have observed [30] that the fluctuations in local forces do coincide with the onset of the non-local contribution to $g(\vec{r})$, at μ_s. This is a new interpretation of the physical mechanism behind the models. This result is presented in Fig. A.8.

In the course of performing these experiments, we have realized that our existing annular apparatus does not attain flows which truly reach the intermediate flow regime ($I \approx 1$). Therefore, we have recently begun an IFPRI-funded collaboration with Nathalie Vriend (Cambridge, UK) in order to investigate that regime in her existing chute flow apparatus. This has permitted us to add a free-surface flow to our project; experiments and analysis are currently underway and will be presented at the Annual Meeting.

Proposed Research Aims (Revised)

In the first funding period, we focused on performing experiments in steady flows that are slow enough to achieve the first quantitative tests of the validity of the NLR models. These have been successful, allowing us to move on to new aims which expand our ability to utilize the models in more contexts. An important horizon is the influence of the boundary conditions on granular flows. To draw an example from ordinary fluids: understanding the no-slip boundary condition has been instrumental to development of the field of fluid dynamics [21]; today, an exciting new horizon is arising through new availability of superhydrophobic coatings [28].

In this renewal proposal, we focus on characterizing the properties of granular slip at boundaries, incorporating our observations into NLRs, and investigating which aspects of a dense granular flow can be controlled by the choice of boundary condition. Detrimental flow behaviors such as intermittency, creeping/stagnant zones, and clogging arise from a complex interaction between the flow-forcing and the boundary conditions. We will be guided by recent preliminary experiments (presented below), and will continue to work with particles of a variety of shapes, beyond circular.

NLR depend on only a small number of empirically-determined parameters. In order for them to be successful as a modeling tool, we need to be able to make flow measurements for a set of particles in one geometry, and then use them to provide predictions for flows in other geometries. For example, the density and viscosity of an ordinary fluid are material constants (with known and understood dependence on temperature and intramolecular interactions) and can be measured outside of the context of any particular flow. The goal of this aim is to provide guidance about how the boundary conditions should be handled for a particular choice of granular materials and boundary property.

Our specific aims for the renewal period are as follows:

Q4: *How does changing the roughness and/or compliance of a boundary change the resulting flow?*

We will perform rheological tests as a function of both variables to quantify the joint effects of these roughness and compliance. Our existing annular apparatus (see Fig. A.1) was designed to be used with exchangeable laser-cut outer boundaries. The leaf-spring boundaries used during the first grant period are tunable by both roughness and compliance. In NSF-funded research, we have observed that the choice of boundary strongly controls the stick-slip statistics of the flow (see Fig. 3) through the relative presence of particle slip at the wall. Similarly, the Vriend group has observed that the roughness at the base of a chute flow controls flow profile and internal stresses [31]. We will laser-cut multiple different

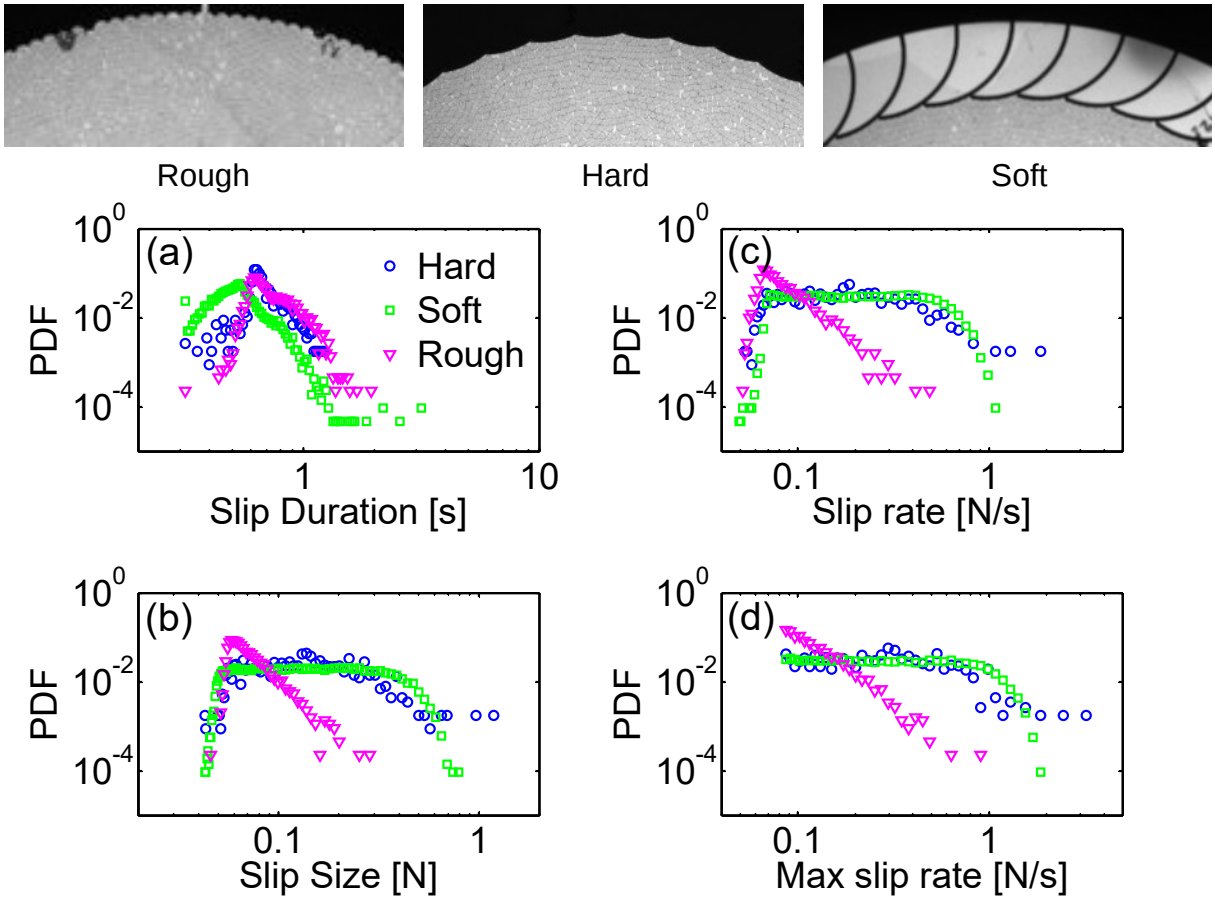

Figure 3: Top row: Sample boundaries of varying roughness and compliance. The walls labeled Smooth/Rough are both non-compliant acrylic, and Soft is smooth and made compliant (able to dilate) via leaf springs of the same shape as the Smooth boundary. We observe that these designs for the outer wall control key aspects of the stick-slip statistics of intermittent flows driven by a linear stiffness ramp. For a series of thousands of stick slip failures, we observe histograms of the (a) slip event duration, (b) total force drop during event, (c) the average rate of force-release, and (d) maximum rate of force-release. These figures are adapted from data collected by Ted Brzinski (Daniels group, publication in prep, [5]) for the three different outer wall geometries. Note that the existing annular apparatus can be modified to operate either via direct-drive (as was done for the data presented in Appendix A), or with a spring-loaded coupling which can generate the stick-slip motion reported in this Figure. For the experiments proposed here, we will focus on the direct-drive setup.

boundaries spanning a range of (roughness, compliance) properties and quantify the effects of these parameters, both independently and jointly. Experiments will be conducted on both smooth and rough particles for completeness.

Q5: *What are the general principles which allow us to correctly set the boundary conditions in NLR models, based on the roughness/compliance of the boundary relative to the particle properties?*

The newest forms of NLRs [14, 15, 18] allow for strong spatial and temporal gradients in both $\mu(\vec{r},t)$ and $I(\vec{r},t)$, but the boundary conditions for the resulting flow fields are typically set by hand from direct observations of the flow profile. We will use the results of **Q4** to construct principles under which these boundary conditions can reasonably be set from a general set of rules about the roughness/compliance of the boundary relative to the particle properties.

Q6: *Are the NLR parameters and boundary conditions determined in one geometry appropriate for use in other geometries?*

A key prediction is that the NLR parameters determined in one geometry will be appropriate for use in other geometries. We will test this prediction directly, by using the results of **Q4/Q5** to make and test predictions about simple observables (e.g. mass-flow rate) for a hopper-flow in which the outer wall boundary properties are identical to those used in the annular rheometer.

Research Plan (Revised)

Our experiments for **Q4/Q5** will primarily be conducted in the existing annular shear apparatus (see Fig. A.1), supplemented by a simple hopper-draining flow for **Q6** (see Fig. 4). Both of these experiments will operate on a single layer of laser-cut particles or a thin (up to 1.5 cm) layer of more realistic granular materials, with the later occurring as time allows. The characterization of the hopper flow (flow field, mass flow rate, boundary deformations) will be conducted via image-processing from a camera.

We currently have the following shapes available (see Fig. 2): stiff photoelastic Vishay particles (mix of ellipses and circles), soft photoelastic polyurethane articles (circles), and non-photoelastic acrylic particles (circles, ellipses, pentagons, stars). These span a variety of stiffnesses, friction coefficients, sizes, and shapes to provide a range of tests. Additional particles will be cut as needed during the experiments described below.

Our timeline is as follows:

Year 1-2: Our existing annular apparatus was designed to be used with exchangeable laser-cut outer boundaries. To complete **Q4**, we will begin by laser-cutting and calibrating the new outer wall panels using the same methods described in [29]. The wall designs will systematically-vary both roughness (the shape of the outer surface) and compliance (stiffness of leaf springs), as shown by the examples in Fig. 3. This could, for instance, be all combinations between 3 roughnesses and 3 compliances for a total of 9 designs.

As a result of the first round of funding, we already know the values of the constitutive parameters (A, b, μ_s) for the cooperative model for four different sets of particles (see Fig. 2). We will chose one rounded and one angular particle type from this list, and perform experiments quantifying the rheology. If needed, we will perform these experiments with photoelastic particles, but hopefully the acrylic particles (easier to use) will be sufficient.

As with our work during the first funding period, we will measure both the bulk rheology (shear stress $\tau(r)$, normal stress P) and individual particle trajectories $\vec{r}_i(t)$. Taking these bulk and local measurements provides all of the information necessary to calculate the local $\mu(I)$ and fluidity, but also to characterize the dependence of the boundary conditions on both the particle-shape and boundary-characteristics.

Year 2: Using the data collected during the first phase of the project, we will seek to find general trends regarding the dependence of boundary condition on the particle shape, boundary shape, and

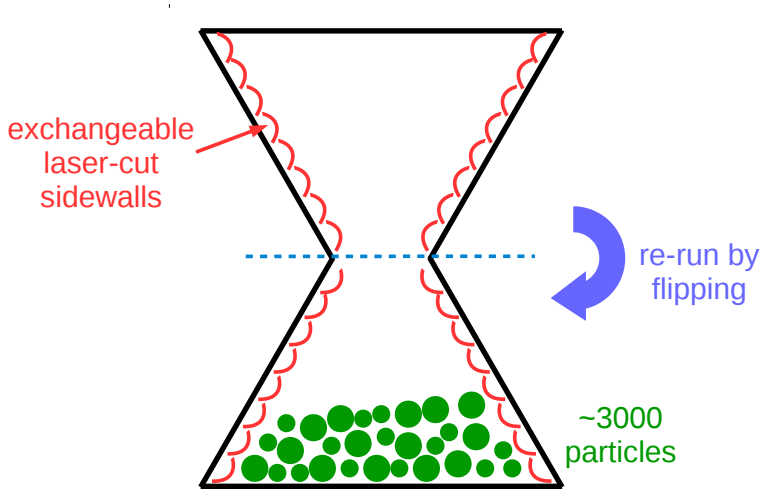

Figure 4: Schematic of 2D hopper, with an hourglass-like flippable design to allow for numerous trials. The sidewalls will be easily exchangeable to allow for reconfigurability to test boundary conditions.

boundary compliance (**Q5**). We will aim to identify general principles present for determining the boundary condition in such fields as $v(\vec{r})$, $\mu(\vec{r})$, and $I(\vec{r})$. For example, in the intermittent flows presented in Fig. 3, we found that wall-slip at the outer wall (present for the low-roughness experiments) is correlated with the presence of longer-duration and large-magnitude slip events. Using the direct-drive scenario (used in [30]), we hope to be able to use the simple NLR models tested so far. However, we will expand our research to include NLRs that allow for spatial and temporal gradients [14, 15, 18] if any of the particle/boundary choices require it.

Year 3: We will conduct simple hopper flow experiments, designed to accommodate the same particles and the same boundary designs used in the annular cell. A schematic is shown in Fig. 4. Using the NLR parameters (A, b, μ_s) already determined for each set of particles, plus the determination of appropriate boundary conditions from **Q5**, we will make predictions for flow/no-flow conditions, mass-flow rates, and flow fields within the hopper. For each set of parameters, we will completed dozens of trials in order to obtain sufficient statistics to make a quantitative comparison with NLR predictions. Hopper-flow experiments have the benefit of allowing access to intermediate flow regimes more readily than our annular Couette apparatus, due to the low confining pressure.

Synergies and Outlook

As in the first round of funding, the apparatus is designed to also permit experiments on thin (up to 1.5 cm deep) three-dimensional flows, in addition to the quasi two-dimensional flows described here. The hope is that we will, during Year 3, be able to conduct preliminary experiments on thin 3D flows in both geometries and test the same ideas in that context. These datasets will also be suitable for use comparing to prior IFPRI-funded work if that data is made available. In addition, our local collaborator Michael Shearer (NCSU Mathematics), has been working on the

mathematical underpinnings of the local $\mu(I)$ rheology [1]. We will work with him and his group to connect our work to theirs.

Estimated Yearly Budget

The budget will pay costs for 1 graduate student (plus tuition) or postdoc each year, working half time on this project. The annular apparatus (including instrumentation, camera, etc.) for the main experiments already exists. The supplies funds will be used to laser-cut new boundary walls for the apparatus, and to construct the hopper flow apparatus and boundaries described in the proposal. Travel funds would be used to report the findings at the annual IFPRI meeting (required for the PI, beneficial for the student/postdoc), plus scientific meetings such as the annual APS March Meeting, Powders & Grains, or the Society of Rheology annual meeting, as funds allow. No overhead is allowed on these funds.

student/postdoc support	\$26 k
supplies (electronics, hardware, particle machining, camera)	\$6 k
travel	\$4 k
Total Direct Costs	**\$36 k**

Appendix A

Nonlocal rheology of dense granular flow in annular shear experiments

Zhu Tang, Theodore A. Brzinski, Michael Shearer and Karen E. Daniels

The flow of dense granular materials at low inertial numbers cannot be fully characterized by local rheological models; several nonlocal rheologies have recently been developed to address these shortcomings. To test the efficacy of these models across different packing fractions and shear rates, we perform experiments in a quasi-2D annular shear cell with a fixed outer wall and a rotating inner wall, using photoelastic particles. The apparatus is designed to measure both the stress ratio μ (the ratio of shear to normal stress) and the inertial number I through the use of a torque sensor, laser-cut leaf springs, and particle-tracking. We obtain $\mu(I)$ curves for several different packing fractions and rotation rates, and successfully find that a single set of model parameters is able to capture the full range of data collected once we account for frictional drag with the bottom plate. Our measurements confirm the prediction that there is growing lengthscale at a finite value μ_s, associated with a frictional yield criterion. Finally, we newly identify the physical mechanism behind this transition at μ_s by observing that it corresponds to a drop in the susceptibility to force chain fluctuations.

A.1 Introduction

Currently, there is no first-principles, general continuum theory of dense dry granular flow that predicts its rheological response as a function of particle size, shape, and friction. A universal form for constitutive laws describing such rheology continues to be a challenging issue, despite promising recent developments [1, 3, 4, 12, 19, 34]. In an empirical approach, constitutive relations are postulated based on considerations of the connection between applied stresses and the properties of flow. In the experiments described here, we test several nonlocal models under various shear and packing conditions, providing insight into not only the relative success of the models, but also

a physical interpretation of the underlying mechanisms.

In a dense granular flow, it is common to characterize the flow rapidity via the dimensionless inertial number [12]

$$I \equiv \frac{\dot{\gamma} d}{\sqrt{P/\rho}}. \tag{A.1}$$

This can be interpreted [12] as the ratio between a microscopic timescale $T = d/\sqrt{P/\rho}$ (the time for a particle of density ρ to fall into a hole of grain size d, under pressure P) and a macroscopic timescale $1/\dot{\gamma}$ (the mean deformation time due to shear rate $\dot{\gamma}$). While the modeling of rapid flows ($I \gg 1$) is in an advanced state [6, 13], intermediate flows ($I \sim 1$) must account for both shear and compression effects [7], and slow flows ($I \ll 1$) remain particularly challenging to model.

For slow to intermediate flows, the dimensionless stress ratio μ is defined as the ratio between the local shear stress τ and the local pressure P:

$$\mu \equiv \frac{\tau}{P}. \tag{A.2}$$

Measurements of $\mu(I)$ were first modeled by purely local considerations: any point with $\mu \geq \mu_s$ (the yield criterion) would be flowing, and those with $\mu < \mu_s$ would be blocked. While these local rheologies have been broadly successful at describing fully-developed flows [12], they fail to quantitatively capture the transition from inertial to quasistatic ($I \ll 1$ but still creeping) flow, [20] explain the dependence of shear band width on geometry and grain size, [8, 22] or describe how shear/vibration in one region of a granular material can fluidize distant regions. [23, 27]

Due to these limitations of local rheology, several nonlocal rheology models have recently been developed. The nonlocal rheology model proposed by Kamrin and Koval [14, 19] extends a local Bagnold-type granular flow law to include a Laplacian term governing the diffusion of *fluidity* via cooperative effects. The nonlocal rheology model of Bouzid *et al.* [3, 4] performs a gradient expansion of a general constitutive relation. In both models, a Laplacian term models the diffusion of nonlocal effects within the granular material, but with a different physical interpretation; we will refer to these models as *cooperative* and *gradient*, respectively. Both of these models have been well-tested in simulations [3, 4, 18, 19, 34], but experimental verifications [14] have been confined to testing the kinematics (speed profiles, including the width of the shear band) rather than directly testing the relationship between applied force and the resulting flow.

In this paper, we report the results of a successful, quantitative comparison between experimental data and each of these models. We have developed a new 2D annular shear apparatus (see Fig. A.1) which is instrumented to measure the shear (τ) and normal (P) boundary forces. By using photoelastic particles [11] as the granular material we can either perform particle tracking (without polariscope) or measure spatiotemporal fluctuations in forces (with polariscope). These methods allow us to measure $\mu(I)$ throughout the material, and provide insight into the underlying mechanisms driving nonlocal rheology.

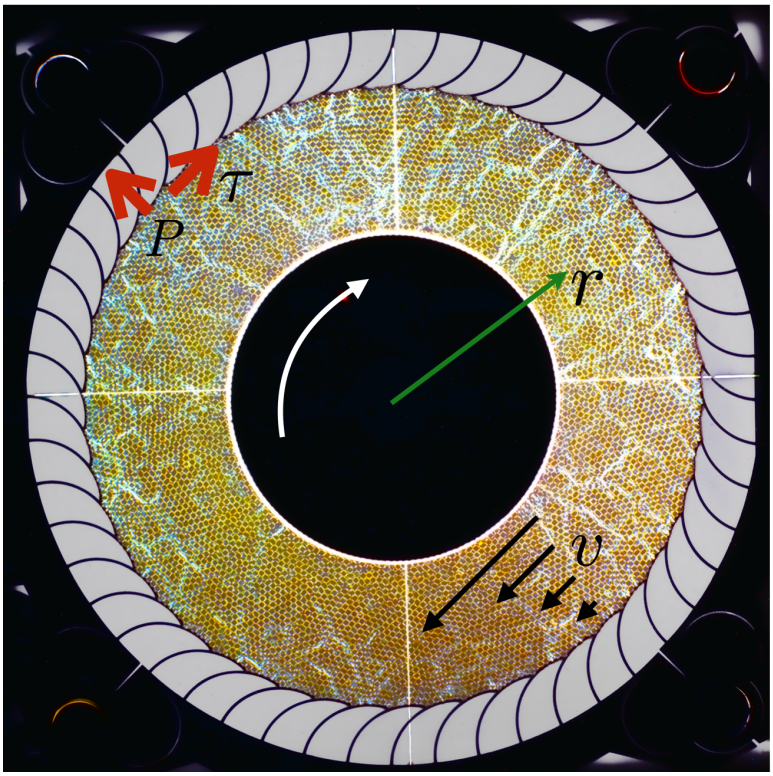

Figure A.1: Top view of annular Couette experiment with ≈ 5000 flat photoelastic particles. Image is a composite of an image of the leaf springs and an image of the force chains, inverted for clarity (dark particles are those experiencing more force). The inner wheel ($R_i = 15.0$ cm $= 26.8d$) rotates at fixed speed, and the outer boundary ($R_o = 28.0$ cm $= 50.0d$) is composed of 52 laser-cut leaf springs. The tips of the leaf springs are calibrated to measure shear (τ) and normal (P) stress. The speed profile $v(r)$ is measured via particle-tracking.

A.1.1 Cooperative model

The cooperative model [14, 19] is based on extending a local Bagnold-type granular flow law to include nonlocal effects. As with Bagnold scaling, there is assumed to be a linear relationship between shear stress and shear rate. This leads to the definition of *fluidity*

$$g \equiv \frac{\dot{\gamma}}{\mu} \tag{A.3}$$

where μ is the dimensionless stress ratio defined in Eq. A.2, and g has units s^{-1}. Motivated by results from numerical simulations, [10] Kamrin and Koval further assumed a linear relationship between local I and μ, but only where μ is larger than a yield ratio μ_s. This relationship, using the Heaviside function $H(\cdot)$, is given by

$$I(\mu) = \frac{(\mu - \mu_s)H(\mu - \mu_s)}{b}. \tag{A.4}$$

The parameter b controls the steepness of the rise of $I(\mu)$; in prior studies, [18, 19, 34] b has been observed to be in the range of 1.0 ± 0.1. In locations where $\mu < \mu_s$, this local rheology would predict no flow ($I = 0$). From this local flow rule and Eq. A.3, they define a corresponding local granular fluidity

$$g_{\mathrm{loc}}(\mu, P) = \frac{(\mu - \mu_s)H(\mu - \mu_s)}{b\mu T}. \tag{A.5}$$

The nonlocal portion of the theory develops from assuming that the granular fluidity g in Eq. A.3 has two contributions: the local g_{loc} (Eq. A.5) and a nonlocal contribution arising cooperatively from the surroundings. This is modeled as a diffusive process taking place over a cooperativity lengthscale ξ:

$$\nabla^2 g = \frac{1}{\xi^2}(g - g_{\text{loc}}) \tag{A.6}$$

For example, particle slips or vibrations or stress redistribution in one part of the system can propagate through to other parts of the system, with the system most sensitive in the vicinity of μ_s. This length scale is proposed to scale with the particle diameter d via the functional form

$$\frac{\xi}{d} = A\sqrt{\frac{1 + H(\mu_s - \mu)}{|\mu - \mu_s|}}. \tag{A.7}$$

Note that this equation is asymmetric around $\mu = \mu_s$. The parameter A controls the strength of this cooperative effect, and has been seen in previous work [18, 19, 34] to be in the range of 0.4 ± 0.1. Because ξ controls the proposed mechanism of nonlocality – how one part of the system influences another – Eq. A.7 is a key relationship to test directly.

Prior work [19] on the cooperative model originally allowed for Eq. A.7 to have a free exponent (found to be near 0.6) instead of the square root. Later papers [14, 18] chose a square root for simplicity, and we have followed that form here. More recently, the cooperative model has been extended to account for time-dependent flow [18, 34]. In this paper, we examine steady flows and therefore take the time-independent cooperative model as our comparison.

A.1.2 Gradient model

The gradient model [3, 4] takes a different definition of the fluidity

$$f = \frac{\dot{\gamma}}{Y} \tag{A.8}$$

where $Y \equiv \mu(I)/\mu_s = \tau/\mu_s P$ is the local stress ratio, relative to the same yield stress ratio μ_s used in the cooperative model. This fluidity f also has units of s^{-1}, and is related to the fluidity used in the cooperative model by $f = \mu_s g$.

The model further assumes that this expression for Y is just the first (local) term in an expansion of the true (unknown) constitutive relation. The full gradient-expansion, taken in higher orders of I, would be

$$Y \simeq \frac{\mu(I)}{\mu_s}\left(1 - \nu_\ell \kappa + \mathscr{O}(\kappa^2) + \cdots\right) \tag{A.9}$$

expressed in terms of $\kappa = d^2\nabla^2 I/I$. In this model, we keep only the lowest order (linear) term containing κ. This gives

$$Y = \frac{\mu(I)}{\mu_s}\left(1 - \nu_\ell \frac{d^2(\nabla^2 I)}{I}\right) \tag{A.10}$$

where the phenomenological constant ν_ℓ is a parameter controlling the magnitude of the higher-order contribution. Previous comparisons with simulations [3] have observed $\nu_\ell = 8$.

Using Eq. A.8 and the local definition of Y, Eq. A.10 can be written as a function of the fluidity f:

$$\dot{\gamma} = \frac{I_{\text{loc}}(f)}{T} - \ell^2 \nabla^2 f \tag{A.11}$$

where T is again the microscopic timescale (determined from measurements of P). Physically, this corresponds to writing the shear rate $\dot{\gamma}$ as the sum of a local term and a nonlocal term. The second (Laplacian) term in Eq. A.11 is the nonlocal contribution, and the parameter ℓ represents the spatial extent of the contributions the local fluidity makes to its surroundings. Prior work has observed that ℓ is on the order of a few grain diameters. [4]

For a homogeneously flowing steady state ($\mu > \mu_s$), the local inertial number I_{loc} would have the same physical meaning as I, with a constitutive relation

$$Y = 1 + a I_{\text{loc}}^n \tag{A.12}$$

Here, the frictional case ($n = 1$) plays the same role as Eq. A.4 with $\mu > \mu_s$ in the cooperative model. We can re-write Eq. A.12 in terms of the fluidity f by taking $Y = \dot{\gamma}_{\text{loc}}/f = I_{\text{loc}}/Tf$. For $n = 1$, the function I_{loc} takes the form

$$I_{\text{loc}}(f) = \frac{Tf}{1 - aTf} \tag{A.13}$$

where the fitting parameter a controls how steeply I_{loc} rises as a function of f. Previous comparisons with simulations [3] have observed $a = 4.3$.

In Eq. A.10, a divergent length scale L arises in the vicinity of $Y = 1$, due to whether or not local effects are present in I ($Y > 1$ corresponds to $\mu > \mu_s$ and vice versa.) This can be illustrated as follows. For $Y > 1$, linearizing Eq. A.10 around a combination of local and nonlocal effects ($I + \delta I$) gives a differential equation of the form $L^2 \nabla^2 \delta I - \delta I = 0$; the solutions of this equation are exponentials with a lengthscale given by $L = d\sqrt{\frac{Y\nu_\ell}{Y-1}}$. However, for $Y < 1$, there are only *nonlocal* effects, and linearization instead takes place around $I = \delta I$, with $\kappa = (1-Y)/\nu_\ell$. The resulting differential equation is therefore $d^2(\nabla^2 \delta I) - \kappa \delta I = 0$, whose solutions are an exponential with different lengthscale, $L = d\sqrt{\frac{\nu_\ell}{1-Y}}$. Written together, the physical lengthscale L is described by the following piecewise function:

$$\frac{L}{d} = \begin{cases} \sqrt{\frac{Y\nu_\ell}{Y-1}} & Y > 1 \\ \sqrt{\frac{\nu_\ell}{1-Y}} & Y < 1 \end{cases} \tag{A.14}$$

Thus, as for the cooperative model, there is again a divergent length scale at μ_s, and again an asymmetry above/below μ_s.

$v(R_i)$ [d/s]	2	0.2	0.02	0.002	2	0.2
# of particles	5610	5610	5610	5610	5760	5760
Φ ($\pm$0.002)	0.819	0.818	0.817	0.817	0.839	0.841
P [kPa]	7.5$\pm$0.4	8.0$\pm$0.4	9.2$\pm$0.4	9.3 $\pm$0.4	12.0$\pm$1.0	9.2$\pm$0.4
T [msec]	2.2$\pm$0.1	2.1$\pm$0.1	2.0$\pm$0.1	2.0$\pm$0.1	1.7$\pm$0.1	2.0$\pm$0.1

Table A.1: Description of the six datasets. The inner wall rotation $v(R_i)$ is the speed set by the motor controller. The number of particles is set by hand to one of two values (corresponding to 4 runs at $\Phi_{\rm lo}$ with 5610 particles and 2 runs at $\Phi_{\rm hi}$ with 5760 particles). The global packing fraction Φ is calculated from number of particles, the area of the particles, and the area of the shear cell (including the measured spring wall dilation). The $\pm$ values correspond to errors in the measurement of the particle size and the fluctuations in the spring wall dilation; these are of similar magnitude, and were added in quadrature. Pressure P is calculated from spatially- and temporally-averaging the normal stress measured at the 52 spring wall arms. The $\pm$ values are the standard deviation of these measurements across both space (52 arms) and time. The microscopic timescale T is calculated based on this pressure and known values of d and ρ.

A.2 Method

A.2.1 Apparatus

Our apparatus consists of a quasi-2D annular shear cell; [16] this geometry allows continuous shearing from the inner wall and visual access to the dynamics of all particles. The particles are a bidisperse mixture of circular (60%) and elliptical (40%) disks cut from 3 mm thick PhotoStress Plus PS-3 polymer from the Vishay Measurements Group (bulk modulus 0.21 GPa, density $\rho =$ 1.15 g/cm^3). The circles have diameter $d = 5.6$ mm and the ellipses have major and minor axes of 6.8 mm and 4.7 mm, respectively; we report length measurements scaled by the circle diameter d (also the geometric mean of the two ellipse axes).

A motor (Parker Compumotor BE231FJ-NLCN with a PV90FB 50:1 gearbox) is attached to the inner wall, providing a constant rotational speed. We measure the inner wall shear stress $\tau(R_i)$ via a torque sensor (Cooper Instruments & Systems Torque Sensor) attached to the central shaft. As shown in Fig. A.1, the stationary outer wall incorporates 52 laser-cut leaf springs. Each of the springs linearly deforms (both radially and tangentially) under stress from the granular material. Via calibrated image processing [29], we obtain quantitative measurements of shear (τ) and normal (P) stresses at each of the 52 spring tips. Values are reported as spatial and temporal averages.

Table A.1 summarizes the six datasets spanning four rotation rates and two packing fractions ($\Phi_{\rm lo}$ and $\Phi_{\rm hi}$). All data is collected after the system reaches a steady state. For inner wall rotation speeds $v(R_i) = 0.02, 0.2$, and 2 d/s, the data are collected after at least one full rotation; for 0.002 d/s, we wait two hours ($1/12$ of a rotation) before collecting data. Images for particle-tracking are collected at 1 fps ($0.02d - 0.2d$/frame), except for the slowest (0.1 fps, $0.02d$/frame) and fastest (4 fps, $0.5d$/frame) runs. For the fastest dataset, we image only one quarter of the whole apparatus, to allow for a faster frame rate. The duration of the experiments is determined by the rotation rate, ranging from 0.5 to 24 hrs so that each run completes 1-2 full rotations at steady state. An additional set of images was taken using a darkfield polariscope, [11] allowing us

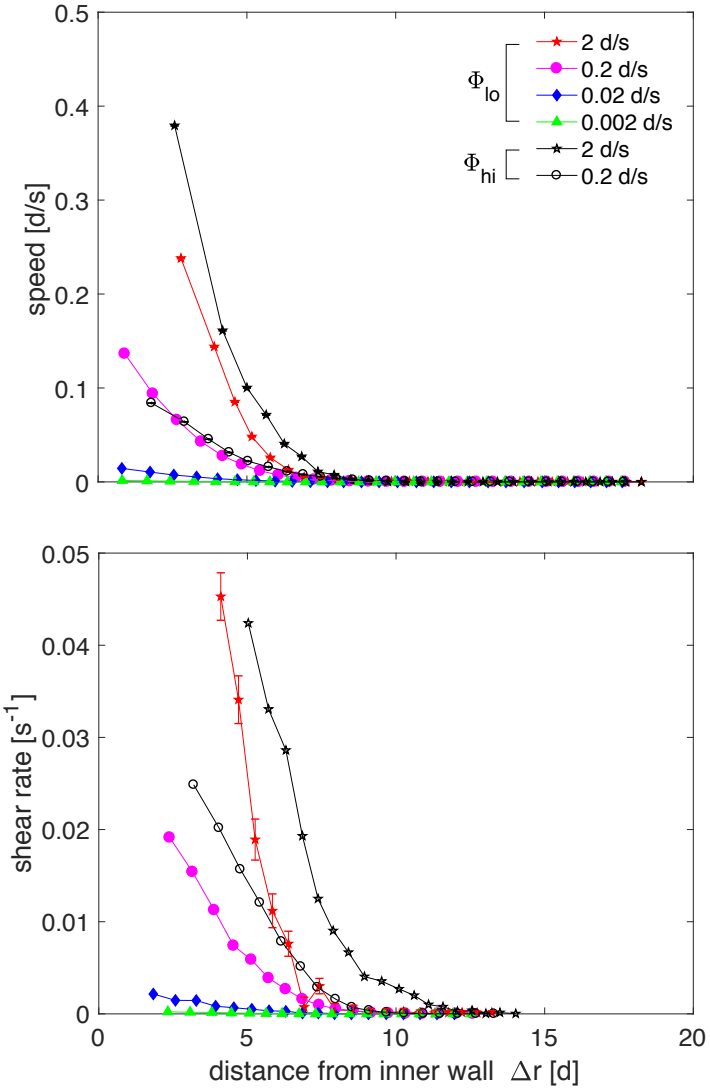

Figure A.2: (a) Speed profiles $v(r)$ and (b) shear rates $\dot{\gamma}$ for all six datasets, measured by particle-tracking. The distance from inner wall is at location $\Delta r = r - R_i$.

to visualize interparticle forces and their fluctuations. We collected this for an additional dataset with $v(R_i) = 2$ d/s and Φ_{hi}, in order to make measurements both above and below μ_s.

A.2.2 Particle tracking

We track the particles in Matlab using a Hough transform (imfindcircles combined with the Blair-Dufresne particle-tracking code. [2] Particle speeds are obtained from taking finite differences of the particle locations along these tracks. For the fastest runs, particle tracks immediately adjacent to the inner wall are inaccessible and data is not reported for those positions. To obtain the azimuthal speed profile $v(r)$, we calculate the average tangential speed v within concentric rings of width $0.65d$ located at different distances from the center. The shear rate profile is calculated by FFT-

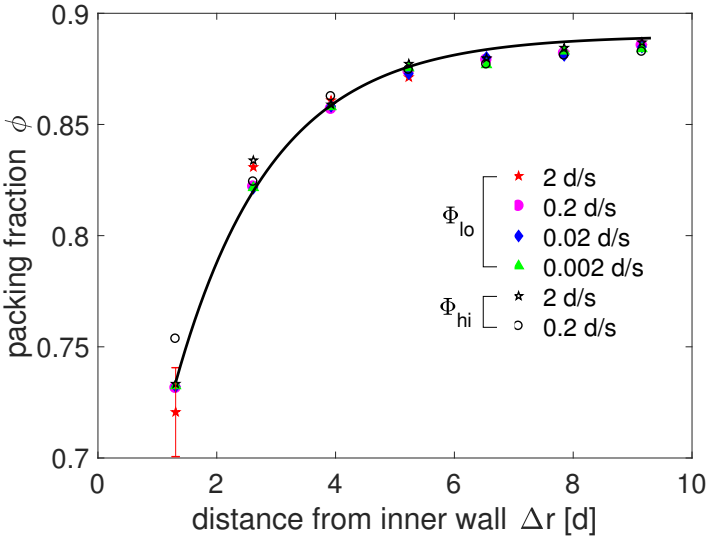

Figure A.3: Local packing fraction profiles $\phi(r)$, for all six datasets. The solid line is a fit to an exponential with decay length $r_0 = (1.67 \pm 0.17)d$, averaged over fits to all six datasets.

derivative of the averaged $v(r)$ profile. In polar coordinates, the azimuthal shear rate is given by $\dot{\gamma}(r) = \frac{1}{2}\left(\frac{\partial v}{\partial r} - \frac{v}{r}\right)$.

The resulting speed and shear rate profiles are shown in Fig. A.2, for all six datasets. Each datapoint is the average over 100 tracked particles (averaged in space), and approximately 2000 frames (averaged in time). All six speed profiles show strong shear-banding, with the speed falling to nearly zero within about $10d$ of the inner wall. Note that data close to the inner wall is excluded from plots; this arises where images are too blurred by motion to confidently report quantitative values. We observe that for datasets at the same Φ, the shear rate is greater for higher inner wall rotation rates, when compared at the same location. For the same inner wall rotation rate, higher Φ have a higher shear rate at same location.

We measure the local packing fraction ϕ as a function of r by dividing images into concentric rings of width $2.5d$. Within each of these rings, we calculate the fractional area of the particles detected; approximately 250 particles are used in each average. The results are shown in Fig. A.3 for each of the six datasets, all following an approximately exponential decay with the same characteristic length. However, for the same wall rotation rate, runs with higher global Φ also have a higher local ϕ near the inner wall.

A.2.3 Inertial number

To measure the spatial dependence of the inertial number $I(r)$ (Eq. A.1) at each point within the experiment, we combine the measured shear rate $\dot{\gamma}(r)$ for each dataset (Fig. A.2b) with the measured (constant) pressure P (Table A.1). In all cases, the values are azimuthally and temporally averaged. We observe a high value of I near the inner wall, and a low value of I near the outer wall across all six datasets, with values ranging from 10^{-8} to 10^{-4}, falling well within the quasistatic [13] regime ($I < 10^{-2}$). These values of I place the majority of our data in the nonlocal regime.

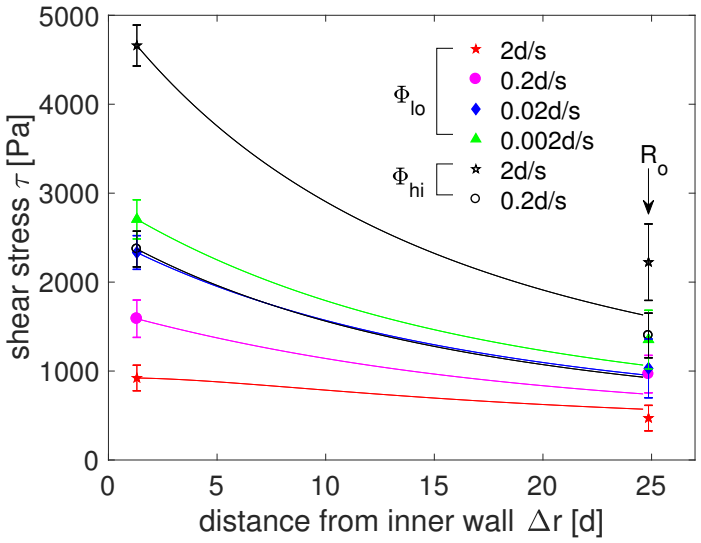

Figure A.4: Modeled shear stress profiles $\tau(r)$, determined from the model given in Eq.A.16, with $\tau_0 = (250 \pm 30)$ Pa and r_0 taken from Fig. A.3. Datapoints at R_i come from the torque sensor, and at R_o from the leaf springs, for each of the six datasets.

A.2.4 Shear and normal stress

By tracking the displacement of the 52 tips on the spring wall boundary (see Ref. [29] for details), we measure the shear stress τ at the inner and outer walls, and the normal stress (pressure) P at the outer wall. We assume that P is constant throughout the system (force balance) and that $\tau(r)$ can be described by accounting for boundary drag in addition to geometric arguments. If no drag with the upper/lower plates were present, then $\tau(r) = S(R_i/r)^2$ where S is the measured shear stress at the inner wall. [19] We assume that an additional contribution, due to basal friction, is related to the local packing fraction $\phi(r)$. As shown in Fig. A.3, $\phi(r)$ takes an exponential form

$$\phi(r) = \phi_0 \left[1 - e^{-\Delta r/r_0}\right] + \phi(R_i). \tag{A.15}$$

where $\Delta r \equiv r - R_i$ is the distance from the inner wall.

Correspondingly, we write a phenomenological model for the shear stress profile:

$$\tau(r) = S_0 \left(\frac{R_i}{r}\right)^2 + \tau_0 \left[1 - e^{-\Delta r/r_0}\right] \tag{A.16}$$

This form is motivated by two main features: the driving from the inner wall ($\tau \propto (R_i/r)^2$), plus an exponential decay from basal fraction (Eq. A.15). The value $r_0 = 1.67d$ comes from Fig. A.3, and we determine parameters (S_0, τ_0) by fitting each of the six datasets to Eq. A.16 subject to the measured endpoints $\tau(R_i)$ (from the torque sensor) and $\tau(R_o)$ (from the leaf springs). The average value $\tau_0 = 250 \pm 30$ Pa is then used for all datasets as our model of basal friction, while retaining the six individual values of S_0 to reflect the driving.

The resulting curves for $\tau(r)$ are shown in Fig. A.4. For the same rotation rate, datasets with higher Φ experience a higher shear stress at the same location. For the same Φ, experiments with lower rotation rates have higher shear stress for the same location.

A.3 Results

A.3.1 $\mu(I)$ rheology

The measurements from §A.2.3 and §A.2.4 can be plotted parametrically to obtain a graph of $\mu(I)$, as shown in Fig. A.5a. For all six datasets, the inner (faster) part of the flow is located on the right side of the graph, at larger values of I. Fig. A.5a provides our first estimate of the value of the yield stress ratio μ_s, which is the upper limit of $\mu(I)$ for the slowest run (rotation rate $0.002d$/s). Because the shear ratio μ approaches μ_s for very slow inertial numbers, the upper limit at low-I has previously been taken as a good estimate of μ_s. [19] This is approximately $\mu_s = 0.26$, a value which will be further confirmed with two additional methods below.

Note the reversal of trends for the two different packing fractions: for Φ_{lo}, decreasing the rotation rate of the inner wheel raises μ, while the opposite is true at Φ_{hi}. This is echoed by the measurements of P (Table A.1) and τ (Fig. A.4). The likely reason for this effect is the dilatancy transition: [32] densely-packed granular materials dilate under shear, while loosely-packed ones compact. As measured by the two-point correlation of free Voronoï volumes in binary disc packings, [35] the 2D dilatancy transition occurs between Φ_{lo} and Φ_{hi}, near 0.827.

A.3.2 Fluidity

Both the cooperative (§A.1.1) and gradient (§A.1.2) models depend on the calculation of the local fluidity. Our experimental measurements of $(\dot{\gamma}, \mu, P)$ in the preceding figures provide values for Eq. A.3 (cooperative model):

$$g_{\text{exp}}(r) = \frac{\dot{\gamma}_{\text{exp}}(r)}{\mu_{\text{exp}}(r)}. \tag{A.17}$$

and Eq. A.8 (gradient model):

$$f_{\text{exp}}(r) = \frac{\mu_s \dot{\gamma}_{\text{exp}}(r)}{\mu_{\text{exp}}(r)}. \tag{A.18}$$

where only $\mu_s = 0.26$ is a fit parameter. The resulting data are shown in Fig. A.6: as expected, the system is most fluid near the inner shearing wall. Note that the ratio between the two fluidities (f, g) is just μ_s. Therefore, we can scale the left and right axes so that only a single set of data points is shown for both.

A.3.3 Comparison to models

For the cooperative model, we obtain $g(r)$ by solving Eq. A.6 using the Matlab ODE-solver *bvp4c*. The two boundary conditions are taken as the value of $g_{\text{exp}}(r)$ nearest the inner wall, and $g(R_o) = 0$. Using Levenberg-Marquardt optimization, we obtain the fitting parameters A and b from the dataset with $v(R_i) = 2d$/s and Φ_{hi}. These two parameters (A, b) are used to plot all of the solid lines in Figs. A.5 and A.6. See Table A.2 for the values and uncertainties.

For the gradient model, the $\dot{\gamma}$ in Eq. A.11 is written as a function of f, and we solve for $f(r)$ (again using *bvp4c*). The boundary conditions of $f(r)$ are determined in the same way as for

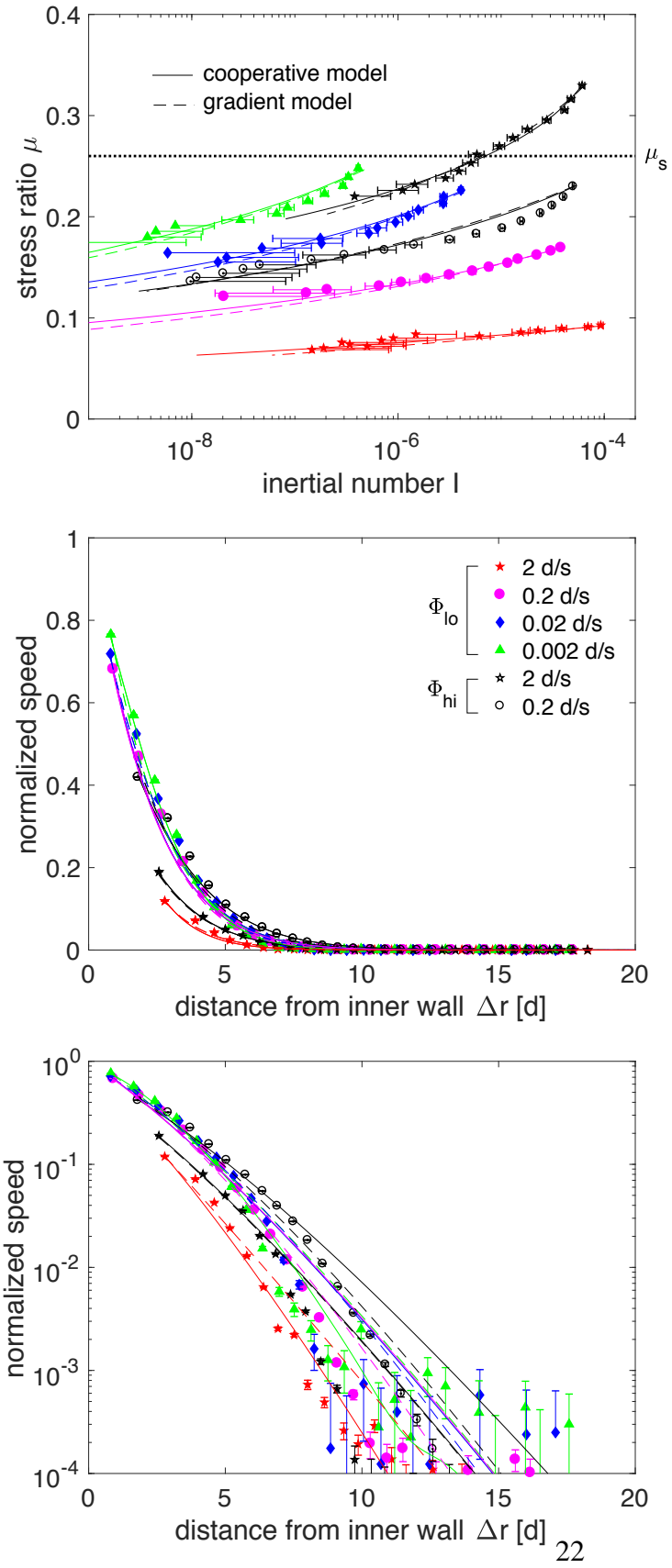

Figure A.5: (a) Stress ratio μ as a function of inertial number I, for all six datasets. The horizontal dotted line indicates the location of $\mu_s = 0.26$ to distinguish the local and nonlocal regions. Speed profiles $v(r)$ for all six datasets, plotted as (b) raw data on a linear axis and (c) normalized on a logarithmic axis. In all cases, solid lines compare to the cooperative model (§A.1.1) and dashed lines to the gradient model (§A.1.2). For comparison, we calculate relative residuals as $R^2 \equiv \langle (a_{\rm exp} - a_{\rm th})^2/(a_{\rm exp}^2)\rangle$, with the average taken over all data points. For (a): $R^2 = 0.224$ for the cooperative model, and $R^2 = 0.215$ for the gradient model. For (b,c): $R^2 = 0.129$ for the cooperative model, and $R^2 = 0.124$ for the gradient model.

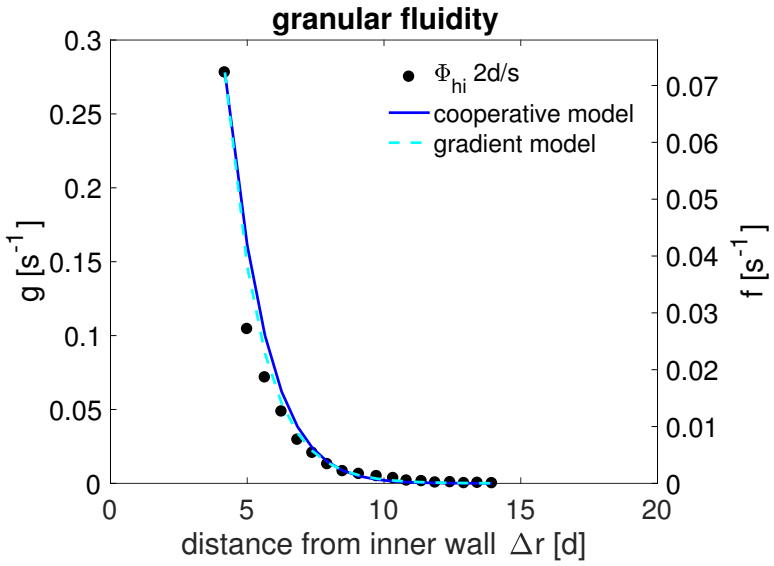

Figure A.6: Experimentally-measured granular fluidity (calculated by Eq. A.17 and Eq. A.18), compared to best fit theoretical curves for both models. The line for the cooperative model g (left axis) is calculated from Eq. A.6 and the line for the gradient model f (right axis) is calculated from Eq. A.11. Since the relationship between the two granular fluidity is $g\mu_s = f$ (see Eq. A.3 and Eq. A.8), the left and right axes have been scaled by μ_s to allow for comparison on a single plot. The dataset was taken at Φ_{hi} and $v(R_i) = 2$ d/s.

	cooperative model		
μ_s	A	b	
0.26 $\pm$0.01	0.250$\pm$0.002	1.1$\pm$0.5	
	gradient model		
μ_s	ℓ	a	ν_ℓ
0.26$\pm$0.01	1.02$\pm$0.02	7.2$\pm$4.3	0.21$\pm$0.03

Table A.2: Fitting parameters for both models, with $\pm$ values representing the sensitivity range. The sensitivity for μ_s (identical for both models) is taken from the full-width-half-maximum of the peak in the inset to Fig. A.7. For the four parameters (A, b, ℓ, a), the sensitivity is determined from the run with Φ_{hi} and $2d/s$ by holding one parameter fixed and allowing the residual to vary up to $R^2 = 0.3$ (rather than the best-fit $R^2 = 0.2$ shown in Fig. A.5a). Similarly, for the lengthscale parameter ν_ℓ, the sensitivity range is for an increase from $R^2 = 0.02$ to 0.03 for the data and fit given in Fig. A.7.

the cooperative model. Using the dataset with $v(R_i) = 2d$/s and Φ_{hi}, we simultaneously fit the parameters a and ℓ using Levenberg-Marquardt optimization. This set of parameters is used to plot all of the dashed lines in Fig. A.5 and A.6.

Using the parameters in Table A.2, we solve the cooperative model (Eq. A.6, using μ_s, A, b) and the gradient model (Eq. A.11, using μ_s, ℓ, a) for all six runs, to get the granular fluidity ($g(r)$ and $f(r)$, respectively).

Recall that the values of $\mu(r)$ were calculated in §A.3.1. For the cooperative model, $I(r) = g(r)\mu(r)T$ and for the gradient model $g(r)$ is replaced by $f(r)/\mu_s$. The resulting parametric plots of $\mu(r)$ vs. $I(r)$ are shown in Fig. A.5a, with the cooperative model represented by solid lines, and the gradient model by dashed lines. Both models show good agreement with the data, with similar R^2 residuals.

We can also compare the speed profiles, as has been done for two other geometries in Ref. [14]. The predicted speed profile $v(r)$ is obtained by numerically integrating $\dot{\gamma} = \mu(r)g(r)$ from the outer wall R_o to the location r (correspondingly, $g(r)$ is replaced by $f(r)/\mu_s$ for the gradient model). The resulting curves are compared with the data on both logarithmic and linear axes in Fig. A.5b,c. Again, we observe that both models agree well with the data, with no significant difference in the residuals for the two models.

Notably, the comparisons in Fig. A.5 were made using a *single set* of parameters, making them inherent properties of the granular material. As can be seen from the sensitivity ranges given in Table A.2, both nonlocal parameters (A, ℓ) are much better-constrained by the data than the local parameters (b, a). This is because we have collected the majority of our data in the nonlocal region.

A.3.4 Nonlocal lengthscale

To directly test the prediction of a diverging lengthscale (ξ or L) at μ_s (Eq. A.7 and A.14), we calculate these quantities from the dataset that spans both the local and nonlocal regimes (Φ_{hi} and rotation rate $2d$/s). The lengthscale ξ is determined from Eq. A.6 using the experimentally-determined values of g_{exp} and its Laplacian, with g_{loc} taken from Eq. A.5 using $\mu(r)$ and the fitting parameter b from Table A.2.

The Laplacian term in Eq. A.6 requires taking a second derivative of the fluidity (either g or f), which is itself calculated from $\dot{\gamma}(r) = \frac{1}{2}\left(|\frac{\partial v}{\partial r}| + \frac{v}{r}\right)$. This requires taking three derivatives of our discretely-sampled $v(r)$ data (see Fig. A.2). Because this is numerically-challenging, we use two complementary methods: the analytical method takes analytical derivatives of an empirical fit to $v(r)$ and the numerical method uses FFT-differentiation. The empirical fit to $v(r)$ is shown in Fig. A.7a, given by:

$$v(r) = v_0 \exp\left[\alpha_3 r^3 + \alpha_2 r^2 + \alpha_1 r + \alpha_0\right]. \tag{A.19}$$

In applying the analytical method, we do not use the experimental fluidity data g_{exp} directly, but instead use this functional form for the calculations.

The lengthscale L for the gradient model is calculated similarly, using $f = \mu_s g$. However, in this case we still have one free parameter to fit. We obtain $\nu_\ell = 0.21$ by fitting Eq. A.14 to the numerical experimental data (blue stars in Fig. A.7b) for $\mu > \mu_s$.

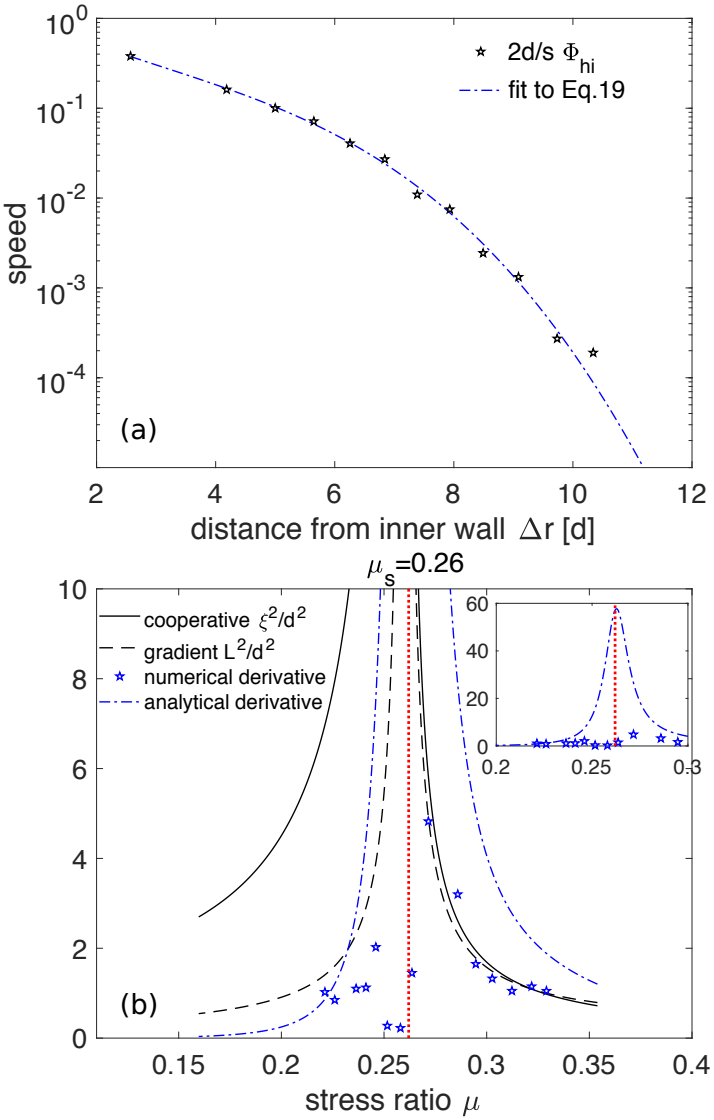

Figure A.7: (a) Speed profile $v(r)$ for the dataset with $\Phi_{\rm hi}$ and rotation rate $2d/\mathrm{s}$. The best-fit curve is given by the best fit to an empirical curve, given by Eq. A.19 with $\alpha_3 = -0.0118$, $\alpha_2 = -0.1096$, $\alpha_1 = -0.8374$, and $\alpha_0 = 0.6512$. (b) Comparison of the measured lengthscale (blue) to the two models (black), scaled by particle diameter d. Both of the models have a divergence near the value $\mu_s = 0.26$ taken from Fig. A.5. For $\mu > \mu_s$ (local regime), the best relative residuals are $R^2 = 0.029$ for the cooperative model (black solid line) and $R^2 = 0.020$ for the gradient model (black dashed line), based on a comparison with the numerically-determined values (blue stars). For $\mu < \mu_s$ (nonlocal regime), the only reasonable comparison to make is between the gradient model (black dashed line) and the measurements based on the analytic derivative (blue dash-dotted line), but the residual is still quite large ($R^2 = 35$, vs. $R^2 = 1052$ for the cooperative model.)

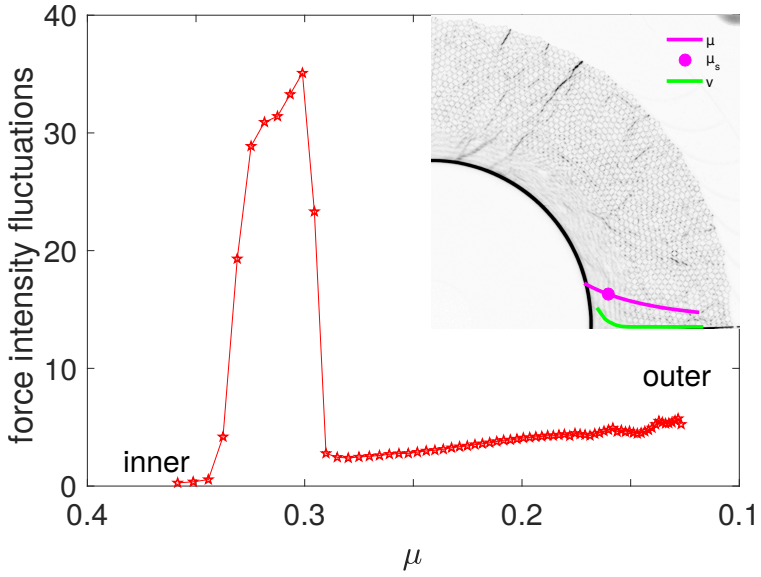

Figure A.8: The variance of the light (force) intensity within concentric rings, plotted parametrically against the value of μ measured within that ring. The sharp drop is at $\mu_s = 0.29$. Inset: Image of force chains, inverted for clarity, so that dark particles are those experiencing more force. Data collected at Φ_{hi} and at rotation rate $2d/\text{s}$. Upper line (magenta) overlays the measured $\mu(r)$ with $\mu_s = 0.29$ marked by the circle. Lower line (green) overlays the measured $v(r)$ for comparison.

The results of these lengthscale calculations give $\xi(r)$, as either a curve (the analytical method, blue dash-dotted line) or a set of discrete points (the numerical method, blue stars), which can be plotted parametrically against $\mu(r)$ to provide $\xi(\mu)$. These two datasets are shown in blue in Fig. A.7b. While the numerical method works well only for $\mu > \mu_s$ (the local regime), it suggests a growing lengthscale near the same $\mu_s = 0.26$ observed in Fig. A.5a. The analysis using the analytically-derived measurement confirms the presence of a clear peak in $\xi(\mu)$ near $\mu_s = 0.26$, spanning both the local and nonlocal regimes. These results provide a second, kinematic, verification of the value of the yield stress ratio μ_s.

Finally, we compare these measured lengthscales to the predictions of the two models, using the parameter values given in Table A.2. For the cooperative model, the prediction is provided directly by Eq. A.7. In Fig. A.7b, we observe that for $\mu < \mu_s$ (nonlocal regime), the gradient model (dashed line) provides a better fit to the observed length scales (blue dash-dotted line, analytical derivatives). This improvement arises through the inclusion of a fit parameter ν_ℓ, which directly controls the shape of $L(\mu)$.

A.3.5 Yield stress ratio μ_s

A third, completely independent, method of determining the yield stress ratio μ_s arises from an examination of the force chain fluctuations. [16] We use the variance of the force chain intensity as a semi-quantitative proxy measurement for the heterogeneity of the force transmission. As shown in Fig. A.8a, the force chains are spatially heterogeneous (and also temporally heterogeneous, not shown). To quantify the radial profile of these fluctuations, we divide a series of images into concentric rings. Within each of these rings, we measure the variance of all measured light intensity values (across both space and time).

In Fig. A.8, we parametrically plot the measured variance against the value of μ measured

within that ring. We observe that near the inner wall (large μ, left side of plot), the fluctuations grow even as the velocity (also fluidity) drops. This is the local regime, where the cooperative length is increasingly long. At $\mu_s = 0.29$, however, the fluctuations abruptly fall as the granular material enters the nonlocal regime. This provides a new physical interpretation of the nature of the change in material properties in the vicinity of μ_s: a susceptibility to force chain fluctuations.

Interestingly, this value of μ_s is quite close, but does not precisely agree with the value ($\mu_s = 0.26$) obtained from particle kinematics and stress measurements. This small difference likely arises from the change in boundary conditions for the two types of experiments: the particle-tracking experiments are performed with a different upper boundary (the upper layer above the particles is clear plastic) from the photoelastic experiments (polaroid sheet). This change in materials likely adjusts the value of τ_0 in Eq. A.16 by a small amount, accounting for the change in drag. We have chosen to use $\mu_s = 0.26$ for the model comparison done in §A.3.3, since this corresponds to the boundary conditions used for the $v(r)$ measurements. Had we chosen to use $\mu_s = 0.29$, this would disagree with the peak observed in the inset to Fig. A.7b, but it would not significantly affect the $\mu(I)$ results.

A.4 Conclusions

In this paper, we presented new experiments on granular rheology which validate the efficacy of two nonlocal models in describing flow properties. A key advance was the introduction of leaf spring boundaries to provide stress measurements rather than simply relying on particle kinematics. This method will be particularly helpful in future experiments without photoelastic particles (which could otherwise measure the stress), where it is desirable to monitor the spatial and temporal fluctuations of the boundary stresses. By making measurements in a photoelastic system, we additionally uncovered a new interpretation for the model's assumption of a diverging length scale at the yield stress ratio μ_s. We observe that this corresponds to a drop in the susceptibility to force chain fluctuations as the material goes from the local to nonlocal regimes.

In order to make direct, quantitative comparisons between experiments and two popular nonlocal models, the availability of boundary stress measurements allowed us to incorporate a drag term to account for basal friction. To test the applicability of the two models, we used one of six runs to determine the fit parameters; these parameters were then capable of fitting the five other datasets across four different rotation rates (spanning four orders of magnitude in inertial number I) and two packing fractions. Furthermore, we directly tested the presence of a growing length scale in the vicinity of μ_s, and found it to be consistent with both models. This observation provides additional support for why both models have been successful under a variety of circumstances [3, 4, 18, 19, 33]. Additionally, we find that the model is able to capture the dilatancy transition, without explicitly including it.

Importantly, we find that while both models can quantitatively describe the experimental data, the cooperative model has one fit parameter fewer. This favors its choice where only $\dot{\gamma}(r)$ and $\mu(I)$ are concerned, but the additional parameter (ν_ℓ) in the gradient model allows it to better-fit the nonlocal lengthscale for $\mu < \mu_s$ (the nonlocal regime). Further tests in spatially heterogeneous

and/or unsteady situations would be important to better-distinguish the two models.

Acknowledgements

We thank Dave Henann, Ken Kamrin, and Philippe Claudin for useful discussions about the project, and Austin Reid for inspiring the boundary wall designs. We are grateful to the National Science Foundation (NFS DMR-1206808 and DMS-1517291) and the International Fine Particle Research Institute (IFPRI) for financial support.

Bibliography

[1] Thomas Barker, DG Schaeffer, Michael Shearer, and JMNT Gray. Well-posed continuum equations for granular flow with compressibility and μ (i)-rheology. *Proc. R. Soc. A*, 473(2201):20160846, 2017.

[2] Daniel Blair and Eric Dufresne. The matlab particle tracking code repository. `http://site.physics.georgetown.edu/matlab/`.

[3] Mehdi Bouzid, Martin Trulsson, Philippe Claudin, Eric Clément, and Bruno Andreotti. Nonlocal Rheology of Granular Flows across Yield Conditions. *Physical Review Letters*, 111(23):238301, 2013. doi: 10.1103/PhysRevLett.111.238301.

[4] Mehdi Bouzid, Adrien Izzet, Martin Trulsson, Eric Clément, Philippe Claudin, and Bruno Andreotti. Non-local rheology in dense granular flows. *The European Physical Journal E*, 38(11):125, 2015.

[5] Theodore A. Brzinski, Karin A. Dahmen, and Karen E. Daniels. Unpublished.

[6] C S Campbell. Rapid Granular Flows. *Annual Review Of Fluid Mechanics*, 22:57–92, 1990.

[7] C S Campbell. Granular Material Flows - An Overview. *Powder Technology*, 162(3):208–229, March 2006.

[8] X Cheng, J B Lechman, A Fernandez-barbero, G S Grest, H M Jaeger, G S Karczmar, M E Mobius, and S R Nagel. Three-dimensional Shear In Granular Flow. *Physical Review Letters*, 96(3):38001, 2006.

[9] P. A. Cundall and O. D. L. Strack. Discrete Numerical-model For Granular Assemblies. *Geotechnique*, 29(1):47–65, 1979.

[10] Frédéric Da Cruz, Sacha Emam, Michaël Prochnow, Jean-Noël Roux, and François Chevoir. Rheophysics of dense granular materials: Discrete simulation of plane shear flows. *Physical Review E*, 72 (2):021309, 2005.

[11] Karen E Daniels, Jonathan E Kollmer, and James G Puckett. Photoelastic force measurements in granular materials. *Review of Scientific Instruments*, 88(5):051808, 2017.

[12] Yoël Forterre and Olivier Pouliquen. Flows of dense granular media. *Annu. Rev. Fluid Mech.*, 40: 1–24, 2008.

[13] Isaac Goldhirsch. Rapid granular flows. *Annual Review Of Fluid Mechanics*, 35(1):267–293, January 2003.

[14] David L Henann and Ken Kamrin. A predictive, size-dependent continuum model for dense granular flows. *Proceedings of the National Academy of Sciences of the United States of America*, 110(17): 6730–5, April 2013.

[15] David L. Henann and Ken Kamrin. Continuum Modeling of Secondary Rheology in Dense Granular Materials. *Physical Review Letters*, 113(17):178001, October 2014.

[16] Daniel Howell, RP Behringer, and Christian Veje. Stress fluctuations in a 2d granular couette experiment: a continuous transition. *Physical Review Letters*, 82(26):5241, 1999.

[17] Pierre Jop, Yoël Forterre, and Olivier Pouliquen. A constitutive law for dense granular flows. *Nature*, 441(7094):727–30, June 2006.

[18] Ken Kamrin and David L Henann. Nonlocal modeling of granular flows down inclines. *Soft Matter*, 11(1):179–185, 2015.

[19] Ken Kamrin and Georg Koval. Nonlocal Constitutive Relation for Steady Granular Flow. *Physical Review Letters*, 108(17):1–5, April 2012.

[20] Georg Koval, Jean-Noël Roux, Alain Corfdir, and François Chevoir. Annular shear of cohesionless granular materials: From the inertial to quasistatic regime. *Physical Review E*, 79(2):021306, 2009.

[21] Eric Lauga, Michael Brenner, and Howard Stone. Microfluidics: The No-Slip Boundary Condition. In: Tropea C., Yarin A.L., Foss J.F. (eds) *Springer Handbook of Experimental Fluid Mechanics.* Springer, Berlin, Heidelberg, 2007.

[22] G D R MiDi. On dense granular flows. *European Physical Journal E*, 14(4):341, 2004.

[23] Kiri Nichol, Alexey Zanin, Renaud Bastien, Elie Wandersman, and Martin van Hecke. Flow-induced agitations create a granular fluid. *Physical Review Letters*, 104(7):078302, 2010.

[24] Eli T. Owens and Karen E. Daniels. Sound propagation and force chains in granular materials. *Europhysics Letters*, 94(5):54005, June 2011.

[25] Eli T. Owens and Karen E. Daniels. Acoustic measurement of a granular density of modes. *Soft Matter*, 9(4):1214–1219, 2013.

[26] O Pouliquen and Y Forterre. Friction law for dense granular flows: application to the motion of a mass down a rough inclined plane. *Journal Of Fluid Mechanics*, 453:133–151, February 2002.

[27] K. Reddy, Y. Forterre, and O. Pouliquen. Evidence of Mechanically Activated Processes in Slow Granular Flows. *Physical Review Letters*, 106(10), March 2011.

[28] John T Simpson, Scott R. Hunter, and Tolga Aytug. Superhydrophobic materials and coatings: a review. *Reports on Progress in Physics*, 78: 086501, 2015.

[29] Zhu Tang, Theodore A. Brzinski, and Karen E. Daniels. Granular rheology: measuring boundary forces with laser-cut leaf springs. *Powders & Grains 2017*, EPJ Web of Conferences 140, 03035, 2017.

[30] Zhu Tang, Theodore A. Brzinski, Michael Shearer, and Karen E. Daniels. Nonlocal rheology of dense granular flow in annular shear experiments. *Soft Matter*, 14: 3040-3048, 2018.

[31] Amalia Thomas and Nathalie Vriend. Personal Communication.

[32] Brian P Tighe. Shear dilatancy in marginal solids. *Granular Matter*, 16(2):203–208, 2014.

[33] Martin van Hecke. Slow granular flows: The dominant role of tiny fluctuations. *Comptes Rendus Physique*, 16(1):37–44, 2015.

[34] Qiong Zhang and Ken Kamrin. Microscopic description of the granular fluidity field in nonlocal flow modeling. *Physical Review Letters*, 118(5):058001, 2017.

[35] Song-Chuan Zhao, Stacy Sidle, Harry L. Swinney, and Matthias Schröter. Correlation between Voronoi volumes in disc packings. *Europhysics Letters*, 97(3):34004, February 2012.

Self-Assembled Monolayers as Nucleating Surfaces to Study Early Formation Pathways of Crystallographic Polymorphs

Thank you very much for carefully reading the proposal and the comments/questions provided. Below you will find our responses to the various issues raised, classified into three categories: One category asking an overarching question about the overall direction of the project, the second category asking detailed questions about specifics of an alternative method proposed in the renewal, and the third category asking about alternative model systems. We hope these responses will help clarify the overall approach we take to the difficult scientific problem of polymorph selection as well as the specific details of the new method.

Responses to questions from IFPRI members

Comment 1:

Why are you moving to it (the blade coating method) so quickly, rather than "drilling down" more deeply into the role that the chemistry of the SAM has in polymorph selection?

Response:

As pointed out in the renewal proposal (page 5, second paragraph), we intend to conduct blade coating experiments *in addition to* the original proposed droplet evaporation studies. In other words, we are, and will be, definitively drilling further down on the role of the SAM chemistry on polymorph selection using the droplet evaporation method. To that end, as proposed in the original project description, during the third year of this IPRI project we have for the first time successfully applied wide-angle x-ray scattering (WAXS) experiments at the Cornell High Energy Synchrotron Source (CHESS) in order to look at the early stages of nucleation and growth of the SAM/solvent directed small pharmaceutical model compound, acetaminophen (ACM) during droplet evaporation. As I will report together with my student during the upcoming IFPRI Annual General Meeting (AGM), with these experiments we were able to unambiguously demonstrate that nucleation and growth occur at and from the SAM/solvent interface, and that this interface not only directs the ACM polymorph, but also ACM crystal orientation. We think this result is a milestone achievement in our studies, which we are extremely happy about. As already discussed in the original IFPRI proposal, these exciting new results now pave the way, in future studies, to dive even deeper into the early stages of nucleation and growth of this model system, *e.g.* using cryo-(scanning) transmission electron microscopy (cryo-(S)TEM), which we will apply to our samples in case we are renewed (see renewal proposal, page 6, final paragraph).

Comment 2:

How are you generating supersaturation? Is it by evaporation alone?
How do you know that polymorph selection is due to the SAM and not to confinement?
Do you know whether shear is important in nucleation? Is rheology important?

Response:

These questions are all targeted at the blade coating method which we proposed in the renewal as a second, alternative approach to droplet evaporation in order to achieve polymorph

selection (*vide supra*). In this method, a solution of the target molecule (at concentrations close to supersaturation) is pulled into a thin film using a doctor blade. Subsequent solvent evaporation then drives the nucleation. As we discuss in the renewal proposal (page 4, first paragraph), recent studies by others have suggested that the one-dimensional (1D) self-confinement of the crystallization front between the surface crust of the blade and the substrate can be responsible for the polymorph selection ability of this so-called solution-shearing process. It has been argued that the 1D self-confinement process is analogous to three-dimensional (3D) nanoscale confinement in porous media known to select for polymorphs of organic crystals. While in the first part of this IFPRI project for the model compound ACM we have established that solvent(s) and self-assembled monolayer (SAM) surface chemistry work together in single droplet evaporation experiments to control crystal polymorph, in these new studies we would like to find out whether for a given solvent/SAM configuration, parameters like blading speed can be used as an alternative to determine polymorph selection. For example, we are interested to investigate whether for a given solvent/SAM pair, which in the droplet evaporation experiments has shown to induce a particular crystal form of ACM, different blading speeds can lead to a switch between monoclinic form 1 and orthorhombic and metastable form 2 of ACM. This would establish that shear can overwrite the polymorph selection induced by the SAM substrate/solvent interface and therefore would be an important factor. Furthermore, as I will present during the upcoming AGM (*vide supra*), we are now able to spatially probe different areas within a thin film during crystallization. With this capability, we should be able to gain insight into where the nucleation is first occurring (solvent-substrate or solvent-air interfaces) and what polymorph is first formed with what orientation. Finally, since this solution-shearing method would have the added advantage of producing selected polymorphs over large areas, potentially in a roll-to-roll manner, without the requirement of a porous medium, we thought this may be industrially relevant and therefore worth investigating *in addition to* the continuation of the droplet evaporation studies (*vide supra*).

Comment 3:

Consider another system with a larger number of polymorphs. For example, ROY?

Response:

In the renewal proposal, in the first paragraph of page 5 we already wrote: "*Besides ACM, both organic as well as inorganic candidate compounds could be screened …. This phase again will provide ample opportunity for project input from IFPRI members, as during this time candidate(s) for further in-depth studies in subsequent years could be identified.*" If there is interest from IFPRI members in us looking at 5-methyl-2-[(2-nitrophenyl)amino]-3-thiophenecarbonitrile (ROY), we would certainly be happy to do that. In fact, when we first started the project, ROY was one of the candidate molecules we looked into. But as a result of the lack of experience at the time we though the less complex molecule ACM would be a better starting point. But now that we have experience from the study of ACM, more complex systems would definitively be worth looking into.

Self-Assembled Monolayers as Nucleating Surfaces to Study Early Formation Pathways of Crystallographic Polymorphs

Proposed Program Synopsis

Understanding and control of crystallographic polymorphism and crystal habit of organic as well as inorganic compounds is scientifically and technologically important to a number of industries. To date, however, the experimental control of polymorphs (crystalline solids with different arrangements of the same constituents) is difficult. Since a polymorph is determined at the nucleation of a crystal, methods that lead to an advanced understanding of early crystal formation pathways and mechanisms are highly desirable. Towards this aim, we propose to continue to work with a model pharmaceutical compound, acetaminophen (ACM), on arrays of self-assembled monolayers (SAMs) from alkane-thiols and -silanes, with different terminal (omega) functional groups, on various substrates (gold, silicon oxide/silicon). In the first part of this program we have successfully demonstrated how these arrays of SAMs in the presence of various solvent systems influence nucleation, crystal growth, orientation, and polymorph selection of ACM during simple solvent evaporation. We found that both solvent and substrate work together to control crystal polymorph. One emerging benefit of using SAMs to study ACM polymorphism was that the polymorph selectivity of a given surface was related to the chemical, stereochemical, and 2-D crystalline structure of the SAM. By studying the relationships between the structure of the crystal and the nucleating surface/solvent pair, we already gained insights into molecular-scale recognition events leading to polymorphism. In the second part of this program these studies will be complemented by a technique referred to as solution-shearing deposition method. This blade-coating (or doctor-blading) technique involves a top shearing plate forming a well-defined gap that drags a solution across a bottom substrate while keeping the bulk of the solution sandwiched between the plate and the substrate. It has recently been demonstrated for an organic semiconductor molecule that the one-dimensional (1D) self-confinement of the crystallization front between the surface crust and the substrate is responsible for the polymorph selection ability of this solution-shearing process. To this end the PI has constructed a fully automated blade-coating device in his laboratory that will be used to screen for appropriate parameters to control ACM polymorphism, including gate height, blading speed, and solvent system. Once appropriate parameters have been identified, *in-situ* grazing incidence wide angle X ray scattering (GIWAXS) experiments during beam time at Cornell's High Energy Synchrotron Source (CHESS) will be conducted to look at local nucleation and growth characteristics. Finally, based on findings of these *in-situ* studies, cryo-scanning transmission electron microscopy (cryo-STEM) will be used on samples for which the nucleation and growth processes have been halted at the earliest stages to identify possible amorphous or poorly crystalline intermediates. One advantage of this application is that all proposed advanced techniques are available either in the lab of the PI (automated blade coating set up) or in Cornell facilities (GIWAXS at CHESS; cryo-FIB and cryo-STEM in CCMR facilities). To accomplish these goals, the PI will continue his successful collaboration with a Cornell MSE faculty, Lara Estroff, with complementary expertise and a proven track record of collaboration under the umbrella of a recently renewed Department of Energy (DOE) grant currently funding efforts on early formation stages of organic-inorganic hybrid self-assemblies. If successful, this research will provide detailed input about the earliest stages in polymorph formation, which may subsequently enable utilization of computational materials science methods for full understanding of the observations.

Background

Controlling crystallographic polymorphism (and shape) is of great importance to many technologically relevant materials used in a wide variety of fields ranging from microlectronics all the way to pharmaceutical and food industries. For example, the crystal structure of an edible ingredient can influence its taste and texture. The pharmaceutical industry is interested in techniques that facilitate the discovery of all possible polymorphs, solvates (*e.g.*, hydrates), and amorphous forms of a molecule.[1-5] There are large variations in the physico-chemical properties (*e.g.*, stability, solubility, dissolution rate) of these different forms. In turn, these properties directly influence the bioavailability of the drugs in different formulations such as tablets for rapid release into the blood stream or patches for slow release over days or weeks. In multiple industries, when developing new materials formulations, it is necessary to know into which other forms the crystalline (or amorphous) material may transform, either during processing or long-term storage. Ritonavir, an anti-HIV drug marketed by Abbott Laboratories, is a well-known example where a new, more thermodynamically stable polymorph, which had poor bioavailability, appeared after the drug had entered the market.[2] To avoid such costly occurrences, it is desirable to know the complete ensemble of accessible crystalline structures (or as many as can be identified) at an early stage in materials development to predict accurately the solid-state transformations.

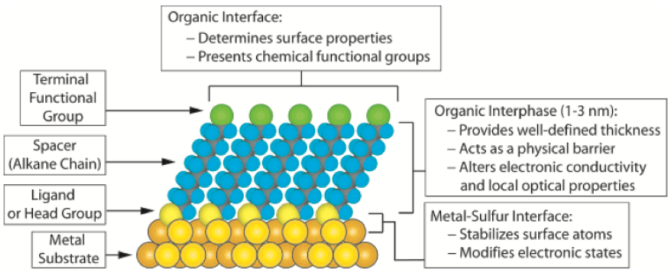

Fig.1. Schematic of ideal alkanethiol SAM on gold.[6]

It is difficult to completely map the phase diagram of a given compound since the underlying mechanisms that determine polymorphism are still largely unknown.[1] In the first funding period of this project we therefore used self-assembled monolayers (SAMs, Fig.1) of alkanethiolates and alkanesilanes on metallic (gold) and (silicon) oxide substrates, respectively, as nucleating surfaces to screen for polymorphs and solvates of a small pharmaceutical model compound, acetaminophen (ACM), see Figures 1-3. Acetaminophen (ACM, Fig. 2) is a well-studied active pharmaceutical ingredient (API) for reducing pain and fever. It has two well-known polymorphs, a monoclinic form I and an orthorhombic form II. Metastable form II is more soluble in aqueous environments and more compressible for tableting because of a layer-by-layer type packing of ACM molecules in the associated crystal structure.[7] The favorable properties of form II allured scientists to find a route to crystallize ACM polymorphs selectively and efficiently. For example, the Wilson Group selectively produced form II by recrystallizing ACM from solutions composed of monosubstituted halobenzoic acid, which they called a multicomponent crystallization technique.[8] Matzger and his

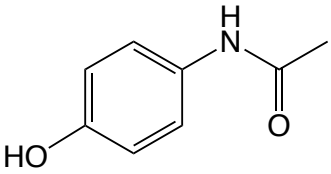

Fig.2. Acetaminophen.

SAMs molecule	*Chemical structure*
11-mercapto-1-undecanol (MUOH)	HO SH
1-undecanethiol (UDT)	SH
Trichloro(octadecyl)silane (OTS)	$SiCl_3$
Trichloro(phenyl)silane (PTS)	$SiCl_3$

Fig.3. Structures of molecules for SAM formation.

coworkers also achieved ACM polymorph selection by use of heterogeneous nucleation on polymer surfaces in aqueous solutions.[9,10] We examined 1-undecanethiol (UDT) and 11-mercapto-

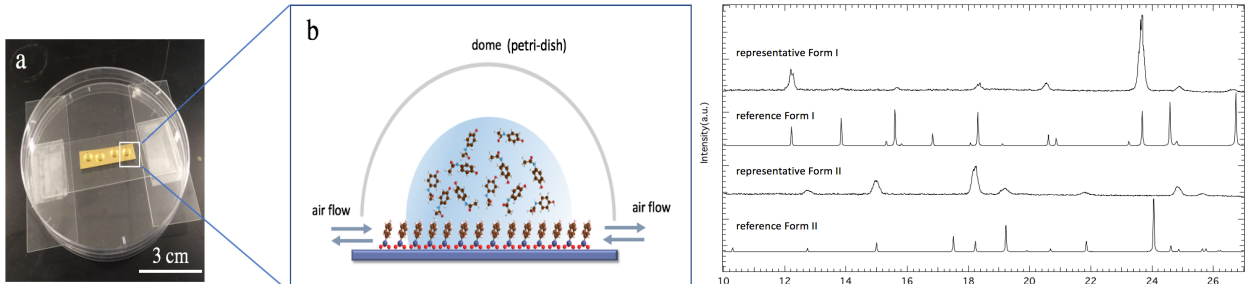

Fig.4. Droplet evaporation set up and schematic (left); PXRD of ACM polymorphs I & II on SAMS together with reference spectra.

1-undecanol (MUOH) SAM chemistries on gold, and trichloro(octadecyl) silane (OTS) and trichloro(phenyl)silane (PTS) on oxide bearing silicon substrates (Fig. 3) in the presence of various solvent systems to investigate their ability to influence the nucleation, polymorph selection and crystal growth of ACM.

Solvent	*SAM Chemistry*	*n*	*Form I*	*Form II*
Ethanol	UDT	20	**80%**	20%
	OTS	18	**94%**	6%
	PTS	14	**93%**	7%
	MUOH	11	9%	**91%**
Water	UDT	9	**93%**	7%
	OTS	15	**87%**	13%
	PTS	10	**100%**	0%
	MUOH	17	**100%**	0%
1,4-dioxane	UDT	11	**100%**	0
	OTS	10	**90%**	10%
	PTS	10	**70%**	30%
	MUOH	10	20%	**80%**
Water/dioxane 20/80	UDT	11	9%	**91%**
	OTS	11	0	**100%**
	PTS	9	0	**100%**
	MUOH	10	0	**100%**

Table 1. Crystallization results for combinations of SAMs and solvent chemistries (n = # droplets in study).

Single droplet evaporation method. Using simple droplet evaporation experiments (Fig. 4, left) and subsequent characterization of the resulting ACM crystals with powder x-ray diffraction (PXRD, Fig. 4, right) we successfully demonstrated how these arrays of SAMs in the presence of various solvent systems influence nucleation, crystal growth, and polymorph selection of ACM during simple solvent evaporation. As summarized in Table 1, we found that both solvent(s) and SAM substrate work together to control crystal polymorph. On hydrophobic surfaces (UDT, OTS, PTS), use of pure solvents resulted in ACM form I (monoclinic), while a mixture of water and dioxane produced form II (orthorhombic). In general, both solvent and SAM surface chemistry act in concert to control polymorph selection. In addition to polymorph selection, we observed that for form II different SAM surface chemistries influence crystal orientation (data not shown). The phenyl-terminated (PTS) SAM surface (Fig. 5, left) nucleated crystals with the phenyl rings oriented approximately perpendicularly to the substrate (*e.g.* (200), (211) and (210) planes lie parallel to the substrate). In contrast, –OH group terminated (MUOH) SAM surfaces (Fig. 5, right) promoted crystallization with the (002) cleavage plane oriented parallel to the substrate.

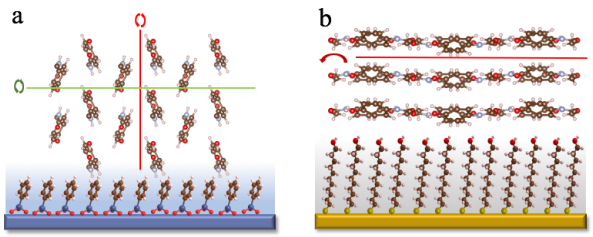

Fig.5. Schematic of proposed molecular interactions btw. form II crystals and different SAMS (see text). Red and green lines indicate crystal planes parallel to (001) and perpendicular to the (002) plane (such as (200) plane), respectively. Arrows indicate angular variations.

Proposed Research

Blade coating method. After establishing, during the first two years of the program, that both solvent and substrate work together to reproducibly control ACM crystal polymorph in simple, quasi-static droplet evaporation experiments, we have recently started to look at experiments more dynamic nature in which the ACM solution is pulled into a thin film via a doctor blade. With this work we follow recent studies that have demonstrated that the one-dimensional (1D) self-confinement of the crystallization front between the surface crust of a blade and the substrate can be responsible for the polymorph selection ability of this so-called solution-shearing process.[11] The 1D self-confinement process is analogous to three dimensional (3D) nanoscale confinement in porous media known to select for polymorphs of organic crystals.[12,13] The solution-shearing method has the added advantage of producing selected polymorphs over large areas, potentially in a roll-to-roll manner, without the requirement of a porous medium, and thus may be

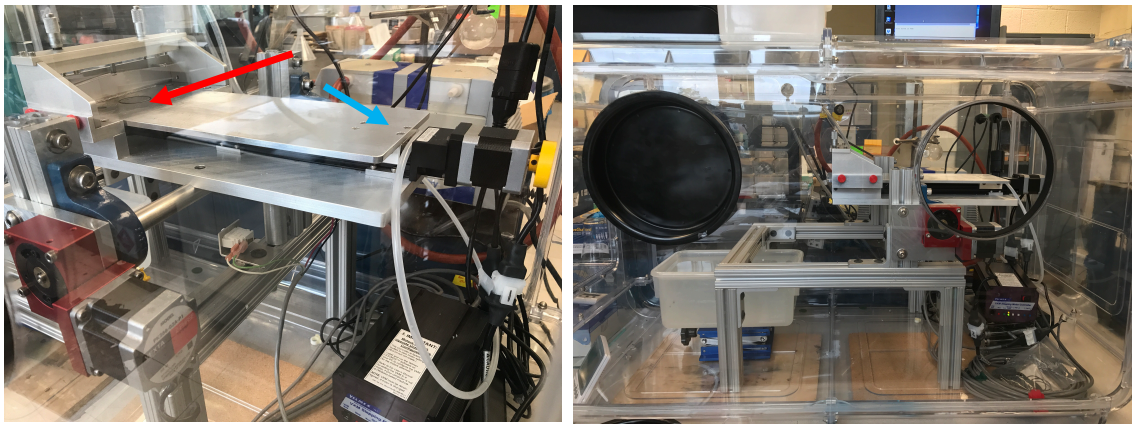

Fig.6. Photographs of fully automated doctor blading set up (left) housed in an atmosphere controlled chamber (right).

industrially relevant. In order to more precisely control the experimental conditions of the doctor-blading process, the Wiesner group has constructed a fully automated system shown in Fig. 6, where a motor-driven table (left photo, blue arrow) moves with controlled speed under a blade (left photo, red arrow) thereby forming a solution film on a substrate that is held on the table via vacuum. The whole system is housed in an atmosphere controlled chamber (Fig. 6, right photo) allowing, *e.g.* to work in well-defined relative humidity (%RH) environments. First, preliminary

Blade	*Solvent*	*Solution Concentration*	*SAM chemistry*	*Temperature*	*Thickness*	*Polymorph*
steel	1,4-dioxane	15 mg/mL	PTS on silicon wafer	RT	76-102	monoclinic
steel	ethanol	15 mg/mL	PTS on silicon wafer	RT	76-102	orthorhombic
steel	1,4-dioxane	15 mg/mL	MUOH on gold	RT	76-102	orthorhombic
steel	ethanol	15 mg/mL	MUOH on gold	RT	76-102	orthorhombic

Tab.2. Preliminary blade coating results showing ACM polymorph selectivity.

results obtained at room temperature for fixed gate height (76-102 microns) and motor speed (300 steps per second) shown in Table 2 suggest that for PTS SAMs on a silicon waver, polymorph selectivity can be achieved varying the solvent from 1,4-dioxane to ethanol.

Building on these very recent and exciting results, we propose to expand these experiments to a range of SAMS, solvents, and doctor blading conditions (for first sets of SAMS and solvents see Fig. 3 and Table 1, *vide supra*) in order to screen a wide parameter set. As discussed for the droplet evaporation experiments, we will use PXRD in order to investigate polymorph structure and crystal orientation of the resulting films in order to establish processing-molecular structure correlations. Besides ACM, both organic as well as inorganic candidate compounds could be screened using this automated doctor-blading device. This phase again will provide ample opportunity for project input from IFPRI members, as during this time candidate(s) for further in-depth studies in subsequent years could be identified.

Subsequent studies. With the droplet evaporation method as well as the blade coating method we are developing reproducible techniques, in which SAMs are exploited to control nucleation, growth, orientation, and crystal polymorphs of acetaminophen. Having these methods established will next allow us to address questions about what happens at the early stages of the crystallization process and how solvent and substrate contribute to polymorphism control. In subsequent investigations, these studies will therefore be complemented by *in-situ* Grazing Incidence Wide Angle X-ray Scattering (GIWAXS) experiments during beam time at Cornell's High Energy Synchrotron Source (CHESS). A successful proposal has already been submitted and first CHESS beam time is now scheduled in order to conduct these studies. We will start with experiments on our ACM model compound, but are open to suggestions of other IFPRI members for alternative candidates.

Using GIWAXS will enable investigation of the structure evolution at the earliest relevant time scales.[14,15] These studies will allow unambiguous identification of amorphous phases and polymorphs as well as possible structural transformations at early times. For example, is the polymorph established at the initial nucleation event or do the different polymorphs form via different pathways, starting from e.g., an amorphous phase or solvate? Does the substrate chemistry and/or solvent choice bias the system towards a specific pathway? Besides employing specific SAMs to select for polymorphs, we will use the solution-shearing deposition (blade coating) method. The top shearing plate forms a well-defined gap that drags a solution across the bottom substrate while keeping the bulk of the solution sandwiched between the plate and the substrate. At the D1 station of the Cornell High Energy Synchrotron Source (CHESS) beamline scientist Detlef Smilgis has developed a small and lightweight shearing apparatus that can be mounted on the sample goniometer upstream of a GIWAXS camera (Fig. 6).[16] The sample mount consists of a vacuum chuck on top of a Peltier element for heating up to 120 °C. The required precision movement of the coating knife parallel to the substrate is achieved using a precision slide and a kinematic mount for blade alignment. The coating knife will be chosen to be at least twice as wide as the sample (see Fig.6), so that excess solution is pushed off the edges of the sample. The speed of the coating knife will be controlled externally: for slow speeds below 1 mm/s a syringe pump controller will be used; for faster shearing speeds up to 25 mm/s a microstepper driven linear stage will be employed. Blade motion and morphology of the deposit will be inspected with a remote-controlled machine-vision microscope acquiring videos at a rate of 8 frames/s simultaneously with X-ray measurements. In

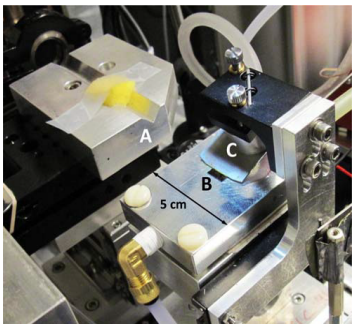

Fig. 6. *In-situ solution shearing set-up at CHESS D1 station: (A) microbeam optics, (B) sample on heated vacuum chuck, (C) shearing blade assembly. Image from ref. 16.*

order to capture the full picture of the shearing process *in-situ*, both spatial and temporal resolution will be considered. The length of the dynamic meniscus ranges from several mm down to 20 μm, which requires the use of a micron-sized X-ray beam, whereas the fast blade motion requires millisecond-scale time resolution. The D1 station at the Cornell High Energy Synchrotron Source delivers of order 10^3 photons/s at 10 keV beam energy, part of which will be focused using a 8 mrad single bounce X-ray focusing capillary with a gain of 800.[17] A fast X-ray area detector (Dectris Pilatus 100 k) will be mounted either vertically or horizontally at a well-defined distance (~200 mm) from the sample. In a recent study this detector was capable of acquiring images at rates of up to 100 frames/s for about 1000 frames thus allowing for highly time-resolved studies of earliest time points in polymorph evolution.

Final stage studies. Based on findings of the *in-situ* studies, in the final stage of this program cryo-(scanning) transmission electron microscopy (cryo-(S)TEM) will be used on samples for which the nucleation and growth processes have been halted at early stages. Studies will provide real space images of amorphous or poorly crystalline intermediates as well as further characterization of crystalline materials via selected area electron diffraction. To this end, early structures on SAM covered substrates or materials obtained by the solution-shearing deposition method will be sputtered with *e.g.* carbon and, where necessary, subsequently cryo-focused ion beam (FIB) milled to expose nanoscopic seeds and their interfaces with the SAM substrates. Transmission electron microscopes (TEMs) have grown to be among the most important tools for the determination of the structure of matter. Organic as well as hybrid organic/inorganic materials, however, still lack high-resolution characterization because of their incompatibility with imaging conditions typically used in materials' electron microscopy. Here, under the guidance of Cornell facility advisor Prof. L. Kourkoutis we will use cryo-(S)TEM to image the organic (and, where appropriate, inorganic) components and their interfaces with the substrate. Cryo-immobilization by rapid-freezing will provide structural preservation, reduced beam damage particularly relevant for organic compounds, as well as the possibility for sample thinning, which is required to reveal the internal structure of thicker specimens. Plunge-freezing, developed in the life sciences for hydrated biological samples,[18-20] will be used to produce thin vitrified films of materials at specific stages of formation. These films can subsequently be transferred under liquid nitrogen into the cryo-(S)TEM. Cornell's Center for Materials Research's (CCMR) electron microscopy facility houses two TEMs equipped for operation at cryogenic temperatures including the analytical FEI Tecnai F20. Sample cooling will be achieved through use of side-entry liquid nitrogen cooled TEM holders. For organic materials like ACM, the imaging resolution will likely be limited by radiation damage, not the performance of the instrument. Thicker materials at later stages of formation will require sample thinning in order to access structures and interfaces. FIB milling, which is routinely used in material science, has recently been adapted for cryo-immobilized soft biological specimens[21-24]. Kourkoutis and Estroff recently expanded these methods to interrogate solid-liquid interfaces.(REF) Here, we will optimize this method for cryo-immobilized organic systems grown on metallic or oxide substrates with the goal of creating electron transparent samples for subsequent analysis by cryo-(S)TEM. Of particular interest are questions of where the nuclei form, i.e., in solution or at the interface, as well as the structure of the nuclei.

References

(1) Bernstein, J. *Polymorphism in Molecular Crystals*; Clarendon Press: Oxford, 2002.
(2) Morissette, S. L.; Almarsson, O.; Peterson, M. L.; Remenar, J. F.; Read, M. J.; Lemmo, A. V.; Ellis, S.; Cima, M. J.; Gardner, C. R., "High-throughput crystallization: polymorphs, salts, co-crystals and solvates of pharmaceutical solids"; *Adv. Drug Deliv. Rev.* **2004**, *56*, 275.
(3) Gardner, C. R.; Walsh, C. T.; Almarsson, O., "Drugs as materials: Valuing physical form in drug discovery"; *Nature Reviews Drug Discovery* **2004**, *3*, 926.
(4) Almarsson, O.; Hickey, M. B.; Peterson, M. L.; Morissette, S. L.; Soukasene, S.; McNulty, C.; Tawa, M.; MacPhee, J. M.; Remenar, J. F., "High-throughput surveys of crystal form diversity of highly polymorphic pharmaceutical compounds"; *Cryst. Growth Des.* **2003**, *3*, 927.
(5) Rodriguez-Spong, B.; Price, C. P.; Jayasankar, A.; Matzger, A. J.; Rodriguez-Hornedo, N., "General principles of pharmaceutical solid polymorphism: a supramolecular perspective"; *Adv. Drug Deliv. Rev.* **2004**, *56*, 241.
(6) Love, J. C.; Estroff, L. A.; Kriebel, J. K.; Nuzzo, R. G.; Whitesides, G. M., "Self-assembled monolayers of thiolates on metals as a form of nanotechnology"; *Chem. Rev.* **2005**, *105*, 1103.
(7) Fachaux, J. M.; Guyot-Hermann, A. M.; Guyot, J. C.; Conflant, P.; Darche, M.; Veesler, S.; Boistelle, R., Pure paracetamol for direct compression, *Powder Technology*, **1995**, 82, 123-128.
(8) Thomas, L. H.; Wales, C.; Zhao, L.; Wilson, C. C., Paracetamol Form II: An Elusive Polymorph through Facile Multicomponent Crystallization Routes, *Cryst. Growth Des.,* **2011**, 11, 1450–1452.
(9) Price, P. C., Grzesiak, A. L., Matzger, A. J., Crystalline Polymorph Selection and Discovery with Polymer Heteronuclei, *J. Am. Chem. Soc.* **2005**, 127, 5512-5517.
(10) Lang, M.; Grzesiak, A. L.; Matzger, A. J., The Use of Polymer Heteronuclei for Crystalline Polymorph Selection, *J. Am. Chem. Soc.,* **2002**, 124, 14834–14835.
(11) Giri, G., Li, R., Smilgies, D.-M., Li, E. Q., Diao, Y., Lenn, K. M., Chiu, M., Lin, D. W., Allen, R. Reinspach, J., Mannsfeld, S. C.B., Thoroddsen, S. T., Clancy, P., Bao, Z., Amassian, A., "One-dimensional self-confinement promotes polymorph selection in large-area organic semiconductor thin films", *Nat. Commun.* **2014**, 5:3573.
(12) Hamilton, B. D., Ha, J.-M., Hillmyer, M. A. & Ward, M. D., "Manipulating crystal growth and polymorphism by confinement in nanoscale crystallization chambers", *Acc. Chem. Res.* **2011**, *45*, 414.
(13) Ha, J.-M., Hamilton, B. D., Hillmyer, M. A. & Ward, M. D., "Phase behavior and polymorphism of organic crystals confined within nanoscale chambers", *Cryst. Growth Design* **2009**, *9*, 4766.
(14) Sirringhaus, H., Brown, P. J., Friend, R. H., Nielsen, M. M., Bechgaard, K. B., Langeveld-Voss, M. W., Spiering, A. J. H., Janssen, R. A. J., Meijer, E. W., Herwig**,** P., de Leeuw, D. M., "Two-dimensional charge transport in self-organized, high-mobility conjugated polymers", Nature **1999**, *401*, 685.
(15) Kline, R. J., McGehee, M. D., Toney, M. F., "Highly oriented crystal at the buried interface in polythiophene thin-film transistors", *Nature Mater.* **2006**, *5*, 222.
(16) Smilgies, D.-M., Li , R., Giri, G., Chou, K. W., Diao, Y., Bao, Z., Amassian, A., "Look fast: Crystallization of conjugated molecules during solution shearing probed in-situ and in real time by X-ray scattering", *Phys. Status Solidi RRL* **2013**, *7*, 177.
(17) Li, R., Cornaby, S., Kamperman, M., Smilgies, D.-M., "Nanocomposite characterization on multiple length scales using μSAXS", *J. Synchrotron Rad.* **2011**, *18*, 697.
(18) Dubochet, J. & McDowall, A. W. "Vitrification of pure water for electron microscopy".

Journal of Microscopy **1981**, *124*, 3.
(19) Dubochet, J. "Cryo-EM—the first thirty years". *Journal of Microscopy* **2012**, *245*, 221.
(20) Kourkoutis, L. F., Plitzko, J. M. & Baumeister, W. "Electron Microscopy of Biological Materials at the Nanometer Scale". *Annual Review of Materials Research* **2012**, *42*, 33.
(21) Marko, M., Hsieh, C., Schalek, R., Frank, J. & Mannella, C. "Focused-ion-beam thinning of frozen-hydrated biological specimens for cryo-electron microscopy". *Nature Methods* **2007**, *4*, 215.
(22) Rigort, A., Baeuerlein, F. J. B., Leis, A. *et al*. "Micromachining tools and correlative approaches for cellular cryo-electron tomography". *Journal of Structural Biology* **2010**, *172*, 169.
(23) Hayles, M. F., de Winter, D. A. M., Schneijdenberg, C. T. W. M. *et al*. "The making of frozen-hydrated, vitreous lamellas from cells for cryo-electron microscopy". *Journal of Structural Biology* **2010**, *172*, 180.
(24) Zachman, M.J., Asenath-Smith, E., Estroff, L.A., Kourkoutis, L.F. "Site-Specific Preparation of Intact Solid-Liquid Interfaces by Label-Free *In Situ* Localization and Cryo-FIB Lift-Out", *Microsc. Microanal.*, **2016**, *22*, 1338-1349.